THE RELATIONSHIP BETWEEN GEOLOGY AND GRADE DISTRIBUTION IN THE BALUBA CENTRE LIMB, ZAMBIAN COPPERBELT

Chama Charles Kapumpa
B.Sc. (Hons.)

A thesis submitted for the award of the degree of Doctor of Philosophy (Ph.D) of the University of London and the Diploma of Imperial College of Science, Technology and Medicine (DIC).

Department of Geology
Royal School of Mines
Imperial College of Science, Technology and Medicine
London SW7 2BP

July, 1995

ProQuest LLC.
789 East Eisenhower Parkway
P.O. Box 1346
Ann Arbor, MI 48106 – 1346

Dedicated to my late sister

Joyce Kamfwa Kapumpa

ABSTRACT

Copper and cobalt mineralisation at Baluba are hosted in tremolite schists and argillites. The principal copper bearing minerals are chalcopyrite, bornite and chalcocite and cobalt occurs as carrollite in the schists and as cobaltiferous pyrite in the argillites. The primary mineralisation is envisaged to be synsedimentary. The 1% copper assay footwall is found to be coincidental with the geological footwall defined by the contact between conglomerates and schists, but the assay hangingwall does not have a corresponding geological marker. A vertical zonation of the orebody into ore mineral groups is noted in the Baluba orebody. A mathematical model that possibly describes the vertical copper grade distribution prior to diagenetic and metamorphic effects is presented.

Petrographic examinations of the Baluba Centre Limb rocks indicate that the rocks have undergone metamorphism of the greenschist facies. The recrystallisation and remobilisation of the metallic minerals has affected the distribution of the copper and cobalt grades within the Baluba Centre Limb rocks.

The geochemistry of the Basement suggests that the Basement schists and granites are possible sources of the rock forming and metallic minerals of the Baluba Centre Limb sediments. Whereas the copper and iron geochemical patterns in the Baluba Centre Limb can be adequately explained by the Basement geochemistry there is a notable deficiency of cobalt in the Basement.

The geochemical patterns displayed in the Baluba Centre Limb rocks appear complex when all the samples are treated together without applying any geological controls to separate them. Clearer geochemical relationships are obtained when the samples are grouped according to lithological and mineralogical classes. The close correlation between cobalt and iron in the pyrites in the hangingwall region signifies the cobaltiferous nature of the pyrite. Statistically it has been observed that the distributions of copper grades are positively skewed and the histograms exhibit frequency distributions which deviate from the normal (gaussian) model. The skewness is, however, not strong enough to fit the log-normal model. The deviation from the normal distribution is attributed to the co-existence of several copper-bearing minerals through the Baluba Centre Limb orebody.

The analysis of variance indicates that the chip sampling method practised at Baluba gives rise to higher sampling variances compared to diamond drill sampling. It is shown that the sampling variance due to chip sampling accounts for about 20-40% of the total variance whereas the sampling variance contribution to total variance in diamond drill sampling is about 10-20%. Evaluation of the precision of copper and cobalt analysis by the AAS procedure at the Baluba mine laboratory indicate detection limits of 0.111% copper and 0.062% cobalt.

Variograms have been constructed in the down-hole direction and in the horizontal plane. The spherical model with a nugget effect is used to fit the experimental variogram data. The fitted variogram models indicate a zonal anisotropy (between the down-hole and horizontal planes), but a geometric isotropy within the horizontal plane. In the down-hole direction the range of influence has been evaluated to be 1.6m in the schist and 8m in the argillites. In the horizontal plane the modelled variograms are isotropic with a range of 100m.

The optimisation of the position of the hangingwall has been evaluated by assessing the influence of internal and hangingwall dilution. Using the effects of internal dilution only, a cutoff grade of 0.75% copper is found to optimise the hangingwall location. If hangingwall dilution is allowed for, in addition to the internal dilution, then a higher cutoff grade of 1.25% copper optimises the hangingwall position. A density of 2.779t/m^3 is obtained for the mineralised sediments of Baluba.

ACKNOWLEDGEMENTS

This research project was sponsored by a scholarship from the Zambia Consolidated Copper Mines Limited, Luanshya Division. I am grateful for their financial support and for the permission to use the materials and data. The support and assistance provided by the Luanshya Division Geology Department during the field work at Baluba mine is acknowledged. The Chief Geologist, geologists and the staff of the Geology, Mining, Analytical and Concentrator departments who provided their assistance in several ways during the field work are sincerely thanked. The senior geologist in charge of the Baluba Centre Limb section, Chalwe Mapoma, was especially a handy colleague to work with during the field work. His assistance with the organisation and management of the numerous mapping and sampling activities is greatly appreciated.

My thanks are extended to Professor Dennis Buchanan for supervising the research. My secondary supervisor, Mr. Colin Dixon, provided field supervision during my first field trip to Baluba mine, in the summer of 1992. His guidance and advice are acknowledged and gratefully appreciated.

I am thankful to Dr. Michael Ramsey for advice on the geochemical analyses. Dr. Chris Halls was helpful with petrographic work and is sincerely thanked. Alban Doyle and Barry Coles provided practical guidance and assistance on geochemical analyses. Other members of the technical staff who provided assistance include Liz Morris, Gillian Ragg, Dick Giddens, Nick Royall and Mark Thompson. They are all gratefully acknowledged. The late Tony Brown offered invaluable advice and assistance with computer-based cartography. He is fondly remembered and his help is acknowledged with deep gratitude. Paul Suddaby and Ella Ng Chieng Hin are thanked for their help with computing facilities.

Geostatistical modelling was achieved mainly with the assistance and guidance provided by the Centre de Géostatistique of the Ecole des Mines de Paris based at Fontainebleau, France. I wish to express my thanks to Dr. Margaret Armstrong and her colleagues at the Centre for their expert advice and help. I would like to sincerely thank the staff at Techpro Mining and Metallurgy, Asford, Kent, who, in the latter stages of my research, provided updated information on the mining operations in the Baluba Centre Limb.

Logistical and administrative support during my stay in London was provided by Zambia Appointments Limited who are the United Kingdom based agents of the Zambia Consolidated Copper Mines Limited. Messrs. Hilton Kelly, Roger Thomson, Ted Avery and Mrs. Sue Gibbs are thanked for their assistance with all the technical and social welfare matters.

I enjoyed the company I shared with fellow members of the Mining Geology research group: Paul Smith, Xingchun Zhang, Dr. Rujian Zhao, Dr. Tom Serenko, Dr. Sean Mulshaw. Wayne and Diane Jennings and family, Francis and Hannah Katakwe and family, Steve Kazumba and other friends and colleagues provided a warm and sincere friendship to me and my family during the period of this study.

Finally, but by no means the least, I wish to acknowledge the company and love I received from my wife Mutinta, and children (Chama Jr. and Changu) and commend their endurance.

TABLE OF CONTENTS

APPENDICES

LIST OF FIGURES

LIST OF PLATES

LIST OF TABLES

CHAPTER 1

INTRODUCTION

1.1 GENERAL

The mining industry is the mainstay of the Zambian economy. Metal exports (principally copper) account for some 90% of the country's Gross National Product. Zambia ranks fourth in the world as a producer of newly mined copper and third as a cobalt producer (Mining Journal, 1994). The production of copper and cobalt in Zambia is undertaken by Zambia Consolidated Copper Mines (ZCCM) Limited which was formed in 1982 by the merger of Nchanga Consolidated Copper Mines (NCCM) Limited and Roan Copper Mines (RCM) Limited. ZCCM operates six copper producing divisions, all located on the Copperbelt Province. In addition to copper and cobalt, ZCCM also mines pyrite (for sulphur production) at Nampundwe mine south-west of Lusaka, the country's capital city. Until 30 June 1994, lead and zinc had been mined at Kabwe mine in the Central Province (Fig. 1.1). ZCCM employs a workforce of some 50,000 personnel. Efforts by the government to diversify into other industries, especially the agricultural sector, are ongoing. However, the mining sector will remain the mainstay of the nation's economy, at least for the foreseeable future.

The Roan Antelope deposit was discovered in 1902 by William Collier. It is alleged that he shot a roan antelope (from which the name of the deposit was derived) near Luanshya stream and noticed that the ground was stained with green malachite where the animal lay. Isolated copper-bearing shale outcrops were discovered nearby. The property was claimed and developed, and production of copper ore at Roan Antelope commenced in 1931.

The Baluba deposit, the focus of this thesis, was discovered in 1928 during mineral prospecting in the North Muliashi area (RCM., 1978).

Baluba mine is located about 15 kilometres northwest of Luanshya town (in the vicinity of 13° latitude, 28° longitude) on the Zambian Copperbelt (Fig. 1.1, Plate 1.1). A pilot operation began in 1966 and full copper and cobalt production at Baluba commenced in 1973. Baluba mine together with the three shafts of Luanshya mine (14, 18 and 28 shafts) are managed collectively by the

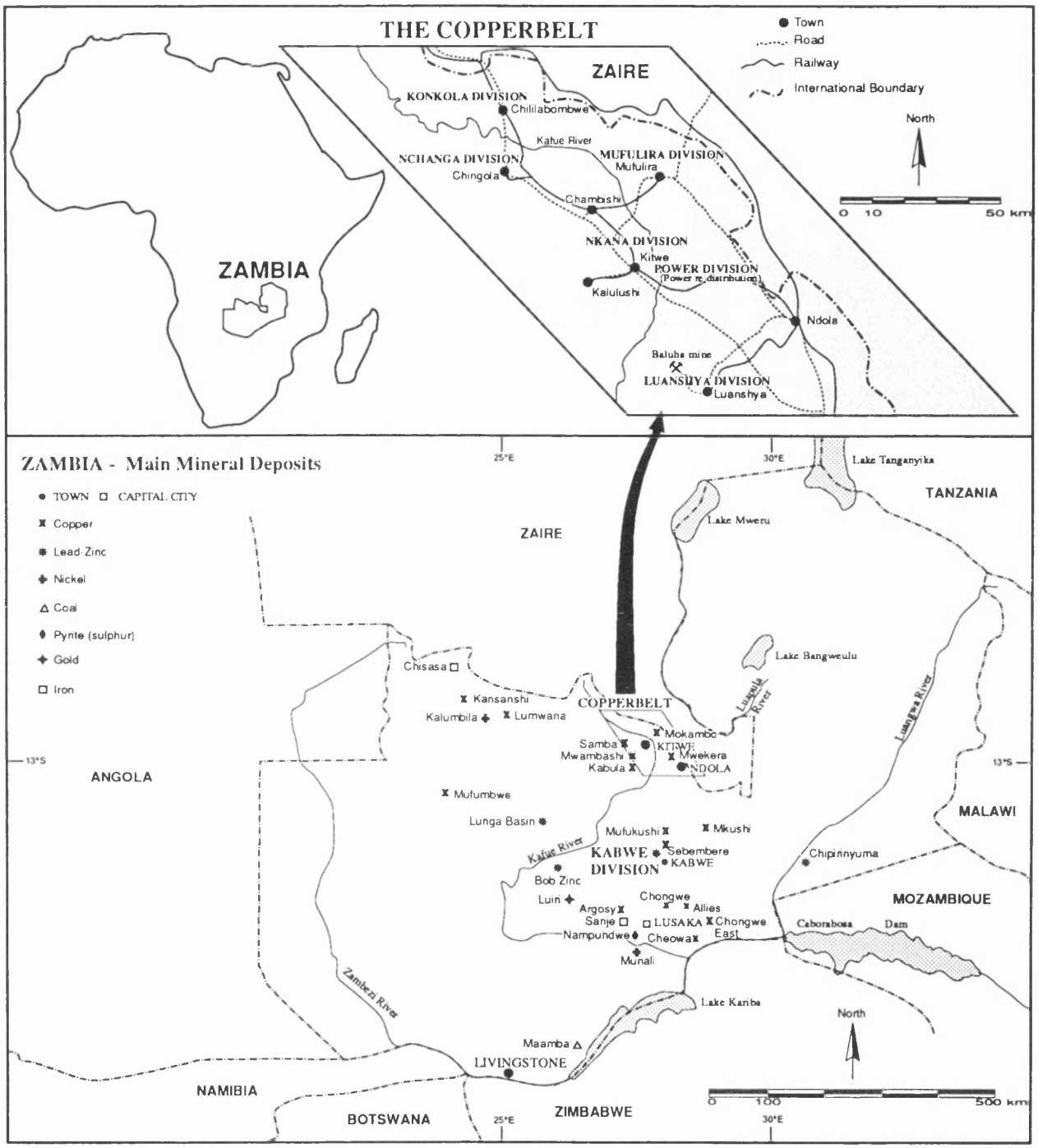

Figure 1.1: Zambian mineral deposits. (Modified from Mining Journal, 1992)

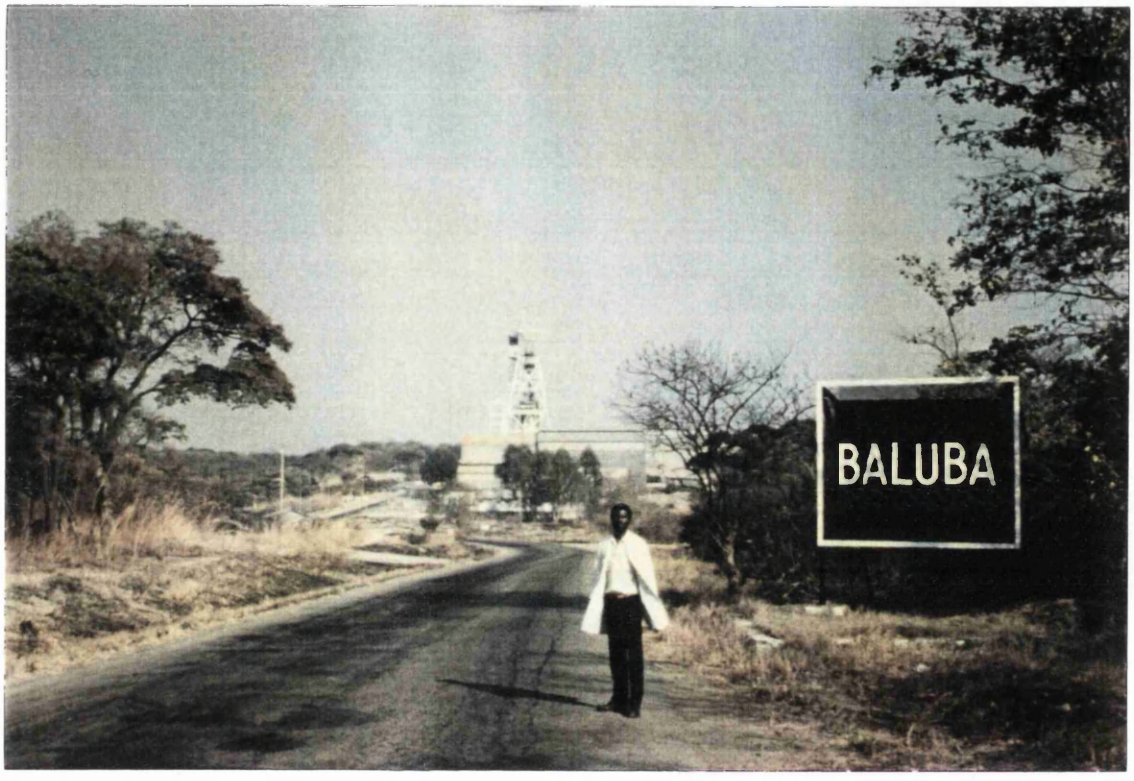

Plate 1.1: Approach to Baluba mine. The two shaftheads can be seen in the background.

Luanshya Division of ZCCM Limited. The Division also operates a concentrator, smelter and engineering support services.

Baluba mine has mineral reserves of about 40Mt at 2.4% copper and 0.15% cobalt, and mineral resources of about 27Mt at 2.3% copper and 0.10% cobalt. In the 1993/94 financial year Baluba produced 2.0Mt of ore grading 1.63% copper and 0.12% cobalt. Baluba accounts for about 6% and 28% of the total ZCCM copper and cobalt production respectively. The Baluba concentrator is located at the main plant area, a distance of 12½ kilometres away from the mine. In the early days of production ore was transported from Baluba mine to the concentrator by locomotives, but since 1977 ore has been transported by cable belt (Mabson, 1976). The concentrates produced at the Baluba concentrator are transported by road and rail to the smelters at Nkana and Mufulira.

Mining at Baluba commenced on the steep north limb where the bulk sub-level open stoping (SLOS) methods have been used. However, since 1990 emphasis of mining has been shifting to the gently steeping centre/south limb area. The change in the structure of the orebody has necessitated changes to the ore extraction methods. The centre/south limb is being extracted using the backfill mining methods; mainly the bench-and-fill, cut-and-fill and drift-and-fill variations (ZCCM, 1990; Baxter and Hooper, 1992). Current mining operations extend to the 580m underground level (at about 720m standard elevation above sea level).

1.2 RESEARCH BACKGROUND

In the Baluba Centre Limb mineralisation with copper and cobalt concentrations which can be mined economically (average grades of about 2% copper and 0.2% cobalt) occurs in the schists and argillites. Copper and cobalt mineralisation decreases to background concentrations (less than 0.1% copper and less than 0.05% cobalt) in the conglomerates and quartzites on the footwall side and in the pyritic argillite on the hangingwall side. The mineral reserves and resources in the Baluba deposit are a function of the cutoff criteria used to define the limits of 'ore' mineralisation.

The definition of ore is determined by the economics of the mining process. Cutoff grades are fundamentally a function of the differences between the revenues and the costs of producing the metal product/s. Revenues are gained from the sale of the product/s and the costs are involved with the

development, extraction, treatment and marketing of the product/s of the mining operation. A mine should be developed in such a way that the poor material is extracted along with the richer material in a blend that would yield a satisfactory product when treated (Lane, 1988). The cutoff grade should be determined by considering how poor the low grade material should get before it is classified as waste and excluded from the orebody. The low grade (waste) material that is included with the ore (intentionally or otherwise) during the exploitation of the mineral reserve constitutes the mining dilution and its effect on the definition of ore should be assessed. The cutoff grades used should be able to clearly demarcate the mineralised rock which can be mined economically (ore). Any uncertainties introduced in the definition of the orebody influence the determination of the reserves and consequently affect the grade control during the exploitation of the reserve.

At Baluba mine the currently applied sampling methods and criteria have been used ever since production commenced in 1973. Similar methods have also been used at the neighbouring Luanshya mines (14, 18 and 28 Shafts) for at least the last thirty years. No documentation is available at Luanshya Division to explain how these methods and criteria were established. The orebody is generally defined by 1% sulphide copper footwall and hangingwall cutoffs. Drill hole and chip sampling are used to define the footwall and hangingwall limits of the orebody. The 1% cutoff grade applied to define the orebody was probably based originally on empirical observations and is essentially arbitrary.

The characterisation of mineralisation is a prerequisite to improving the estimation and utilisation of the mineral reserves and resources. To achieve this requires a rigorous approach to the collection of samples, analytical control of the sample assays, interpretation of the resulting assay values and the choice of the most appropriate method/s to use in the estimation of the reserves and resources.

Figure 1.2 shows how copper and cobalt grades vary vertically in the Baluba orebody. From Figure 1.2 it can be seen that the assay footwall coincides with a geological footwall contact which is defined by the boundary between a quartzose footwall conglomerate and the transitional schists. The footwall conglomerates visually appear devoid of metallic mineralisation (see Maps 11 and 12 in Appendix J) and the footwall contact is distinctive in underground exposures and in drill cores (see Plate 1.2). The footwall limit of the orebody is essentially determined from geological mapping and core logging. The change in assay grades near the hangingwall is subtle and occurs within the argillites. Unlike the footwall which is easily manifested by geological features, there is no readily discernable geological

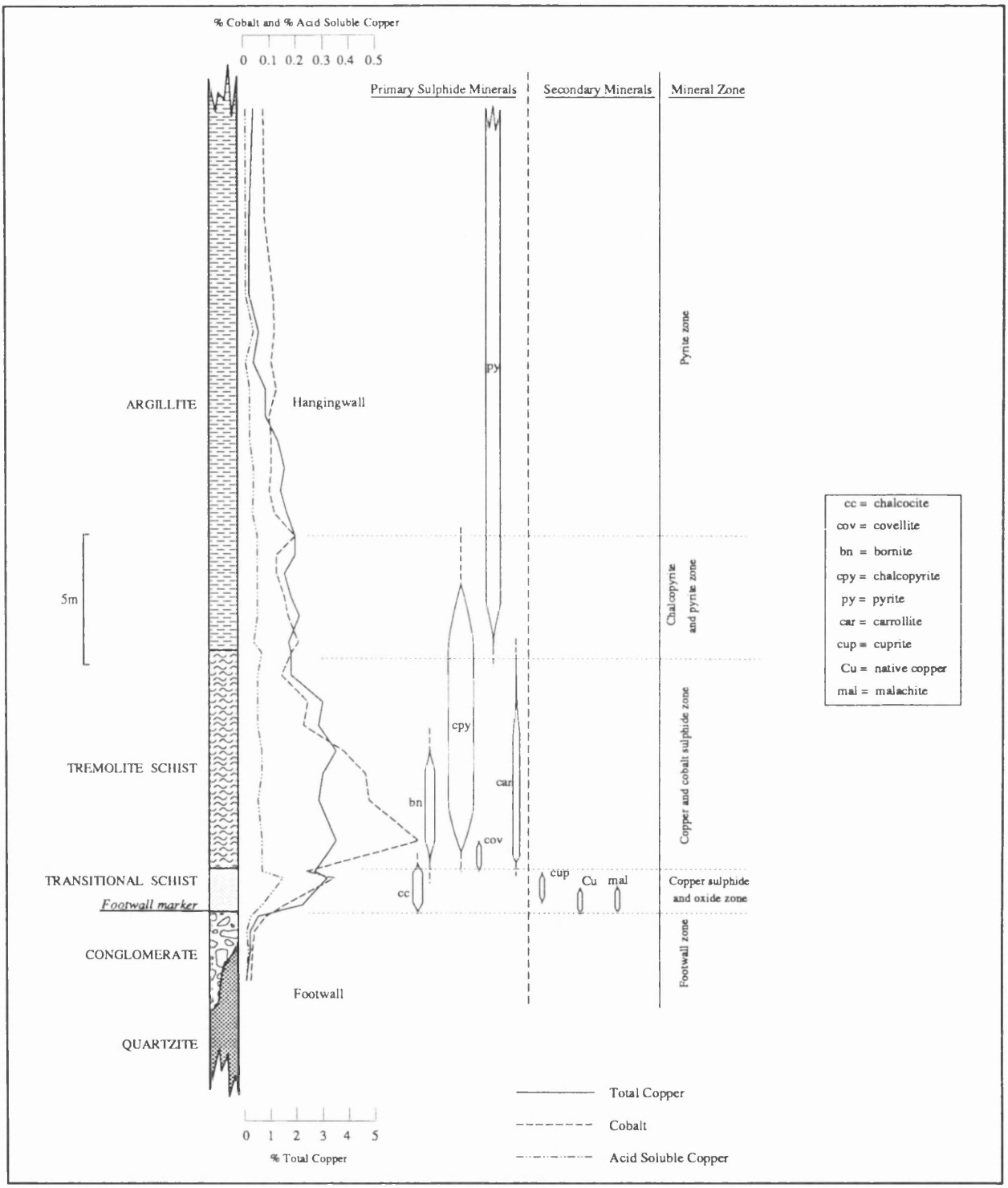

Figure 1.2: Model of vertical metallic mineral zonation in the Baluba orebody. The model is essentially a composite drill hole profile. It has been constructed by averaging the sampling data from drill holes in the Baluba Centre Limb (data in Appendix A - on disk accompanying thesis). The process used to derive the data on which the model is based is described in Appendix B. The contact between the conglomerate and the transitional schist has been taken as the origin (footwall marker).

Plate 1.2: View of the 470m Level, Block A, No.2 Crosscut, showing the footwall contact. The pinkish conglomerate at the base of the orebody is devoid of copper and cobalt mineralisation. The contact between the conglomerate and the dark greenish transitional schist marks the geological footwall which is also coincident with the assay footwall boundary (see Fig. 1.2).

Plate 1.3: View of the 490m Level, Block K, Vent. Raise, showing the hangingwall contact. The 1% copper assay hangingwall is located within the argillites and has no corresponding geological contact associated with it. Contrast with the footwall which is essentially geologically fixed. The geology of the sidewall represented in this plate is presented in Map 9 in Appendix J.

Plate 1.2

Plate 1.3

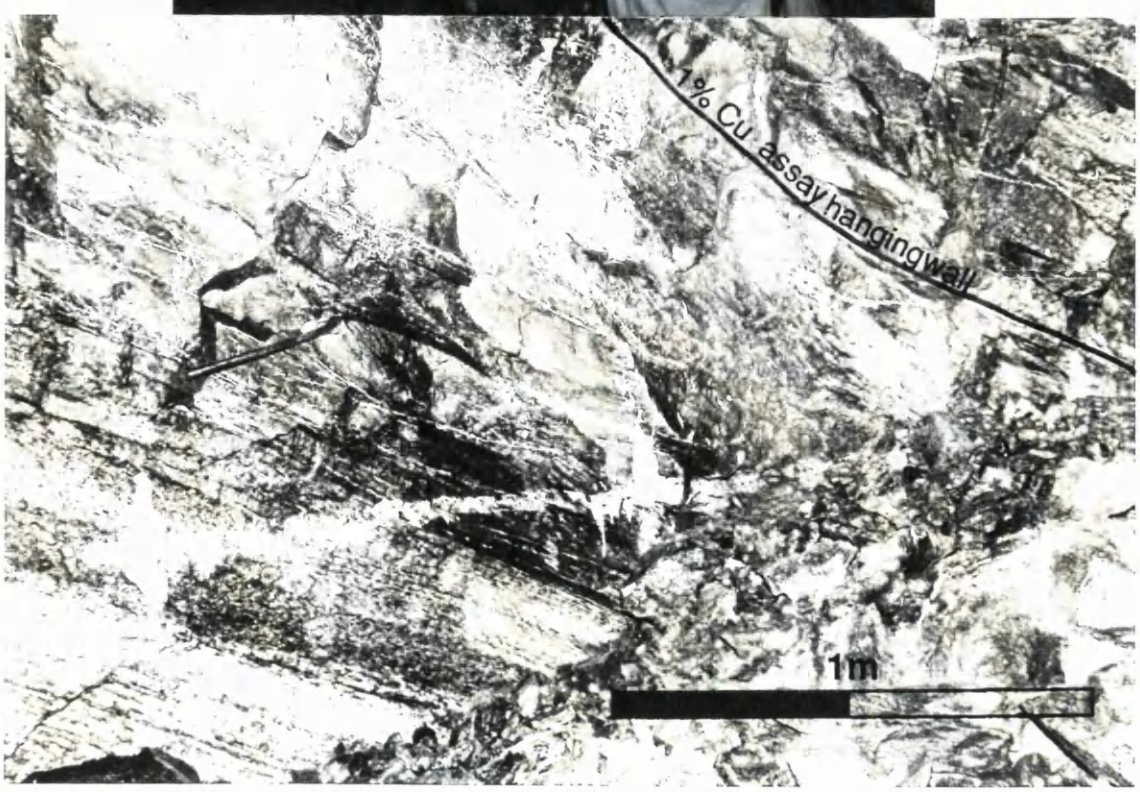

feature associated with the assay hangingwall boundary of the orebody (see Plate 1.3). It is not uncommon to find that within argillite copper grades fluctuate about the critical 1% level used to define the hangingwall boundary. In addition the grade information is not always available in the hangingwall region where it is critical to define the orebody boundary. The drill holes do not extend much beyond the 1% copper assay hangingwall.

Copper and cobalt concentrations are reported to two decimal places as metal percentages by the assay laboratory. There are two assay values of copper reported (total copper and acid soluble copper) and one value of cobalt. Acid soluble copper represents the proportion of copper that is not amenable to sulphide froth flotation and is related to the amount of copper oxide and carbonate minerals present. Acid soluble copper is informally referred to as 'oxide' copper. The terms acid soluble copper and oxide copper are, however, not strictly synonymous because a small proportion of the oxides is extractable by froth flotation (Simmonds, 1979). The term acid soluble copper rather than oxide copper will be used in this study. The copper extractable by froth flotation is equivalent to the total copper less acid soluble copper (see Appendix C). Generally, the concentration levels of acid soluble copper in the orebody are consistent and negligible at about 0.1% compared to the total copper which is at least 2% (see Fig. 1.2).

Baluba mine produces both copper and cobalt. In Figure 1.2 it is noted that whereas copper grades drop considerably from the main orebody (above 2%) into the hangingwall (below 1%), cobalt grades remain at similar levels in the near-hangingwall region as in the orebody at 0.1-0.2%. In defining the footwall and hangingwall bounds of the orebody it would be reasonable to consider the effect of cobalt mineralisation alongside copper. Although a 0.2% cobalt cutoff grade has been applied at Baluba in the past to determine the hangingwall limit of the orebody; this criterion has been used selectively, lacking the consistence and uniformity to be applied to all areas of the deposit. This is particularly due to the fact that cobalt assays are not analysed for all the samples. A study of the relationship between copper and cobalt concentrations in the deposit should lead to understanding how copper and cobalt could be used concurrently in the determination of the footwall and hangingwall. To this end it is important to study the behaviour of copper and cobalt mineralisation in the orebody and in the immediate hangingwall region above the currently applied 1% copper assay cutoff limit.

Given the problems associated with the definition of the hangingwall of the orebody, it is essential to review the cutoff grades used to define the orebody, and in particular assess whether the position of the hangingwall could be determined with greater reliability. Changing the position of the hangingwall by applying a different cutoff grade to that currently used should consider the effects of waste dilution on mining. In-situ dilution has an impact on the grade control and affects the reconciliation between the reserves and milled ore.

The mineral reserves are reported as two parameters; the grade and the tonnage of the mineralised rock. Apart from the optimisation of methods related to grade estimation it is important that the estimation of tonnage is also carried out as accurately as possible. A schematic plan showing the sources of uncertainties in the activities related to the estimation of mineral reserves and resources is illustrated in Figure 1.3.

The density used to convert the volume of rock into mass is a key factor as uncertainties arising when densities are variable through a mineral deposit can have implications on the reserves and hence mine life (de Ruiter, 1985). A uniform tonnage factor of 2.67tonnes/m^3 is used throughout the Baluba deposit for the sulphide ores. This is an oversimplification given the variable distribution of the copper and cobalt bearing minerals within the deposit (see Fig. 1.2).

The minimisation of the uncertainties associated with the estimation of copper and cobalt grades in the Baluba Centre Limb is the main issue that will be addressed in this study. The procedures associated with the acquisition, analysis and interpretation of the data used for the estimation of mineral reserves and resources will be assessed with a view to determining if improvements could be made to the methods and practices currently used at Baluba.

1.3 RESEARCH OBJECTIVES

The objectives of this study are:

(i) To establish the relationship between grade distribution and the geological characteristics in the Baluba Centre Limb deposit.

(ii) To review the current sampling methods used at Baluba and evaluate the sampling and analytical variances associated with them.

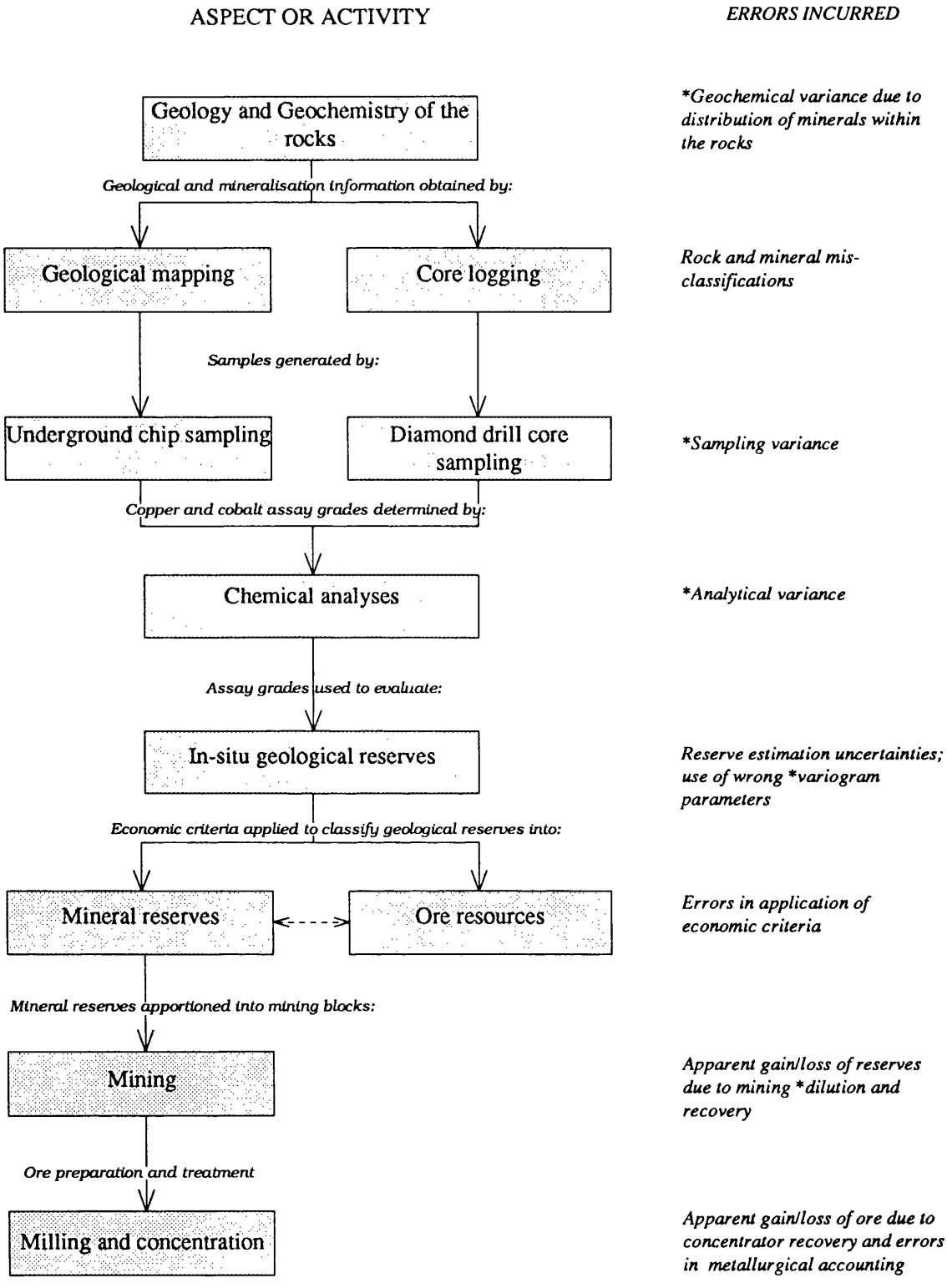

Figure 1.3: Schematic chart showing sources of uncertainty incurred from the stage of geological mapping through to ore milling. * marks the sources of uncertainty which this study will address.

(iii) To use the Baluba case as an example to establish a new insight into how the mineralogical characteristics of the Copperbelt-type rocks influence the approach to geostatistical applications.

(iv) To suggest a method that could be applied to optimise the determination of the hangingwall limit of the orebody by utilising the geological, geochemical, mineralogical and geostatistical characteristics of the Baluba Centre Limb.

The achievement of these objectives would lead to:

(i) understanding how the statistical and geostatistical observations are related to, and how they can be explained by, the geology of the deposit.

(ii) improving the quality of sampling by proposing modifications to current sampling practices and/or introducing new procedures so that uncertainties introduced through sampling and chemical analysis are minimised.

(iii) optimising the location of the hangingwall boundary of the orebody .

(iv) improvement in reserve estimations and grade control.

1.4 RESEARCH STRATEGY

Sources of the information and data on which this study has been based are divided into two categories: the primary and secondary (derived) sources. Primary sources of information constitute records of geological mapping and sampling of underground development exposures including information obtained by core logging. The secondary sources of information constitute the petrological, mineralogical and chemical analytical data that has been generated from this study. Examples of geologic and sampling logs and descriptions of the samples used in this study are presented in Appendix A.

The primary and secondary sources of information complement each other and the data derived from both sources has been used in statistical and geostatistical analysis and modelling. The integration of the geological information, data analysis and modelling is illustrated in Figure 1.4.

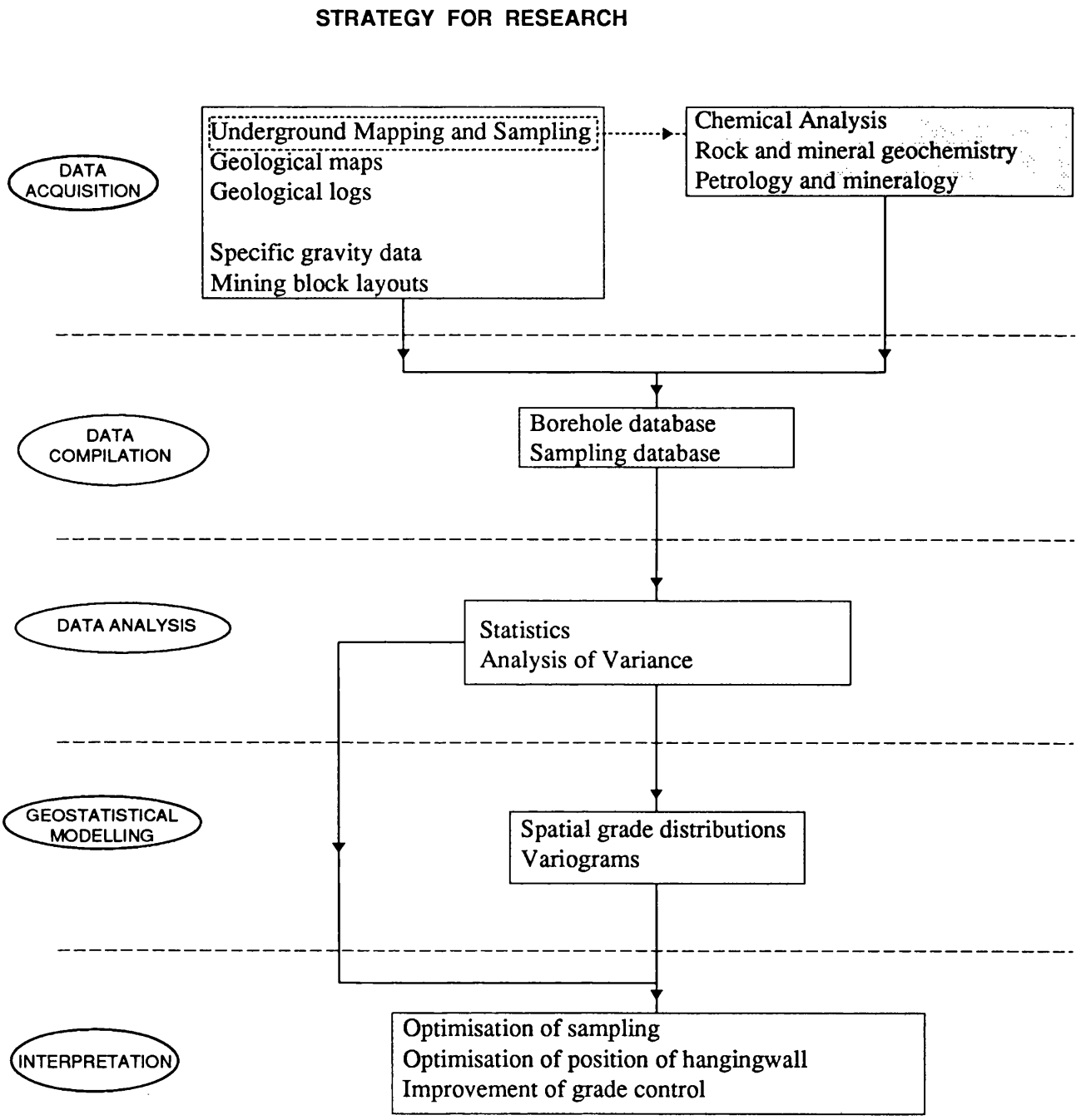

Figure 1.4: Research Strategy

1.5 FIELD SEASONS AND SAMPLING

The geological and sampling data used in this work were collected during two field mapping seasons. The first mapping season was carried out for ten weeks between July and September 1992, and the second for six weeks in August and September of 1993. Mapping and sampling were carried out at Baluba mine, Luanshya. Exposures in underground development excavations (drives, crosscuts and raises) were mapped and sampled.

Secondment to the Centre de Géostatistique of the Ecole des Mines de Paris based at Fontainebleau, France, was undertaken in order to attend a course in advanced mining geostatistics. The secondment period was from October to December 1992. The course covered included linear geostatistics, computing applications in geostatistics and mineral economics.

1.6 STRUCTURE OF THESIS

Chapter 2 discusses the geological setting of the Copperbelt region and of the Baluba area. The nature of mineralisation and ore genesis are reviewed. In Chapter 3 the petrology and paragenesis of the metallic minerals of the Baluba mine area are discussed. The effects of metamorphism on the host rock and metallic mineralisation are investigated. Chapter 4 addresses the geochemistry and mineralogy of the Baluba Centre Limb rocks and minerals. The geochemical and mineralogical relationships are assessed. Chapter 5 discusses the uncertainties associated with sampling and chemical analytical procedures used in the acquisition of the copper and cobalt assay data for Baluba. The concepts and results arising from the analysis of variance and the estimation of precision and accuracy are presented. Chapter 6 addresses geostatistical modelling. Variogram modelling results for the Baluba Centre Limb are presented. In Chapter 7 the optimisation of the hangingwall and of the density for the Baluba Centre Limb orebody are considered and the effects of dilution are addressed. Chapter 8 presents the conclusions arising from the research. Suggestions for further work to be carried out in order to complement, apply and/or verify the findings of this research are highlighted. Recommendations of the parameters to use in sampling and reserve estimation in the Baluba Centre Limb are presented.

CHAPTER 2

GEOLOGY

2.1 PREVIOUS WORK

The geology of the Zambian Copperbelt has been reviewed by various workers since the 1920s. Early publications on the geology of the Zambian Copperbelt include papers by Bancroft and Pelletier (1929), Bateman (1930) and Schneiderhöhn (1932). These works were followed by publications on the geology of the Copperbelt by Garlick (1953, 1964). A comprehensive, definitive account of the geology of the Copperbelt is presented in a book edited by Mendelsohn (1961). All these early publications concentrate on the copper mineralisation without particularly discussing the role of cobalt. Cobalt mineralisation in the context of Copperbelt deposits is discussed by Annels (1974) and Annels and Simmonds (1984). Brown (1992) discusses the sources of mineralisation in the Zambian Copperbelt-type deposits.

The geology of Baluba has been covered as part of the descriptions of the Roan-Muliashi basin geology in publications by Brummer (1955), Mendelsohn (1959), and Fleischer *et al.* (1976).

2.2 REGIONAL GEOLOGY

2.2.1 Structural Setting

The structure of the Zambian Copperbelt formed mainly in response to the Lufilian Orogeny (circa 600 Ma). The Copperbelt occupies an area which is about 160 kilometres long at the southern extremity of the 800 kilometre long Lufilian fold belt (Fig. 2.1). The Lufilian belt is an arcuate system of folds which was formed by pressure acting northwards or northeastwards. It stretches from Angola through northwestern Zambia, the Shaba region of Zaire and then back into Zambia. The Lufilian Arc is flanked by the Kibaride fold belt and the Kasai shield on the west and by the Bangweulu block and the Irumide fold belt on the east. It is separated from the Zambezi fold belt in the south by the Mwembeshi dislocation. Accounts of the relationship between the Lufilian fold belt and the Copperbelt structure and copper-cobalt mineralisation are given in various publications (Brock, 1963; Ramsay and Ridgeway, 1977; Raybould, 1978; Unrug, 1989). The Copperbelt sediments have been subjected to relatively mild flexural folding (Perry and Wiik, 1972).

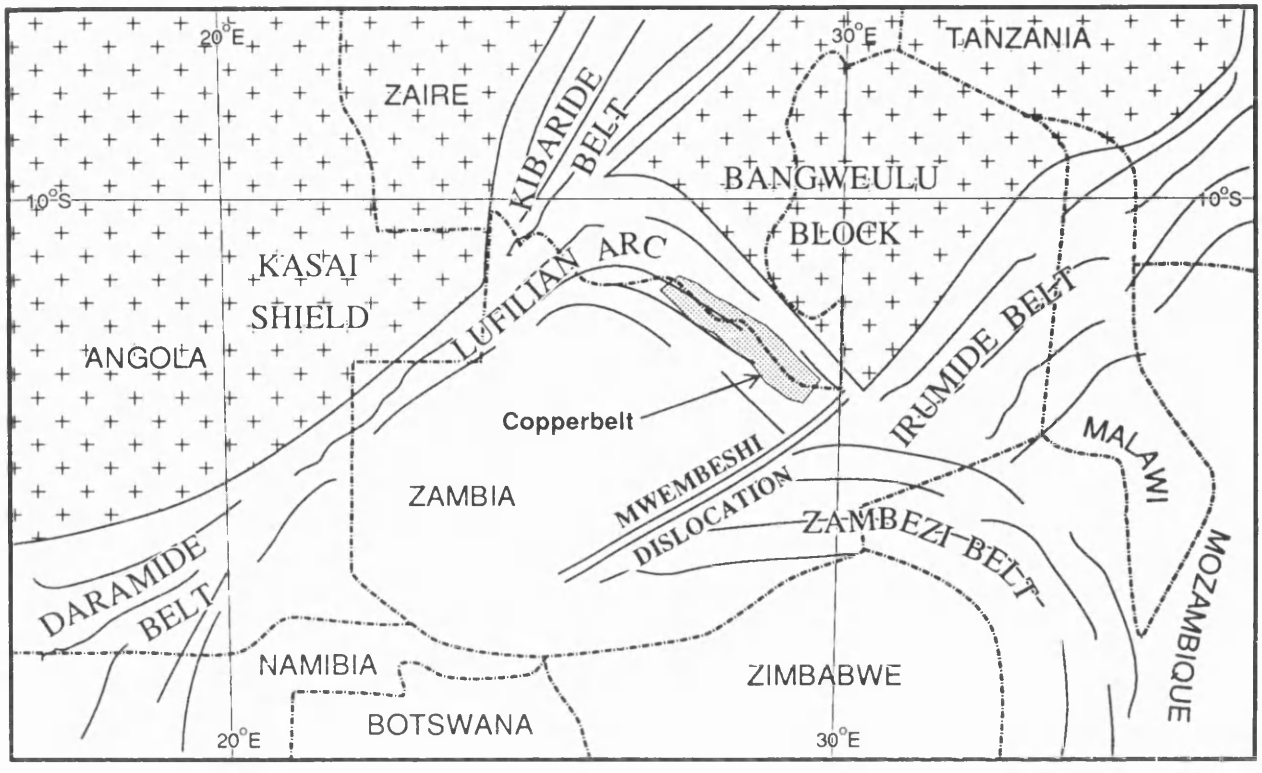

Figure 2.1: Simplified structural map of Zambia showing the position of the Lufilian Arc. (After Raybould, 1978).

The present day structure of the Zambian Copperbelt is dominated by the Kafue Anticline which trends approximately NW-SE. For nearly 50 kilometres through the Copperbelt the Kafue River follows the anticlinal axis and exposes the Lufubu schists in the Basement and the granite intrusives. The Kafue Anticline bisects the Copperbelt into the northeast and southwest flanks (Fig. 2.2).

The copper-cobalt bearing Lower Roan sediments strike sub-parallel on either side of the anticline and outcrop along the margins of structural depressions. Mufulira Mine and the now inoperative Bwana Mkubwa Mine (Ndola) lie on the northeast flank of the anticline and constitute the quartzite deposits. The rest of the mines lie on the southeast of the anticline, stretching from Konkola Mine in the northwest to Luanshya (Roan Antelope) Mine in the southwest (Fig. 2.2). These constitute the ore shale deposits. The host rock in the quartzite deposits is typically a sericitic quartzite with a greywacke facies in parts. Copper and cobalt mineralisation in the ore shale deposits is hosted in impure dolomites and argillites. On the northern side of the Copperbelt, at Nchanga and Konkola,

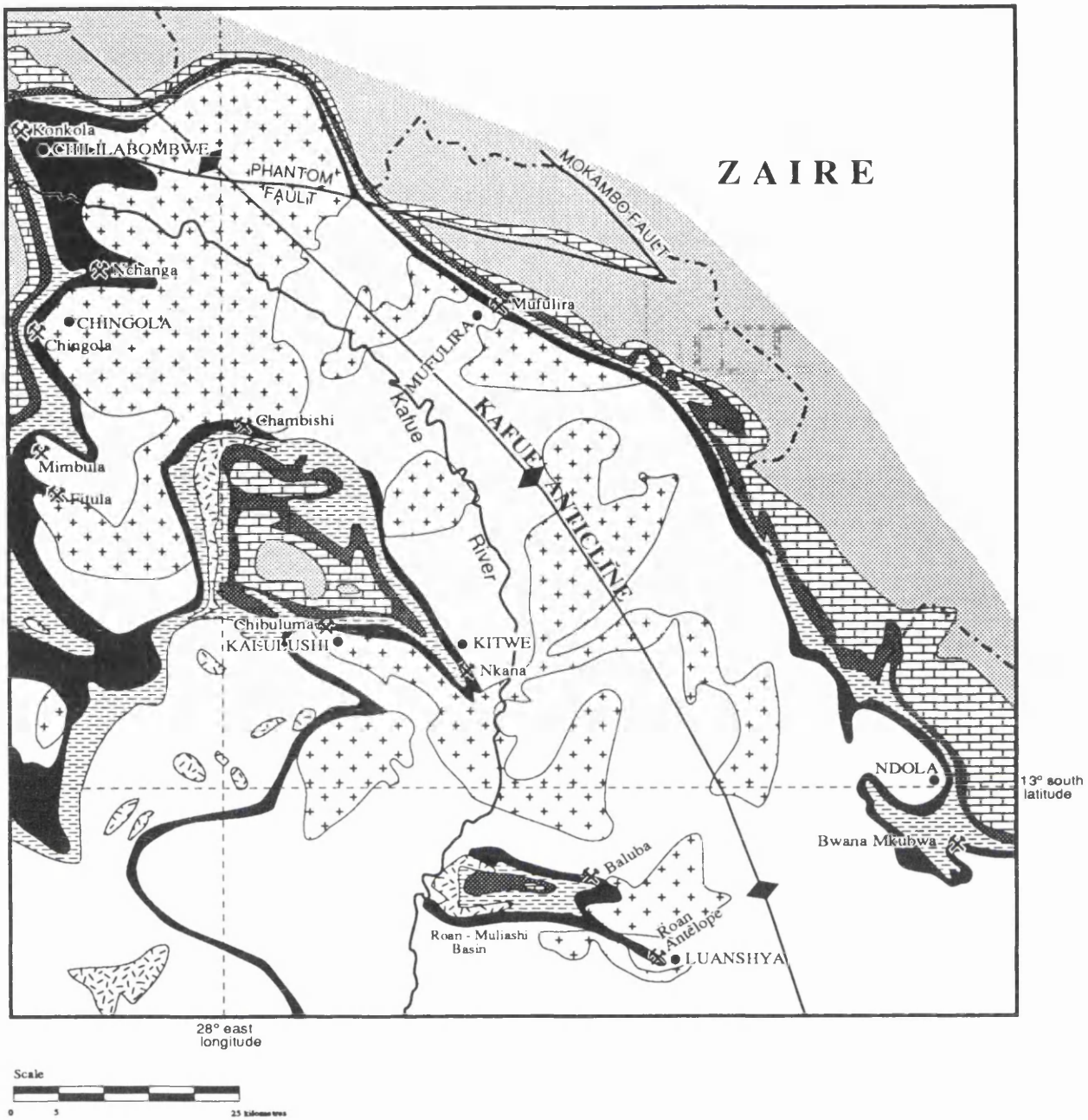

SYSTEM	SERIES	GROUP	ROCK TYPE
KATANGA	KUNDELUNGU	MIDDLE	Sandstone
		LOWER	Limestone, Dolomite, Shale
	MINE	MWASHIA	Carbonaceous Shale
		UPPER ROAN	Dolomite, Argillite
		LOWER ROAN	Quartzite, Conglomerate, Schist, argillite
	UNDIFFERENTIATED KATANGA		Quartzite, Conglomerate, Schist
	UNCONFORMITY		
MUVA / LUFUBU	BASEMENT COMPLEX		Schist, Gneiss, Quatzite, Conglomerate

INTRUSIVES

Gabbro

Granite

Figure 2.2: Geology of the Zambian Copperbelt (Modified after Mendelsohn, 1961)

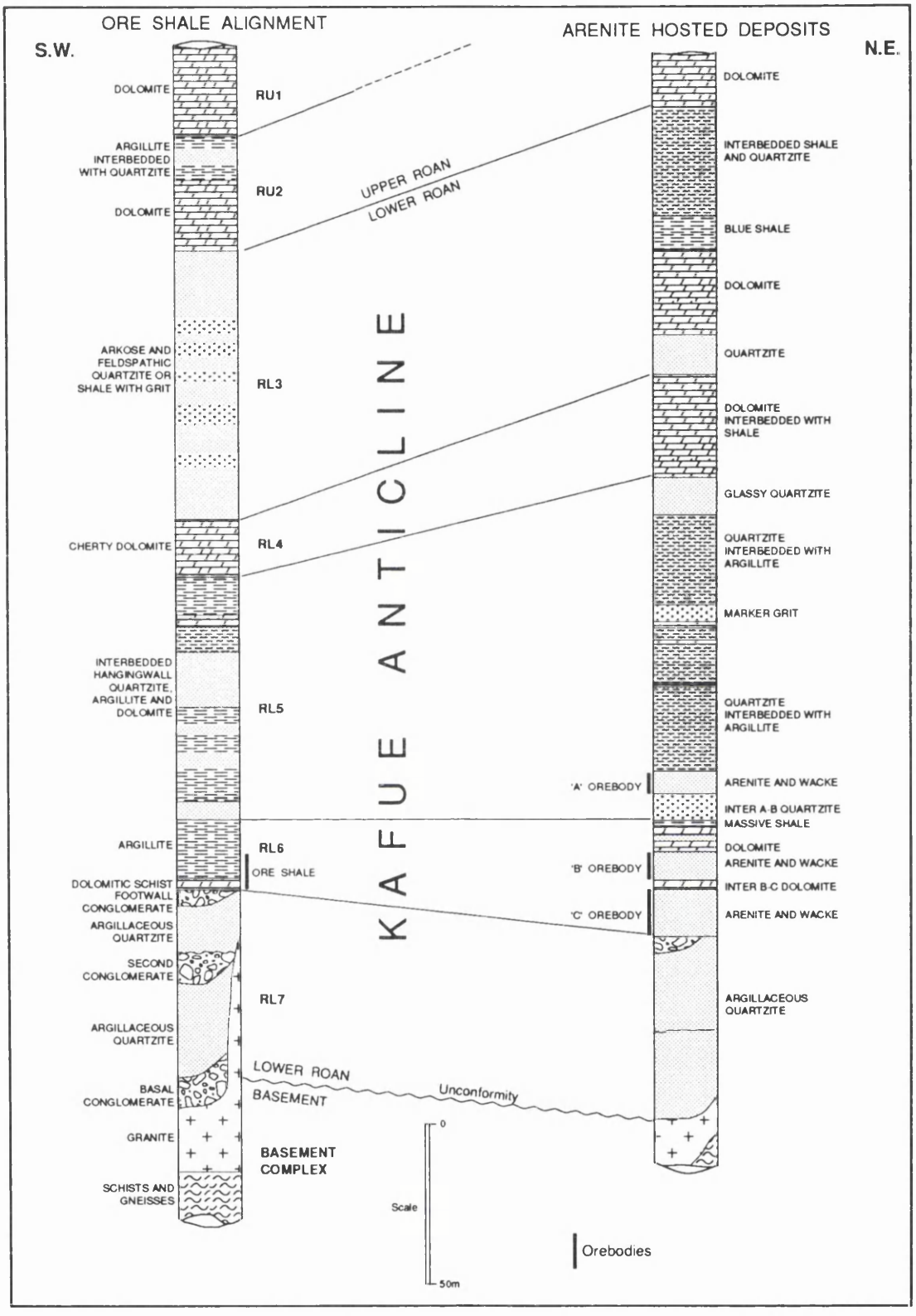

Figure 2.3: Correlation of the Copperbelt stratigraphy across the Kafue Anticline. On the southwest of the anticline the copper (with cobalt) mineralisation is hosted in shales (argillites) while on the northeast the copper (without cobalt) mineralisation is hosted in arenites and wackestones. (Modified from Binda and Mulgrew, 1974).

the dolomite is absent. There is a 20 kilometre separation of the Lower Roan sediments between those on the eastern and those on the western flanks of the Kafue Anticline.

The Phantom fault on the northern side of the Copperbelt is the major fault in the region. On the eastern extreme the Phantom fault joins the Mokambo fault which extends into the Shaban Copperbelt of Zaire (Fig. 2.2). There is little faulting in the mine areas.

2.2.2 Stratigraphy

Stratigraphically the Copperbelt rocks range from the Basement Complex of the Lufubu System (Archean) to the Katanga System which comprises the Mine Series (late Proterozoic). A stratigraphic column of the Copperbelt correlating the south-western and north-eastern flanks of the Kafue Anticline is presented in Figure 2.3.

2.2.3 Mineralisation

It is generally agreed that the Lufilian Arc structure played an important role in the localisation of the basin in which sedimentary deposition took place. The deposition basin was parallel to the old Katanga Sea shoreline; sediments were deposited in valleys carved out of the Katanga Basement (Bowen and Gunitalaka, 1977). The ore deposits of the Copperbelt are confined to the Lower Roan Group and in plan exhibit a continuous, sinuous outcrop pattern. Cobalt mineralisation is associated with copper on the south-western side of the Kafue Anticline but not on the north-eastern side. Cobalt grading over 0.1% is found at Nchanga, Nkana, Chibuluma and Baluba. Cobalt-poor deposits with at least 50ppm (0.005%) but less than 0.1% cobalt are found at Konkola, Chingola and Luanshya (Roan Antelope).

Whereas some copper deposits occur exclusive of, or with little cobalt (less than 50ppm), there are no known occurrences on the Copperbelt of cobalt mineralisation in the absence of copper (Annels, 1984). Annels (1984, 1989) notes that the cobalt occurrences are closely related to areas in which sill-like amphibolites (basic igneous rocks) are found. He suggests that the cobalt areas were probably bound by transverse and rift faults along which the magmatic solutions could have leaked (Fig. 2.4). Although the link between the occurrence of cobalt and the basic magmatic amphibolites is logical, the physical presence of the transverse/rift bounding faults is not apparent in the structures of the

Copperbelt rocks. Therefore, it is difficult to ascribe basic magmatism as a source of cobalt mineralisation.

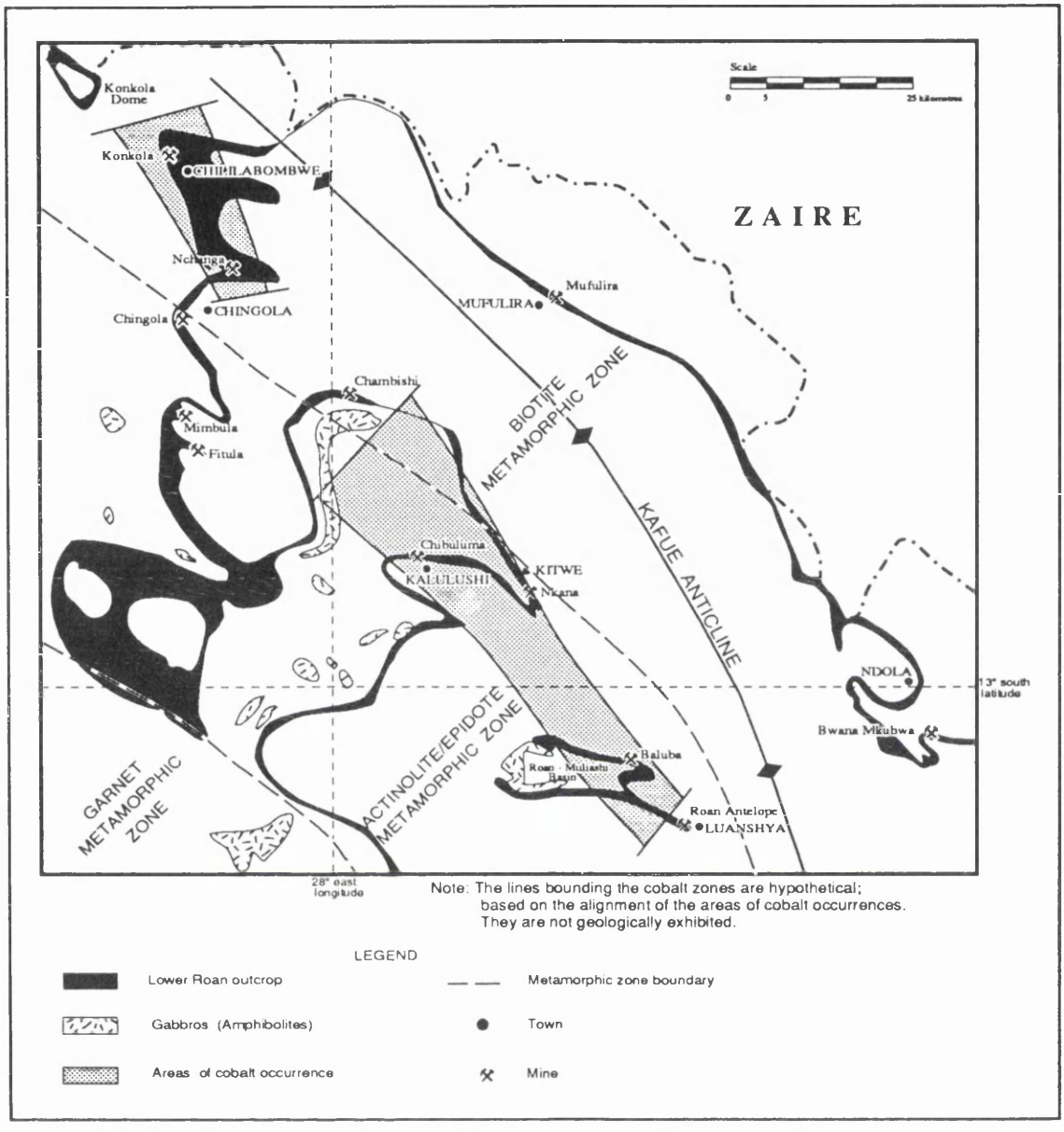

Figure 2.4: Metamorphic zones and areas of cobalt occurrences on the Zambian Copperbelt (After Annels and Simmonds, 1984)

2.2.4 Metalliferous mineralisation

The Copperbelt deposits are essentially iron-, copper- and cobalt-sulphide deposits with local secondary oxidation. The sulphides are disseminated through the host rocks and are also concentrated along bedding and schistosity planes and also occur in massive form in veins. The

principal copper sulphide mineral is chalcopyrite and cobalt occurs in the form of carrollite. Pyrite is the commonest sulphide in the hangingwall formations. Some of the pyrite is cobaltiferous.

Oxidation and leaching of the sulphides is common up to about 50 to 60 metres below the surface. In most deposits there is local partial oxidation to depths of over 800 metres below the surface. The main supergene minerals are malachite, chalcocite, cuprite and chrysocolla.

2.2.5 Metamorphism

Metamorphism of the Copperbelt rocks is associated with the Lufilian Orogeny (see Fig. 2.1). The common mineral assemblage in the Copperbelt rocks is:

quartz + feldspar + carbonates (calcite/dolomite) ± micas (biotite/muscovite/sericite) ± amphiboles (tremolite/actinolite) ± epidote ± chlorite ± sulphides (pyrite + chalcopyrite + bornite + chalcocite).

The host rock mineralogy characterised by the co-existence in equilibrium of the minerals chlorite, epidote, tremolite/actinolite and biotite indicates that the rocks have undergone a low grade greenschist facies metamorphism. A pervasive schistosity has developed in the dolomitic/tremolitic rocks and scapolitisation is common in the argillites.

Metamorphism is estimated to have taken place at temperatures of around 200°C and pressures of about 6kb. The metamorphic grade increases westward and southwestward of the Copperbelt, reaching the garnet facies in the south west part of the Copperbelt (see Fig. 2.4).

2.2.6 Zonation

The concept of zonation of the Copperbelt deposits into metallic mineral groups is envisaged within the context of the sedimentary precipitation of the minerals by Garlick (1953, 1964, 1989) and is supported by Mendelsohn (1989). Renfro (1974) and Brown (1992) explain the zonation using a diagenetic model of ore formation.

The zonation can be explained by the chemical reactions within the Cu-Fe-S-O-H system. The sulphides can be considered to have initially precipitated from solution at ambient temperature and pressure conditions (around 25°C and less than 1kb) during the deposition of the sediments in shallow basins. The deposition is assumed to have been in a reducing and alkaline environment and that there was an excess supply of sulphide provided through the bacterial reduction of sulphate. Bass Becking

and Moore (1961) state that the anaerobic bacterium *desulphovibrio desulpfuricans* is the chief agent for the reduction of sulphates. They demonstrated that in natural present-day environments complex metallic sulphides could be precipitated by sulphate reduction starting from simple copper and iron sulphides .

Roberts (1963) identified chalcopyrite as a product of the reactions between Fe^{2+} and Cu^{2+} sulphides at low temperature, provided Fe^{2+} and Cu^{2+} were in approximately equal molarities. In solutions with excess copper chalcopyrite was replaced by bornite, covellite and chalcocite. It has been suggested that at low temperatures and in an alkaline environment chalcopyrite would form via reactions between precursor iron sulphides and dissolved copper salts (Zeiss *et al.*, 1916; Cowper and Rickard 1989) . With increasing temperatures during the regional metamorphism (to around 200°C), and in the presence of excess copper, the precursor iron sulphides and chalcopyrite react to form chalcocite, bornite and covellite A possible series of reactions involved is presented in Table 2.1.

A block model showing the zonation of the Copperbelt deposits into primary copper sulphides is illustrated in Figure 2.5. In general the zoning pattern from the shoreline seawards (and from the footwall upwards) is chalcocite through bornite and chalcopyrite to pyrite.

Primary copper sulphide minerals:	barren →	chalcocite →	bornite →	covellite →	chalcopyrite →	pyrite
		Cu_2S	Cu_5FeS_2	CuS	$CuFeS_2$	FeS_2
Lateral Zonation	*Nearshore*	----------	----------	----------	---------- →	Offshore
Vertical Zonation	*(Footwall)*					*(Hangingwall)*

The copper oxides and native copper shown in the zonation model for Baluba which occur close to the footwall (see Fig. 1.2) were late redox products of the primary sulphides.

Table 2.1: Zonation in the Copperbelt orebodies explained by the possible chemical reactions involved in the precipitation of the primary copper sulphides.

(a) Sedimentary deposition phase: Initial formation of metastable iron sulphides and chalcopyrite at low temperatures (<100°C).

(i) $Fe^{2+} + 2S^{2-} \longrightarrow FeS_2$

(ii) $Cu^{2+} + FeS_2 \longrightarrow CuFeS_2$

(b) Regional Metamorphic phase: Precipitation of coper and iron sulphides at increased temperatures and pressure (100-200°C, ~6kbar)

(iii) $CuFeS_2 + Cu^{2+} \longrightarrow Cu_2S + FeS$

FeS unstable in the presence of excess sulphur and is converted to FeS_2

(iv) $5Cu_2S + 2FeS_2 \longrightarrow 2Cu_5FeS_4 + FeS$

(v) $Cu_5FeS_4 + 2FeS_2 \longrightarrow 2CuFeS_2 + FeS + 3CuS$

(vi) $FeS + S^{2-} \longrightarrow FeS_2$

Pyrite crystallises as the copper becomes depleted

Decreasing availability of copper

Constant supply of sulphur

FeS = pyrrhotite
FeS_2 = pyrite
$CuFeS_2$ = chalcopyrite
CuS = covellite
Cu_5FeS_4 = bornite
Cu_2S = chalcocite

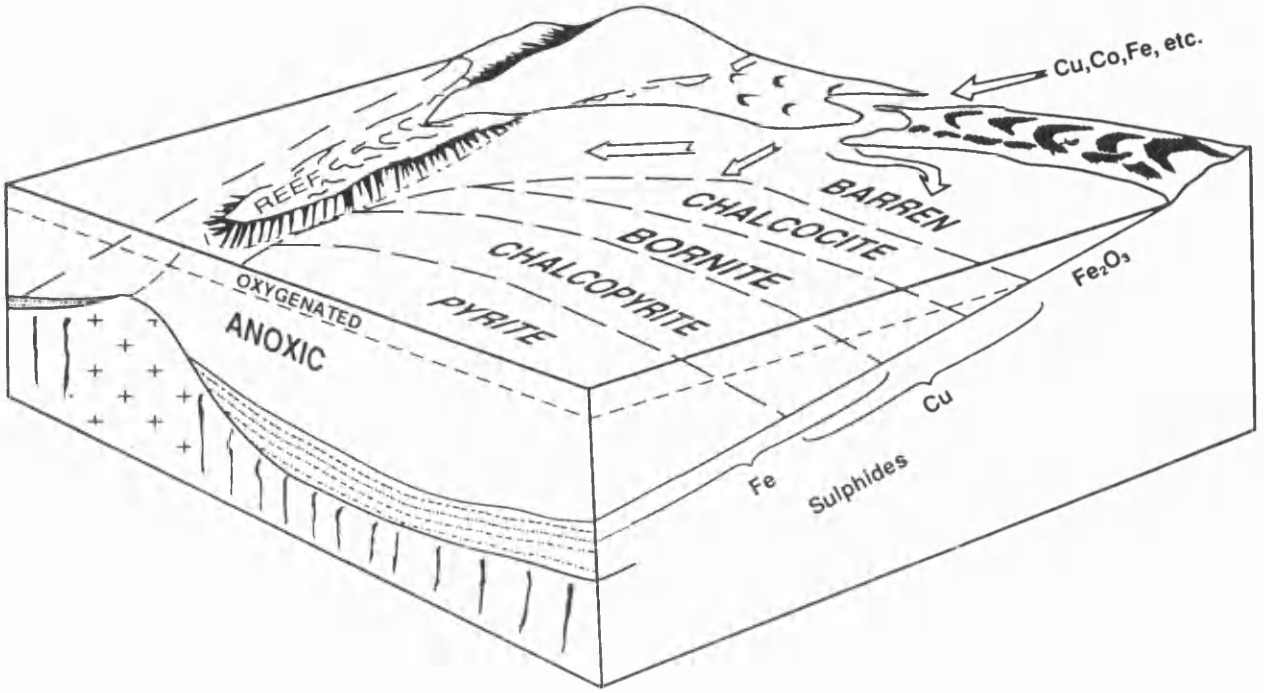

Figure 2.5: Lateral and vertical zonation of the primary copper and iron sulphides explained in the syngenetic model of ore genesis. (After Garlick, 1976).

2.2.7 Ore genesis

Models of ore genesis for the Copperbelt span the whole range from syngenetic through to epigenetic and are described below.

Syngenetic model

The earliest proponents of the syngenetic explanation for the genesis of the Copperbelt copper and cobalt mineralisation were Schneiderhöhn (1932) and Lindgren (1933). Schneiderhöhn likened the Copperbelt deposits to those of the Central European Kupferschiefer mineral province. Lindgren proposed a theory of sedimentary ore deposition, with subsequent low grade metamorphism. Extensive work based on the syngenetic model was undertaken by Garlick (1953, 1964, 1989), and Garlick and Fleischer (1972).

In the syngenetic model it is envisaged that iron, copper and cobalt metals were derived by erosion from the provenance area and that the conversion of metals to metal sulphides was aided by bacterial reduction of sulphates to sulphides induced at low Eh and high pH conditions. Deposition took place in shallow sea water in the shelf zone. For such large volumes of metal to have been deposited, the erosion of a large area of the basement with normal crustal geochemical abundances of copper (and cobalt) would be required. Alternatively, a smaller hinterland which had metalliferous lodes already enriched above geochemical background levels in copper (and cobalt) could provide the required metals (Garrard, 1972).

In the syngenetic model it is generally acknowledged that the primary mineralisation was later affected by metamorphic events, but it is argued that metamorphism in itself was not part of an ore forming process.

Diagenetic model

The diagenetic model to account for genesis of the Copperbelt ores has been suggested by Renfro (1974) and has also been favoured by Brown (1984, 1992). Renfro considers the process of sabkha (salt lake) formation as a modern equivalent for the introduction of the metals into the Copperbelt deposits. During sabkha formation precipitation takes place in unconsolidated sediments at the margins of large bodies of water with a water table close to the surface. Evaporation creates a hydraulic pressure, causing the sea water and terrestrial water to simultaneously flow towards the sabkha. The terrestrial water contains dissolved metals which are precipitated at the sea-land fringe. In the diagenetic model precipitation of the sulphides takes place at the oxidation/reduction interface, referred to by Brown (*op. cit.*) as a *redoxcline*.

Epigenetic model

Bancroft and Pelletier (1929) proposed that mineralisation on the Copperbelt was epigenetic. Gray and Parker (1929) stated:

> *"..... it appears that the copper was introduced into the rock after its formation and probably after it had been folded."*

In the epigenetic model granite magmatism is regarded to be the most likely source of the metals. The metals are inferred to have been carried in magmatic hydrothermal solutions which were enriched in copper and cobalt. The support for the epigenetic explanation is the proximity of copper

deposits to the intrusive granites (see Fig. 2.2). Bateman (1930) noted that the association between granites and mineralisation was not just coincidental but had implications to the genesis of ore mineralisation.

Later proponents of epigenesis have suggested that the restriction of cobalt mineralisation to narrow, structurally controlled zones (see Fig. 2.4) can be explained by cobalt being derived from basic hydrothermal solutions ascending rift structures (Raybould, 1978; Annels, 1984). There is an apparent close spatial relationship between the gabbros (amphibolites), which are intrusive into the Upper Roan, and the cobalt mineralisation in the underlying Lower Roan.

Comment on the ore genesis models

The syngenetic model of deposition is generally accepted amongst the practising mine geologists on the Zambian Copperbelt and is favoured by the author. The main argument for the syngenetic model is that there is generally no evidence that there has been addition of new elements [metasomatically] into the sediments after the primary sedimentation. The concept of metal-bearing fluids generated from a granite magma as being the source of the metals as suggested in the epigenetic model is not convincing given that all the granites have been dated to be older than the mineralised Lower Roan sediments (Garlick and Brumer, 1951; Cahen, 1970; Drysdall *et al.*, 1972) and therefore magmatism was pre-deposition. The sulphide minerals in the veins of the Lower Roan sediments were introduced by lateral secretion from adjacent wall rocks. The veins acted only as local channel ways for the mineralising solutions. There are few faults on the Copperbelt (see Fig. 2.2) and there is no evidence of faulting having provided channel ways for the transportation of mineralising solutions.

2.3 BALUBA AREA GEOLOGY

2.3.1 Structural Setting

The Baluba deposit is part of the Roan-Muliashi Basin, an east-west trending synclinorium on the western side of the Kafue Anticline (see Fig. 2.2). The Roan-Muliashi synclinorium extends northwards to form a subsidiary Baluba synclinorium (Fig. 2.6(a)). The Baluba deposit has a plan length of approximately 3km and a width of about 1½km. Like the overall Copperbelt structural trend, the Baluba deposit structure was formed mainly in response to the Lufilian Orogeny. Davis (1954) explains that the deformation of the Roan-Muliashi sediments was essentially plastic in character. The Baluba synclinorium is refolded into a synclinal and anticlinal structure containing

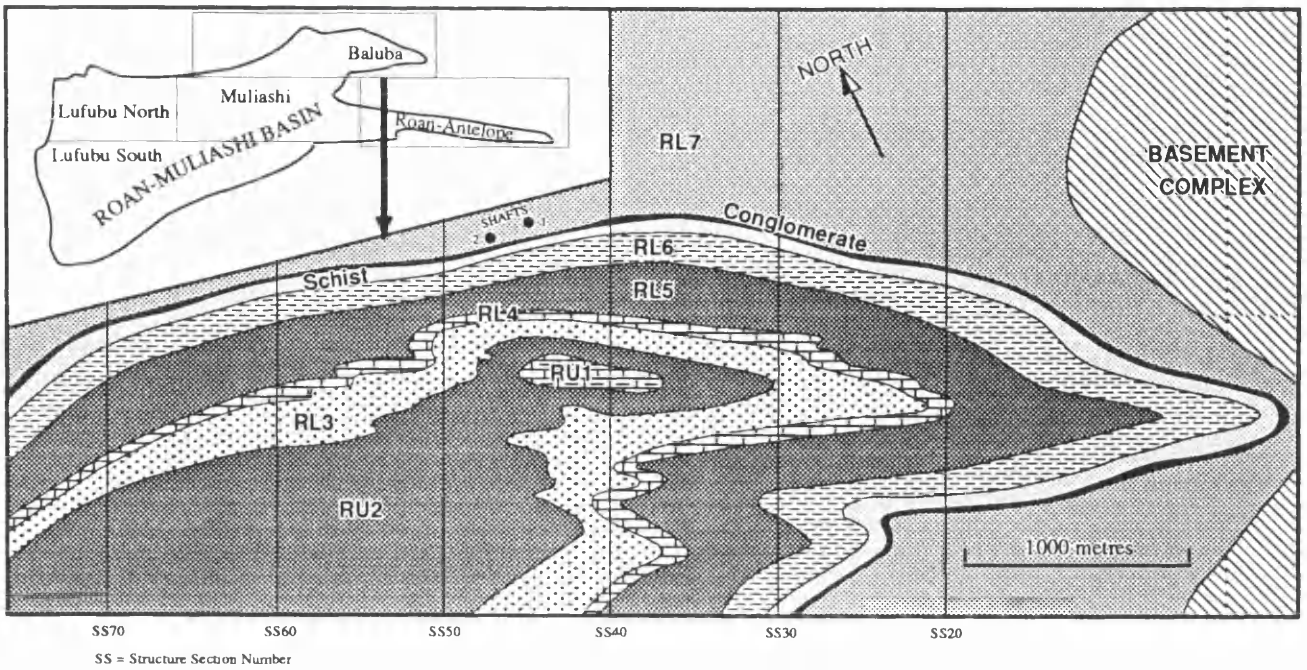

(a) Baluba: Generalised plan

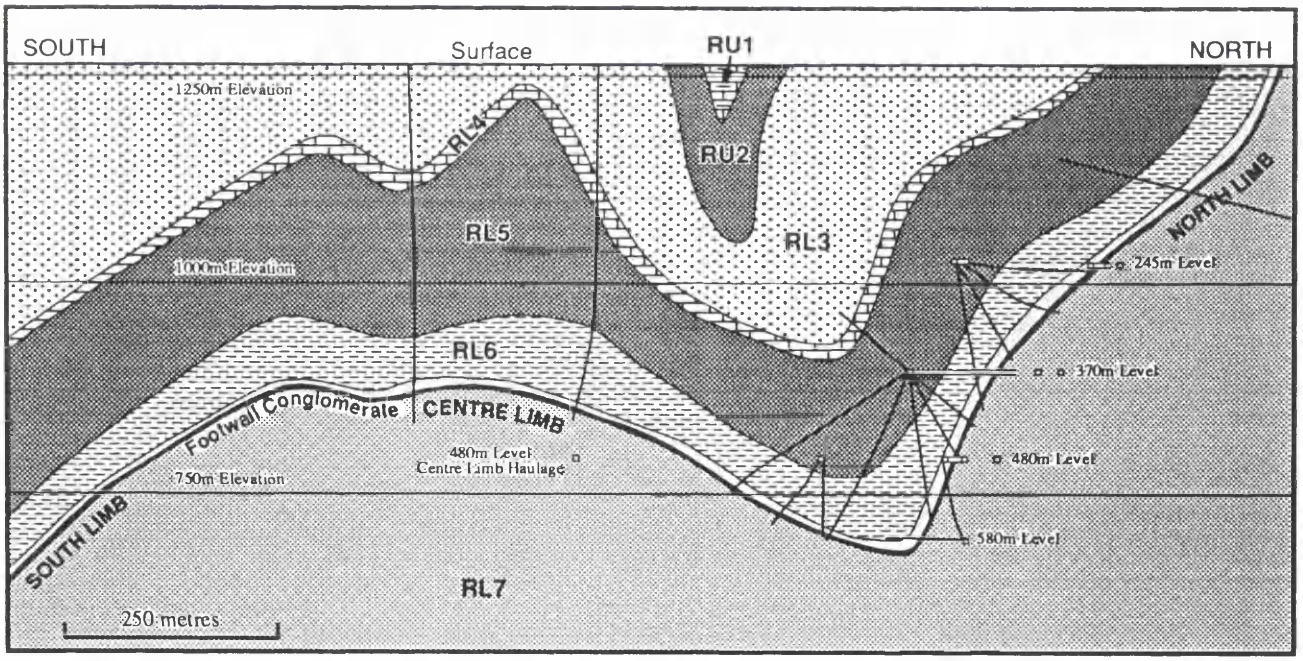

(b) Baluba: SS40 section

Figure 2.6: Geology of the Baluba area. (a) is the generalised plan of Baluba. (b) shows the cross section along Structure Section 40 (SS40 on the plan). The footwall conglomerate indicates the position of the base of the orebody.

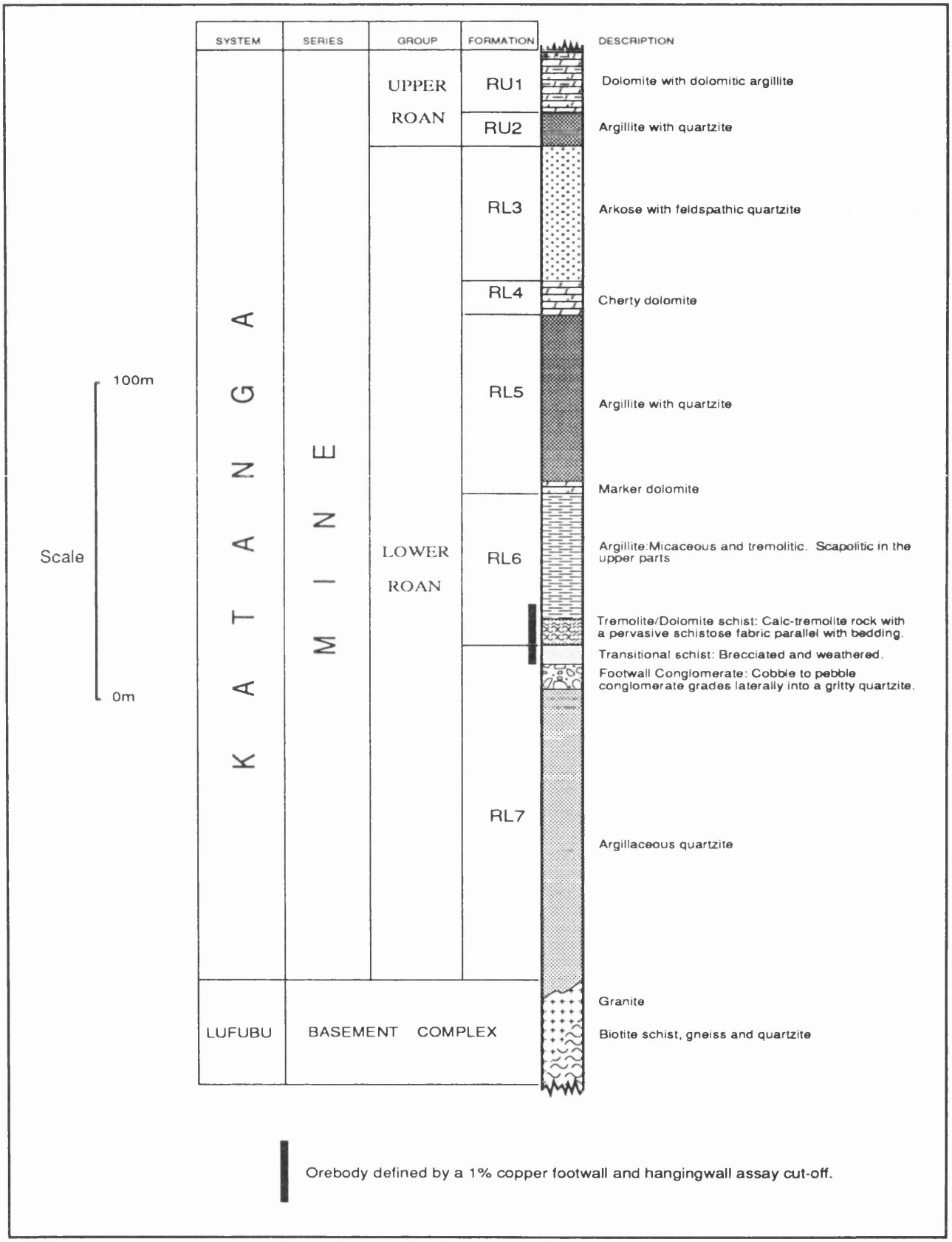

Figure 2.7: Stratigraphy of Baluba and nomenclature used to define the formations

three limbs; a steeply dipping north limb (with dips ranging from 50° to vertical) which flattens towards the centre limb (horizontal to 30° dips) and steepens again on the south limb (Fig. 2.6(b)). The shallowness of the dips in the Baluba Centre Limb can be seen in the plans and sections derived from mapping of underground development excavations (see Maps 1 to 7 in Appendix J). The Baluba synclinorium opens out from east to west, having a gentle north-west plunge of 10-20°. To the west and south the Baluba syncline merges into the Muliashi synclinorium of the main Roan-Muliashi basin. The deepest ore occurrence in Baluba is in the west, around structure section 55, on the north limb/centre limb trough at about 800m below the Baluba surface (500m elevation above sea level).

On the straighter, steep North Limb of Baluba the veins are commonly unfolded, but in the crest and trough areas of the Centre Limb the veins are ubiquitously dragfolded. Schistosity in the tremolite schists is concordant with bedding (see Maps 2 and 3 in Appendix J). No mesoscale faulting is observed in Baluba but occasionally small scale faults (with throws of centimetre scale) have been noted in underground development exposures (see Map 9 in Appendix J).

2.3.2 Stratigraphy

The rocks present in the Baluba area fit the general Copperbelt stratigraphy. The footwall sediments comprise quartzites, sandstones and conglomerates and lie unconformably over the Basement granites and gneisses. The copper and cobalt mineralisation is hosted in calcareous tremolitic schists and argillites. At the base of the orebody the schist is auto-brecciated and there is leaching and oxidation. The schist in this leached and oxidised section of the orebody is referred to as the transitional schist. The hangingwall formations comprise argillites, quartzites and dolomites. The Baluba stratigraphy is illustrated and described in Figure 2.7.

2.3.3 Sedimentation as related to the structure

The granite domes were important in the control of the deposition of the Katanga sediments. The pre-Katanga granites formed protuberances between which the depositional basins formed and into which the sediments were deposited. Sedimentation was syn-orogenic.

The arenaceous, clastic sediments (conglomerates, quartzites) are confined to the footwall side of the mineralised bodies and rest against the old granites. The arenaceous nature of the footwall sediments

indicates that the source detrital material was subjected to little attrition suggesting that the sediments were not deposited far away from their source. The arenaceous sediments are located close to the granites which are the possible source of the detrital material from which they were formed. The argillaceous sediments are found on the hangingwall side of the mineralised bodies. The hangingwall sediments are much finer grained than the sediments close to the footwall. This suggests that they had undergone abrasion over longer distances and were therefore deposited farther from the source area.

2.3.4 Mineralisation and Zonation

The Baluba deposit comprises iron-, copper- and cobalt-sulphide mineralisation with local secondary oxidation. The principal copper-sulphide mineral is chalcopyrite and cobalt occurs mainly in the form of carrollite. Pyrite is the commonest sulphide mineral in the hangingwall argillites and some of the pyrite is cobaltiferous. There is ubiquitous secondary oxidation and enrichment of the primary sulphides in the transitional schist. The metallic mineralisation occurs as disseminated grains in the schists and argillites and also as massive mineralised veins, mainly in the argillites (see Maps 8, 9 and 10 in Appendix J). The orebody defined by 1% copper footwall and hangingwall is about 10m to 15m thick. Zonation with reference to the Roan Antelope and Baluba orebodies has been addressed by Davis (1954), Brummer (1955), Mendelsohn (1962), Binda (1969) and Vink (1972).

From Figure 1.2, in Chapter 1, five metal mineral zones are identified, in a sequence from the footwall to the hangingwall, thus: (i) barren *footwall zone*, (ii) *mixed copper sulphide and copper oxide zone*, (iii) *Copper sulphide and cobalt sulphide zone*, (iv) *chalcopyrite and pyrite zone* and (v) *pyrite zone*. The mineralisation and grade variation associated with the zones are summarised in Table 2.2.

It is noted that the primary sedimentary zonation of the sulphide minerals has been maintained. The contacts between the zones are gradational and the zones commonly overlap. Vink (1972) explains the widths of the primary sulphide mineral zones to be a reflection of the Eh-pH conditions under which each metal sulphide phase was stable.

Table 2.2: Vertical zonation of the Baluba orebody into metal mineral groups. The relationship between the zones and copper-cobalt grade variation is highlighted (see also Fig. 1.2).

Zone	Lithology	Metallic mineral assemblage	Copper and cobalt grades	Mineralisation
Pyrite	Argillite	pyrite + chalcopyrite	0.05-1.5% TCu < 0.1% ASCu ~0.1% Co	Hangingwall
Chalcopyrite + pyrite	Argillite	chalcopyrite + pyrite + carrollite	1-2% TCu < 0.1% ASCu 0.1-0.2% Co	Orebody
Copper + cobalt sulphides	Tremolite Schist	chalcopyrite + bornite + carrollite	1-3% TCu < 0.1% ASCu 0.2-1.0% Co	
Copper sulphide + copper oxide	Transitional Schist	chalcocite + cuprite + native copper + malachite + chrysocolla + carrollite	> 2% TCu 0.1-0.2% ASCu 0.2-1.0% Co	
Footwall	Quartzites and Conglomerates	Copper and cobalt background mineralisation	< 0.5% TCu < 0.1% ASCu < 0.05% Co	Footwall

Tcu = Total copper ASCu = Acid soluble copper

N.B. The distinction between total copper and acid soluble copper is essentially based on the recoverability of copper in the mill. The acid soluble copper component is lost to tails (see Appendix C).

2.4 DISCUSSION

It has been noted in this chapter that the geology and stratigraphy of Baluba fit that common to the Copperbelt ore shale deposits on the western side of the Kafue Anticline. The Lufilian Orogeny is closely related to the formation of the fold structures in the Copperbelt deposits and it is also associated with the metamorphism. The ore genesis theories for the Copperbelt deposits span from syngenesis to epigenesis. The source of copper can readily be related to the Basement geochemistry but the source of cobalt remains questionable. The mineralisation in the Copperbelt deposits essentially comprises copper and cobalt sulphides. The main copper bearing minerals are chalcopyrite, bornite and chalcocite and the main cobalt-bearing minerals are carrollite and cobaltiferous pyrite.

The assay footwall in the Baluba deposit is found to be coincidental with the geological footwall contact between the conglomerates and schists. This contrasts with the assay hangingwall which has no corresponding geological contact and is currently determined based on the 1% copper assay cutoff.

The vertical zonation of the Baluba deposit into metallic mineral groups is noted. The variation of copper and cobalt grades is related to the mineral zones. The relationship between the lithostratigraphic nature of the orebody, mineral zonation and the related copper and cobalt grade variations are important in the demarcation of the orebody.

CHAPTER 3

PETROLOGY AND PARAGENESIS

3.1 INTRODUCTION

The copper and cobalt grade distributions observed in the Baluba Centre Limb rocks are controlled by the inherent mineralogical, structural and textural characteristics of the sedimentary depositional and subsequent diagenetic and metamorphic effects on the rocks. The zonation model presented in Chapter 1 (see Fig. 1.2) shows the distributions of the copper- and cobalt-bearing minerals within the different horizons of the orebody. In this section the relationships between the primary sulphide minerals will be assessed. The consequences of metamorphism on the sulphide mineral recrystallisation and paragenesis will also be addressed.

3.2 PETROGRAPHY AND METAMORPHISM

The petrography of the Baluba Centre Limb rocks is diagnostic of the epidote-amphibolite grade of metamorphism in the greenschist facies. There is an absence of the higher metamorphic grade minerals such as hornblende, kyanite or garnet (Garlick and Fleischer, 1972). The mineral assemblages of the Baluba Centre Limb rocks are summarised in Table 3.1.

Table 3.1: Mineral assemblages of the Baluba Centre Limb rocks.

Quartzite / conglomerate	Rock forming minerals:	Qtz+KFeld+Micas+Trem+Epid+Rut
	Metal bearing minerals:	*Non-visible copper- and cobalt-bearing minerals
Schists	Rock forming minerals:	Calc/Dol+Trem+Micas+KFeld+Plag+Epid+Chl
	Metal bearing minerals:	Cpy+Bn+Cov+Cc+Car+Cup+Mal+Nat.Cu
Argillites	Rock forming minerals:	Micas+Trem+KFeld+Scap+Epid+Sphene+Chl
	Metal bearing minerals:	Py+Cpy

Qtz=quartz, KFeld=alkali feldspar, Trem=tremolite, Epid=epidote, Rut=rutile, Calc=calcite, Dol=dolomite, Plag=plagioclase, Chl=chlorite, Cpy=chalcopyrite, Bn=bornite, Cov=covellite, Cc=chalcocite, Car=carrollite, Cup=cuprite, Mal=malachite, Nat.Cu=native copper, Py=pyrite

* No copper- or cobalt-bearing minerals were observed in the quartzites or conglomerates. The copper and cobalt mineralisation in the footwall is most likely due to solid solutions of copper and cobalt in silicates.

Footwall Conglomerate

The conglomerate has a pinkish grey colour. The clasts are of a cobble to pebble size and comprise quartz and quartzite. The clasts are sub-spherical, rounded and are moderately sorted. The matrix consists mainly of medium grained, granular quartz, calcite/dolomite, potassic feldspars, biotite, and tremolite. Rutile occurs as an accessory mineral. The potassic feldspars noted in the Baluba Centre Limb rocks are mainly orthoclase and microcline (Plate 3.1(a)). The plagioclase feldspar is rarer than the alkali feldspars and occurs as albite. In underground exposures, drill cores, hand specimens and under the petrographic microscope the conglomerates appear devoid of metallic mineralisation (see Plates 3.1(a) and 3.6).

Schists

The schists are light-greenish grey, the greenish tinge being due to the presence of the green mica and amphibole minerals. Calcite±dolomite, amphibole and micas are the prominent minerals in the schists. Feldspar and epidote also occur in minor amounts and the feldspars occur in both the potassic and plagioclase forms (Plate 3.1(b)). The principal mica mineral is a brown biotite (Plate 3.2(a)) and some muscovite is also common. The schists are generally medium grained but where fine grained the micas occur as sericite. In the proximity of the footwall contact the schists are brecciated and leached. This section of the schists is referred to as the transitional schist. It is more siliceous than the rest of the schist lithology.

The schist lithology is the principal host of copper and cobalt mineralisation. The primary metallic sulphide mineral phases in the tremolite schist are the copper-bearing chalcopyrite, bornite and chalcocite and the cobalt-bearing carrollite. The sulphide minerals occur as disseminated grains in the groundmass and along schist partings. In the altered transitional schists there is secondary oxide mineralisation and sulphide enrichment. The metallic minerals in transitional schists occur as secondary chalcocite and covellite, malachite and chrysocolla. Native copper plates (centimetre wide on average and up to about 1m wide) also occur in the transitional schists.

Argillites

The argillites are grey to black and fine grained. They comprise micas, tremolites, feldspars, quartz and accessory amounts of epidote and sphene. Scapolite occurs as conspicuous white porphyroblasts in the upper sections of the argillites (Plate 3.3). The metallic mineralisation in the argillites consists

of chalcopyrite and pyrite which occur as fine grained disseminated grains in the groundmass and also in the massive form along the veins.

3.2.1 Effects of metamorphism

The structure and metamorphism of Baluba are both intimately related to the Lufilian Orogeny. Folding is the main structural feature of the Baluba Centre Limb as discussed in Chapter 2. In the rocks of the Baluba Centre Limb the primary macroscale sedimentary structures such as bedding and cross-bedding have generally been preserved and metamorphic induced features have been superimposed onto these structures.

The footwall conglomerates are massively bedded and show little macroscale metamorphic textural effects. In the calcic rocks there is a pervasive schistosity texture (Plates 3.4(a), 3.4(b)) and a weak schistose fabric is displayed in parts of the argillite. The schistosity is concordant with bedding and there is a tendency of the schistosity to a gneissose texture in parts of the tremolite schists (Plate 3.4(c)) indicating an increase in the metamorphic grade. Metamorphic veins are prominent in the argillites and the veins are ubiquitously dragfolded (Plates 3.5(a), 3.5(b)). In the argillites there is a development of an axial planar cleavage.

Recrystallisation

Recrystallisation of the metallic as well as silicate mineral phases is clearly exhibited in the Baluba Centre Limb rocks and indicates the equilibration of the minerals in response to metamorphism. In the conglomerates the quartz grains generally occur in a polycrystalline form and under the microscope exhibit undulose extinction indicating that the conglomerates have undergone stress due to metamorphism (see Plates 3.1, 3.6). The quartz grain boundaries commonly display triple junctions indicating re-equilibration due to metamorphism (Plate 3.6). Twinning and alteration of the feldspars is common (Plates 3.1, 3.6).

The amphibole mineral in the Baluba Centre Limb rocks is of a tremolite-actinolite type. Tremolite appears to have formed after dolomite (Plate 3.7(a)).

$$10(Ca,Mg)CO_3 + 8SiO_2 + H_2O \text{ -------} \rightarrow Ca_2Mg_5Si_8O_{22}(OH)_2 + 3CaCO_3 + 7CO_2$$

Dolomite Quartz Tremolite Calcite

Tremolite commonly occurs in its usual prismatic form but some of the tremolite has been altered to a fibrous, asbestos form (Plate 3.7(b)). Some of the tremolites in schists exhibit an acicular form and exhibit undulose extinction (Plate 3.8) indicating that the rocks have undergone some metamorphic stress. Some biotites have broken down to a green chlorite (see Plate 3.2(b)).

The sulphide minerals show both cataclastic and plastic responses to metamorphic stress. The brittle, euhedral carrollite crystals, for example, display cataclastic fracturing while the copper sulphides show a plastic response with the mineral elongation aligned with the schistosity direction (Plates 3.9(a), 3.9(b)). The copper-sulphide minerals are overprinted by later metamorphic minerals - tremolite, biotite, rutile, sphene - (Plates 3.10(a), 3.10(b)) indicating that the sulphide mineral formation was pre-metamorphic.

Metamorphic veins

Recrystallisation of rock forming and metallic minerals into veins is common. Two types of metamorphic veins are identified in the Baluba Centre Limb:

(i) Continuous veins which are concordant with bedding. These are commonly dragfolded and are filled with calcite/dolomite, quartz, tremolite/actinolite and the sulphide minerals (see Plate 3.5(a) and Maps 9, 10 in Appendix J)

(ii) Discordant veins which have their longest dimension parallel to the fold axis. They are straight, usually narrower than the continuous veins and cut perpendicularly across the beds. The discordant veins are commonly filled with pink microcline feldspar (Plate 3.11).

The mineral constituents of the veins are all found in the immediate surrounding country rock as well. This suggests that there has been no addition of new elements metasomatically to alter the primary mineralogy and that the minerals which recrystallised in the veins were not transported from afar. Rather, the minerals were locally recrystallised into the veins by lateral secretion from the immediate country rock during metamorphism (Brummer, 1955; Mendelsohn, 1961; Vink, 1972).

3.3 METALLIFEROUS MINERAL PHASE RELATIONSHIPS AND PARAGENESIS

The co-existing sulphide mineral phases in the Baluba Centre Limb can be seen in Figure 1.2 and are tabulated in Table 3.1. Table 3.2 gives the key petrographic features observed in the Baluba Centre Limb rocks that have been used to ascertain the paragenesis of the primary sulphide minerals.

Table 3.2: Paragenetic relationships of the metallic sulphide minerals in the Baluba Centre Limb deposit.

Sulphide mineral	Co-existing mineral assemblages	Features	Crystallisation	Illustrations
Chalcopyrite	cpy + py + bn + car ± cc/cov	- subhedral crystal form - cpy is replaced by bn - cpy and bn occur in mymmerkitic exsolution - cpy replaces car - cpy is replaced by cov	- cpy crystallisation earlier than cov - Some cpy earlier than bn but some contemporaneous with bn (in solid solution) - cpy crystallisation later than car	- Plate 3.12(a) - Plate 3.12(b) - Plate 3.13(a) - Plate 3.13(b)
Bornite	bn + cpy ± car ± cc/cov	- subhedral to anhedral crystal form - bn replaces cpy - bn and cpy occur in mymmerkitic exsolution - bn is replaced by cc	- Some bn later than cpy but some contemporaneous with cpy (in solid solution) - bn crystallisation earlier than cc	- Plate 3.12(a) - Plate 3.12(b) - Plate 3.13(b)
Covellite	cov + cpy ± bn	- subhedral to anhedral crystal form - cov replaces cpy	- cov crystallisation later than cpy	- Plate 3.13(a)
Chalcocite	cc + bn ± cpy	- subhedral to anhedral crystal form - cc replaces bn	- cc crystallisation later than bn	- Plate 3.13(b)
Pyrite	py + cpy ± car	- Always as euhedral cubic crystals - Does not replace any other mineral phase	-Early crystallisation	-Plate 3.14
Carrollite	car + cpy ± bn	- euhedral crystal form - car is replaced by cpy	- car crystallisation earlier than cpy	- Plate 3.12(a) - Plate 3.15

Abbreviations:
py = pyrite, car = carrollite, cpy = chalcopyrite, bn = bornite, cov = covellite, cc = chalcocite

Plate 3.1: Feldspar minerals

The feldspar in the Baluba Centre Limb rocks is mainly the alkali type (orthoclase and microcline). Plagioclase is rare and where it occurs it is always associated with the alkali feldspars.

(a) Transmitted light photomicrograph (a) shows microcline in the centre of the field with typical cross hatched 'tartan' twinning. The other minerals in the photo are quartz, pink carbonate near the right edge and small biotite grains displaying high birefringence colours. Sample CK6496; Conglomerate. Crossed polars. Width of field = 1.7mm.

(b) Transmitted light photomicrograph (b) shows feldspar in three forms: simply twinned orthoclase feldspar (Orth), multiple twinned plagioclase (Plag) and cross hatched twinned microcline (Micr). Width of field = 0.42mm. Crossed polars. Sample CK6498; Tremolite Schist. Width of field = 0.42mm. Location of both (a) and (b): 470m block A, crosscut 10 (see Map 11 in Appendix J).

Plate 3.1

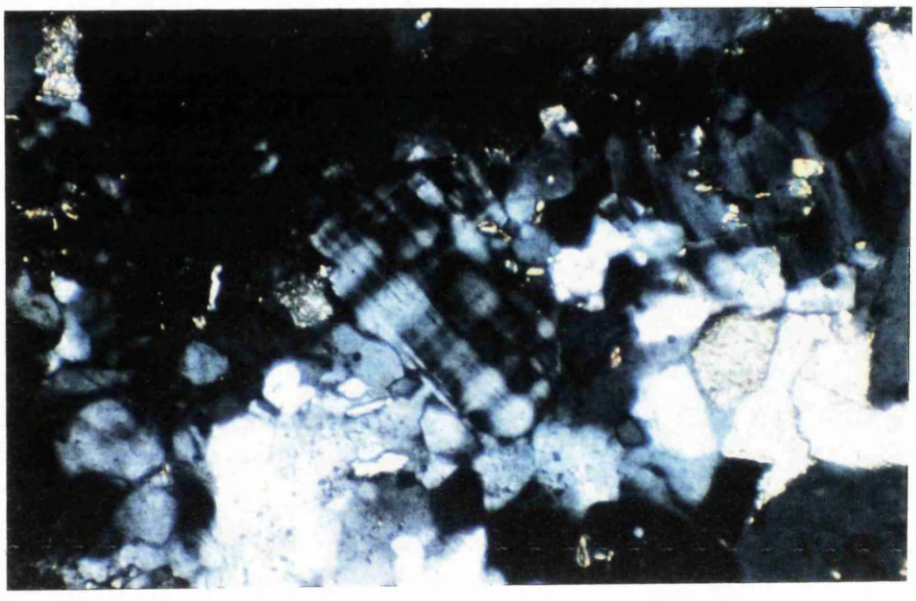

(a)

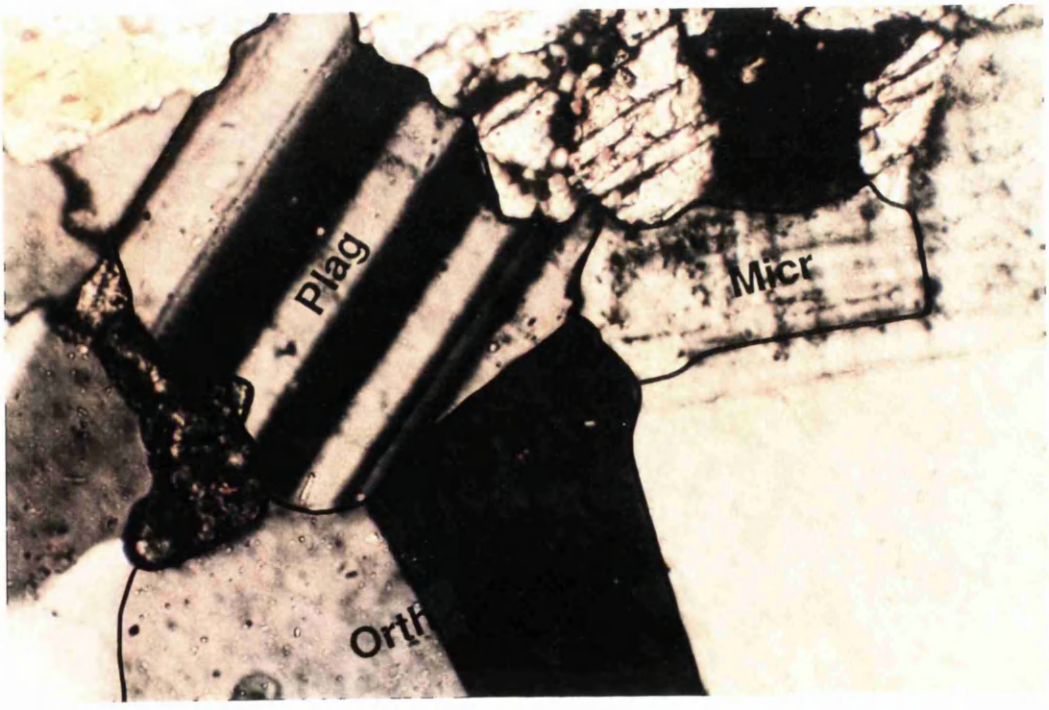

(b)

Plate 3.2: Metamorphic minerals - Biotite

In the transmitted light photomicrograph (a) two generations of biotite are recognised. The early biotites are aligned with schistosity while the late metamorphic biotites cut across the schistose fabric. The early biotites are also cut by the hexagonal epidotes (Epid). The opaque minerals are chalcopyrite and pyrite. Sample CK6487; Argillite. Plane polarised light. Width of photo view is 1.7mm. 463m block A, crosscut 2.

In transmitted light photomicrograph (b) biotite is seen to have been altered to chlorite (Chl), the latter which is characterised by its fibrous form and pronounced green pleochroism. The remnant dark biotite pleochroic haloes are evident. Other minerals in this field are carbonates (calcite/dolomite) and the opaque mineral is chalcopyrite. Sample CK6500; Tremolite Schist. Plane polarised light. Width of photo view is 1.7mm. Location: 470m block A, crosscut 10 (see Map 11 in Appendix J).

Plate 3.2

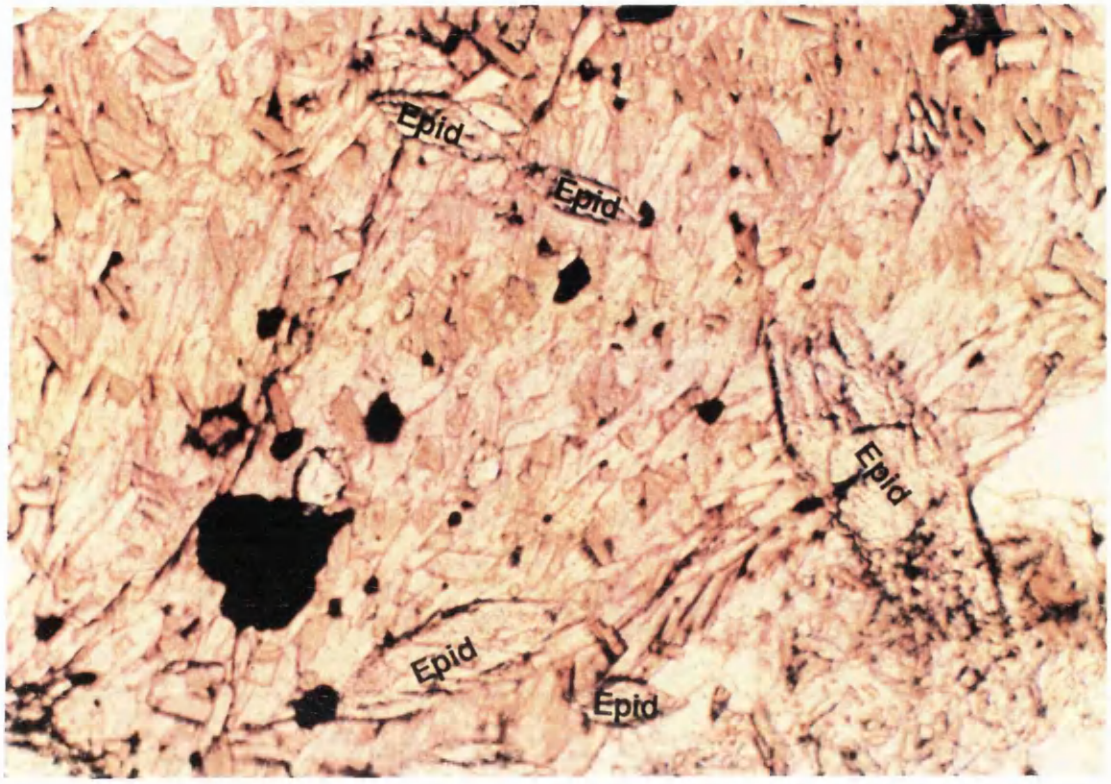

(a)

(b)

Plate 3.3: Metamorphic minerals - Scapolite

Photograph (a) of the hand specimen shows white scapolite porphyroblasts in a dark grey to black biotitic groundmass in argillite. The scapolite porphyroblasts give the rock a distinct spotted texture. Sample CK5886. 470m block A haulage.

Transmitted light photomicrograph (b) shows two late, metamorphic scapolite porphyroblasts clustered with inclusions of earlier biotite and the opaque pyrite. The porphyroblasts are set in a biotite matrix. Sample CK6487; Argillite. Crossed polars. Width of view = 4.4mm. 463m block A, crosscut 2.

Plate 3.3

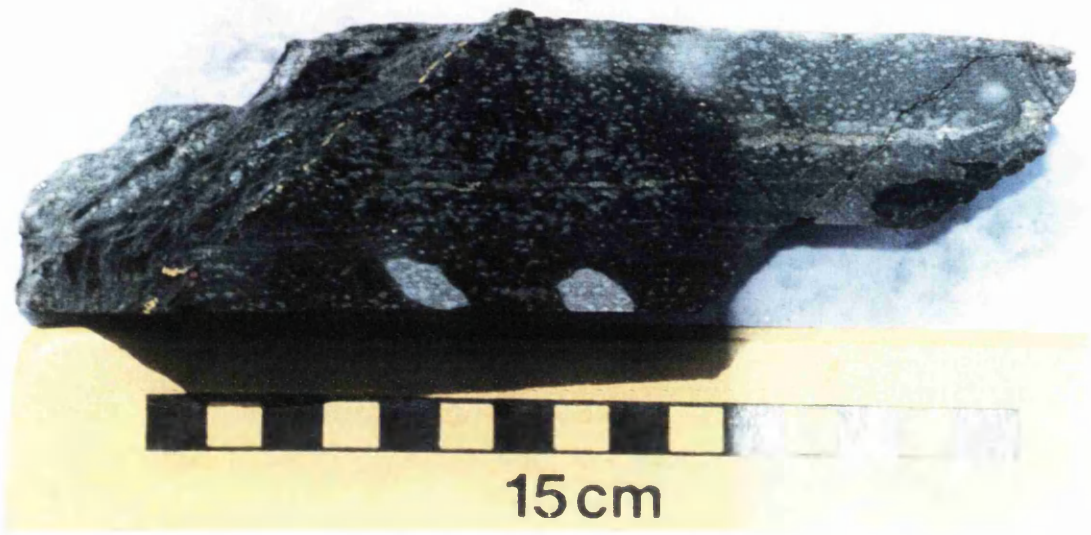

(a)

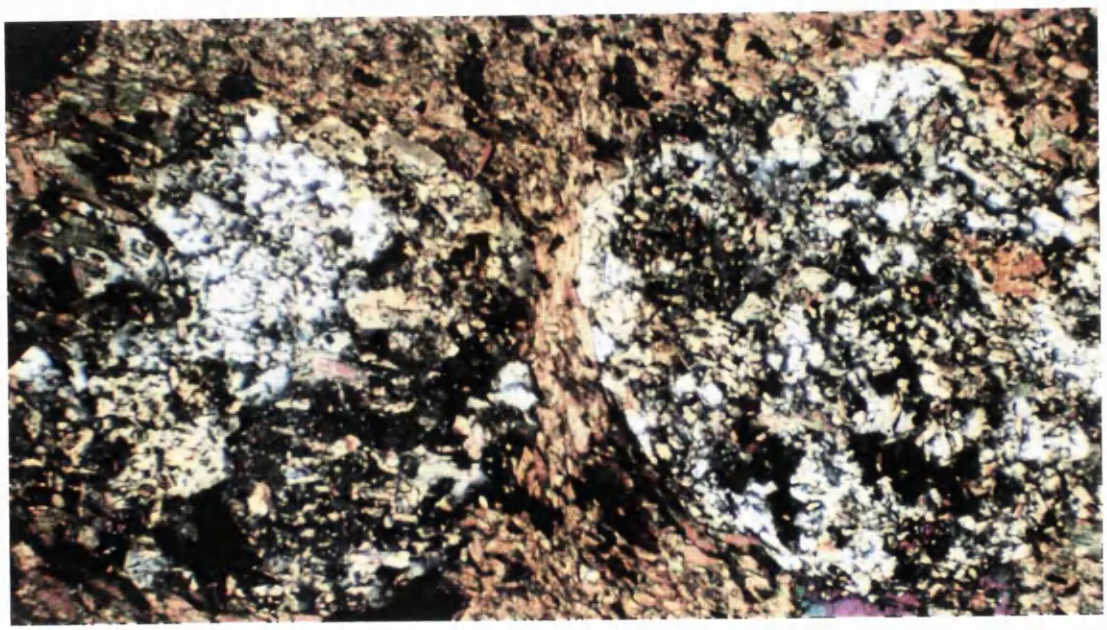

(b)

Plate 3.4: Metamorphic textures in calc-tremolite schist.

(a) Tremolite schist overlain by argillite. The schistosity in the tremolite schist is concordant with bedding. Photograph taken looking north-westward (335 °). Location: 490m block K, SS48 Vent Raise Crosscut. (See Map 9 in Appendix J for the geological section of the 490m block K, SS48 Vent Raise sidewall).

(b) Schistosity defined by the segregation of black, flaky biotite bands from green tremolite bands. Disseminated yellow chalcopyrite grains are evenly distributed in the rock. Sample CK5892; Tremolite Schist. Hand specimen. Location: 490m block K, SS48 Vent Raise Crosscut (see Map 9 in Appendix J).

(c) Schistose texture tending to gneissosity. The light green tremolite bands become discontinuous in the centre of this hand specimen displaying a pseudo-augen gneiss texture. Massive chalcopyrite (yellow) mineralisation is noted. Some chalcopyrite has been replaced by purple/blue bornite; seen on the right hand side of the specimen. Specimen CK5885; Tremolite Schist. Hand specimen. Location: 470m block A, haulage.

Plate 3.4

(a)

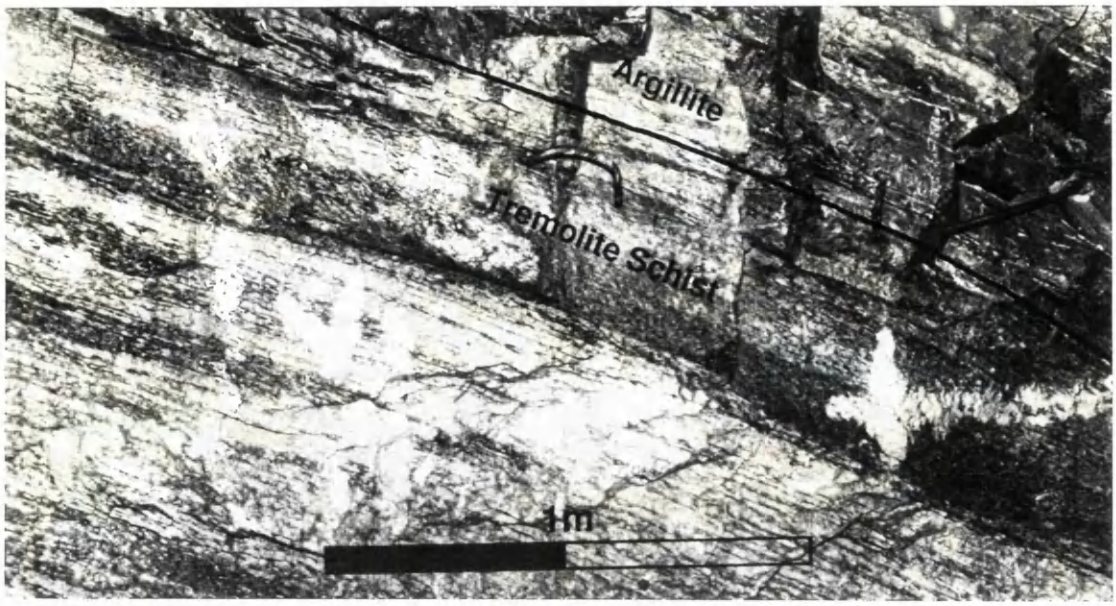

(b)

(c)

Plate 3.5: Dragfolding in argillite.

In photograph (a) the calcite filled veins in argillite are dragfolded. The folds are concordant to the bedding direction. Photograph taken looking south-eastward (165°). Location: 475/463m block A, Access crosscut.

Photograph (b) shows dragfolding seen on a smaller scale in a hand specimen. Massive chalcopyrite is restricted to the calcite vein while in the groundmass chalcopyrite occurs as disseminated grains. The segregation of mineralisation into the massive form associated with metamorphic recrystallisation affects the grade distribution within the orebody. Specimen CK588; Argillite. Location: 475/463m block A, access crosscut (see Map 8 in Appendix J).

Plate 3.5

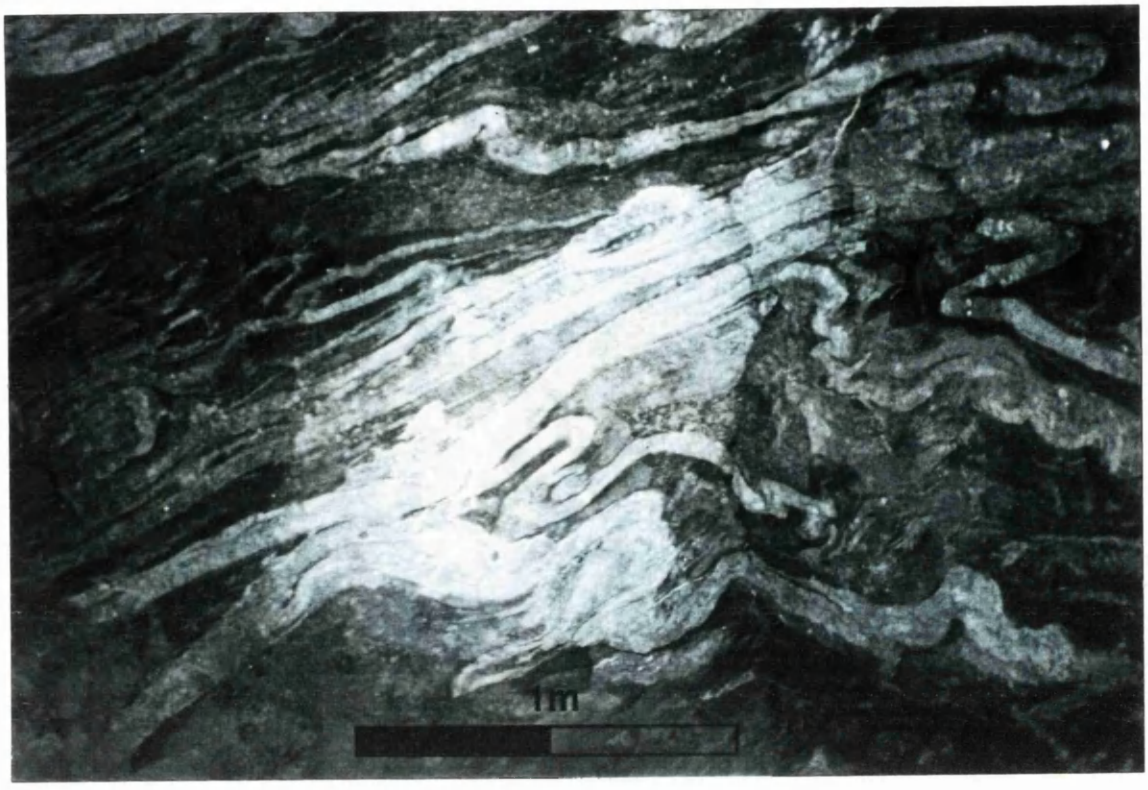

(a)

(b)

Plate 3.6

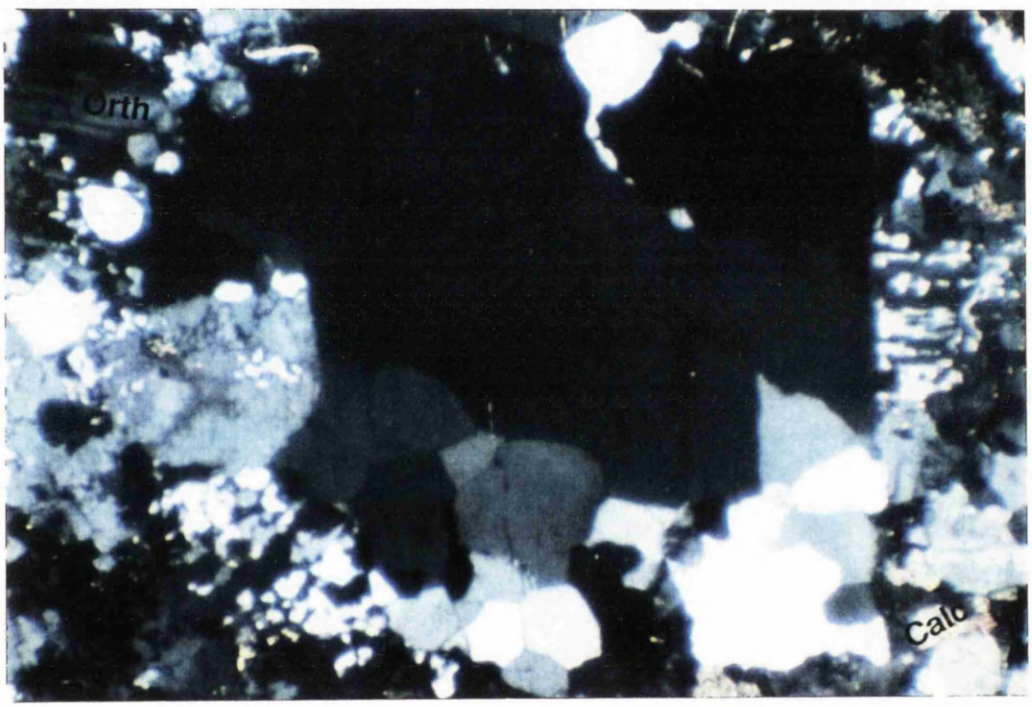

Plate 3.6: The pervasive effect of metamorphism is clear in this photomicrograph. Polycrystalline quartz exhibits triple junctions which are indicative of re-equilibration due to metamorphic recrystallisation. Other minerals in this section are microperthite feldspar (Orth), small brown biotites, Calcite (Calc) and small tremolite laths. Sample CK6496; Conglomerate. Width of field = 4.4mm. Location: 470m block A, crosscut 10 (see Map 11 in Appendix J).

Plate 3.7: Tremolite - Formation and alteration

Reflected light photomicrograph (a) shows dolomite (Dol) alteration to tremolite (Trem) in a dolomite vein. The opaque mineral is chalcopyrite. Sample CK5879. Crossed polars. Width of field is 4.4mm. Location: 475/463m block A, access crosscut (see Map 8 in Appendix J).

Reflected light photomicrograph (b) shows tremolite in its usual prismatic form on the right hand side. On the left side tremolite is observed breaking down into a fibrous form; tending to an asbestos type. Sample CK5887; Tremolite Schist. Crossed polars. Width of field is 1.7mm. Location: 490m block K SS48 vent raise crosscut (see Map 9 in Appendix J).

Plate 3.7

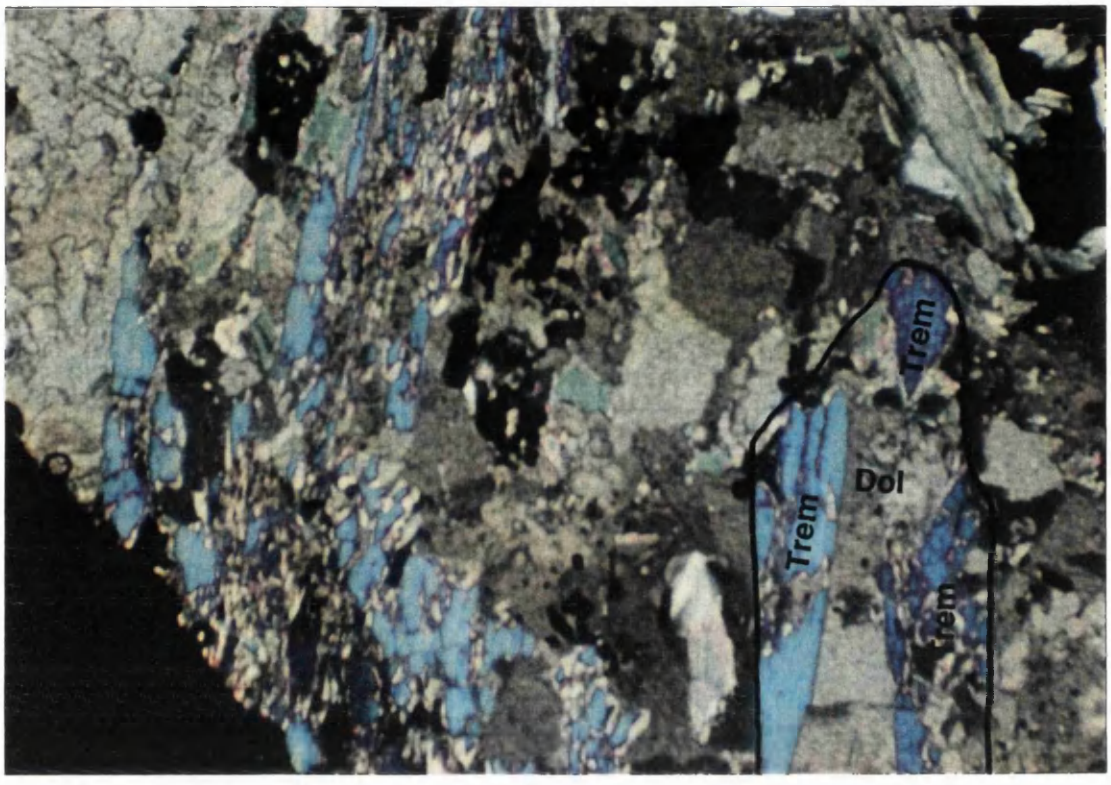

(a)

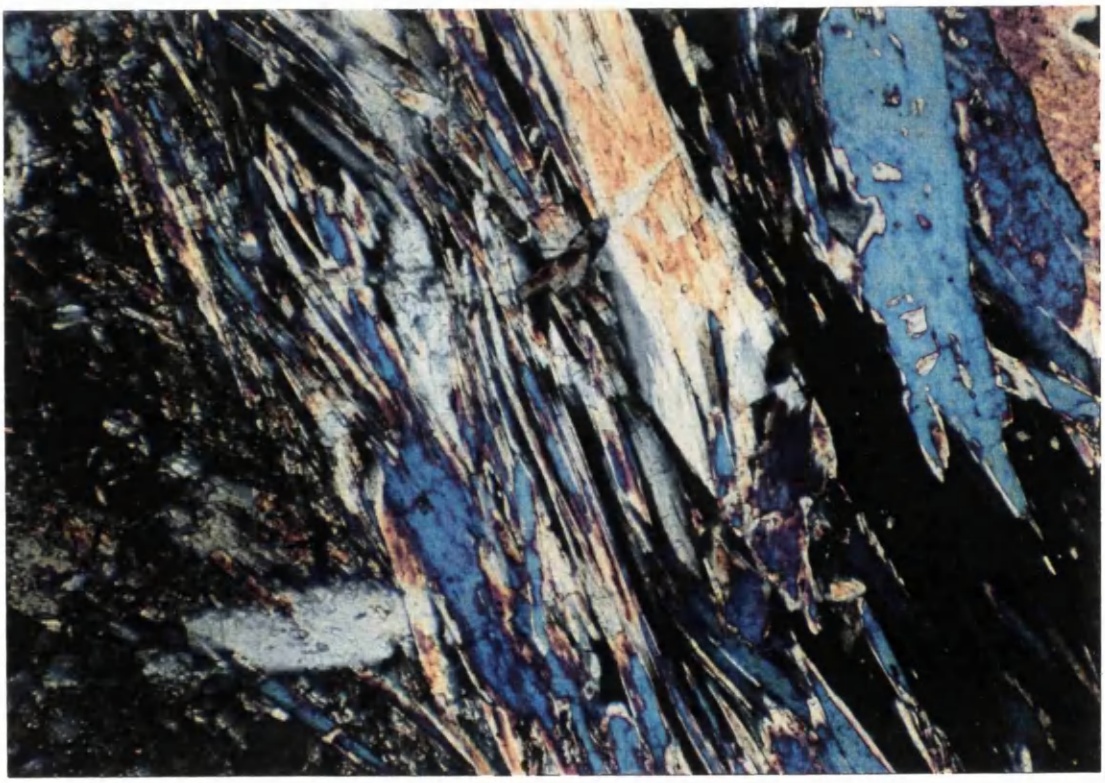

(b)

Plate 3.8

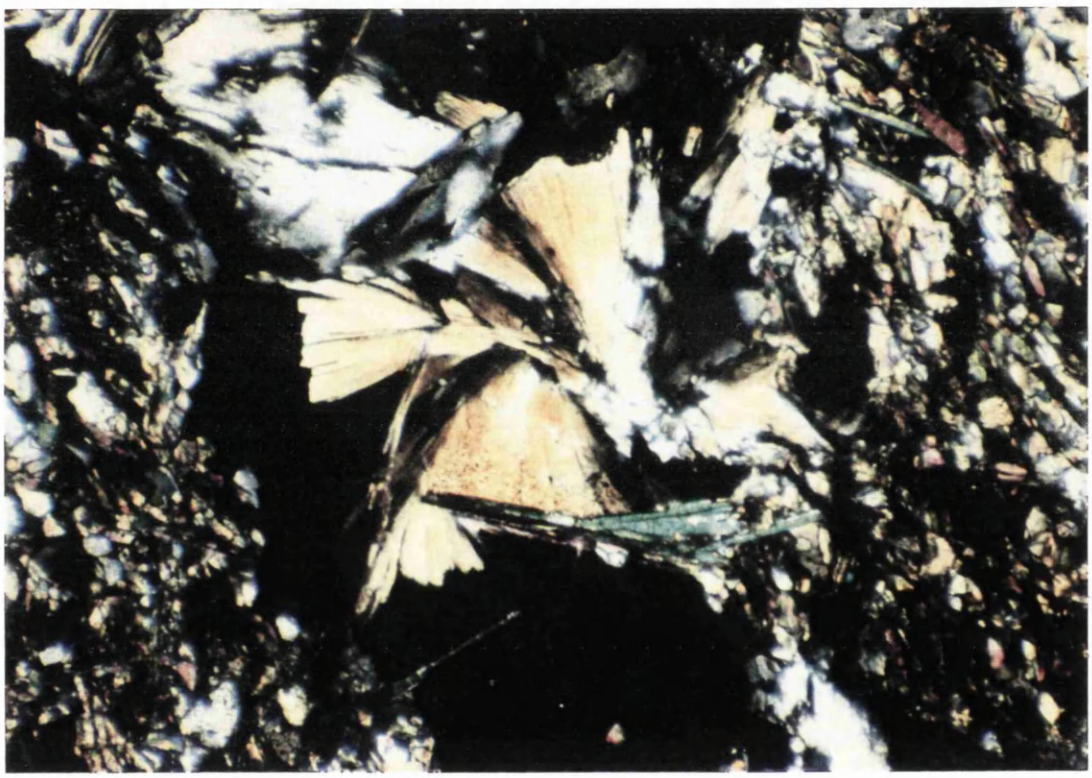

Plate 3.8: Transmitted light photomicrograph showing acicular tremolites. The fan-like, undulose extinction, indicates that the tremolites have undergone some metamorphic stress. The fine grained mineral with high polarisation colours on the right and left of the tremolites is biotite. The tremolites overprint the opaque sulphide mineral (pyrite). Sample CK5879. Crossed polars. Width of field is 1.7mm. Location: 475/463m block A, access crosscut 2 (see Map 8 in Appendix J).

Plate 3.9: Metamorphic effects on metallic sulphide minerals

Transmitted light photomicrograph (a) shows the opaque chalcopyrite elongated along schistosity, signifying a plastic response to metamorphic stress. The other minerals in this section are biotites seen on the left and centre of the field and calcite on the right side. The conformity of chalcopyrite to the schistosity indicates that primary chalcopyrite crystallisation is pre-schistosity and therefore pre-metamorphic. Sample CK5883; Argillite. Plane polarised light. Width of field is 4.4mm. Location: 475/463m block A, access crosscut (see Map 8 in Appendix J).

The carrollite in reflected light photomicrograph (b) is cataclastically fractured indicating the brittle nature of the mineral. Carrollite has not conformed to the schistose texture in the host rock but has maintained its euhedral form. Sample CK6491; Tremolite Schist. Width of field is 2.14mm. Location: 490m block K, crosscut 1 (see Map 12 in Appendix J).

Plate 3.9

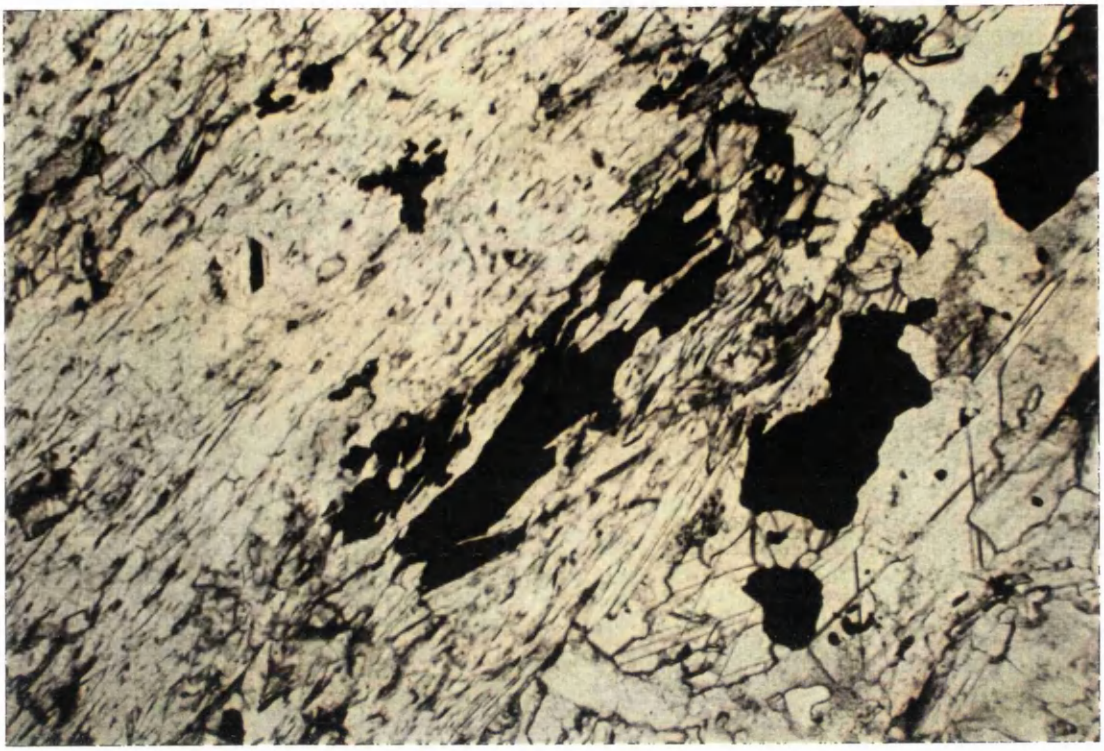

(a)

(b)

Plate 3.10: Relationship between sulphides and metamorphic minerals

Transmitted light photomicrographs showing chalcopyrite overprinted by metamorphic minerals.
In (a) opaque chalcopyrite is overprinted by tremolite laths. Sample CK 6487; Argillite. Crossed polars. Field width = 1.7mm.
Location: 463m block A, crosscut 2.

In (b) chalcopyrite is overprinted by a hexagonal epidote crystal seen in the centre of the field. A small rhomb shaped, yellow-brown crystal on the top right is sphene. Sample CK6490; Transitional Schist. Crossed polars. Width of field = 1.7mm. Location: 490m block K, crosscut 1 (see Map 12 in Appendix J).

Plate 3.10

(a)

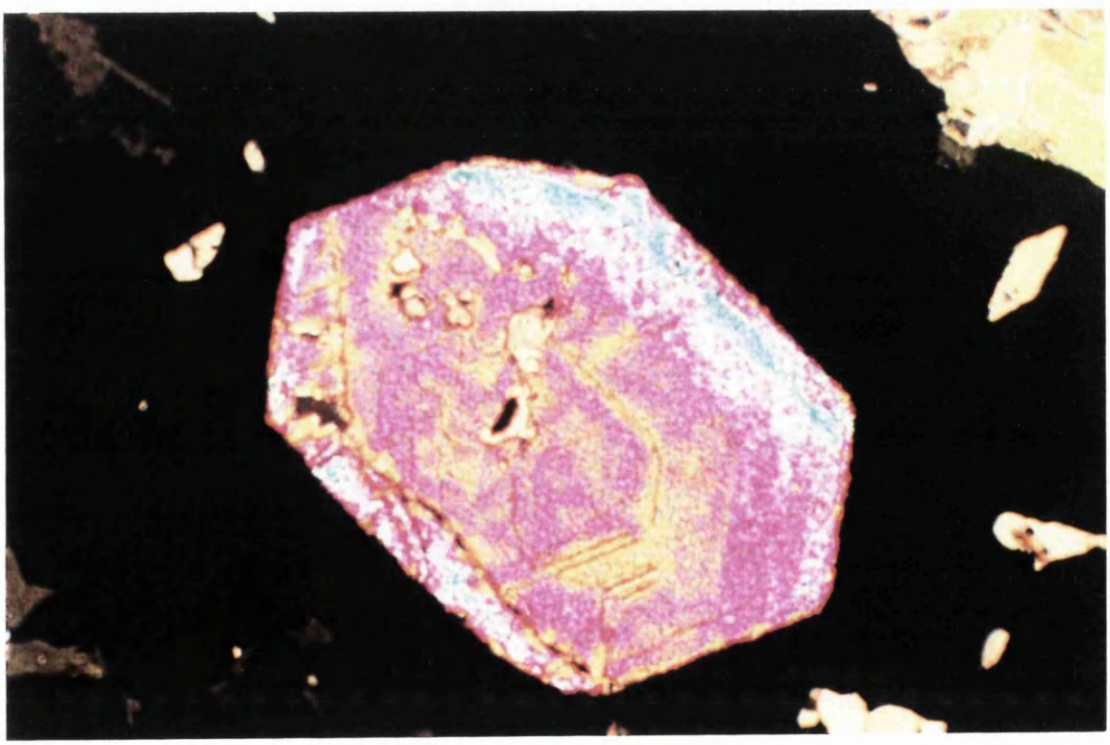

(b)

Plate 3.11

Plate 3.11: Discordant microcline-filled vein in argillite orientated normal to bedding. Location: 460m Block K haulage.

Plate 3.12: Intergrowth and replacement textures of chalcopyrite and bornite.

Reflected light photomicrographs showing the relationships between chalcopyrite and bornite.

In (a) a well formed early euhedral carrollite (Car) crystal has later chalcopyrite (Cpy) nucleating around it. The chalcopyrite is in turn replaced by bornite (Bn). Hence in this photograph the crystallisation order is carrollite followed by chalcopyrite and then bornite. Sample CK6488; Tremolite Schist. Width of field is 0.55mm. Location: 490m block K, crosscut 1 (see Map 12 in Appendix J).

In (b) the yellow chalcopyrite (Cpy) is in mymmerkitic intergrowth with purple bornite (Bn). The mymmerkite texture signifies that the two minerals are in solid solution and therefore crystallised simultaneously. Sample CK5890; Tremolite Schist. Width of field = 0.55mm. Location: 490m block K, SS48 Vent Raise Crosscut (see Map 9 in Appendix J).

Plate 3.12

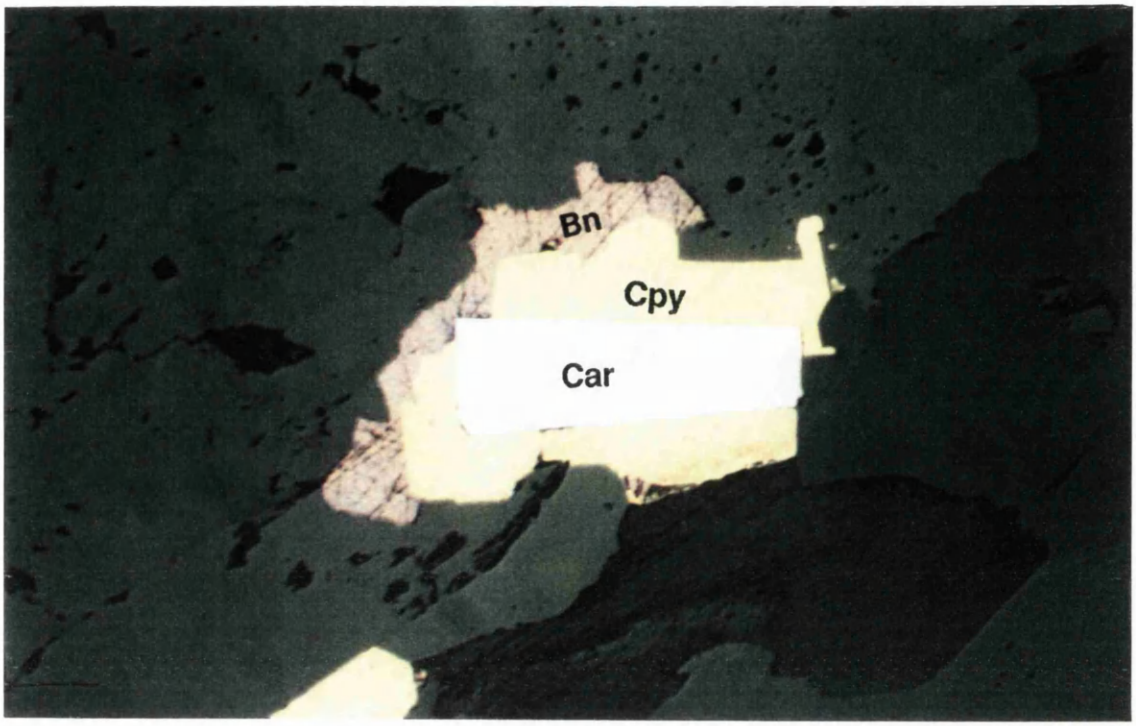

(a)

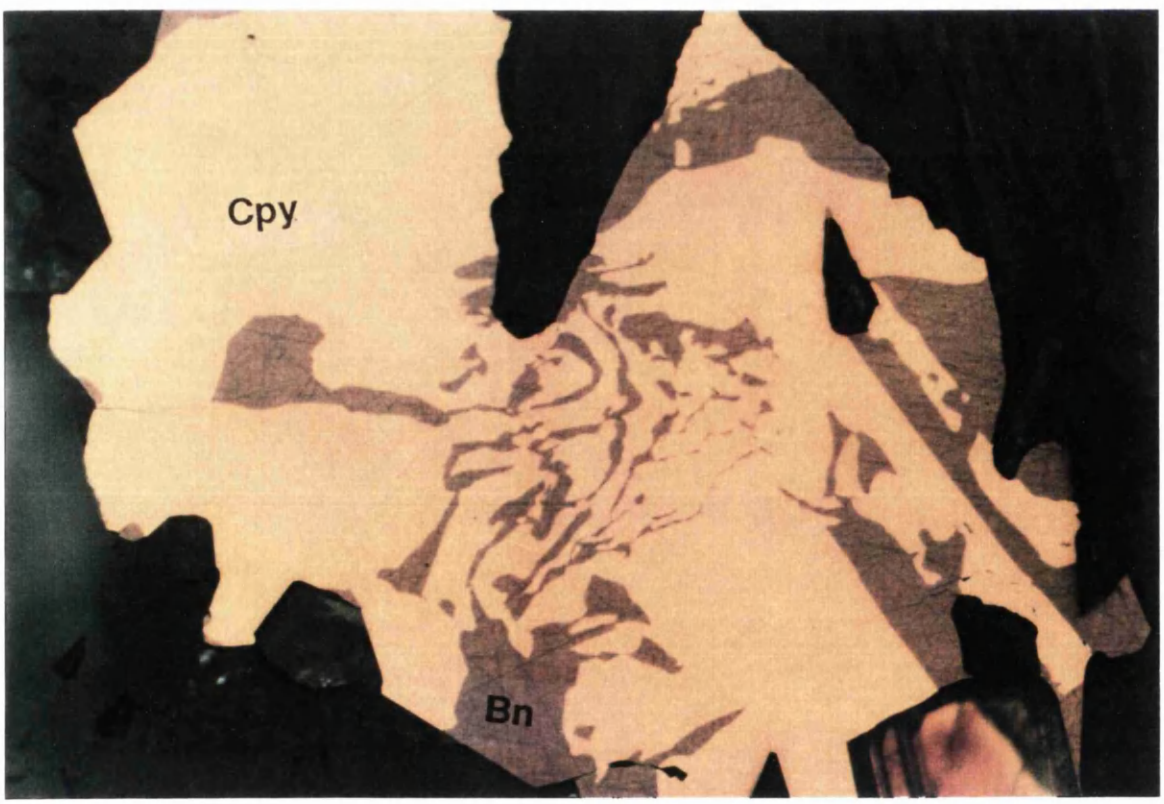

(b)

Plate 3.13: Chalcopyrite-covellite-bornite-chalcocite replacement textures

Reflected light photomicrograph (a) shows yellow chalcopyrite replaced by laths of blue covellite and displays a distinct covellite skeletal texture. Replacement of covellite after chalcopyrite indicates that covellite crystallised after chalcopyrite. Sample CK6498; Transitional Schist. Width of photo view is 2.14mm. Location: 470m block A, crosscut 10 (see Map 11 in Appendix J).

Reflected light photomicrograph (b) shows chalcopyrite (Cpy) almost completely replaced by bornite (Bn) which in turn is replaced by chalcocite (Cc). The crystallisation order represented is chalcopyrite followed by bornite and then chalcocite. Sample CK5892; Tremolite Schist. Width of field = 0.55mm. Location: 490m block K, SS48 Vent Raise Crosscut (see Map 9 in Appendix J).

Plate 3.13

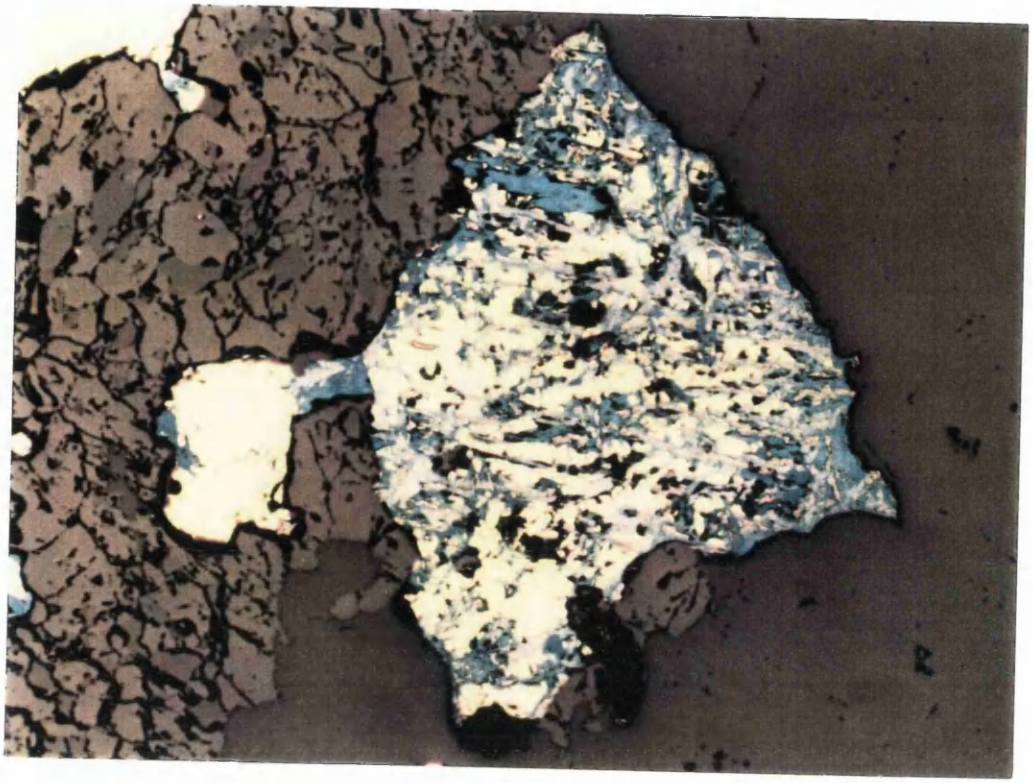

(a)

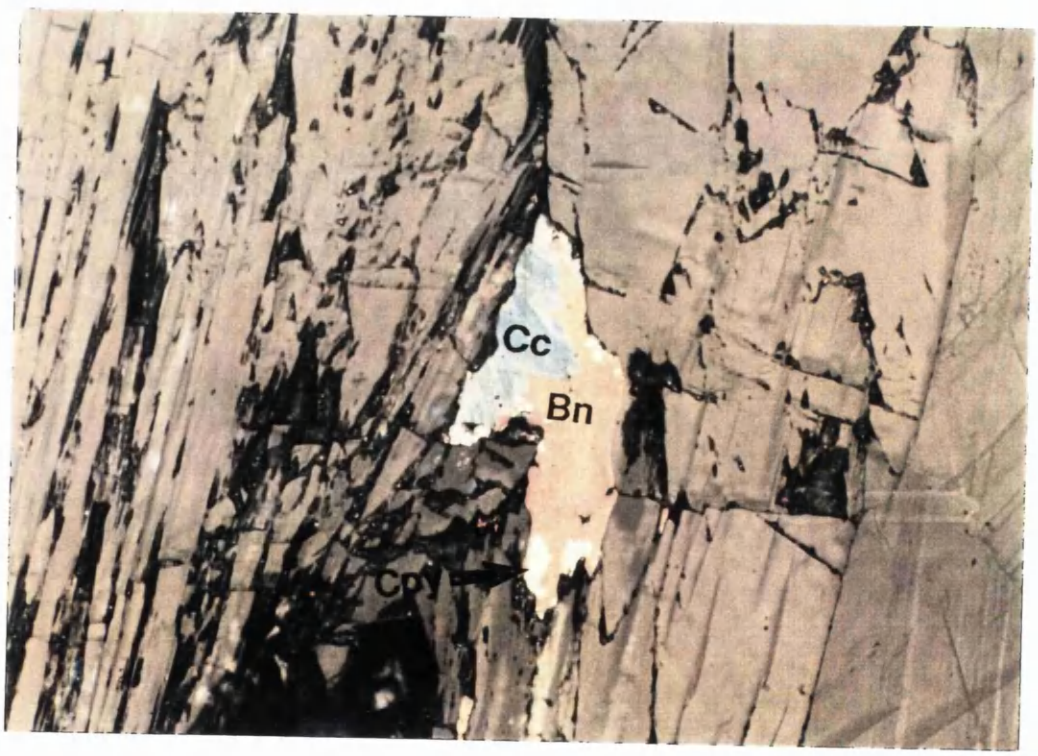

(b)

Plate 3.14

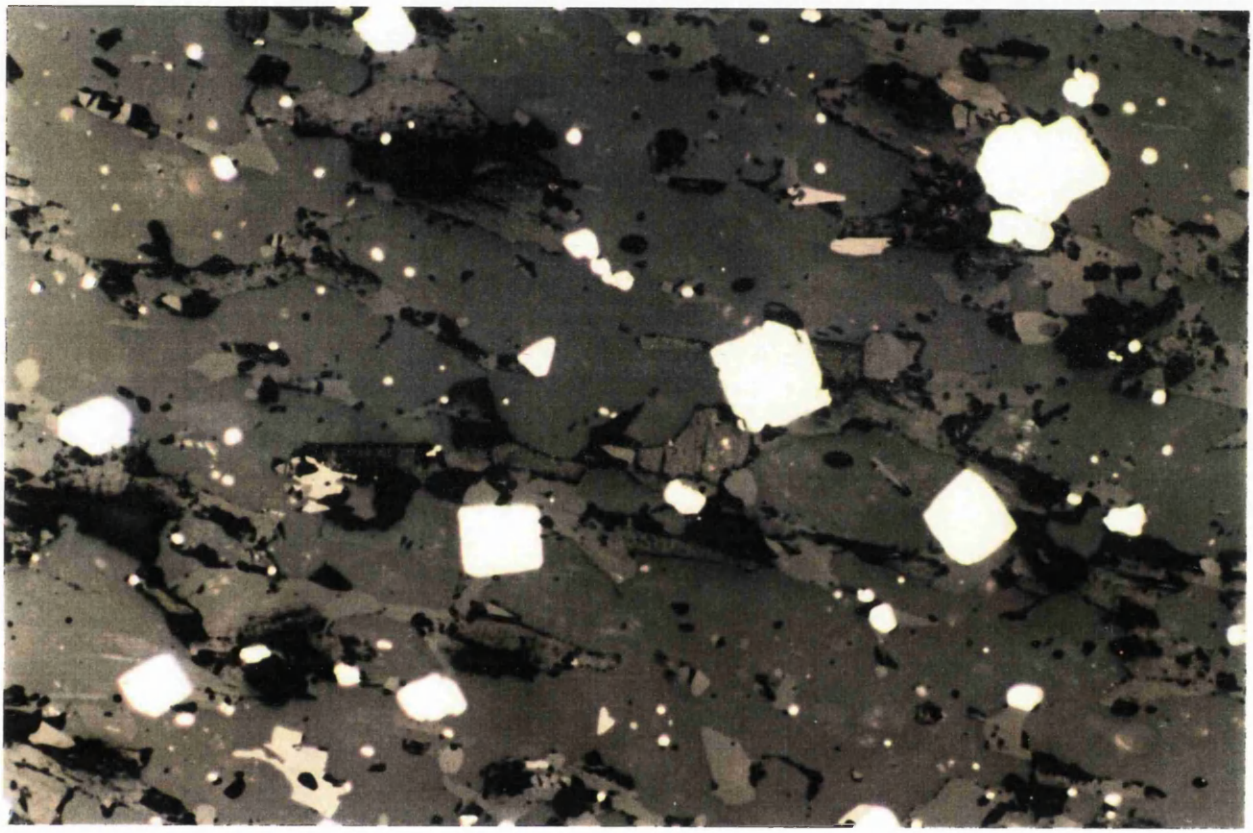

Plate 3.14: Reflected light photomicrograph showing early, well formed, euhedral pyrite cubic crystals disseminated in argillite. Sample CK376. Width of photo view is 1.09mm. Location: 463m block A, haulage.

Plate 3.15

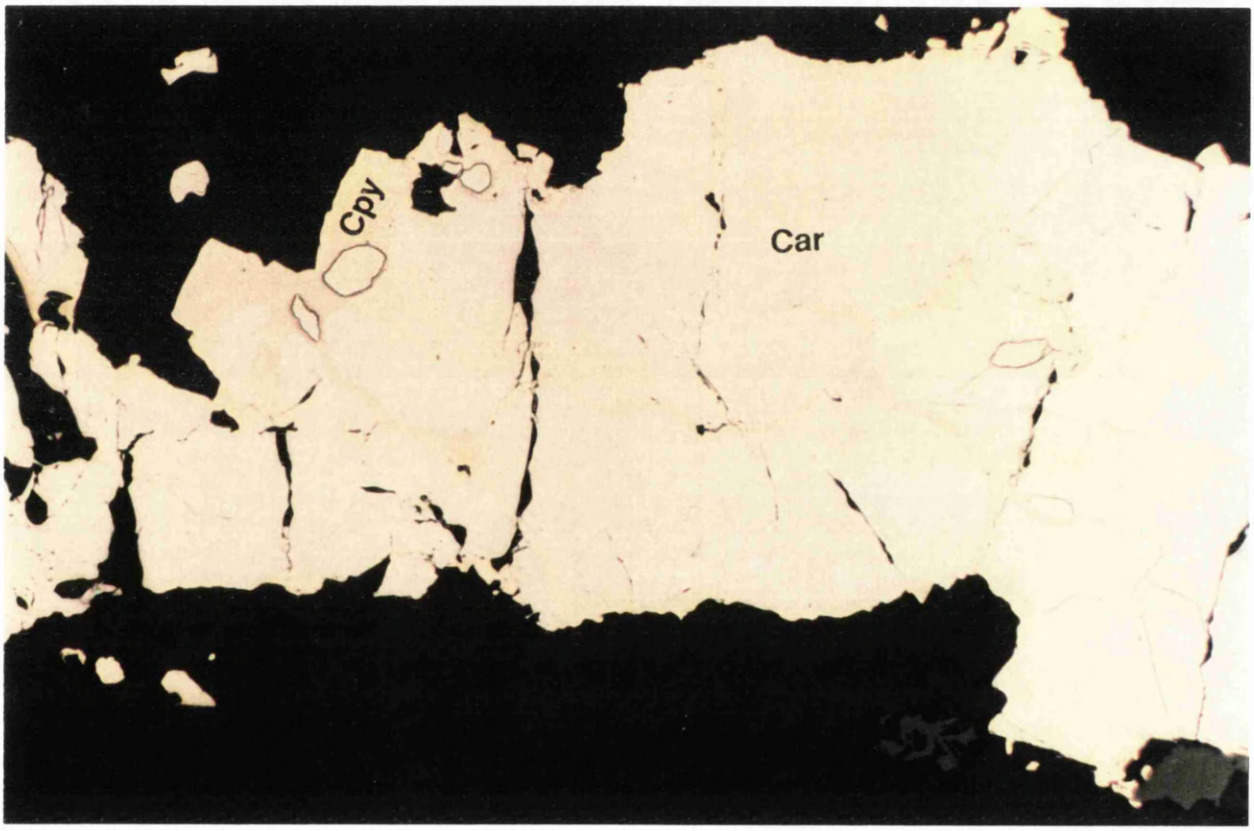

Plate 3.15: Reflected light photomicrograph illustrates carrollite (Car) being replaced by chalcopyrite (Cpy) along fractures. This signifies that the crystallisation of carrollite was earlier than that of chalcopyrite. Sample CK5893; Argillite. Width of field is 2.14mm. Location: 470m block A haulage.

It can be seen from Figure 1.2 that chalcopyrite is the commonest metallic sulphide in the Baluba Centre Limb orebody. The prevalence of chalcopyrite indicates that the mineral formed under a wide range of stability conditions. Chalcopyrite occurs mainly in the subhedral to anhedral crystal form and is commonly replaced by bornite, covellite and chalcocite (see Plates 3.12 (a), 3.13(a), 3.13(b)). Some of the bornite occurs in a mymmerkitic texture with chalcopyrite (Plate 3.12(b)), indicating that some bornite crystallised under the same conditions as chalcopyrite.

Pyrite generally occurs as crystalloblastic, cubic crystals and shows little or no alteration (see Plate 3.14). The stability of pyrite indicates that crystallisation of pyrite was early. Pyrite appears to be incompatible with bornite and chalcocite, indicating that the formation of pyrite took place under different stability fields to those of bornite and chalcocite. Carrollite has been replaced by the later chalcopyrite and the growth of chalcopyrite after carrollite has been noted (Plates 3.12(a), 3.15).

It appears that the recrystallisation of the primary sulphide minerals must have taken place isochemically. There has been no addition of elements to change the bulk metallic mineral chemistry. All the elements that make up the sulphide minerals seem to have been present during the primary sedimentation. The alteration and recrystallisation of the various mineral phases was determined by the temperature and pressure stability fields for the mineral phases (see Table 2.1, Chapter 2).

Table 3.3 presents the paragenetic sequence of the primary sulphide minerals in Baluba Centre Limb.

Table 3.3: Baluba Centre Limb sulphide mineral paragenetic sequence.

Pyrite	———
Carrollite	———
Chalcopyrite	———
Bornite	———
Covellite	———
Chalcocite	———

3.4 DISCUSSION

In this chapter it has been established that the effects of metamorphism in Baluba Centre Limb rocks are clearly exhibited. The metamorphism is intimately related to and accompanied the orogeny. The mineral assemblages, textures and mineralogy observed in the Baluba Centre Limb rocks are indicative of greenschist metamorphism. Evidence of metamorphic segregation and recrystallisation is displayed in both the metallic and rock-forming minerals.

It has been noted that the paragenetic sequence of the metallic sulphide minerals mainly manifests the recrystallisation accompanying post-sedimentary events. It is apparent that the formation of metallic minerals was pre-metamorphic. It has been noted that the recrystallisation and remobilisation of the metallic minerals due to metamorphism have had an effect on the distribution of the copper- and cobalt-bearing minerals, and hence the copper and cobalt concentrations within the Baluba Centre Limb deposit. The remobilisation of the minerals into veins during metamorphism is thought to have been by lateral secretion and the transport of the minerals has been localised to the vicinity of the source country rock. As a consequence, the selective enrichment of copper and cobalt minerals from the disseminated form into the massive form of mineralisation (along veins) mainly affects the short scale grade continuity.

CHAPTER 4

GEOCHEMISTRY AND MINERALOGY

4.1 INTRODUCTION

In this chapter the whole rock geochemistry and mineral chemistry in the Baluba Centre Limb rocks will be assessed. The geochemical and mineralogical patterns in the different lithologies will be correlated to the associated petrography and will also be used to explain some possible implications on the ore genesis. The chemistry of the copper- and cobalt-bearing minerals in the Baluba Centre Limb influence the concentrator recoveries of copper and cobalt. A study of the mineral chemistry of the copper- and cobalt-bearing minerals will provide some information on the characteristics of copper and cobalt within the structures of the metallic minerals. In particular, the nature of cobalt mineralisation in the different sections of the mineralised sediments will be analysed by assessing the variability of cobalt concentration within the cobalt bearing minerals.

Geological processes generally give rise to what statistically appears as 'noisy' geochemical sampling data owing to the complexities of the phenomena involved in the formation of the rocks and the associated mineralisation. To unravel the complexities of the patterns displayed by the geochemical sampling data it is important to relate the statistics to the primary geological processes and controls. The statistical patterns of geochemical assay grades in the Baluba Centre Limb deposit will be analysed and interpreted with reference to the different lithological and mineralogical characteristics associated with the mineralisation.

4.2 ANALYTICAL TECHNIQUES USED TO ACQUIRE GEOCHEMISTRY AND MINERALOGY DATA

Whole rock geochemical data was acquired using the Inductively Coupled Plasma - Atomic Emission Spectrometry (ICP-AES) analysis. The concentrations of a selection of major and minor elements were determined. The mineral chemistry was determined by the use of the Scanning Electron Microscope (SEM) fitted with an electron microprobe attachment for quantitative analysis. The ICP-AES analytical procedures used to analyse the samples and the SEM procedure utilised for mineralogical analysis are described in Appendix D. The results of the ICP-AES analyses are

presented in Appendix E.I and the results obtained from the SEM analyses are presented in Appendix E.II.

4.3 ROCK FORMING MINERALS

The summary of the major whole-rock oxide compositions in the Baluba Centre Limb rocks categorised by lithologies is presented in Table 4.1.

Table 4.1: Mean concentrations of major oxides in the Baluba Centre Limb rocks.

Lithology	Number of samples	% Na_2O	% K_2O	% CaO	% MgO	% TiO_2
*Basement (schists and granites)	-	3.5	4.0	1.7	0.9	5.6
Footwall (Quartzites/Conglomerates)	11	0.32	3.09	7.14	3.51	2.64
Calcareous Schists	33	0.70	2.85	12.85	10.82	3.21
Mineralised argillites (cupriferous)	12	0.65	3.67	9.61	10.30	4.27
Hangingwall argillite (pyritic)	26	0.48	4.29	6.05	7.95	4.77

* The values for the Basement rocks compiled from Mendelsohn (1961). The rest of the values in the table are mean concentrations calculated in this study from the ICP-AES data for Baluba Centre Limb samples.

(i) Alkaline oxides (Na_2O and K_2O)

In the Basement rocks the concentrations of K_2O and Na_2O are similar, at around 3.5% to 4% by weight, as seen in Table 4.1 and Figure 4.1.

The concentration of Na_2O decreases in the Katanga meta-sediments to below 1% while K_2O concentrations remain at similar levels in the sediments as in the Basement. It is assumed that the Katanga sediments were derived from the Basement detrital material. Mendelsohn (1961) suggests that the low Na_2O and high K_2O in the sediments can be explained by the loss of Na_2O in the sediments, perhaps metasomatically, while K_2O has been retained. The persistence of K_2O is manifest by the prevalence of alkali feldspars compared to plagioclases in the Baluba Centre Limb sediments (see plate 3.1).

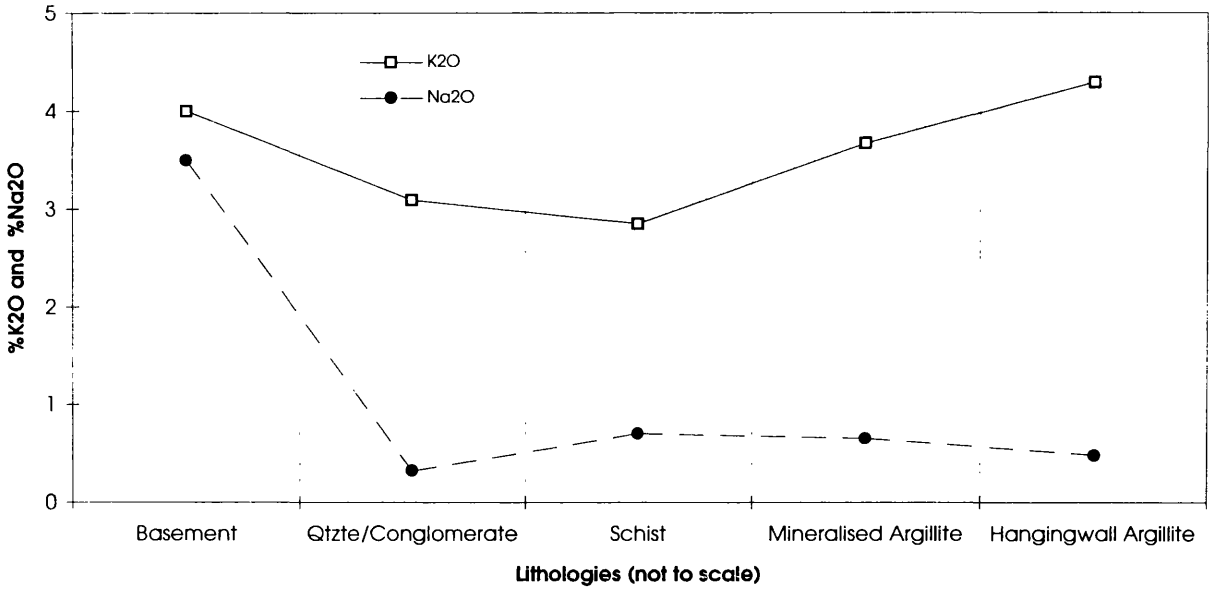

Figure 4.1: The concentrations of Na_2O and K_2O in the Basement are approximately the same. The Na_2O becomes substantially depleted in the Katanga meta-sediments while K_2O remains at similar levels as in the Basement. Some Na would have been lost during the sedimentary deposition or during the ensuing diagenetic or metamorphic processes.

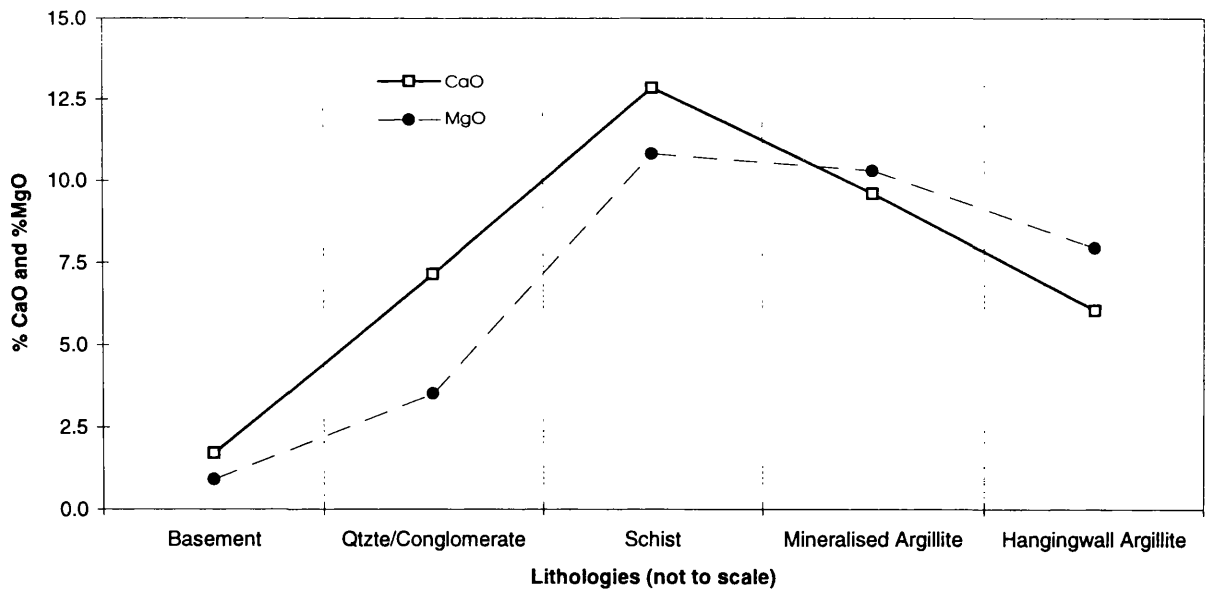

Figure 4.2: The CaO and MgO concentrations increase from the Basement into the Katanga meta-sediments. This signifies that Ca and Mg must have been derived from the Katanga sea waters rather than from the Basement hinterland.

(ii) Lime (CaO) and Magnesia (MgO)

The schists, which host the bulk of copper and cobalt mineralisation, are carbonate-rich. They are calcic and dolomitic. The footwall meta-sediments generally lack carbonate minerals. A depletion of MgO and CaO is expected in the footwall rocks with respect to the schists and argillites. Apart from calcite and dolomite the other major common Mg- and Ca-bearing rocks in the Baluba Centre Limb are tremolite, mica (biotite) and chlorite. These minerals too are more common in the schists and argillites than in the footwall sediments further supporting the lack of Ca and Mg in the footwall rocks.

Figure 4.2 illustrates that the Basement and footwall meta-sediments (quartzite and conglomerate), have low MgO and CaO levels compared to the schists and argillites. Therefore the source of Mg and Ca would not have been the Basement provenance area but from the sea water.

4.4 METALLIC SULPHIDE MINERALS

4.4.1 Mineral chemistry

To analyse the compositional variations of the metal bearing minerals the Baluba Centre Limb metallic sulphide minerals have been divided into four classes:

(i) Cu-S system (chalcocite and covellite),

(ii) Cu-Fe-S system (bornite and chalcopyrite),

(iii) Co-Cu-S system (linnaeite and carrollite),

(iv) Fe-S system (pyrite).

The compositional ranges of sulphide minerals determined by SEM are presented in Table 4.2 and graphically summarised in Figure 4.3.

From Table 4.2 and Figure 4.3 it is noted that:

(i) the minerals with the more varied compositions are carrollite and pyrite. These are also the cobalt bearing minerals.

(ii) the carrollites of Baluba Centre Limb are seen to be depleted in copper and enriched in cobalt compared to the theoretical carrollite stoichiometry.

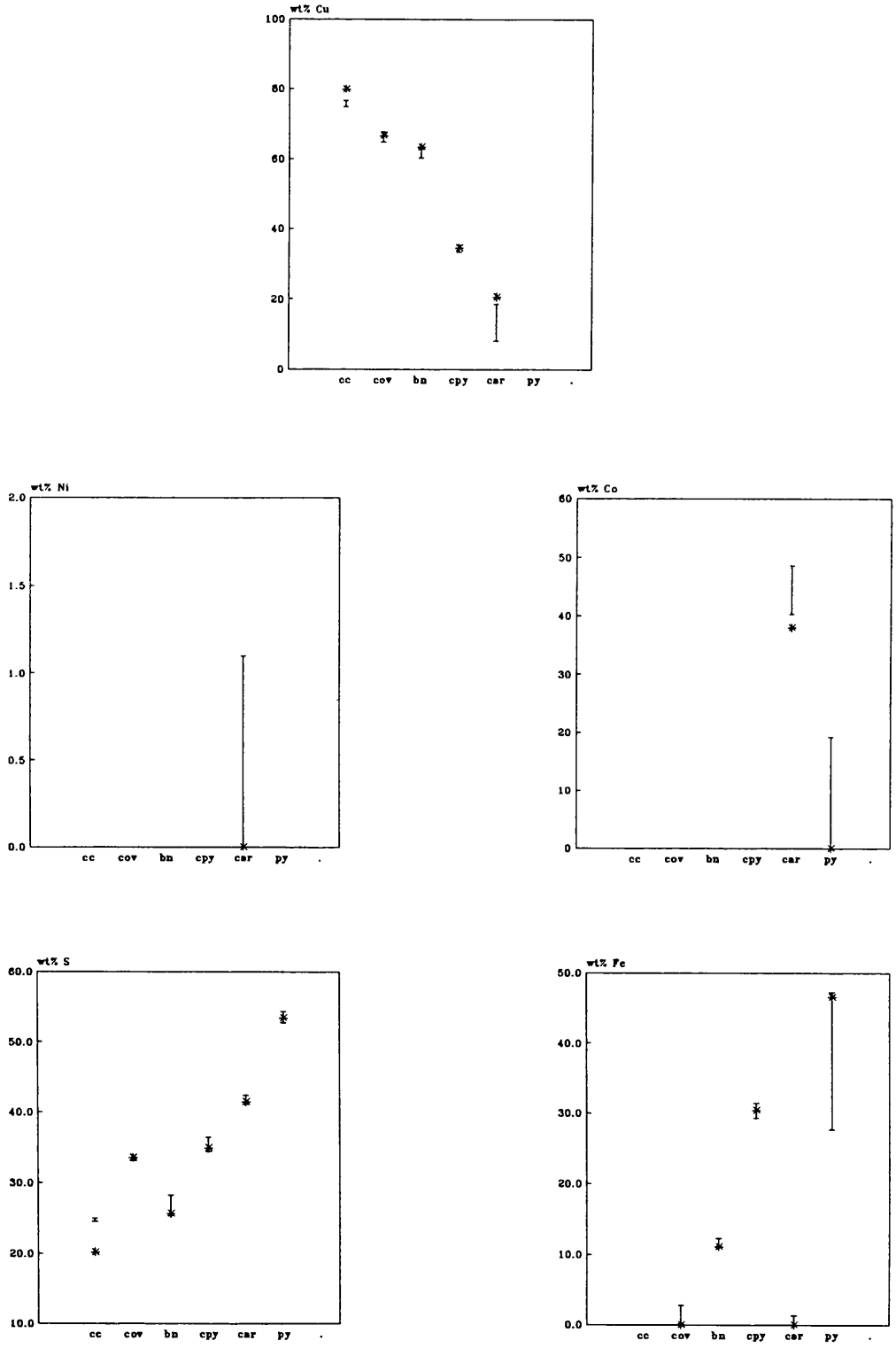

Figure 4.3: Summary of compositions of sulphide minerals in Baluba Centre Limb. The vertical lines (I) show the range of compositions obtained from SEM analyses of Baluba Centre Limb samples and the asterisks (*) indicate the theoretical stoichiometric compositions of a pure mineral.

(iv) the cobaltiferous nature of the pyrites is indicated. In the Baluba Centre Limb pyrite samples, the cobalt content reaches a maximum of 19.2% by weight.

Table 4.2: Mineralogy of the sulphide minerals found in Baluba Centre Limb.

		Weight % of element in mineral									
		Copper		Cobalt		Nickel		Iron		Sulphur	
Mineral	Formula	[1]A	[2]B	[1]A	[2]B	[1]A	[2]B	[1]A	[2]B	[1]A	[2]B
Pyrite	FeS_2	-	0	-	0	-	-	46.6	46.7	53.4	53.3
[3]Co- pyrite	$(Fe,Co)S_2$	-	0	[4]24.2	5.0	-	-	[4]23.0	42.0	52.8	53.5
Chalcopyrite	$CuFeS_2$	34.5	34.7	-	0	-	-	30.4	30.6	35.0	35.0
Bornite	Cu_5FeS_4	63.3	61.8	-	0	-	-	11.1	11.8	25.6	26.6
Covellite	CuS	66.5	65.9	-	0	-	-	-	1.7	33.5	33.3
Chalcocite	Cu_2S	79.9	75.5	-	0	-	-	-	0.1	20.1	24.9
Carrollite	Co_2CuS_4	20.5	15.4	38.1	42.7	-	0.2	-	0.4	41.4	41.6

Notes:
1. Columns labelled A are theoretical stoichiometric elemental compositions of the minerals.
2. Columns labelled B are elemental compositions of minerals measured on Baluba Centre Limb samples by Electron Microprobe quantitative analysis.
3. Co-pyrite = Cobaltiferous pyrite
4. Cobalt and iron proportions in cobaltiferous pyrite based on the ratio of cobalt to iron of 1:1.

It is observed that the compositions of the cobalt-bearing minerals deviate considerably from the theoretical stoichiometries, but that the copper bearing sulphides in Baluba Centre Limb have compositions which are almost indistinguishable from the theoretical stoichiometries. The mineralogy of the cobalt-bearing minerals is naturally varied and able to accommodate a wide solid solution series (Tarr, 1935) compared to the copper-bearing minerals.

As noted in the zonation model in Chapter 1 (Fig. 1.2), the *pyrite zone* generally represents the hangingwall of the Baluba Centre Limb orebody. The cobaltiferous nature of the pyrites in the hangingwall region is important because it indicates that cobalt mineralisation continues beyond the assay hangingwall boundary of the orebody defined on the basis of copper only.

(i) Co-Cu-S System (Linnaeites)

Linnaeites have the general formula AB_2X_4 where:

Site A can be occupied by Co, Cu, Fe, Ni or Zn, Site B by Co, Cr, Fe, In, Ni or Sb, and Site X by S or Se.

Tarr (1935) presents six major members of the linnaeite group of minerals as: (i) Linnaeite, Co_3S_4, (ii) Siegenite, $(Ni,Co)_3S_4$, (iii) Carrollite, $CuCo_2S_4$, (iv) Polydymite, Ni_3S_4, (v) Violerite, $FeNi_2S_4$ and (vi) Daubreelite, $FeCr_2S_4$.

No pure Cu_3S_4 or Fe_3S_4 salts are known to exist in nature (Tarr, 1935). When Cu and Fe occur in the linnaeite system they appear with Co, Ni or Cr - never alone. The term carrollite is applied to the copper-rich but nickel-poor linnaeites. The compositions of some Copperbelt carrollites are presented in Table 4.3.

Table 4.3: Compositions of Copperbelt carrollites.

Location	Chemical composition range (mean in brackets) - in weight percent					Source of data
	Copper	Cobalt	Iron	Sulphur	Nickel	
1. Baluba	8.05-18.66 (15.70)	40.29-48.65 (42.44)	0-1.37 (0.33)	41.10-42.42 (41.62)	0-1.09 (0.18)	This study
2. Baluba	19.79-21.92 (20.86)	37.95-39.88 (38.92)	0.25-0.25 (0.25)	40.70-41.36 (41.03)	0.48-0.49 (0.48)	Annels *et al.*, 1983
3. Chibuluma	19.5-20.0 (19.8)	37.0-38.0 (37.5)	0-0.65 (0.32)	41.5-41.5 (41.5)	0.2-1.8 (1.0)	Darnley and Killingworth, 1962
4. Chibuluma	19.23-21.12 (19.98)	36.86-39.70 (38.53)	0.49-0.82 (0.64)	39.35-40.54 (39.87)	0.41-2.53 (1.06)	Craig *et al.*, 1979
5. Chibuluma	19.37-20.82 (20.29)	36.86-39.04 (38.07)	0.49-0.82 (0.62)	39.35-40.02 (39.64)	0.45-2.53 (1.09)	Annels *et al.*, 1983
6. Nkana South Orebody	8.75-17.19 (12.97)	41.25-48.23 (44.74)	0.19-1.01 (0.60)	41.55-41.96 (41.76)	0-0.97 (0.48)	Richards, 1965
7. Nkana South Orebody	6.8-10.2 (8.65)	39.9-49.9 (44.55)	1.6-8.6 (5.2)	40.4-41.9 (41.2)	0-1.1 (0.38)	Riley, 1980
8. Chambishi Southeast	11.53-19.40 (15.41)	37.20-45.48 (41.20)	0.12-2.49 (0.55)	40.57-43.02 (41.26)	0.15-1.60 (0.40)	Annels *et al.*, 1983
9. Nchanga	9.2-15.0 (13.15)	36.6-42.2 (39.98)	0-1.5 (0.75)	39.8-44.1 (41.90)	0-9.9 (2.48)	Garrard, 1972
Carrollite	20.5	38.1	0	41.4	0	Theoretical stoichiometry
Linnaeite	0	58.0	0	42.0	0	Theoretical stoichiometry

Analyses on the Baluba Centre Limb carrollite samples indicate that they are cobalt-rich compared to the theoretical carrollite stoichiometry, but are cobalt-poor compared to linnaeite (Fig. 4.4). Owing to the low copper content and the elevated cobalt content in the linnaeites, Richards (1965) suggested that the term copper-rich linnaeite rather than carrollite was more appropriate for the Copperbelt linnaeite-group minerals. However the Baluba Centre Limb samples and the other linnaeite-group minerals for the Zambian Copperbelt presented in Table 4.3 indicate that their compositions are closer to carrollite than to linnaeite.

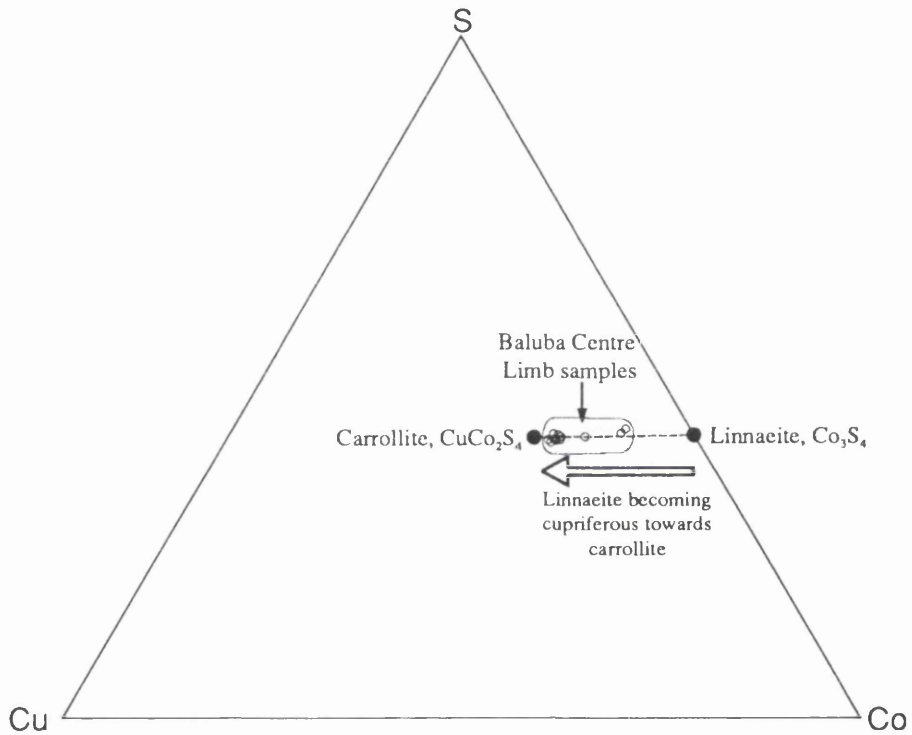

Figure 4.4: Cu-Co-S ternary plot showing the composition of the linnaeite minerals. Baluba Centre Limb linnaeite-group minerals plot between carrollite and linnaeite.

Generally for the Zambian Copperbelt, the term carrollite, therefore, seems suitable despite the departure in the mineralogical composition of analysed samples from the composition of pure carrollite.

(ii) Fe-S System (Pyrite)

The mineralogy of pyrite is important because, as observed in Figure 4.3, some of the Baluba Centre Limb pyrites contain cobalt. It is probable that the pyrite found in the Baluba (and some other Copperbelt) orebodies belong to the pyrite (FeS_2) - cattierite (CoS_2) isomorphous series. It appears that cobalt and iron are interchangeable over a range of compositions from FeS_2 to CoS_2 (Notebaart and Vink, 1972). The pure cattierite end member, CoS_2, has not been reported for any Copperbelt deposit, but has been described for the Shaban (Katangan) Copperbelt in neighbouring Zaire (Kerr, 1945). The cobaltiferous nature of the pyrites in Zambian Copperbelt deposits is demonstrated in Table 4.4.

Table 4.4: Compositions of Copperbelt pyrites.

Location	Chemical composition range (mean in brackets) - in weight percent					Source of data
	Iron	Cobalt	Copper	Sulphur	Nickel	
1. Baluba	27.73-47.34 (43.32)	0-19.21 (3.58)	0	52.69-54.34 (53.57)	0	This study
2. Baluba	29.07-47.59 (38.08)	0.84-19.14 (10.51)	0-0.80 (0.24)	49.04-51.59 (50.36)	0-2.8 (0.09)	Annels *et al.*, 1983
3. Chibuluma	24.5-24.9 (24.7)	20.5-21.3 (20.9)	0-0.3 (Trace)	52.2-52.4 (52.3)	0-0.3 (0.03)	Riley, 1965
4. Nkana South Orebody	35.0-44.6 (39.8)	0.9-10.5 (5.7)	0	52.4-53.4 (53.0)	0	Richards, 1965
5. Chambishi Southeast	25.04-45.52 (37.01)	0.13-20.21 (8.25)	0-0.14 (0.04)	51.62-53.01 (52.31)	0	Annels *et al.*, 1983
6. Nchanga	33.8-46.9 (40.35)	0.7-12.1 (6.4)	0	50.9-53.8 (52.35)	0	Garrard, 1972
Pyrite	46.7	0	0	53.3	0	Theoretical stoichiometry

The Baluba Centre Limb pyrite samples examined in this study indicated that they contain up to 19.2% cobalt (see Table 4.4). The range of composition of the pyrite minerals in the Baluba Centre Limb is presented as a Fe-Co-S ternary plot in Figure 4.5 to show variations in iron, cobalt and

sulphur in the pyrites. It is noted that the Baluba Centre Limb pyrite samples range in composition from pure pyrite to pyrite in which 50% of the Fe has been replaced by Co. These results concur with the assertions of Annels and Simmonds (1984) who suggest that a significant proportion of iron in the Baluba pyrites lies in solid solution with cobalt.

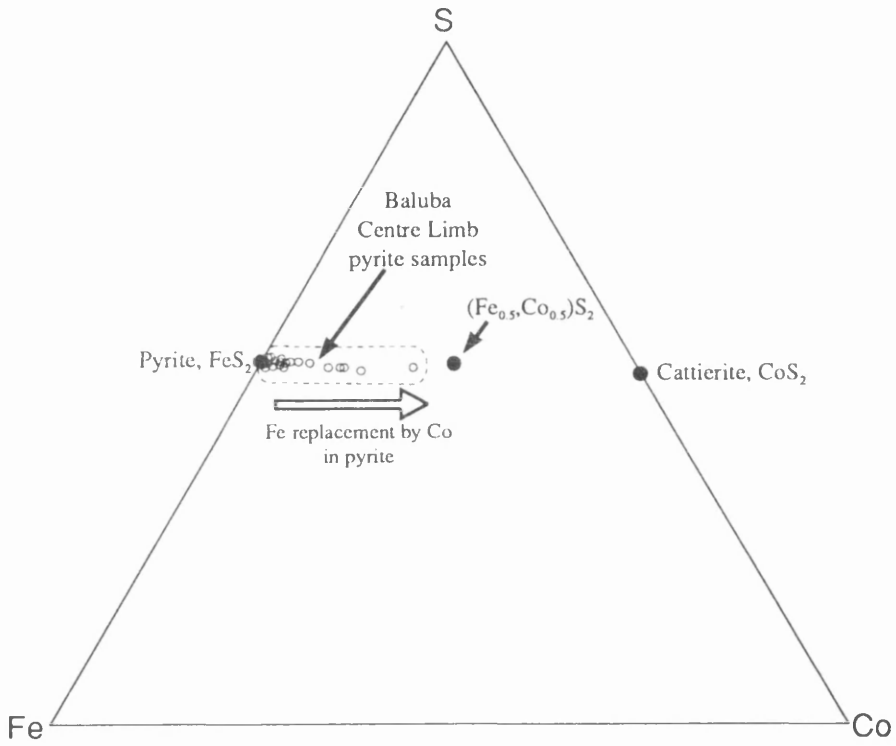

Figure 4.5: Fe-Co-S ternary plot showing the range of composition of the Baluba Centre Limb pyrites. The tendency for the pyrites to become cobaltiferous is demonstrated.

4.4.2 Whole-rock geochemistry

(i) Copper-cobalt relationship

Copper- and cobalt-bearing minerals occur in the schists and argillites. As seen in the zonation model (Fig. 1.2) the highest copper and cobalt assay grades occur in the lower section of the schists.

The footwall, clastic meta-sediments (quartzites and conglomerates) are virtually devoid of copper- and cobalt-bearing minerals. In this study no copper- or cobalt-bearing minerals were identified petrographically in the footwall rocks. The background copper and cobalt mineralisation (less than

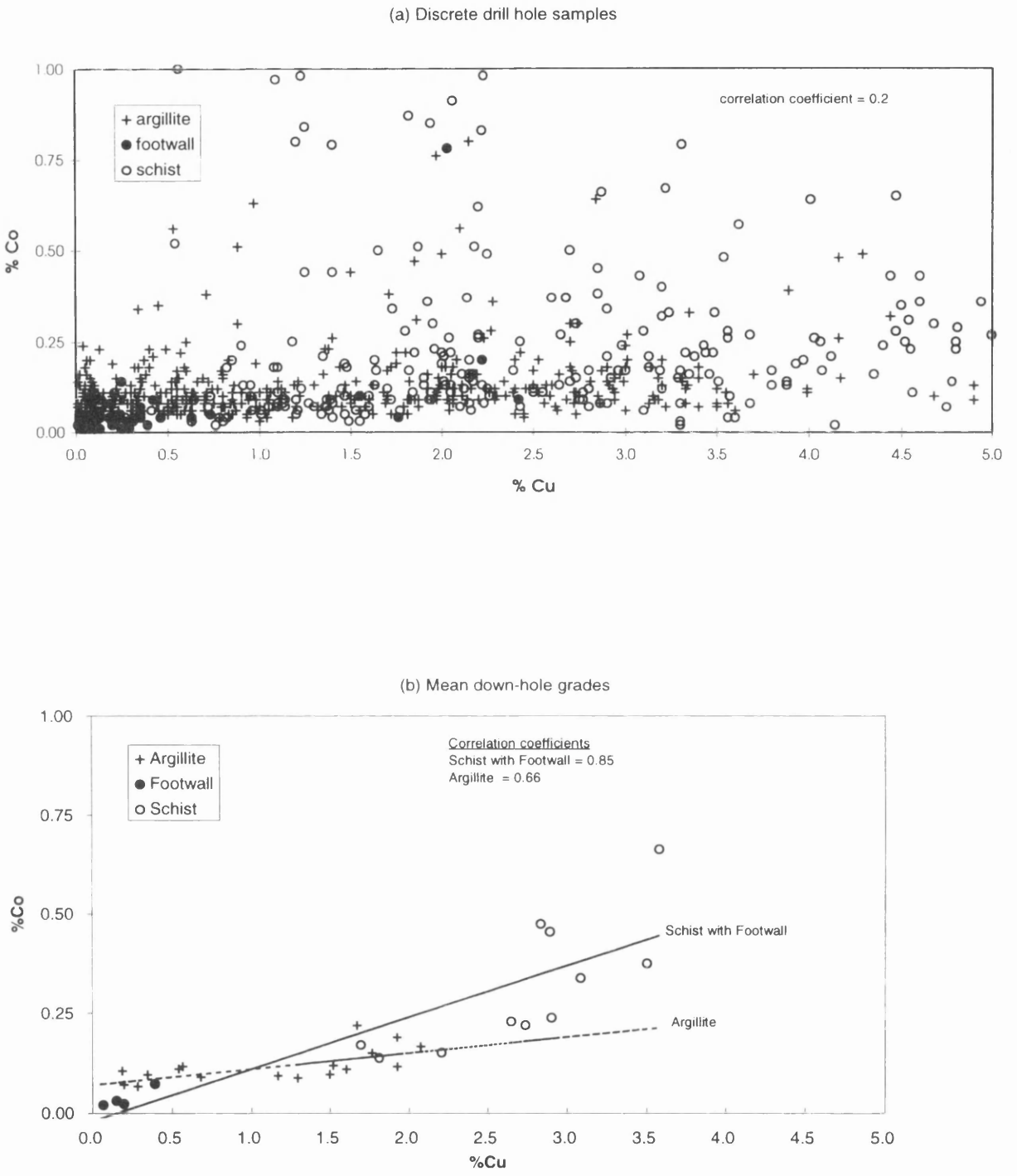

Figure 4.6: Plot (a) shows the apparent absence of a direct relationship between copper and cobalt when discrete drill hole samples are used. By using mean grades down the drill hole profile (the data base used to draw up the zonation model in Fig. 1.2) a linear correlation is discernable as shown in (b).

0.5% copper and less than 0.05% cobalt) in the footwall is due to copper and cobalt solid-solution in the silicate minerals.

Although copper and cobalt occur in the same horizons in the Baluba Centre Limb orebody the correlation between copper and cobalt was found to be poor when the discrete drill hole samples were used (Fig. 4.6(a)). There was an improvement in the correlation between copper and cobalt when the mean grades along the drill holes (Fig. 4.6(b)) were used, i.e. the weight averaged grades that were used to construct the zonation model in Chapter 1.

The copper-cobalt mineralisation trend in the argillites can be segregated from that in the schists and footwall sediments. The cobalt in argillites occurs in the form of cobaltiferous pyrite while in schist it occurs in the form of carrollite. It is seen in Figure 4.6(b) that the linear regression line for the schist and footwall crosses the plot close to the origin and has a steeper gradient than that in the argillite. The low grade, background cobalt mineralisation in the footwall is assumed to be of a similar generation as that in the schists; of the carrollite type. Copper and cobalt co-exist within the carrollite structure, hence the intersection of the regression line close to the origin. Based on the carrollite stoichiometry, cobalt cannot be expected to occur in the absence of copper within the schists.

The regression line of copper-cobalt correlation in the argillites has a cobalt intercept value of 0.07% and a gradient approaching zero. The intercept signifies that cobalt exists in the absence of copper within the argillites. This is attributed to the existence of cobalt within the pyrite structure (see section 4.4.1). Cobalt exists in the absence of copper in the cobaltiferous pyrites and the independence between cobalt and copper mineralisation within the argillites accounts for the constant, shallow, near-zero gradient of the regression line.

(ii) Cobalt-Nickel relationship

While the Copperbelt copper deposits are cobaltiferous (see Chapter 2) nickel is virtually absent. For the Baluba Centre Limb, the average concentration of nickel in the samples analysed in this work was about 30ppm compared to about 3% copper and 0.3% cobalt. No nickel-bearing minerals were identified in petrographic examinations of the Baluba Centre Limb rocks. The whole-rock nickel

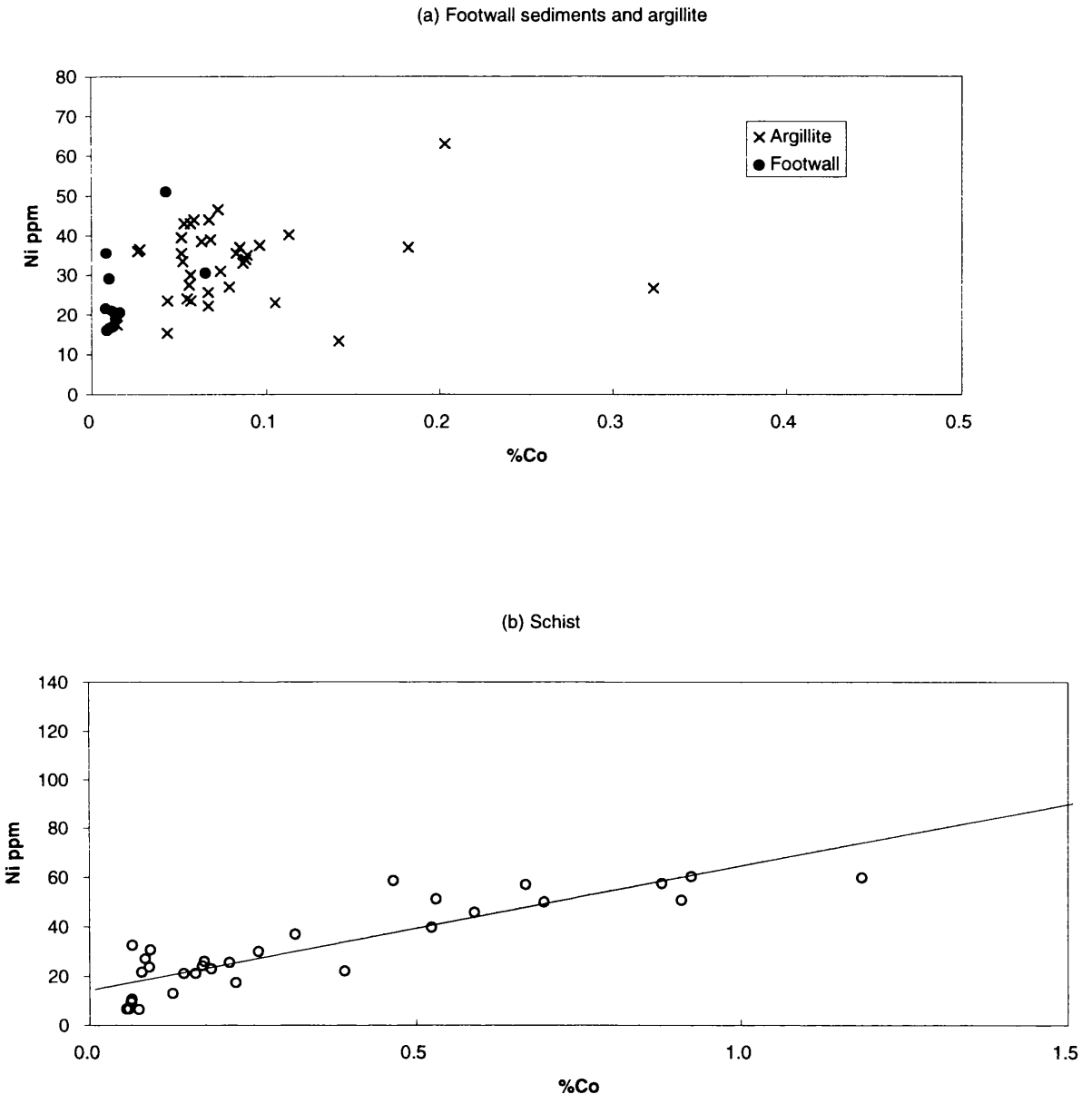

Figure 4.7: Plot (a) demonstrates the absence of cobalt-nickel correlation in the footwall sediments and argillites. In (b) the linear correlation between cobalt and nickel concentrations in the schists is indicated. The data used are the ICP-AES analyses of a mixture of 80 underground drill hole, chip and grab samples from Baluba Centre Limb (see Appendix E.I).

assays obtained by the ICP-AES chemical analyses (Appendix E.I) are considered to be due to nickel solid-solution in sulphide mineral phases.

In Figure 4.7(a) a lack of correlation between cobalt and nickel is observed in the footwall sediments and in the argillites. The cobalt concentration in these lithologies is lower compared to that in the schists as was illustrated in the zonation model (Fig. 1.2). It would seem, therefore, that at low cobalt concentrations nickel occurs in solid solution in the silicate as well as sulphide mineral phases, hence the lack of direct correlation between cobalt and nickel in the footwall and argillites. Higher cobalt concentrations occur in the schists. A linear correlation between cobalt and nickel is observed in schists (Fig. 4.7(b)). Since cobalt mineralisation in the schists is due to carrollite as depicted in Figure 1.2, it can be assumed that the nickel in the schists is contained within the carrollites. This assertion is supported by the nickel which was quantitatively detected in carrollites (see carrollite SEM analyses, Appendix E.II). The positive intercept on the nickel axis in Figure 4.7(b) indicates that nickel exists in the presence of cobalt in solid solution in the carrollites.

(iii) Iron-cobalt relationship

As noted in the pyrite mineralogical analyses (section 4.4.1), some pyrites in the upper sections of the argillite (hangingwall region) from the Baluba Centre are cobaltiferous. A direct relationship between iron and cobalt in the pyritic argillites can be expected (assuming that the iron contained in silicates and titaniferous minerals in argillites is negligible compared to the iron contained in pyrites). Figure 4.8 shows plots of the iron-cobalt correlation in the Baluba Centre Limb samples.

The regression line in Figure 4.8 (b) intersects the iron axis at just over 1%. No cobalt is associated with iron concentrations of less than about 1%. If the iron concentration is taken to be approximately proportional to the amount of pyrite present in the argillite, then Figure 4.8(b) indicates that cobalt only appears in the pyrites as the pyrite concentration increases.

(iv) Copper-iron-sulphur relationship

The variation in the composition of copper, iron and sulphur in the Baluba Centre Limb rocks is presented in the Cu-Fe-S ternary diagram in Figure 4.9.

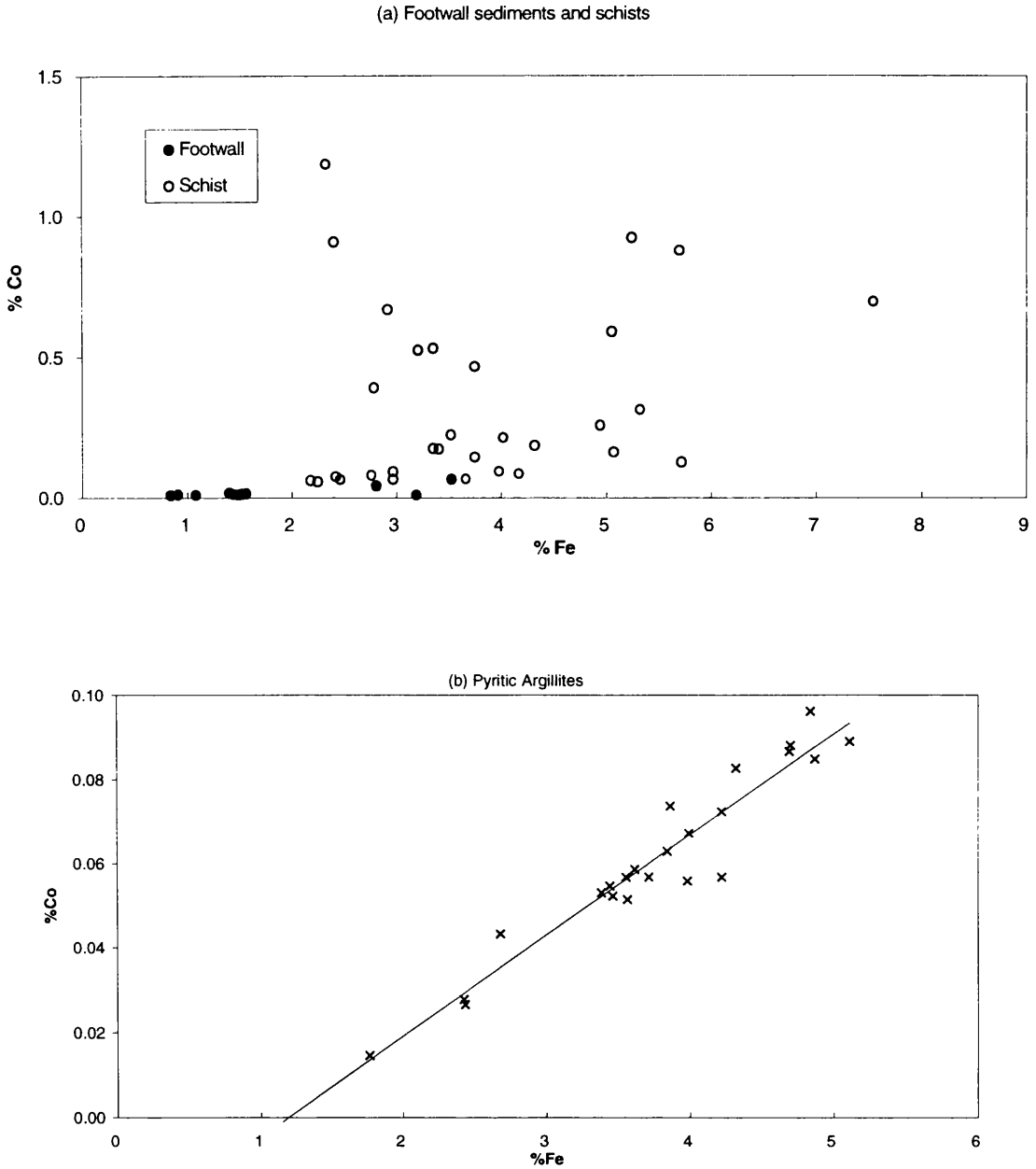

Figure 4.8: Plot (a) shows the absence of correlation between iron and cobalt in the footwall sediments and in the schists. This is because of the co-existence of a mixture of Cu-Fe-S and Cu-Co-S minerals in the footwall sediments. The outlying schist samples enriched in cobalt indicate the effect of cobalt mineralisation due to carrollite($CuCo_2S_4$); causing an increase in cobalt concentration without a corresponding increase in iron. (b) shows a plot of cobalt against iron in the pyritic argillite samples. The linear correlation between iron and cobalt in the pyritic argillites is demonstrated. Since the iron in the upper parts of the argillites is mainly due to pyrite mineralisation the correlation between iron and cobalt concurs with the assertion that cobalt occurs in solid-solution within the pyrites in the argillites. The data used are the ICP-AES analyses of a mixture of 80 underground drill hole, chip and grab samples from Baluba Centre Limb (see Appendix E.I).

other Cu-Fe-S bearing minerals. This is in agreement with chalcopyrite being the commonest sulphide mineral in the Baluba Centre Limb deposit.

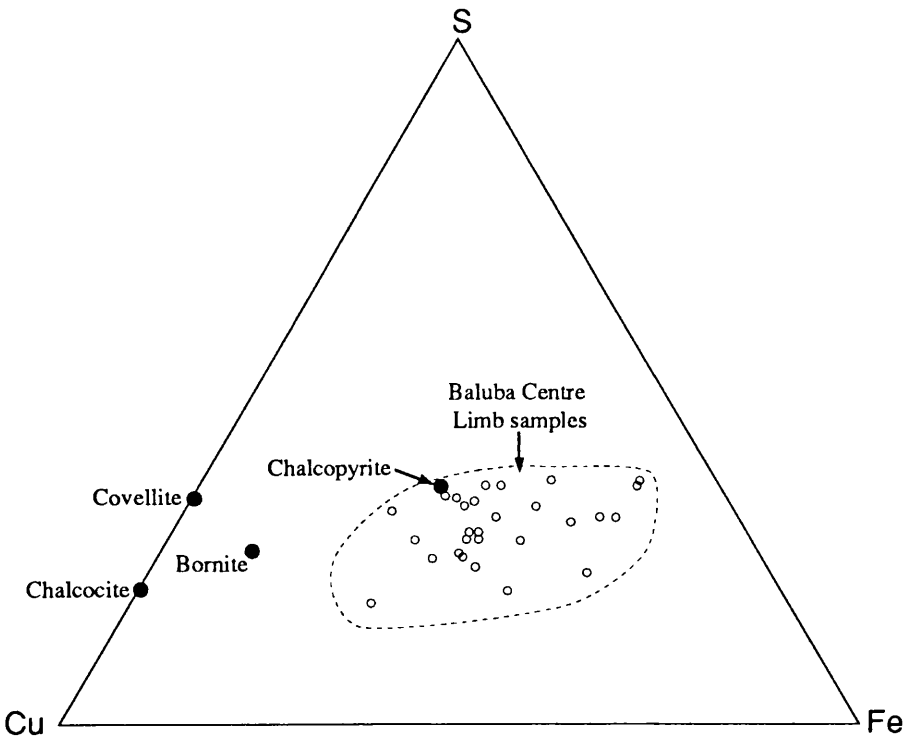

Figure 4.9: Cu-Fe-S ternary plot of the Baluba Centre Limb rocks.

4.5 UNIVARIATE STATISTICS OF COPPER

4.5.1 Data source

The data set used for the statistical analysis has been derived from the assay grades generated by diamond drill core sampling in the Baluba Centre Limb. The assay data together with the geological information used have been extracted from geological logs of underground diamond drill cores. 26 drill holes containing a total of 911 samples analysed at the Baluba mine laboratory have been used for the statistical analysis. The format of the data used is described in Appendix A and the data base is contained on a floppy disk enclosed with this thesis. The pattern of the intersection of the drill holes through the mineralised horizons is not a regular grid. The plan showing the locations of the projected footwall intersections of the drill holes used is presented in Figure 4.10 (enclosed in the pocket at the back page).

Missing and Zero values

The number of samples on which total copper assay values are available is greater than the number of samples with either acid soluble copper or cobalt assay values. All the 911 samples used in this study had total copper assay grades. Of these, 842 samples had accompanying acid soluble copper assays and 883 had cobalt assays. The discrepancy in the number of assays arises because some of the samples have not had the concentrations for acid soluble copper and/or cobalt determined at the mine assay laboratory. This situation arises when there are chemical shortages at the mine assay laboratory and only the total copper concentration is determined.

In addition to the samples with missing acid soluble copper and cobalt values, there are those samples whose acid soluble copper and/or cobalt values are reported as zero. These are assays from samples in which the acid soluble or cobalt concentrations are very low and hence close to, or below the analytical procedure's detection limit. It is, however, not uncommon for some of these low grade samples to be reported as blank assays, hence unclear as to whether they are zero assays or undetermined values.

Statistically, a distinction must be made between the samples with missing, undetermined acid soluble copper and cobalt assay values and those whose assays are reported as zero. Accepting the convention that the low-concentration samples should be recorded as zero and the undetermined assays left as blank values, there are four categories to which samples with missing and zero assays may belong:

(i) samples not analysed and whose assays are correctly recorded as blank values;
(ii) samples not analysed but whose assays are wrongly recorded as zero;
(iii) samples with low, below detection limit assays correctly recorded as zero and
(iv) samples with concentrations below the detection limit wrongly recorded as blank values

To avoid the danger of mixing the missing and the zero sample values, acid soluble and cobalt assay values have not been used in the univariate statistical analysis.

Sample support regularisation

The support of the variable associated with a sample is defined by the volume, shape and orientation of the sample. Bigger samples have larger volumes, hence greater support, and should have a greater influence on the statistics than the smaller samples. If the statistics are calculated using assay grades from the samples of unequal lengths a bias is introduced due to the different supports associated with the sample grades. To remove this bias, it is advisable to regularise the samples to a constant length so that the support of all the samples is constant. Regularisation of sample volumes is described in general terms thus:

$$z_v(x) = \frac{1}{v} \int_{v(x)} z_v(y)\, dy \qquad \textbf{(4.1)}$$

where $z_v(x)$ is the grade of the regularised samples (of a regular sample volume x)
$z_v(y)$ is the grade of the original samples (of variable sample volumes y)

Strictly the support of the samples should be their volumes. However, if the core diameter is constant then the volumes of the cores is directly proportional to their lengths.

In the Baluba Centre Limb the lengths of core samples on which the assay values were determined was not uniform. The lengths of the core samples ranged from 0.2m to 2.0m, with the two commonest core lengths being 0.5m and 1.0m (see Fig. 4.11). The drill holes used in this study were all the same diameter: of AX sized core (about 32mm in diameter). Regularisation of the support was achieved by regularising the sample lengths.

It is justified to regularise the sample lengths to a length which is also the commonest in the original samples. This ensures that as many as possible of the generated regularised samples retain the characteristics of the original 'real', actual samples after the regularisation process. Based on the histogram of the core lengths displayed in Figure 4.11 the regularisation length for the Baluba Centre Limb data should be a choice of either 0.5m or 1.0m, the two commonest sample lengths of the original samples. For example consider a 2m long drill core that is sampled in 1.0m, 0.4m and 0.6m pieces. Regularization of this drill core to uniform 0.5m and 1.0m lengths is illustrated in Figures 4.12(a) and 4.12(b) respectively.

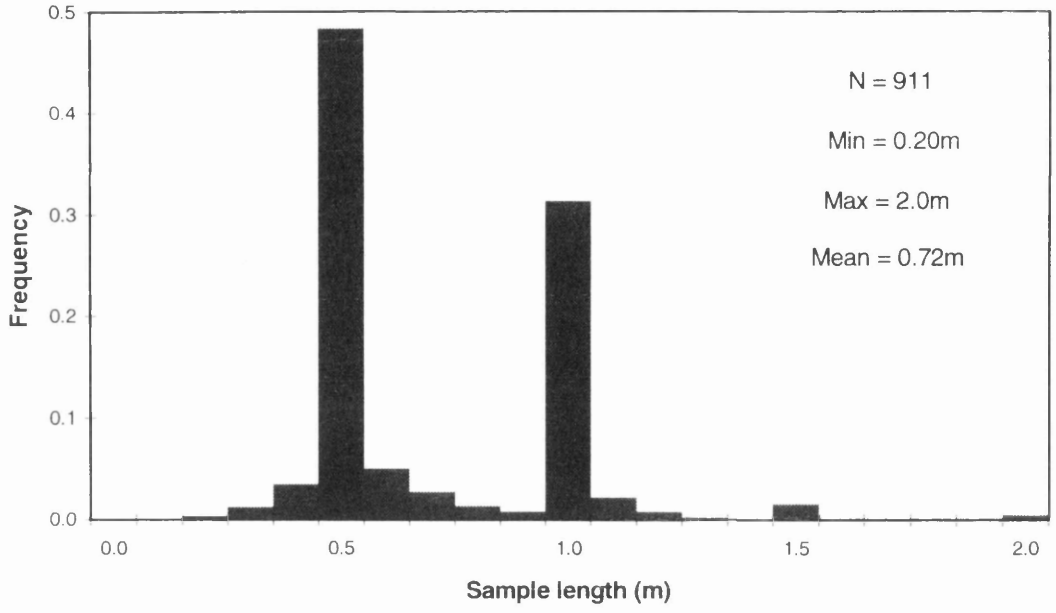

Figure 4.11: Histogram of sampled core lengths in the Baluba Centre Limb drill holes

In regularising to a 0.5m length, samples whose original widths are longer than 0.5m have to be split into shorter constituent lengths after regularisation. There is a danger that if the regularised length is much shorter than the average length of the actual samples, some of the regularised samples could arise from the same original sample. This would effectively result in replicating assay grades of actual samples. The assumption that the within-sample variance is zero is clearly not correct since the petrological, geochemical and mineralogical data presented earlier in this chapter indicate that there is mineralogical and mineralisation heterogeneity in the rocks. It is improbable that if the first two 0.5m regularised samples which come from the same original sample were analysed they would both result in a grade of exactly 2% equitably distributed between them (Fig. 4.12(a)).

If, on the other hand, the samples were regularised to a 1.0m uniform length, the grade of the first sample would remain the same in the unregularised and the regularised samples since the length of both the original and the regularized sample remains unchanged at 1.0m; the sample is not altered at all. The second and third samples of the original core which are less than 1.0m wide are composited to produce a 1.0m regularised sample. The average grade assigned to the second 1.0m regularized composite is the weighted average grade of the 0.4m and 0.6m samples (Fig. 4.12(b)).

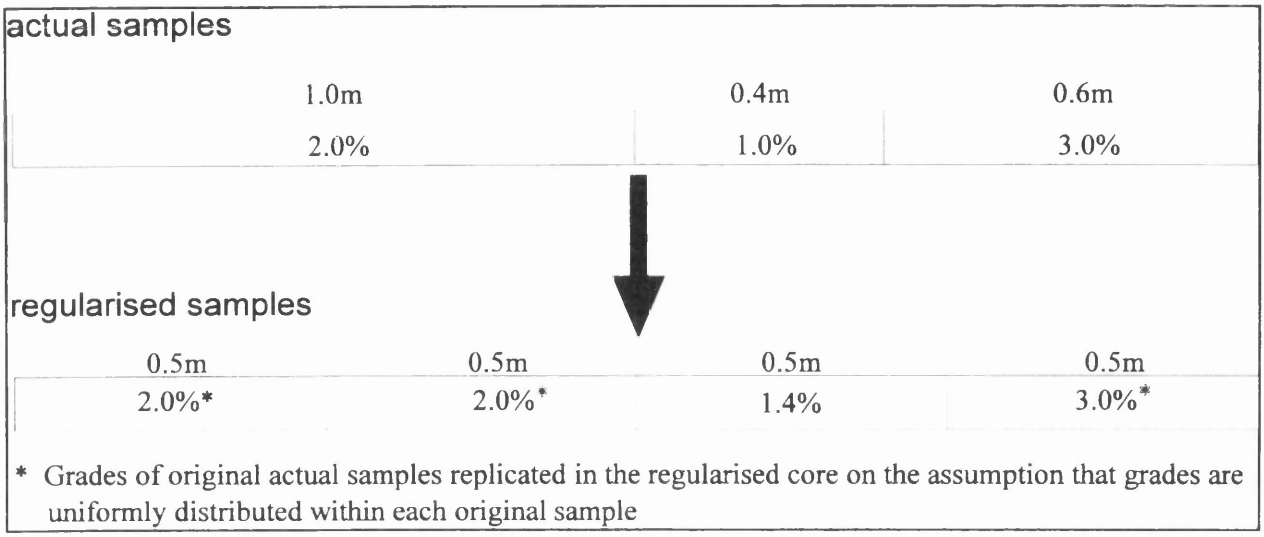

(a): Sample regularisation to a length shorter than the mean of the original sampled core lengths.

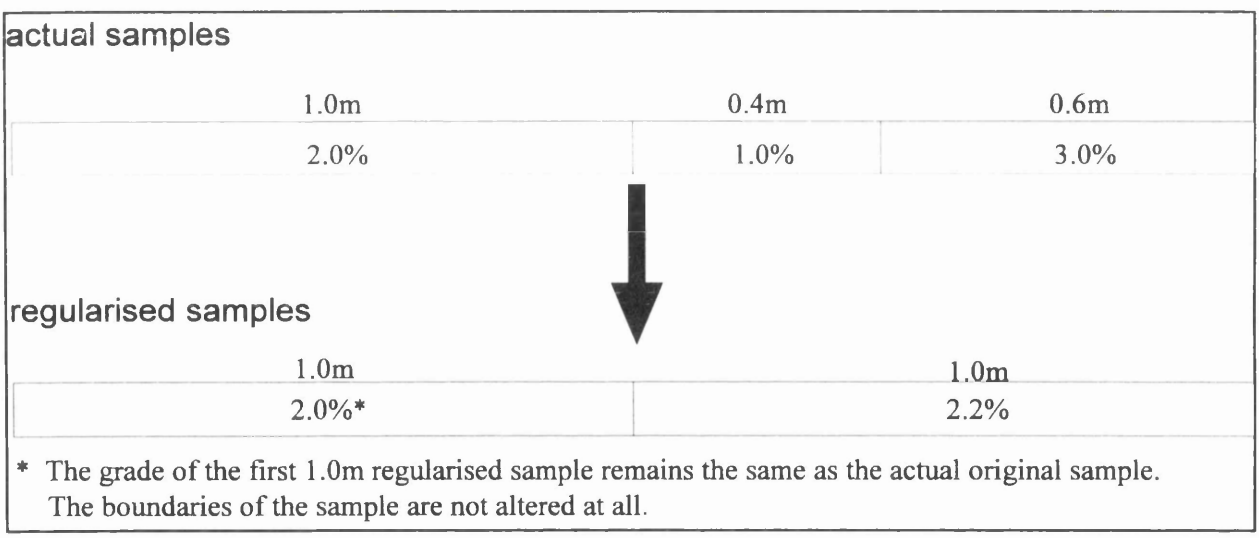

(b): Sample regularisation to a length longer than the mean of original sampled core lengths

Figure 4.12: Sample regularisation

It is reasonable to assign the average grades of the shorter original samples to the accumulated longer regular samples as exemplified in Figure 4.12(b). This process has a physical justification. If the

metal content in a regularised longer piece of 1.0m were analysed it would be expected to be equivalent to the weighted average grade of the shorter constituent cores of 0.4m and 0.6m.

To avoid the risk of sample grade replication that could arise when samples are regularised to a shorter length as displayed in Figure 4.12(a), 1.0m rather than 0.5m has been chosen to be the regularised length for the Baluba Centre limb samples. Generally, the length of the reconstituted regular samples should not be smaller than the mean length of the actual samples, otherwise the reconstitution process results in the artificial creation of information (Journel and Huijbregts, 1978). The generated 1.0m composite samples have 649 values of total copper grades, 352 of acid soluble copper and 627 of cobalt.

Univariate statistics

The organisation and presentation of large data sets into coherent, smaller groups is essential to enable the features observed in the data to be effectively assessed. In this section the statistics will be evaluated on samples grouped into lithological and mineralogical classes as geological controls. The total data set was in the first instance sorted into three lithological categories; the footwall sediments (quartzites and conglomerates), schists and argillites. The argillite category was further split into two sub-groups based on the metallic mineralogy. The pyrite mineralisation was taken as the distinction between the cupriferous (ore) and the hangingwall argillite. The lower part of the argillite in which chalcopyrite is the main sulphide mineral was classified as the cupriferous argillite and the higher part of the argillite where pyrite is the main sulphide mineral was classified the hangingwall argillite.

(i) Variance and coefficient of variation

Distributions of some variables show that the standard deviation is proportional to the mean of the variable under review. The Baluba Centre Limb copper grades have been found to exhibit a proportional effect between the standard deviation and the mean (Fig. 4.13). Because of the proportional effect the absolute variances should not be compared without due regard to the mean grades of the samples under review. The variance in copper grades in the schists, for example, is expected to be higher than that in the footwall rocks. The higher variance of the grades in the schists would not necessarily signify greater variability than that of the grades in the footwall; it could merely be a consequence of the proportional effect. Owing to the presence of the proportional effect,

it is desirable that to compare the variability in the various lithologies an estimator which took into account the relationship between the means and variances of the grades be used.

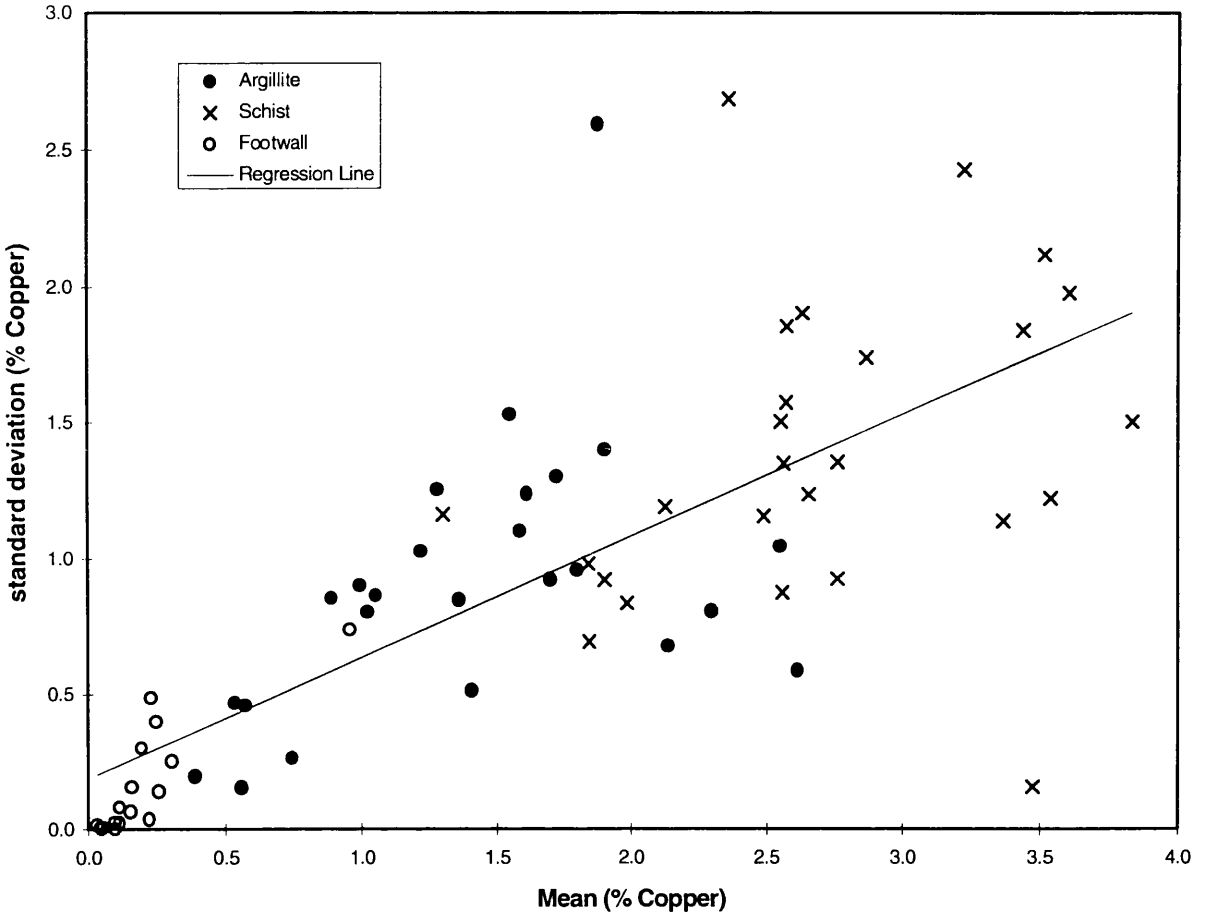

Figure 4.13: Mean-variance proportional effect demonstrated in the Baluba Centre Limb rocks. The lithologies with higher mean grades display higher variances than those with lower mean grades. The data used were 26 drill holes located in the Baluba Centre Limb (data on disk accompanying thesis - Appendix A). Each point represents the mean copper grade and the corresponding variance within a lithological class along each drill hole.

The coefficient of variation incorporates the standard deviation and the mean (coefficient of variation = standard deviation ÷ mean). It identifies the presence of extreme data values in a distribution. Data which are derived from the same population would be expected to display similar coefficients of variation. Care should, however, be taken in interpreting the coefficient of variation as it is only correctly applied if all the data values in the distribution are positive. The coefficient of variation results may be distorted when dealing with log-transformed data since grades less than 1% give rise to negative values when log-transformed. The coefficient of variation has been used to interpret the

distributions of the actual and the regularised samples, but not of the log-transformed grade data for the Baluba Centre Limb samples.

From histograms of copper grades displayed in Figures 4.14 and 4.15 and Tables 4.5 and 4.6, the determination of the coefficient of variation for the Baluba centre Limb samples indicates that:

(i) the regularised samples exhibit smaller coefficient of variation than the irregular samples. This implies that there is generally a tendency to normal distributions as a result of sample regularisation.

(ii) The coefficient of variation is lower in the orebody lithologies (cupriferous argillites and schists) than in the footwall (quartzites/conglomerates) and hangingwall (pyritic argillites) lithologies. The presence of even a trace of high copper mineralisation is quite sensitive to the distributions the low grades in the footwall and hangingwall, hence the high levels of coefficient of variation.

(ii) Skewness

The coefficient of skewness for a normal (Gaussian) distribution is zero. Positive values of the coefficient of skewness indicate positive skewness and the histograms of such distributions show a long tail on the high values side. The opposite applies for the negatively skewed distributions. The magnitude of the coefficient of variation indicates how long the tail of the distribution extends.

For the Baluba Centre Limb copper distribution it is noted that the magnitude of the coefficient of skewness (disregarding the sign) for the distributions of the copper grades of the unregularised samples within the footwall and hangingwall is higher than that of the distributions of grades within the mineralised schists and argillites (Fig. 4.14 and Table 4.5).

The coefficient of skewness for the distributions in the mineralised schists and argillites decreases when the grades of the regularised samples are used. The distributions of the grades of the regularised samples exhibit a positive skewness. The distribution of the natural logarithms of the grades show a negative skewness. If the grades in the schists and argillites were from a 'true' lognormal distribution it would have been expected that the absolute magnitude of skewness of the log-transformed grades would be closer to zero than that associated with the untransformed grades of the irregular or regularised samples. The samples in the mineralised argillite actually show a

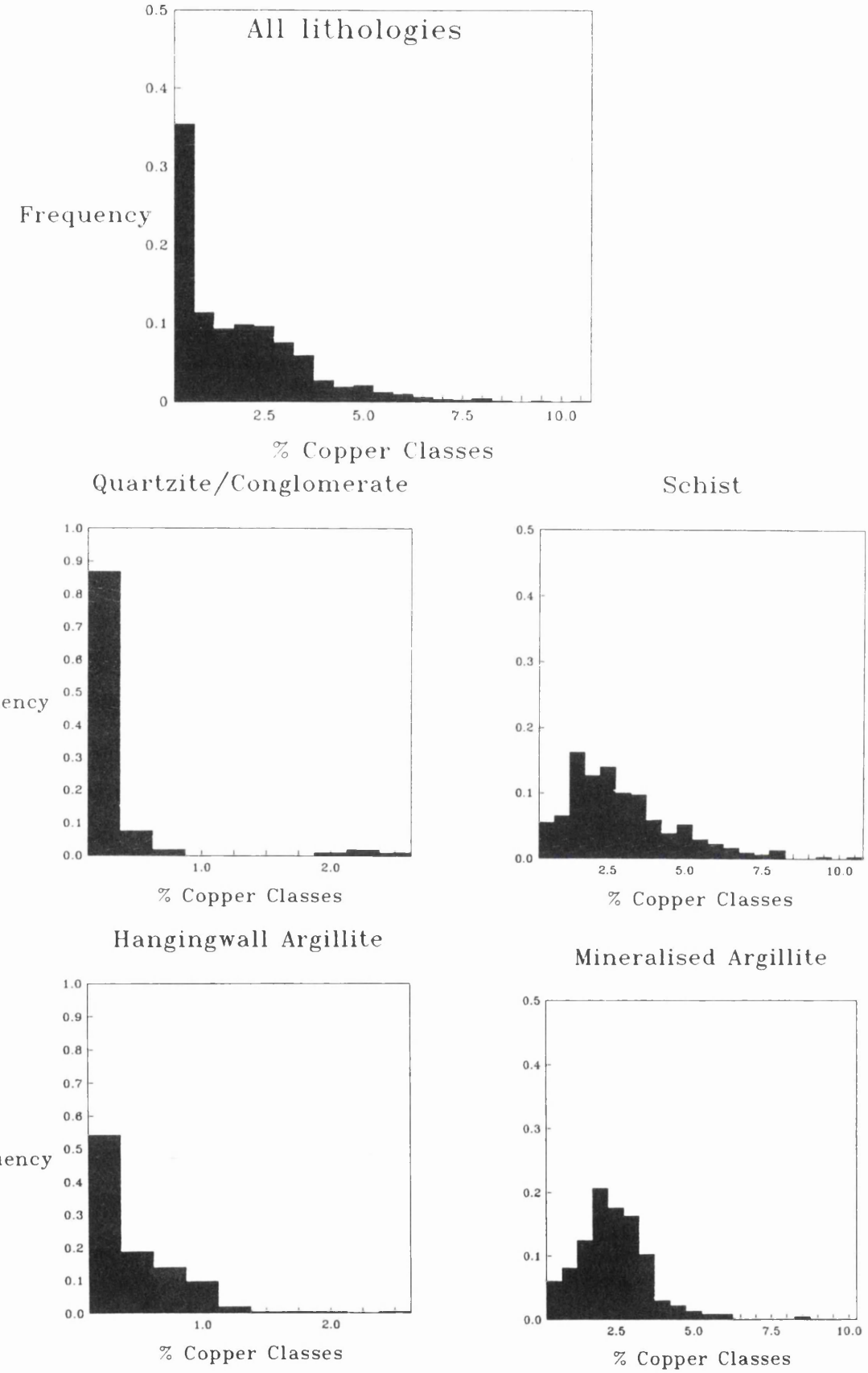

Figure 4.14: Histograms of copper grades in unregularised samples.

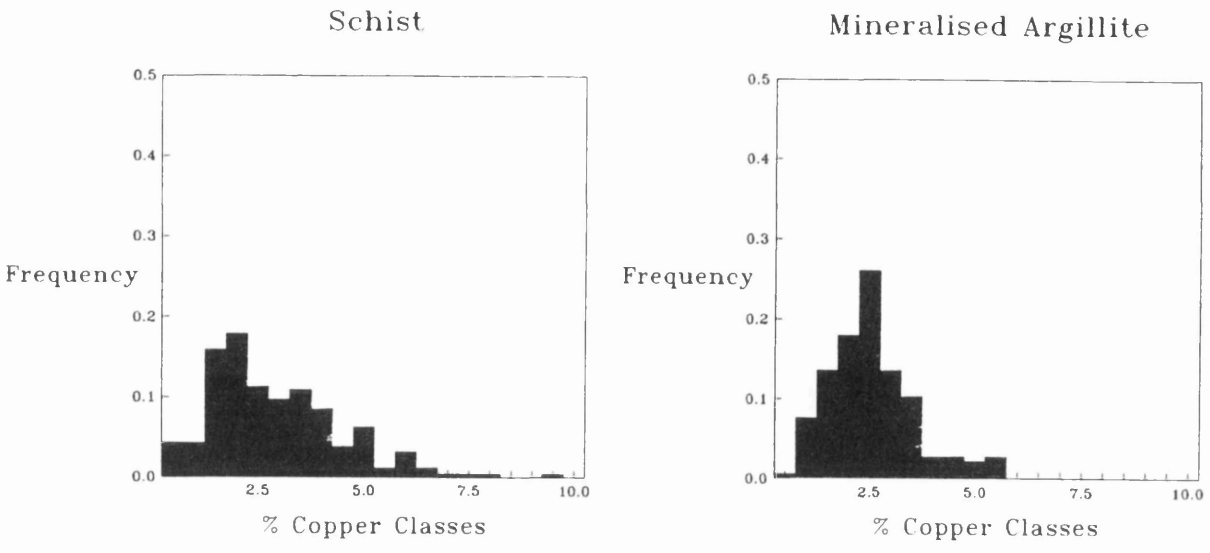

(a) Untransformed copper grades

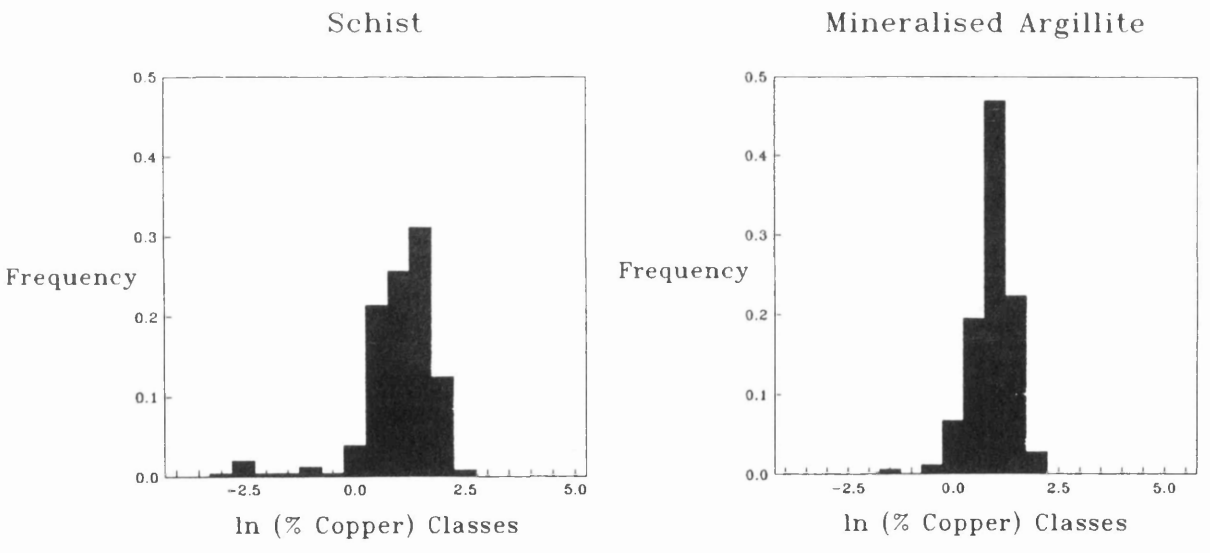

(b) Log-transformed copper grades

Figure 4.15: Histograms of copper grades in 1m regularised samples.

larger magnitude of skewness for the distribution of the logarithms of the grades than for the untransformed grades. Therefore in the mineralised sediments, it would seem that a shift towards the normal distribution is achieved by regularising the samples and that there is little or no further shift towards normality by using the logarithms of the grades.

A summary of the skewness and coefficient of variation of the copper grades of actual, unregularised samples in the mineralised and footwall and hangingwall lithologies of Baluba Centre Limb is provided in Table 4.5. A summary of the results on regularised samples in the mineralised lithologies (the schists and argillites), is given in Table 4.6.

Table 4.5: Statistics summary of copper grades in actual unregularised core samples in the Baluba Centre Limb.

Lithological group	Number of samples	Mean % Cu	Variance $\%^2$ Cu	Coefficient of Skewness	Coefficient of variation
All	911	1.58	2.58	1.41	1.01
Footwall	106	0.20	0.16	4.32	2.02
Schist	533	2.51	2.28	1.36	0.60
Cupriferous Argillite	229	2.19	1.31	1.01	0.52
Pyritic Argillite	268	0.33	0.12	1.71	1.03

Table 4.6: Statistics summary of copper grades in regularised core samples in the Baluba Centre Limb.

Lithological group	Grade transformation	Number of samples	Mean % Cu	Variance $\%^2$ Cu	Coefficient of Skewness	Coefficient of variation
Schist	Untransformed	257	2.65	2.30	0.98	0.57
	Log-transformed	257	0.79	0.44	-2.25	0.84
Cupriferous Argillite	Untransformed	179	2.23	0.81	0.54	0.40
	Log-transformed	179	0.71	0.21	-1.06	0.65

4.6 DISCUSSION

In this chapter it has been shown that the variations in the rock geochemistry are related to the petrography of the Baluba Centre Limb rocks. The compositions of the copper bearing minerals in the Baluba Centre Limb have been found to be essentially consistent with the theoretical stoichiometries, but the compositions of cobalt bearing minerals deviate considerably from the theoretical compositions. Hence, the copper metal content in the orebody is basically a function of

the concentration of the copper-bearing minerals within the rocks but the cobalt content depends on the concentration of the cobalt-bearing minerals within the rocks as well as the mineralogical variation of cobalt within the minerals.

Carrollite is the principal cobalt bearing mineral in the schists but cobalt is contained in cobaltiferous pyrite in the upper portions of the orebody in the argillites. Some carrollites were observed to contain nickel. This is interpreted to be the nickel in solid-solution within the carrollite structure. The cobaltiferous nature of pyrite has been established. The existence of cobalt within the pyrites in the argillites is significant because cobalt mineralisation persists beyond the limits of the orebody currently defined by a 1% copper assay cut off. Any attempts to exploit the cobalt in the hangingwall region of the orebody would require the careful analysis of the pyrites within the argillites.

The departure from the normal (or lognormal) distribution obtained for the copper assay grades in the Baluba Centre Limb is due to the mixture of mineralisation from different groups of copper-bearing minerals. The apparent outliers which appear in the histograms were signified by the increase in skewness and are most likely due to small scale variations in mineralisation. Partial simplification of the data is obtained when the data is classified into lithological and mineralogical categories.

Sampling is not carried out through the entire lithological spans in the footwall and hangingwall. The distributions obtained in the footwall and hangingwall sections are therefore of incomplete, truncated populations. To get a fuller picture of the distribution would require sampling deeper into the footwall and hangingwall margins of the orebody to cover their entire lithological extents.

CHAPTER 5

SAMPLING AND ANALYTICAL QUALITY CONTROL

5.1 INTRODUCTION

The uncertainties introduced during sampling and chemical analyses have an effect on the confidence that can be attached to the assay grades of samples. Hence the necessity to estimate the sampling and analytical variances, and to estimate the precision and accuracy associated with the analyses. The difference between the value attached to the sample (the estimator) and the true value represents the sampling error. If the assay data are to be used with confidence in describing mineralisation then it is desirable that the chemical analyses be as close as possible to the true values (accurate) and that the analyses should be reproducible (precise). Sampling should be able to take into account the variations brought about by the distributions of the minerals within the rocks.

The objective of this chapter will be to assess the sampling methods currently used at Baluba and to estimate the uncertainties associated with them. Sampling variances associated with diamond drill and chip sampling of the different lithologies will be evaluated. The precision and accuracy associated with the analytical methods currently applied will also be evaluated.

5.2 ANALYSIS OF VARIANCE

The Analysis of Variance (ANOVA) method separates the total measured variance into three components; analytical, sampling and geochemical variances. Geochemical variance is a measure of the variation of concentration of minerals within the samples. It is an intrinsic aspect of mineralisation as it arises from the distribution of the minerals within the rock and it is essentially a measure of the heterogeneity of the mineralisation. Sampling and analytical components of variance on the other hand are introduced during sampling and chemical analysis and are compounded onto the geochemical variance.

The three components of variance need to be estimated in order to measure the significance of the variances introduced by sampling and chemical analysis (Ramsey *et al.*, 1992). It is essential that the sampling and analytical components of variance be minimised so that the estimated variance reflects the true geochemical variance as closely as possible.

A measurement of an analyte concentration can be represented as:

$$x = x_{true} + \varepsilon_s + \varepsilon_a \qquad (5.1)$$

where x is the measured concentration,
x_{true} is the true geochemical concentration,
ε_s is the sampling error and
ε_a is the analytical error.

If the sources of variation are independent then the total variance can be stated thus:

$$\delta^2_t = \delta^2_g + \delta^2_s + \delta^2_a \qquad (5.2)$$

where δ^2_t is the total variance,
δ^2_g is the geochemical variance,
δ^2_s is the sampling variance, and
δ^2_a is the analytical variance.

The sum of the sampling and analytical variances is the technical variance (δ^2_{tech}):

$$\delta^2_{tech} = \delta^2_s + \delta^2_a \qquad (5.3)$$

$$\therefore \delta^2_t = \delta^2_g + \delta^2_{tech} \qquad (5.4)$$

It is difficult to determine what absolute levels of uncertainty (sampling, analytical and geochemical) should be allowed in a sampling and chemical analytical scheme. In geochemical applications the acceptable limits of variances are somewhat arbitrary. Ramsey *et al.* (1992) and Ramsey (1993) have suggested, based on the experience from geochemical sampling campaigns, that for a clear description of the natural geochemical variance the technical variance should comprise no greater than 20% of the total variance, otherwise the geochemical information becomes distorted. Using the same criterion, it is suggested that the analytical variance should comprise no more than 20% of the technical variance, or equivalent to 4% (20% of 20%) of the total variance (see Fig. 5.1). If the technical variance is found to be greater than 20% of the total variance then there is a need to reduce the technical variance component. This is usually achieved by reducing the sampling variance

component rather than the analytical variance component. However, if in addition the analytical variance exceeds 4% of the total variance then the technical variance can be reduced by improving the analytical precision.

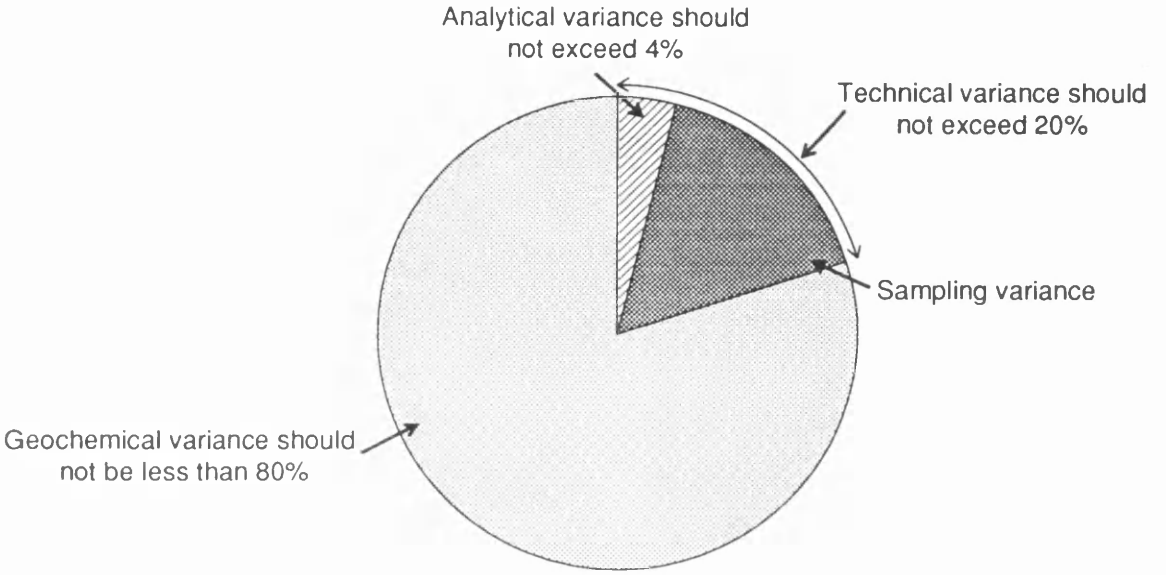

Figure 5.1: Pie chart showing the maximum allowable analytical and technical variances in analysis of variance (After Ramsey *et al.*, 1992).

5.2.1 Analysis of Variance in Baluba Centre Limb

Diamond drill and chip sampling are the main sampling methods used at Baluba. Diamond drill samples are continuous while chip samples are discrete, point samples (see Table 5.1). It is expected that diamond drill sampling should give rise to lower sampling variances than chip sampling since diamond drill samples are more complete compared to the discontinuous chip samples. The total continuum of mineralisation is not obtained during chip sampling and some information about mineralisation continuity between sampling points might be missed. The lack of continuity in chip samples renders them less representative [than drill hole samples] of the rock mass they represent.

71 samples from drill holes BL0016, BL0031, BL0032 and BL0033, and 55 chip samples from blocks A, B, C, J and K were used for the ANOVA estimation. The sampling data used for the ANOVA evaluation is given in Appendix F.I. The locations of the drill holes and chip samples are presented in the plans and sections in Figure 4.10 and in Appendix J.

To estimate the three components of total variance requires that duplicate samples are available and that duplicate analyses are carried out on each sample.

Table 5.1 Comparison of diamond drill and chip sampling.

Diamond drill sampling	Chip sampling
- *continuous samples (subject to high core recovery)	- discrete samples
- core diameter is regular (or controlled) and the size of samples is determined by sample width	- irregularly shaped samples of unequal volumes
- little contamination	- liable to contamination on the surfaces of development walls
- can sample areas that are not physically accessible	- can only sample accessible areas that have been opened up by development excavations
- expensive drill machinery and skilled manpower required	- requires cheap hand held tools and manpower is easily trained

Note: *High core recovery is important in the acquisition of representative samples (Ranta *et al.*,1984). Drill cores can be relatively free from bias if the core recovery during drilling were 100 percent (Peters, 1987; Dixon, 1979). However, differential core losses may occur in diamond drill holes, especially in the softer parts of the rock (see Plate 5.1).

Analytical variance was evaluated from analytical duplicates, sampling variance from sample duplicates and geochemical variance from differences between the samples. The sampling scheme applied is shown in Figure 5.2.

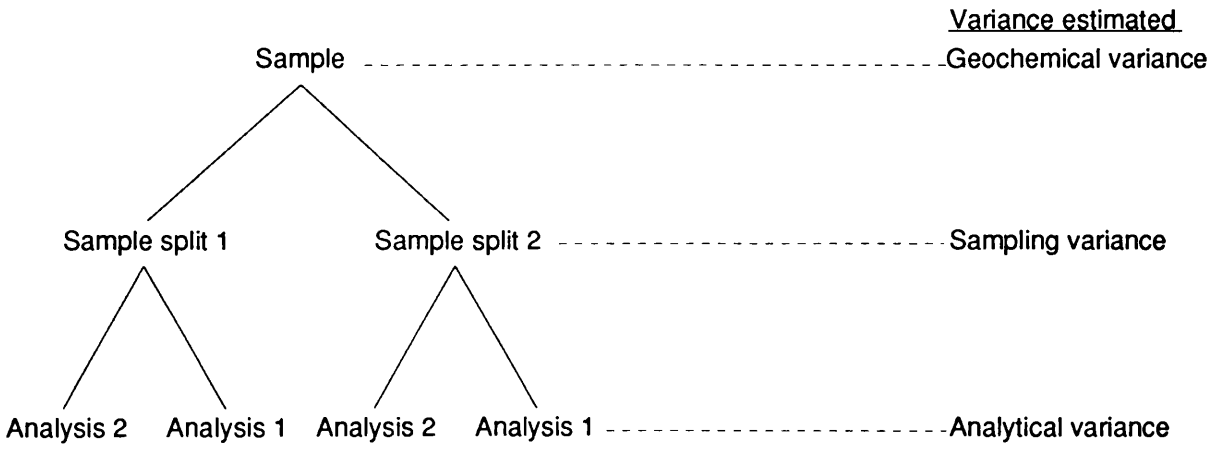

Figure 5.2: Sampling and analysis design for the analysis of variance for Baluba Centre Limb.

Plate 5.1: Diamond drill sampling

The plate shows diamond split drill core. The main advantage of diamond drill sampling is the continuous nature of the core obtained. The continuity of the diamond drill cores is, however, subject to the recovery of the drilled core. In weak ground (e.g. in the pyritic argillite in this plate) some core may be lost during drilling. The rows in the core box are 1.5m long. Drill hole BD239, 560m SS44 Return Airway Crosscut.

Since the aim in this study is to compare the two methods of sampling (diamond drill and chip sampling) in Baluba Centre Limb, the results are presented in Table 5.2 as percentage contributions of the component variances to the total variance rather than as absolute variances to allow the comparison between the two sampling methods.

Table 5.2: Baluba Centre Limb analysis of variance results - copper.

		% contribution to total variance				% contribution of analytical variance to technical variance
	Mean (%)	Analytical δ^2_a	Sampling δ^2_s	Technical δ^2_{tech}	Geochemical δ^2_g	
Diamond Drill Sampling						
Argillite	1.282	3.7	15.8	19.5	80.5	19.0
Schist	2.317	0.2	12.5	12.7	87.3	2.3
Chip Sampling						
Argillite	0.346	-	-	*38.3	61.7	-
Schist	2.887	-	-	*23.1	76.9	-

* The analytical and sampling variance components were not determined separately for the chip samples because duplicate analyses were not carried out on the chip samples.

From Table 5.2 it can be noted that:

(i) The technical variance component in argillite is greater than that in schist for both diamond drill and chip sampling. This is a function of the remobilisation of the metal-bearing minerals into metamorphic veins as discussed under the geology of Baluba and under metamorphism (see Chapters 2 and 3). The argillite samples are more heterogeneous than the schist samples. In effect this means that a substantial proportion of the total variance in argillite is induced by sampling, and is not true geochemical variance.

(ii) The chip samples have a larger technical variance than the diamond drill samples. The chip samples are discrete and more discontinuous than the diamond drill samples. Therefore there is a higher probability of obtaining selective and biased samples during chip sampling than during diamond drill sampling.

(iii) Although analytical and sampling variance components in chip sampling could not be segregated, it can be assumed that, as for diamond drill sampling, the analytical variance component of chip samples is small compared to sampling variance since the analytical determinations on both diamond drill and chip samples were identical. The analytical variance for diamond drill samples is less than the maximum allowable levels, 4% of total variance or 20% of technical variance.

Sampling variance is a function of the variability of the metallic mineralogy and is also affected by the sample size compared to the mineral size. A smaller sampling variance would be expected in a rock comprising one metallic mineral only (mono-mineralic) compared to one comprising a mixture of metallic minerals (poly-mineralic). Within either the mono- or poly-mineralic category a higher sampling variance can be expected if the mineralisation occurs in a mixture of the disseminated and massive type rather than if the mineralisation is of one texture only.

In terms of copper-bearing minerals the mineralisation in the schists is poly-mineralic (mixed copper sulphides and oxides) but is evenly disseminated. Copper mineralisation in the argillites is mono-mineralic (chalcopyrite) but occurs in the disseminated as well as massive forms.

ANOVA results presented in Table 5.2 indicate that the sampling variance component is greater in the argillites than in the schists. From Table 5.2 it would seem that the mineralisation texture is more critical to sampling variance than the variability in the metallic minerals.

Based on the ANOVA results, there appears to be a need to reduce the technical variance component associated with chip sampling. This could be achieved by reducing the sampling variance component since the analytical variance component is smaller than the critical limits (20% of the technical variance or 4% of the total variance as shown in Figure 5.1). The geochemical variance of the chip samples in argillites accounts for less than half of the total variability associated with the samples. The target should, therefore, be to reduce the technical variance associated with chip sampling to a level closer to 20% of the total variance; the maximum level of technical variance allowable.

5.3 ANALYTICAL DATA QUALITY CONTROL

5.3.1 Precision

Precision is the measure of agreement between replicate analyses. The difference between the first and replicate analyses is a measure of the analytical error (Equation 5.5).

$$error = | c_1 - c_2 | \qquad (5.5)$$

Precision terms have been calculated for the Baluba Centre Limb using 142 pairs of duplicate analyses carried out in the Baluba mine laboratory on drill holes BL0016, BL0031, BL0032 and BL0033. Precision has been estimated for the Baluba laboratory AAS analysis by evaluating how the replicate analyses differ from one another. The data for precision analysis for the Baluba Centre Limb is presented in Appendix F.II.

Assay checks

The repeatability of analyses can in the first instance be checked by examining whether replicate analyses deviate significantly from the 45° line on the scatter plot. Poor precision can also be indicated if the spread of pairs of replicate analyses is such that a significant number of them plot outside prescribed confidence limits (usually 95% confidence).

In Figures 5.3 and 5.4 the Baluba Centre Limb copper and cobalt replicate analysis pairs have been plotted against each other in order to evaluate the analytical error on the AAS copper and cobalt analyses of the Baluba laboratory. The slopes of the regression lines of less than 1 are obtained and indicate that for both copper and cobalt analyses there was a slight underestimation of the replicate analyses compared to the initial ones (Tables 5.3 and 5.4). The regression lines deviate from the 45° lines but t-tests indicate that the deviations from the 45° lines are not statistically significant. The t-values of the deviations of the duplicate analysis points from the linear regressions are smaller than the theoretical t-distribution values at the 95% confidence levels. It is noted that all the replicate pairs fall within the 2 standard deviation limits.

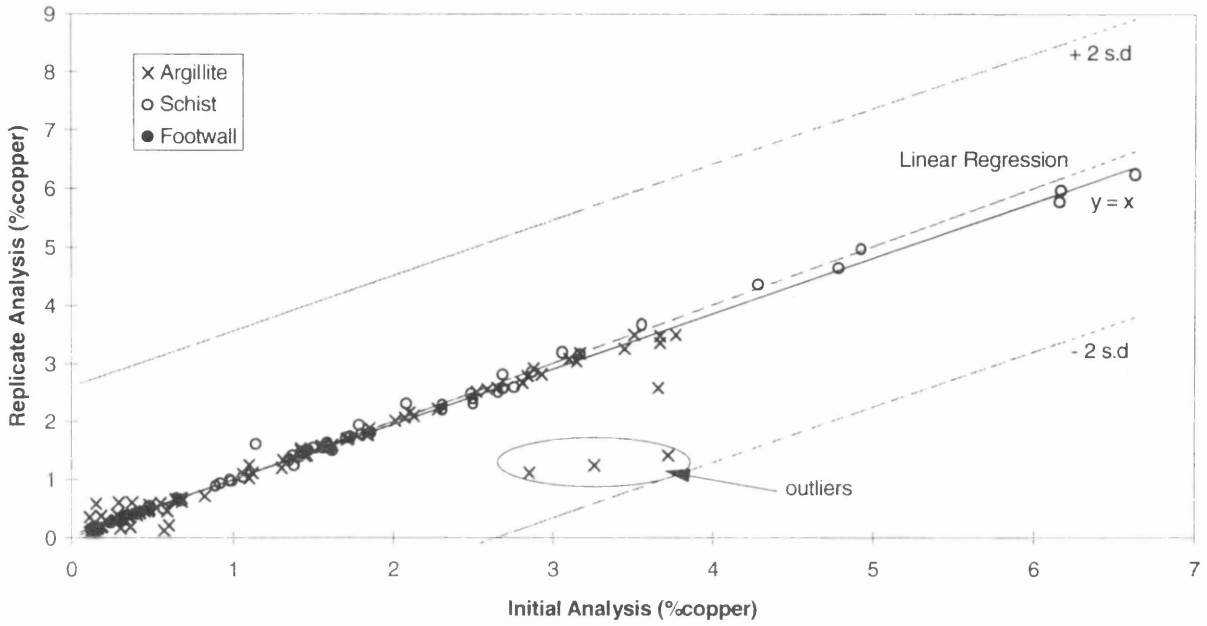

Figure 5.3: Baluba laboratory AAS replicate analyses for copper. The three outlying replicate analyses of the argillite samples in drill hole BL0016 are attributable to operator bias. The three outlier samples were reported by the assay laboratory as possible spurious analyses and have been excluded from the regression analysis.

Table 5.3: Baluba AAS copper duplicate analyses (concentration in % copper)

Number of samples =	142
Mean =	1.527
Standard deviation =	1.303
Regression coefficient =	0.066
Standard error of coefficient estimation =	0.316
Slope of regression line =	0.963
Standard error of slope estimation =	0.020
Degrees of freedom =	140
Mean of differences between duplicates =	-0.010
Theoretical t-value at 95% confidence =	1.980
Calculated t-value =	0.951

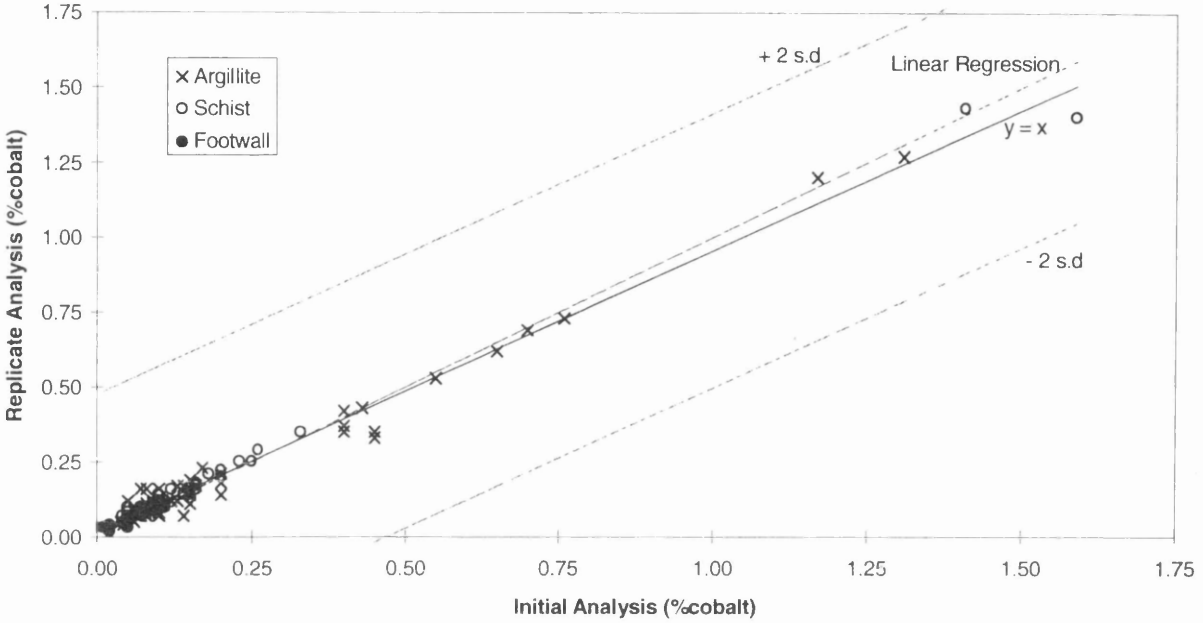

Figure 5.4: Baluba laboratory AAS replicate analyses for cobalt

Table 5.4: Baluba AAS cobalt duplicate analyses (concentration in % cobalt)

Number of samples =	142
Mean =	0.173
Standard deviation =	0.234
Regression constant =	0.021
Standard error of constant estimation =	0.053
Slope of regression line =	0.919
Standard error of slope estimation =	0.019
Degrees of freedom =	140
Mean of differences between duplicates =	-0.007
Theoretical t-value at 95% confidence =	1.980
Calculated t-value =	0.790

Precision estimation

Precision is related to concentration by the following equation:

$$s_c = s_o + kc \qquad (5.6)$$

where s_c is the standard deviation of analysis,
s_o is the standard deviation of analyses at zero concentration,
k is the limiting high level precision and
c is the analyte concentration.

The relationship in Equation 5.6 assumes that the precision of the analytical method (s_c) varies as a linear function with concentration. The function s_o is an estimate of the precision at zero concentration and is related to the detection limit of the analytical method used.

The graphical procedure described by Thompson and Howarth (1976) is used to obtain the precision terms s_o and k using the relationship defined in Equation 5.6. The procedure is described as follows:

(i) Calculate means for pairs of duplicate analyses and also evaluate the absolute differences between the pairs, i.e. $(x_i + y_i)/2$ and $|x_i - y_i|$

(ii) Arrange the means of pairs of analyses into an ascending order.

(iii) Split the means into groups containing 11 pairs each.

(iv) Obtain the means for each of the groups of 11 sample pairs and evaluate the median of the differences between the pairs in each group of 11. Repeat for successive groups of 11. The last group is ignored if it contains less than 11 pairs.

(v) Carry out weighted linear regression with the means of 11 analytical pairs in each group as the x variable and the medians of differences as the y variable.

Using the procedure described above s_o is represented by the y intercept on the graph and k by the slope of the graph (see Equation 5.6). To allow for the Gaussian distribution s_o and k, and their respective errors are multiplied by a factor of 1.048 (Thompson and Howarth, 1976).

Once s_o and k have been estimated they can be used to quantify the precision, p_c, at a given concentration.

$$p_c = 2s_c / c \qquad (5.7)$$

The factor of 2 in Equation 5.7 is used because the precision is estimated at 2 standard deviations which approximately corresponds to the 95% confidence level.
Substituting Equation 5.6 into 5.7 leads to:

$$p_c = 2s_o / c + 2k \qquad (5.8)$$

Equation 5.8 can be split into two components; $2s_o/c$ and $2k$. The factor $2s_o/c$ is the precision at zero concentration and $2k$ is the precision at high level concentrations.

To estimate the precision terms the 142 pairs of AAS analysis duplicates have been classed into 12 groups of 11 analytical pairs each (total = 132 pairs), with a last group of 10 analytical pairs not used in the precision evaluation. The last group of the 10 pairs which were not used in the precision estimation were at the high concentration range. In the application of precision estimation to evaluate the detection limit the samples with low concentrations are more critical and therefore the exclusion of the samples with high concentrations does not seriously affect the determination of the detection limit.

Table 5.5: s_o and k values in the precision determination for the Baluba Centre Limb copper and cobalt samples analysed by the AAS method (copper and cobalt concentrations as %).

	s_o	se(s_o)	p(s_o)	Detection Limit	k	se(k)	p(k)	High level precision
Copper	0.005	0.014	0.075	0.111	0.022	0.015	0.230	0.030
Cobalt	0.006	0.007	0.425	0.062	0.061	0.076	0.482	0.101

se = standard error: estimate of the error of the measurements from the mean value.
p = probability: estimate of the chance that the estimated values will fall outside the 95% confidence limits.

The regression lines in Figures 5.5 and 5.6 have positive intercept and slope values (s_o and k respectively). However, the relevance of these parameters depends on whether they are significantly different from zero statistically. If both the initial and replicate analyses were the same the difference between the analytical pairs would be zero and the regression line would be horizontal, i.e. a line of zero intercept and zero slope. The statistical null test is that the intercept and slope values should be rejected if they are not significantly different from zero at 95% confidence (i.e. probability less than 0.05).

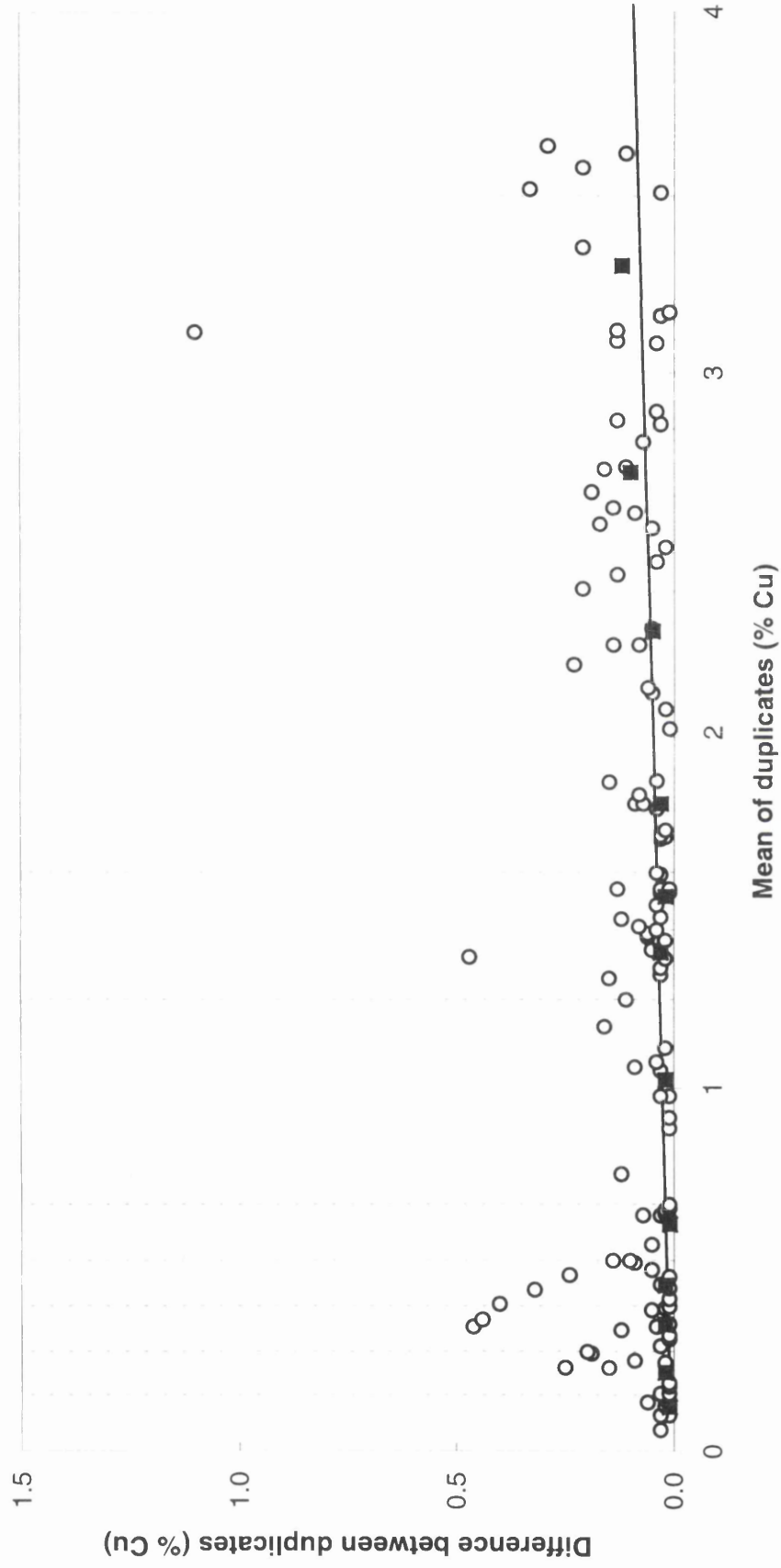

Figure 5.5: Determination of precision of copper analysis of Baluba Centre Limb samples. In this figure and in Figure 5.6 the open circles have the means of pairs of analyses on the x-axis and the differences between the pairs on the y-axis. The black squares have the averages of the means within each group of 11 pairs as the x-axis and the medians of the differences within each group as the y-axis. The groups are separated by dotted vertical lines.

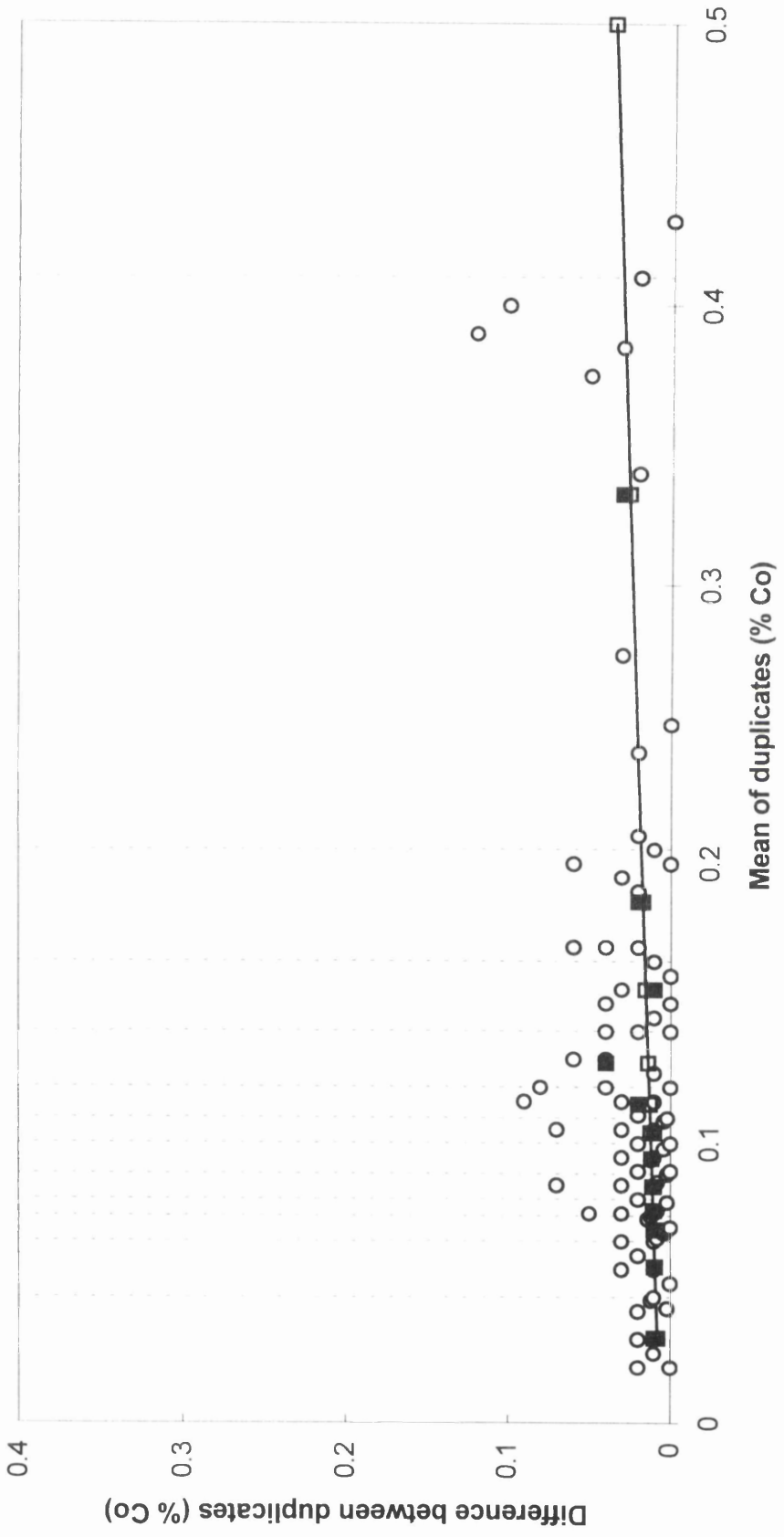

Figure 5.6: Determination of precision of the cobalt analysis in the Baluba Centre Limb samples.

From Table 5.5, it is seen that the probabilities of all the s_0 and k are greater than 0.05 and therefore the s_0 and k values for both copper and cobalt analyses are not significantly different from zero. The s_0 and k parameters evaluated from Figures 5.7 and 5.8 could therefore not be taken as the detection limit and high level precision estimates respectively. The detection limits for copper and cobalt have been calculated according to the Maximum Method Detection Limit relationship suggested by Ramsey *et al.* (In press) as:

$$MMDL = 3(s_o + 2.228\ se(s_o)) \qquad \textbf{(5.9)}$$

The standard error is multiplied by 2.228 which corresponds to the t-distribution with (n-2) degrees of freedom at 95% confidence (12 - 2 = 10 degrees of freedom in this case). The detection limit values obtained are 0.111% and 0.062% for copper and cobalt respectively.

As the estimates of k (for both copper and cobalt) are not significantly different from zero, the high level precision has been evaluated using the relationship suggested by Ramsey *et al.* (In press) :

$$k = \frac{grand\ median\ of\ differences\ between\ analytical\ duplicates}{grand\ mean\ of\ analyses} \qquad \textbf{(5.10)}$$

The high level precision parameters were evaluated as 0.030 and 0.101 for copper and cobalt respectively.

5.3.2 Accuracy

In the estimation of precision the replicate analyses have been compared between themselves without regard to the 'true' value of an analyte. Accuracy, on the other hand, is a measure of the nearness of an analysis to the true value and therefore the true concentration of the analyte (or assumed best estimate thereof) must be known to estimate accuracy. Bias measures the deviation of the measured value from the true one (Equation 5.11).

$$Bias = x_{true} - x_{measured} \qquad \textbf{(5.11)}$$

Since the true values of analytes are prerequisite to the estimation of accuracy, it is essential to have standard analytical samples whose 'exact' concentrations are known.

Bias can also be evaluated by comparing results obtained from two analytical methods, one of whose measurements are known with greater certainty and are therefore assumed to be the true values. The bias between two analytical methods can be translational, rotational or a combination of the two. Translational bias occurs when the bias is not proportional to the concentration of the analyte but is constant through the entire range of concentrations under review. On the scatter diagram the points plot along a line parallel to, but offset from the line y = x. The test for translational bias is that the intercept on the y-axis is non zero, i.e. the graph does not pass through the origin. Rotational bias results when the bias is proportional to concentration. On the scatter plot the rotational bias line goes through the origin but progressively deviates from the y = x line as the concentration increases. A combination of the two biases gives a non zero y-axis intercept and is also not parallel to the y = x line. Schematic illustrations of the three types of bias are shown in Figure 5.7.

If $y = bx + a$ is the equation of the regression line between analyses of samples by methods x and y, and the standard errors of the slope and constant of the regression line are se_b and se_a respectively, then translational bias is indicated by a value of a outside the range $0 \pm 2se_a$ where $2se_a$ represents the minimum detectable translational bias at 95% confidence limits. Similarly rotational bias is indicated by a value of b which lies outside the limits $1 \pm 2se_b$ (additive of 1 applied because this is the slope of $y = x$, which represents a perfect fit line with no bias).

The pulps (100μm nominal size) of 28 samples initially analysed at the Baluba mine laboratory using the AAS method were re-analysed by the ICP-AES method at Imperial College. It was assumed that the Baluba laboratory conditions were less stringent than those under which the analyses were carried out at Imperial College and therefore the Imperial College analyses were used as estimates of 'true' values. The samples and analytical data used for the determination of accuracy are presented in Appendix F.III.

Simple linear regression analysis is a method used to fit the best straight line through bivariate data points and has been used to estimate the accuracy of the Baluba laboratory analyses. Simple linear regression parameters are defined in Table 5.6.

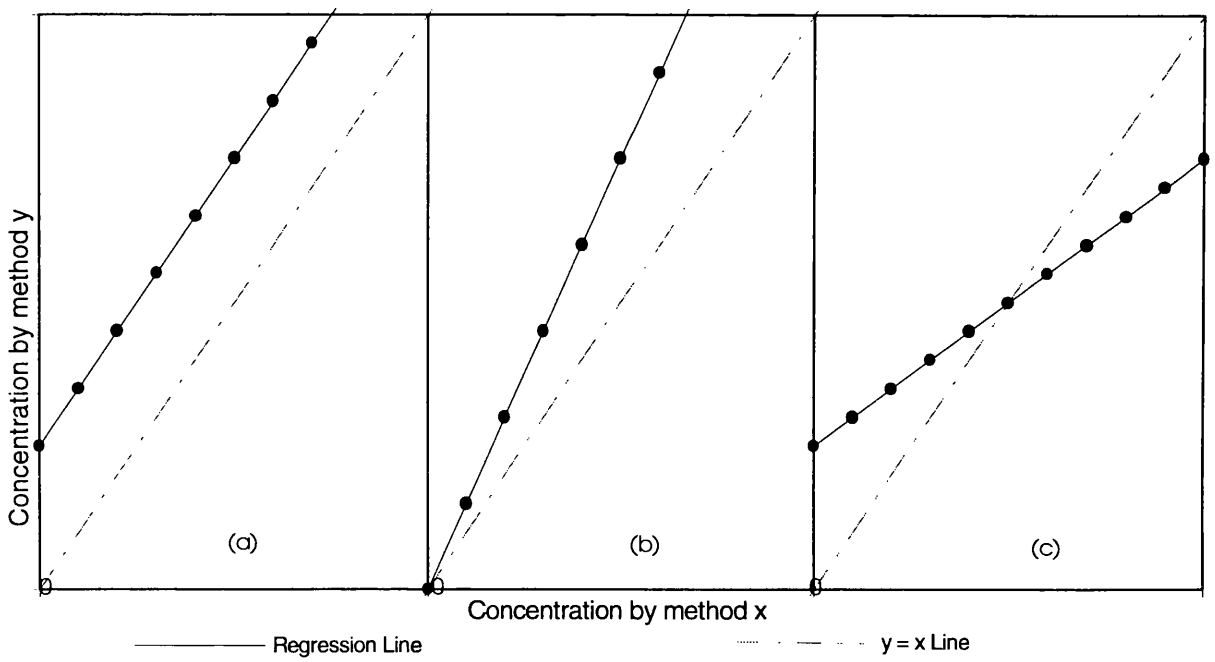

Figure 5.7: Schematic representations of bias showing: (a) translational bias, (b) rotational bias and (c) combination of the two types of bias.

The application of the simple linear regression to estimate the accuracy of Baluba copper and cobalt analyses is presented in Figures 5.8 and 5.9 and the results in accompanying Tables 5.7 and 5.8 respectively.

Table 5.6: Definitions of the simple linear regression statistics

Statistic	Estimate of stastic
Weight, w_i	1
Mean, x_m	$\Sigma x_i / n$
Slope, b	$\frac{\Sigma(x_i-x_m)(y_i-y_m)}{\Sigma(x_i-x_m)^2}$
y intercept, a	$y_m - bx_m$
Standard error factor, s	$\sqrt{\frac{\Sigma (y_i-a-bx_i)^2}{n-2}}$
Standard error on b, se_b	$s / \sqrt{(x_i-x_m)^2}$
Standard error on a, se_a ...	$s\sqrt{\frac{\Sigma x_i^2}{n\Sigma(x_i-x_m)^2}}$

From the data presented in Tables 5.7 and 5.8 it is observed that the linear regression for both copper and cobalt analyses gave non zero y-axis intercepts and were also not parallel to the $y = x$ line.

Baluba and Imperial College (IC) copper and cobalt analyses can be related by the following equations:

$$Baluba\ Cu = (0.984 \times IC\ Cu) + 0.021 \qquad \textbf{(5.12)}$$

$$Baluba\ Co = (0.985 \times IC\ Co) + 0.018 \qquad \textbf{(5.13)}$$

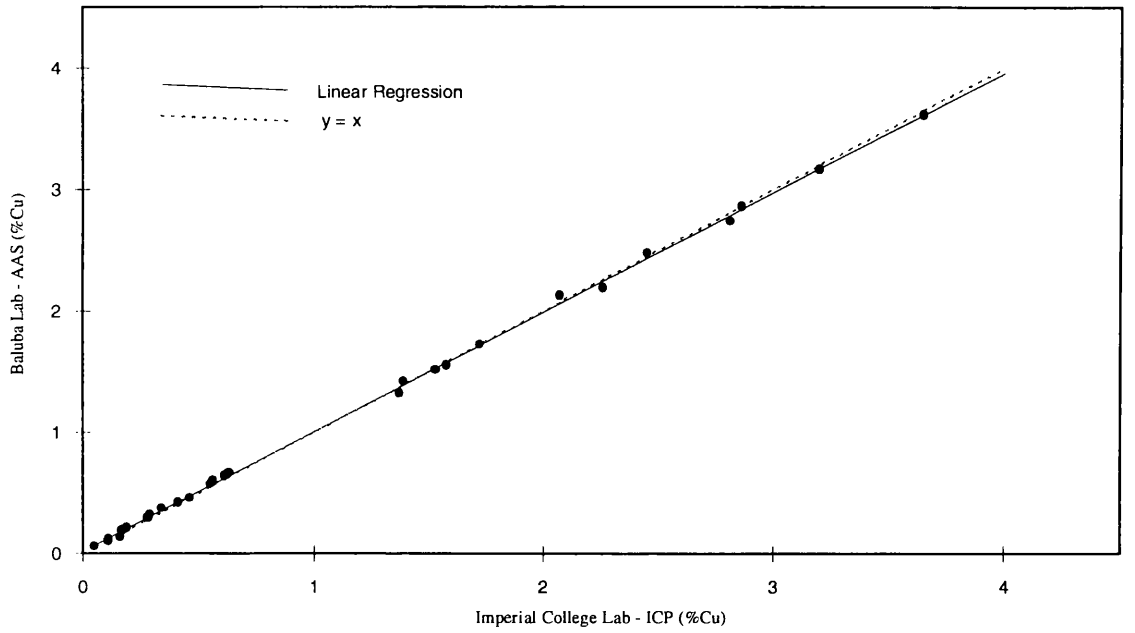

Figure 5.8: Determination of accuracy of copper analyses in Baluba Centre Limb samples

Table 5.7: Linear regression results for copper.

Mean of Imperial College analyses	1.158%
Mean of Baluba analyses	1.160%
Slope of regression, b	0.984
y intercept, a	0.021
Standard error on slope, se_b	0.00010
Standard error on intercept, se_a	0.00015
Rotational confidence range, $1 \pm 2se_b$	0.9998 to 1.0002 (4 dp)
Translational confidence range, $0 \pm 2se_a$	-0.0003 to 0.0003

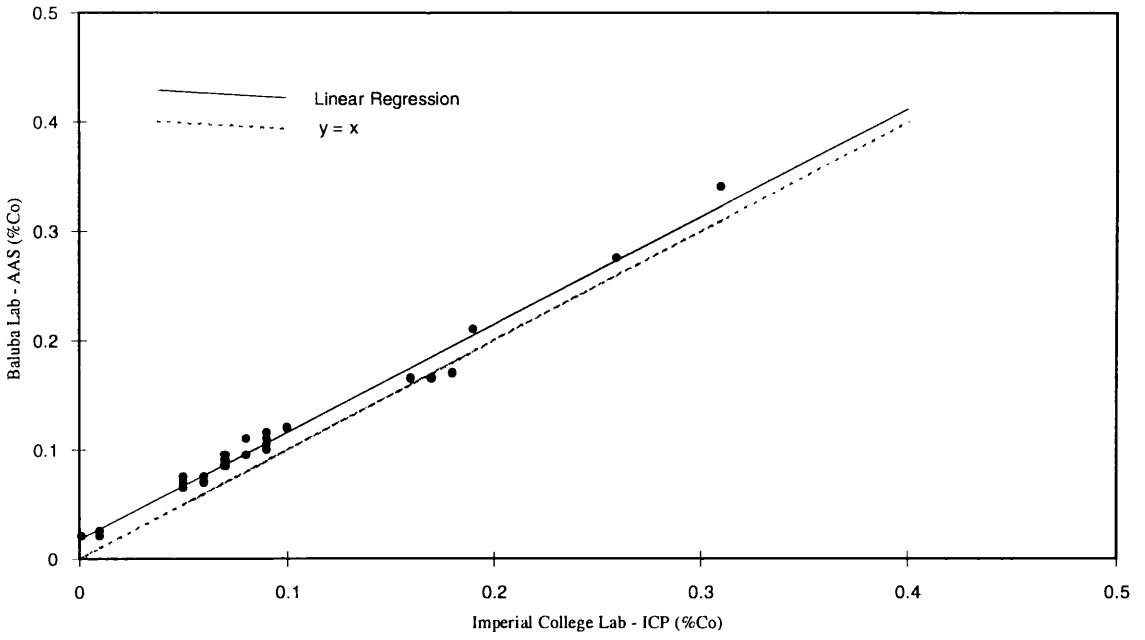

Figure 5.9: Determination of accuracy of cobalt analyses in Baluba Centre Limb samples

Table 5.8: Linear regression results for cobalt.

Mean of Imperial College analyses	0.093%
Mean of Baluba analyses	0.109%
Slope of regression, b	0.985
y intercept, a	0.018
Standard error on slope, se_b	0.00074
Standard error on intercept, se_a	0.00009
Rotational confidence range, $1 \pm 2se_b$	0.9985 to 1.0015 (4 dp)
Translational confidence range, $0 \pm 2se_a$	-0.0002 to 0.0002

5.4 DISCUSSION

Results of the analysis of variance show that the contribution of the sampling variance introduced in chip sampling is larger than the ideal limits. The sampling variance associated with chip sampling therefore most likely distorts the variance due to the true geochemical effects and there is a need to improve the chip sampling method in Baluba Centre Limb by reducing the sampling variance component. It is observed that the sampling variance is more sensitive to the texture of mineralisation than to the mineralogy of the metallic minerals. The argillites which contain massive sulphide mineralisation along the veins and disseminated mineralisation in the groundmass gives rise to a higher sampling variance than the schists which comprise disseminated mineralisation of a mixture of copper-bearing minerals.

The detection limits obtained in this study, 0.111% for copper and 0.062% for cobalt, are notably higher than those normally achieved in pure geochemistry applications. Nevertheless, in applied geochemistry applications, such as mining, other analytical factors must be weighed against the need to achieve greater precision and accuracy. The speed and cost of analysis are critical when handling large suites of samples. Using the results obtained in this study, it would be assumed that copper and cobalt grades of concentrations lower than 0.111% and 0.062% respectively, can not be precisely determined at the Baluba laboratory as they are below the minimum threshold. These detection limits should be taken as local laboratory parameters and not necessarily representative of the AAS analytical method *per se*. Though higher than the detection limits normally achieved in pure geochemical applications these levels are well below the mean grades found in the Baluba Centre Limb rocks and the cut-off grades applied. Therefore there does not seem to be a practical need to improve the existing analytical procedures.

Accuracy estimations indicate that there was a slight bias between the analyses of copper and cobalt concentrations carried out at the Baluba laboratory (determined by the AAS method) and the analyses carried out by the ICP-AES method at Imperial College.

CHAPTER 6

GEOSTATISTICS

6.1 INTRODUCTION

Matheron (1971) defines geostatistics as *"The application of the theory of regionalised variables to the estimation of mineral deposits (with all that this implies)."* A regionalised variable has a spread in space and also exhibits a spatial structure. It has a random aspect which accounts for local irregularities and a structured aspect which reflects large scale properties of the phenomenon. Geostatistics is based on the precept that the characteristics of points which are close together are better correlated than those of points which are farther apart. This postulation leads to the concept of continuity.

Geostatistics relies on a tool known as the variogram to reflect and quantify the mineralisation continuity that is otherwise recognised subjectively using geology alone. The variograms of copper grades will be used to evaluate geostatistical characteristics in the Baluba Centre Limb and assess how they relate to the geology. Sampling and analytical variances obtained by the analysis of variance method in Chapter 5 will be compared with the nugget variances obtained in the semi-variograms. It is planned that the results obtained in this study will subsequently be incorporated into the geology and mining reserve models at Baluba mine.

6.2. THE VARIOGRAM

Structural analysis is the geostatistical procedure of describing the spatial distribution of variables. It is the first and vital step of any geostatistical study (Journel and Huijbregts, 1978). The variogram is the basic diagnostic geostatistical tool used for structural analysis and it is defined as the expectation (or mean) of the squares of differences between variables separated by a specified distance (Equation 6.1).

$$2\gamma(h) = E\,[Z(x_{i+h}) - Z(x_i)]^2 \qquad \textbf{(6.1)}$$

where h is the vector distance that separates the pairs of variables under review. h is called the lag,
$Z(x_{i+h})$ and $Z(x_i)$ are two variables which are separated by a lag h,
N(h) is the total number of pairs which are a lag h apart,
$\gamma(h)$ is the semi-variogram at lag h.

The value of the variogram, $2\gamma(h)$, depends on the vector distance, $|h|$, and direction, α, along which the variogram is calculated. The variogram measures the average grade variability over space.

The experimental variogram, $\gamma^*(h)$, is calculated as:

$$\gamma^*(h) = \frac{1}{2N(h)} \sum_{i=1}^{N(h)} [Z_{(x_i+h)} - Z_{x_i}]^2 \qquad \textbf{(6.2)}$$

The idea behind the variogram is that points which are closer together are more likely to be similar, hence better correlated, than those which are farther apart. The rate of increase of the variogram indicates how quickly the influence of a sample drops off with distance and measures the continuity of the variable under review. Generally the value of the semi-variogram, $\gamma(h)$, increases with the vector distance, $|h|$. If the variable under study is stationary, the variogram reaches a limiting maximum value at a certain lag spacing. The distance at which this limiting value is reached is called the range, a, of the variogram and beyond this distance the samples are no longer auto-correlated.

The manner in which the semi-variogram, $\gamma(h)$, increases for small values of the distance, h, is characteristic of the degree of spatial continuity of the variable under study. Theoretically the value of the semi-variogram is zero when h=0 because the sample is being compared to itself. However, it is noted in practice that most variables exhibit a short distance variability. This short distance variance is called the nugget effect and is represented by a discontinuity at the origin of the variogram (Fig 6.1). The nugget effect reflects the built-in random nature of mineralisation whose variability is not predicted by the spatial relationship between the samples (Clark, 1979c). Samples which are very close together - approaching h = 0 - still show a significant difference in their values. The nugget effect represents the variability related to structures smaller than the shortest lag used in the variogram. Part of the nugget effect could also be a result of sampling and chemical analysis measurement errors.

The difference between the maximum variogram value and the nugget is called the sill, C. In essence the variogram is made up of two components; the nugget effect which estimates the non-spatial, random variability and the sill which relates to the degree of spatial variability. The total of the nugget variance and the sill should be approximately equal to the total variance of the assay grades if the variable under review is stationary.

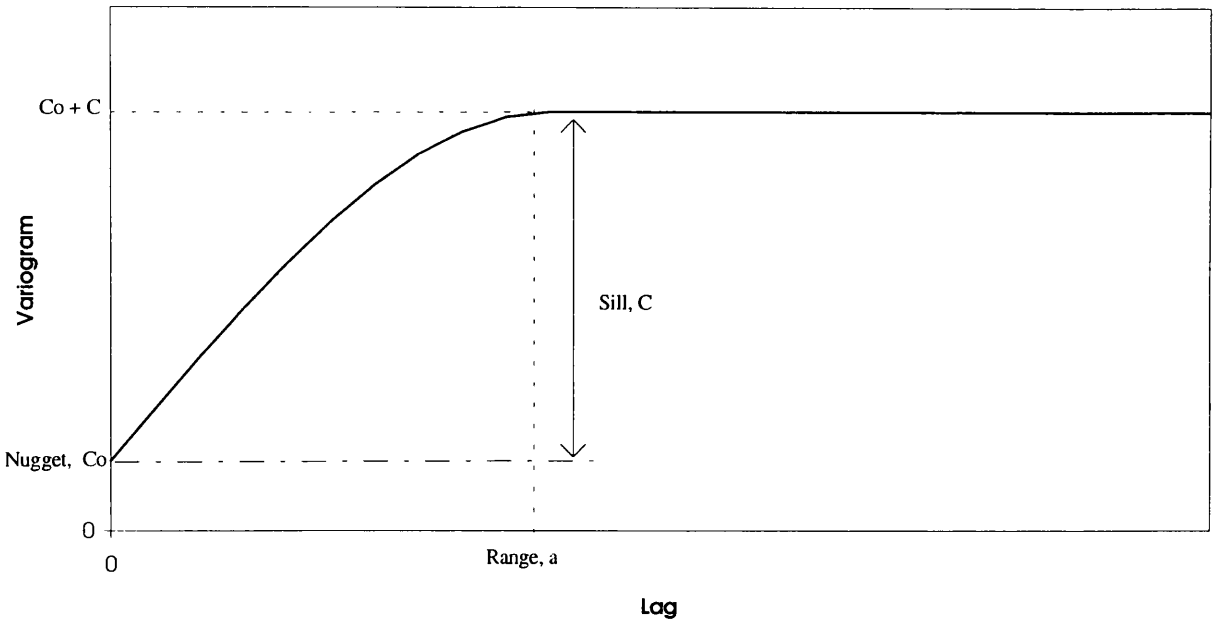

Figure 6.1: Definitions of the parameters used to define a bounded variogram model

$$C_{0^+} C \approx variance \qquad (6.3)$$

Anisotropy arises when the continuity of the phenomenon under review is different in various directions. There are two types of anisotropy; geometric and zonal. In geometric anisotropy the range changes with direction but the sill remains constant. In zonal anisotropy the sill changes with direction while the range remains the same.

There are many theoretical variogram models but the most commonly used are the spherical, exponential, gaussian, linear and pure nugget models.

6.3 BALUBA CENTRE LIMB VARIOGRAM MODELLING

6.3.1 Data Used

The data used to calculate the variograms consisted of 911 core samples from 26 diamond drill holes located in the Baluba Centre Limb (data on the disk - Appendix A). The drill holes were selected from the area lying between Structure Section 46 and Structure Section 50, covering some 350m along strike and about 275m across strike. The drill holes are not regularly spaced. Their locations are presented in Figure 4.10 (map enclosed in the pocket of the back cover of the thesis). Block 'A'

has the greatest density of drill holes, the orebody intersections being located at about 20m intervals along strike and 20-50m across strike.

Variogram construction and modelling were carried out with the aid of the GeoEas (Geostatistical Environmental Assessment) computer software in the Geology Department at Imperial College and the MAGMA (Management for Geostatistics Mining Applications) software at the Centre de Géostatistique, Fontainebleau, France.

6.3.2 Experimental variograms

In the construction of three dimensional variograms, the down-hole direction often plays an important role since it normally corresponds to the direction along which there is the greatest grade variability compared to any of the horizontal directions. This is indeed what would be expected of the Baluba Centre Limb orebody given that there is a lithostratigraphic as well as vertical zonation into metallic mineral groups. Grades within individual layers (litho-strata) and mineral zones are expected to have a pronounced lateral continuity but to change rapidly across the strata, along the down-hole direction. Therefore for geostatistical structural analysis of the Baluba Centre Limb the down-hole variograms have been calculated separately from the variograms in the horizontal plane.

Copper grades of actual samples were used to construct down-hole variograms but the horizontal variograms obtained using the actual samples were very 'noisy' and did not present a clear structure. Grades were averaged within each lithology and the average grades used to construct the horizontal variograms. The process used to evaluate the down-hole and horizontal variograms is illustrated in Figure 6.2 and in Table 6.1.

As seen in Chapter 4, the length of the actual samples down the drill holes ranges from 0.2m to 2.0m, with the mean length of 0.72m (see Figure 4.10). Down-hole variograms have been calculated using the lag spacings of 1.0m with a 0.5m tolerance.

Laterally the variograms have been evaluated along the directions 120°, 030° and 045° in order to detect the anisotropy. The 120° direction corresponds to the direction of the Centre Limb/South Limb axial trace, which is effectively the mean strike direction in the Baluba Centre/South Limb area.

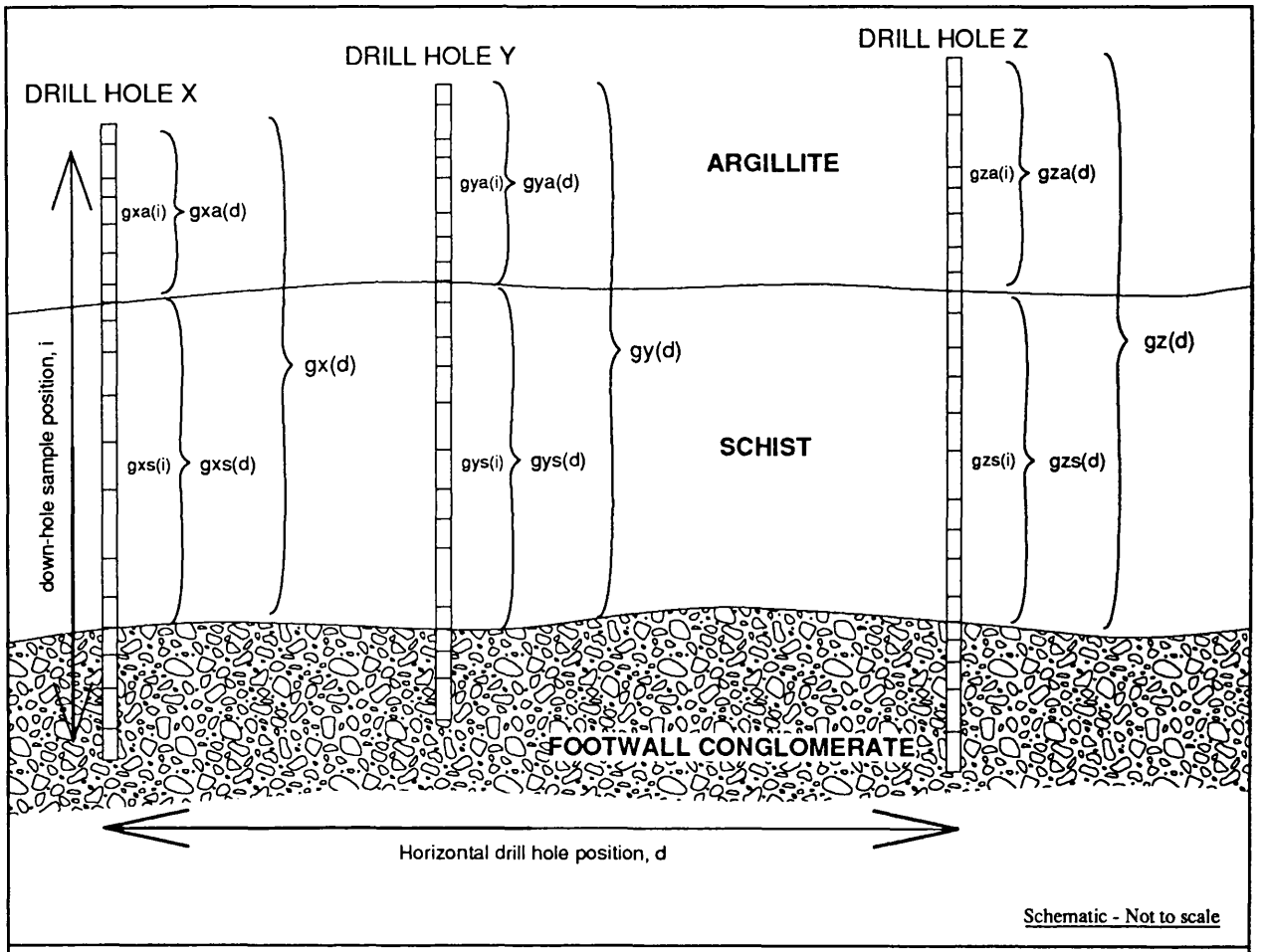

The following suffixes are used to identify the grades, g, of the samples:
x,y,z: drill hole identifiers,
a, s: distinguish between samples located in argillite and schist respectively,
i is the position of a sample down a drill hole,
d is the planar position of the drill hole (where a drill hole is inclined the position of *d* used is that of the footwall contact).

Examples:
gxa(*i*) is the discrete sample along drill hole X, within the argillite located at *i*,
gys(*d*) is the composite sample generated by weight averaging discrete samples in the schist lithology along drill hole Y which is located at *d*,
gz(*d*) is the composite sample for drill hole Z which is located at *d*. The composite sample is generated by weight averaging samples from both the argillite and schist lithologies.

Figure 6.2: A schematic example to illustrate how the experimental variograms were evaluated in the down-hole and horizontal directions. The spacing of samples in the down-hole direction is much smaller than that in the horizontal direction. *i* is typically about 0.5-1.0m while *d* is about 10-50m. The grades of discrete samples are used in the construction of the down-hole variograms while the composited grades are used to calculate horizontal variograms.

Table 6.1: Sample pair differences used in the evaluation of the experimental variograms for copper in the Baluba Centre Limb. Refer to Fig. 6.2 for the explanation of the symbols used.

Lithology	(i) Down-hole .....(1)	(ii) Horizontal .....(2)
Argillite	[gna(i) - gna($i+h$)]	[$gn_1a(d)$ - $gn_2a(d+h)$]
Schist	[gns(i) - gns($i+h$)]	[$gn_1s(d)$ - $gn_2s(d+h)$]
Argillite + Schist combined	[gnϵ(i) - gnϵ($i+h$)] ..... (3)	[$gn_1(d)$ - $gn_2(d+h)$]

Notes:
n is the drill hole identifier.
(1) In the down-hole direction variograms were evaluated along individual drill holes. The variogram values at each lag were weight averaged using the number of pairs for each drill hole as a weighting factor.
(2) To calculate experimental variograms in the horizontal directions the composite grades were used. Grades were composited into lithological groups and differences evaluated between mean grades for the drill holes. Note that in the evaluation of the variograms in the horizontal plane $n_1 \neq n_2$.
(3) To calculate the combined-lithology experimental variogram in the down-hole direction all samples from the argillites and schists down a drill hole were used without segregation by lithology, ϵ = (a or s).

The 030° direction is the direction perpendicular to the strike and approximately aligns with the orientation of structure section lines (see Fig. 4.10). The third direction was used because if variograms are examined in only two perpendicular directions it is possible to miss the anisotropy. The spacing of the drill hole intersections of the orebody is about 10-50m laterally on average. The lag spacing in the horizontal plane was chosen as 25m with a 12.5m tolerance. The tolerance applied on the horizontal angle was ± 22.5°. The results obtained for the down-hole and horizontal experimental variograms for copper are presented in Appendix G.

6.3.3 Variogram modelling

As the experimental variogram cannot be used in kriging, a mathematical model has to be fitted to it. As a general guide, it is suggested that the theoretical variogram model should be fitted to the experimental data points using only points on the experimental variogram for lag spacings of up to half the maximum span of the sample field (Journel and Huijbregts, 1978; Clark, 1979a: Royle, 1979). The experimental variogram points at lag spacings longer than half the total field range are usually calculated from too few sample pairs to be reliably used for model fitting.

Single-sill spherical models were fitted to the experimental variograms by iteratively choosing the nugget, sill and range values. The goodness of fit of the model to the experimental data was

determined visually. The model used to describe the experimental variograms is given in Equation 6.4.

$$\gamma(h) = C\left(\frac{3h}{2a} - \frac{h^3}{2a^3}\right) + C_0 \quad \text{..... for } |h| \le a \qquad \textbf{(6.4)}$$

$$= C + C_0 \quad \text{..... for } |h| > a$$

where C is the sill
C_0 is the nugget effect
h is the lag
a is the range of influence

(a) Down-hole variograms

The down-hole variograms are shown in Figure 6.3. For the down-hole variograms the classical statistical sample variance was used in fitting the total variogram value using the relationship that the variance is approximately equal to the total of the nugget effect and sill (see Equation 6.3). The down-hole variogram modelling results are presented in Table 6.2.

Table 6.2: Baluba Centre Limb down-hole variogram model results for copper

Lithology	Variable	Range, a (metres)	Nugget Effect,C_0 ($\%^2$)	Sill, C ($\%^2$)	Relative Nugget Effect $(C_0/C_0+C)*100$
Combined	Copper	6.5	0.45	2.20	17.0%
Schist	"	1.6	0.45	2.70	14.3%
Argillite	"	8.0	0.30	1.19	20.1%

(i) Nugget effect and sill

From Table 6.2 it is seen that although the absolute nugget effect is slightly higher in the schists than in the argillites the relative nugget effect ($C_0/(C_0+C)$) is greater in argillite. This implies that the nugget effect has a greater impact on the total variance in argillite than in schist. The higher relative nugget effect in argillite can be explained by the contrast in the mineralisation between the massive sulphides along the mineralised veins and the disseminated mineralisation in the groundmass (see Plate 3.5(b)). The mineralised veins behave like 'nuggets'. As for the analysis of variance in Chapter 5 it

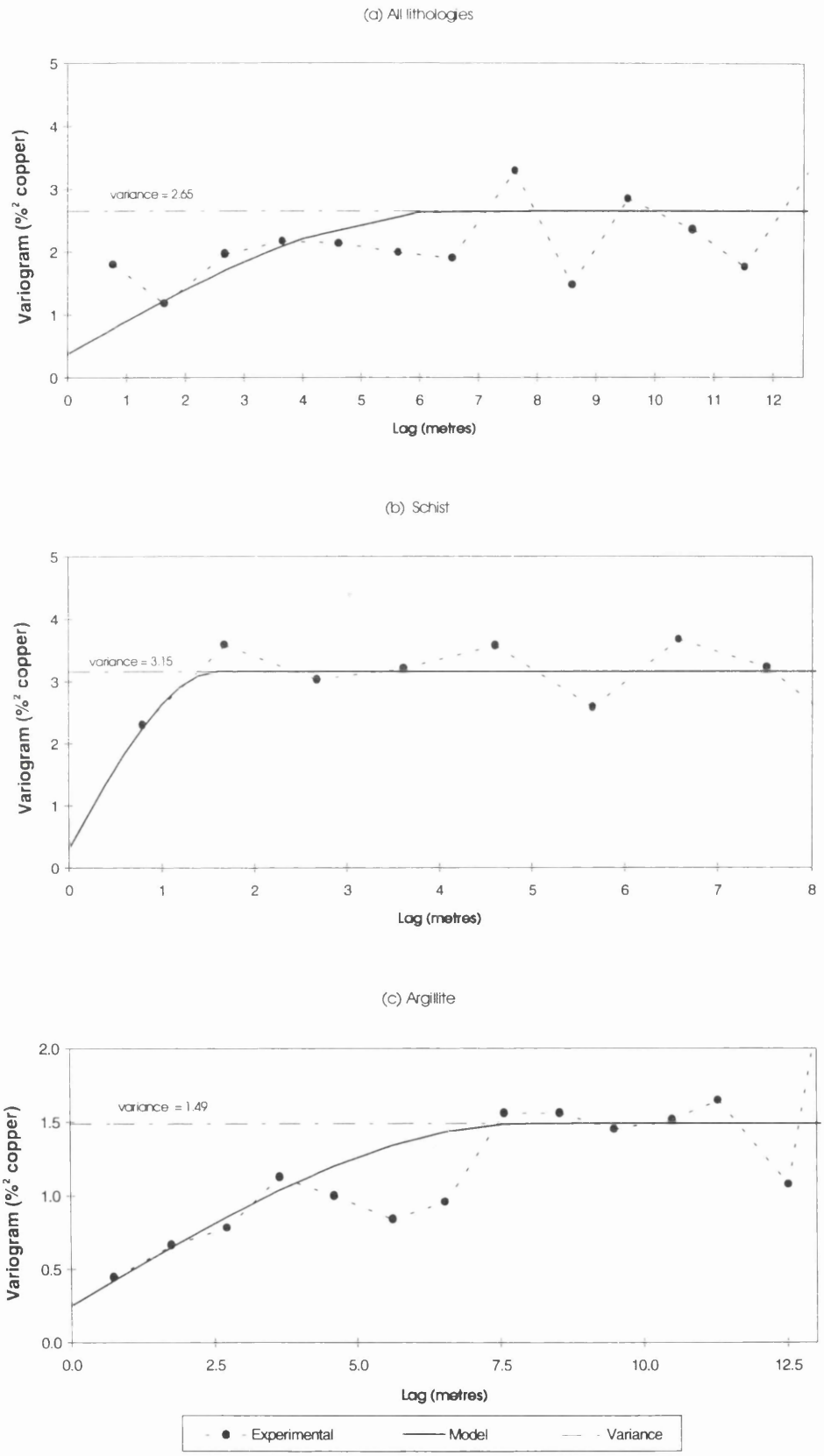

Figure 6.3: Baluba Centre Limb down-hole variograms for copper

appears that the texture of the mineralisation is more critical to the assessment of the relative nugget effect.

The copper variogram in schist could either be a pure nugget effect or one with a very short range (about 1.5m). The nugget effect may represent the variability that was not accessible at the scale of sampling. It might require some closer spaced sampling in the schists to verify whether the phenomenon displayed is pure nugget effect or not.

Mineralisation in schists is generally more evenly disseminated than in the argillites. On average the mineralised grains in the groundmass and along schistosity planes in the schists are of a centimetre scale or less. This is in contrast to the massive mineralisation in the argillites which is associated with mineralised veins of decimetric size. The sampling spacing is 0.5m to 1.0m on average and at this scale of sampling the nugget effect in the argillite is segregated from the sill since the cause of the nugget is comparable to the scale of sampling. In the schists, on the other hand, the sampling is too wide (over-regularised) and all that is measured at such sampling scale is the total variance; the nugget effect is not isolated from the total variance. This gives the impression of a pure nugget effect in schists.

(ii) Range

The ranges obtained in the down-hole variograms can be explained in view of the differences in the nature of copper mineralisation in argillite and schist. The copper in argillite is exclusively due to chalcopyrite mineralisation whereas in schist there is a mixture of copper sulphides and oxides (see Fig. 1.2). Therefore the copper mineralisation in argillite can be considered to be due to the same mineral population (chalcopyrite) but that in the schist due to a mixture of mineral populations (mixed sulphides and oxides). Hence the copper grades in argillite are correlatable over a longer distance than those in the schists.

(iii) Comparison of down-hole variogram modelling results and Analysis of Variance (ANOVA) results

In Chapter 5 the total variance was split into analytical, sampling and geochemical components using the ANOVA approach. It was deduced that the technical variance which is the sum of analytical and

sampling variances is a resultant of analytical and sampling processes used to acquire the assay data. The technical variance can be likened to the nugget effect in the variogram scheme.

In geostatistical literature (Gy, 1974; Krige, 1978; Clark, 1979b; Annels, 1991) it has long been recognised that there is a similarity between the nugget effect and errors due to sampling and chemical analysis (the technical variance in ANOVA terminology). In particular Rendu, 1981, states:

> *" A [second] source of discontinuity at the origin is the presence of sampling and assaying errors: if it were possible to take a repeat sample exactly in the same place, the two observed values would differ and the value of the variogram for the distance h=0 would be equal to the mean squared sampling and assaying error. ..... in practice the two sources of discontinuity cannot be separated and add up to a total discontinuity defined as the nugget effect."*

The comparison between the nugget effect results obtained in variogram modelling and the technical variance results derived in the analysis of variance for the Baluba Centre Limb (Chapter 5) is presented in Table 6.3. The variogram results used are those for the down-hole direction and the analysis of variance results those for the drill holes. The horizontal variogram results were not suitable for comparison with the analysis of variance results owing to the reduction in the variogram values which is brought about by the regularisation effect in the horizontal plane which results from compositing of the samples into lithological groups (see Fig. 6.2).

Table 6.3: Comparison between the relative nugget effect obtained in variogram modelling and the technical variance obtained in the Analysis of variance for the Baluba Centre Limb rocks.

Lithology	Variogram modelling	Analysis of variance
	%Relative Nugget Effect[1]	% Technical Variance[2]
Combined	17.0	21.2
Schist	14.3	12.8
Argillite	20.1	19.5

1. Relative Nugget Effect = Nugget effect ÷ (Nugget Effect + Sill)
2. Technical variance component of total variance = SOS (sampling + analytical) ÷ SOS (sampling + analytical + geochemical)
SOS = Sum of squares

Generally the relative nugget effect can be expected to be approximately equal the technical variance component of total variance. This is because the nugget effect includes the sampling and analytical measurement errors (equivalent to the technical variance in ANOVA). The proportion of the technical variance to the total variance can therefore be taken as a guide to the level of the nugget effect that can be expected in variogram modelling.

(b) Horizontal variograms

The lateral direction variograms are presented in Figure 6.4. The results of horizontal variogram modelling are presented in Table 6.4.

Table 6.4: Baluba Centre Limb horizontal variogram model results for copper

Lithology	Variable	Range, a (metres)	Nugget Effect, C_0 ($\%^2$)	Sill, C ($\%^2$)
Combined	Copper	100	0.10	0.25
Schist	"	100	0.10	0.40
Argillite	"	100	0.10	0.30

As shown in Figure 6.2 the weight averaged composite samples have been used in the calculation of the horizontal variograms. The generation of the composite samples is a method of sample regularisation. As a consequence of the regularisation effect the horizontal variograms calculated using the composite samples exhibit a lower variance (and hence variogram) than the corresponding variograms calculated using the discrete samples in the down-hole direction.

It is noted that the horizontal variograms are isotropic. The range along different horizontal directions remains constant within each lithological group and also remains the same between the lithologies. This implies that there is a geometric isotropy.

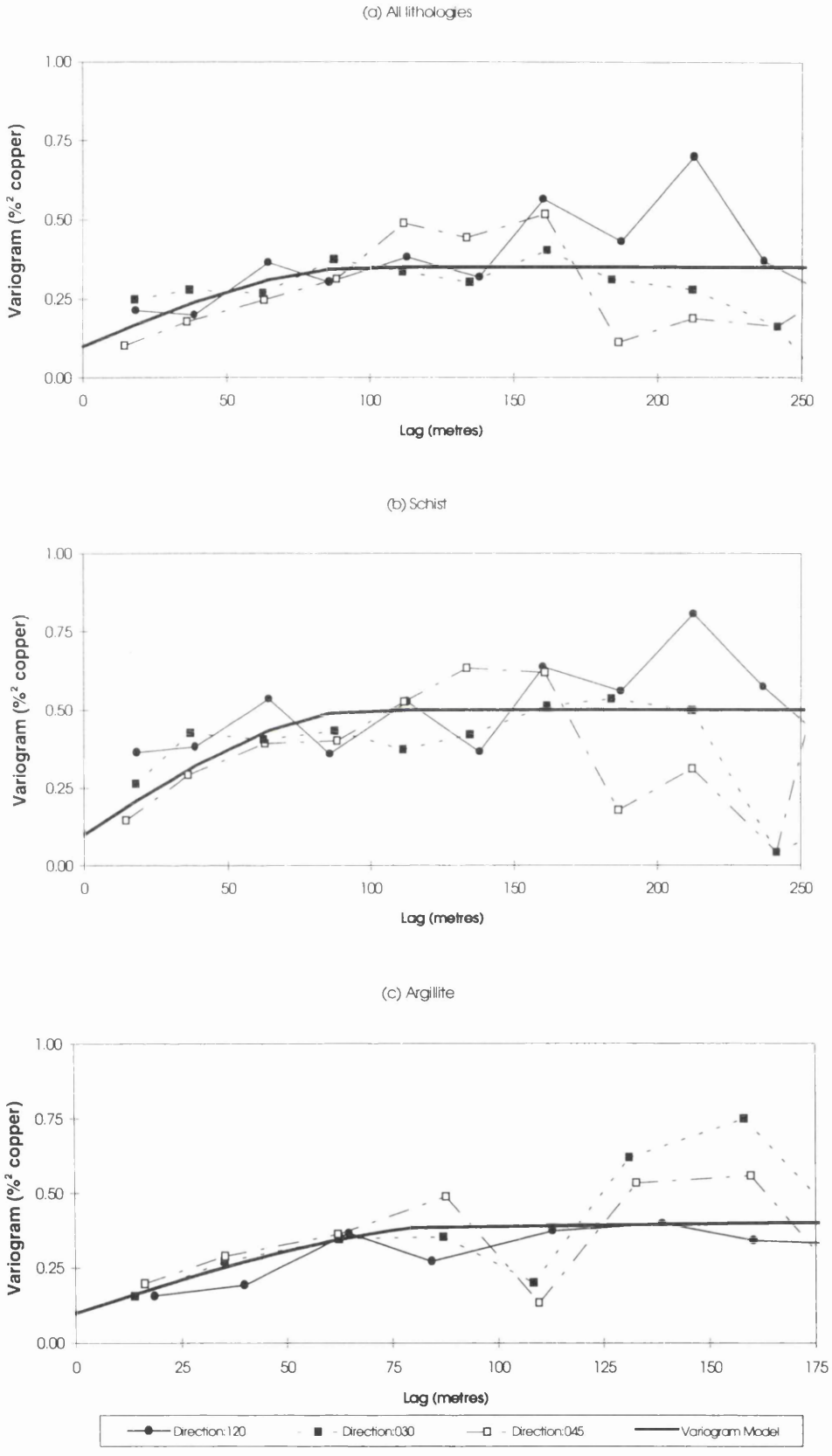

Figure 6.4: Baluba Centre Limb horizontal variograms for copper

6.4 SIGNIFICANCE OF THE GEOSTATISTICS RESULTS

Geology should provide the controls to the geostatistical methods that are applied in assessing a mineral deposit. Journel and Huijbregts (1978) recommend that grade estimations should not be isolated from geology and mining layouts. In this chapter the relationship between geology and geostatistics in the Baluba Centre Limb has been demonstrated. The variograms have been modelled using the geological controls and it can be expected that the reserve estimations based on these variogram models will be geostatistically and geologically reliable. The geostatistical results have been explained using the geological and mineralogical characteristics of the rocks.

The relationship between sampling and analytical errors on one hand and the nugget effect on the other has also been shown. The relative nugget effect obtained from variogram modelling is found to be related to the contribution of sampling and analytical variances to the total variance, as evaluated using the ANOVA method in Chapter 5. The technical variance (sampling + analytical variance) seems to indicate the minimum level of relative nugget effect expected in variogram modelling. If the contribution of the technical variance to the total variance increases beyond levels of reliability it is possible for the variograms to display a nugget effect as a consequence of the sampling and analytical errors, even in a field where a nugget effect due to spatial micro-structures was not present. The purpose of the variogram is to present a measure of the spatial continuity of the variables. A high technical variance screens the estimation of the true spatial variability component. Therefore the geostatistical evaluation is intimately influenced by the precision and accuracy of the sampling and analytical processes used to generate the data of the variables under review.

Geostatistical reserve estimation methods, such as kriging, require the variogram model parameters in their application. Therefore the variogram modelling results obtained in this study will provide an important input into the Baluba Centre geological and mining reserve schemes at Baluba mine. The estimation variance calculated by geostatistical methods depends on the variogram model parameters. Once the variogram model has been fitted to the experimental data, the parameters obtained can be used to determine the optimal drill hole spacing, laterally, and the sample spacing down the drill holes. The optimum sample spacing is dictated by geostatistics, mining method and associated block layouts and by the time and cost of sampling *inter alia* (de Wijs, 1972). The sampling pattern derived using geostatistical parameters ensures that the intervals between adjacent samples are close enough to

produce auto-correlation between the samples. The results obtained in this study will be used at Baluba mine to optimise the sample spacing.

CHAPTER 7

HANGINGWALL POSITION SELECTION AND DENSITY DETERMINATION

7.1 INTRODUCTION

A cutoff grade is any grade that is used to separate which part of the deposit should be mined and which one should be left in-situ. In this chapter the basis for selecting the optimum cutoff grade/s or a set of cutoff parameters will be determined. The objective will be to achieve a grade or a relationship combining several grades such that the uncertainty of defining the limits of the orebody is minimised. Unless the footwall and hangingwall limits of the orebody are confidently defined, all subsequent mineral reserve evaluations are liable to be affected by the uncertainty associated with the determination of the bounds of the orebody.

Currently at Baluba mine a 1% cutoff grade based on sulphide copper (total copper less acid soluble copper) is used to define the footwall and hangingwall bounds of the orebody for mining. The sampling and cutoff practices currently applied at Baluba are described in Appendix C. Owing to the negligible concentration levels of acid soluble copper (~0.1%) in relation to total copper (~2%) coupled with the fact that some samples are not analysed for acid soluble copper (as highlighted in Chapter 4), the total copper values rather than sulphide copper will be used in this chapter in the assessment of the position of the hangingwall.

Copper grades of discrete samples within drill holes intersections in the Baluba Centre Limb can be quite variable. The fluctuation in grades is especially critical in the argillites where the hangingwall boundary of the orebody is fixed on the basis of grades only as opposed to the footwall which is geologically fixed (see Plate 1.2, Chapter 1). It is not uncommon for the copper grades to lie close to the 1% copper cutoff. The fluctuations of grades close to the hangingwall introduces some uncertainty in the positioning of the hangingwall limit of the orebody.

The optimisation of the definition hangingwall limit of the orebody should ultimately result in the improvement of mineral reserve estimations, minimisation of mining dilution and improvement in the grade control.

In this chapter copper and cobalt assays of samples drawn from 40 drill holes located in Baluba Centre Limb will be used to assess the optimal location of the hangingwall in the Baluba Centre Limb orebody. The 40 drill holes comprise the 26 drill holes which were used in deriving the zonation model in Chapter 1 and in the geostatistical analysis and an additional 14 drill holes. The additional data set was available in the later stages of the research after the zonation model, statistical and geostatistical analyses had been evaluated and was only used in the hangingwall optimisation study. The drill hole data bases are presented in Appendix A.

7.2 DILUTION

When a cutoff grade is used the mineralisation is segregated into ore and waste. Some of the waste may, however, be drawn together with the ore during mining and hence introduces waste dilution. The dilution can be intentional or unintentional. Intentional dilution is due to the low grade (waste) material that is added to the ore in order to make the thickness up to the minimum mining width (Annels, 1991). Internal dilution is a special case of intentional dilution and occurs when low grade material is contained wholly as waste pockets within ore mineralisation. Internal dilution is inevitable and usually uncontrollable at larger scales of mining (David, 1988).

Unintentional dilution occurs due to the introduction of waste material to the ore by unwanted means. Unintentional dilution includes the waste introduced to ore as a result of over-drilling (and the resultant over-break of the rock) and also due to the gravitational collapse of the hangingwall rock. Ground stability conditions of the hangingwall rock are critical in the assessment of unintentional dilution. Unlike internal dilution in which the waste is wholly contained within the ore, it is possible to exclude hangingwall waste from the ore. Hangingwall dilution is usually controllable by supporting the hangingwall using roof bolts.

7.2.1 Modes of occurrence of internal dilution in Baluba Centre Limb

When a 1% copper cutoff grade is applied to determine the orebody span using assay data of drill hole (or chip) samples in Baluba Centre Limb, invariably some samples with assay grades lower than 1% copper are contained between samples which assay higher than 1% copper. The internal dilution appears as waste patches within an otherwise continuously mineralised orebody.

Key to Figure 7.1

Orebody as defined currently at Baluba mine, using a 1% copper assay cutoff.

Assay hangingwall position currently used (as indicated in the geological logs).

Figure 7.1: Modes of internal dilution displayed in the Baluba Centre Limb drill holes using a 1% copper assay cutoff. The position of the footwall is characterised by the conglomerate/schist contact. There is some subjectivity in the positioning of the hangingwall. The ideal scenario is represented in (a) where a continuous orebody is defined. In (b) the dilution occurs in the schist. The two situations represented in (c) and (d) where all or part of the dilution is in the argillites causes difficulty in positioning of the hangingwall. In (c) there are two possible positions of the hangingwall, A or B. B was chosen in this case. The situation in (d) is even more flexible, with four possible positions for the hangingwall, A, B, C and D.

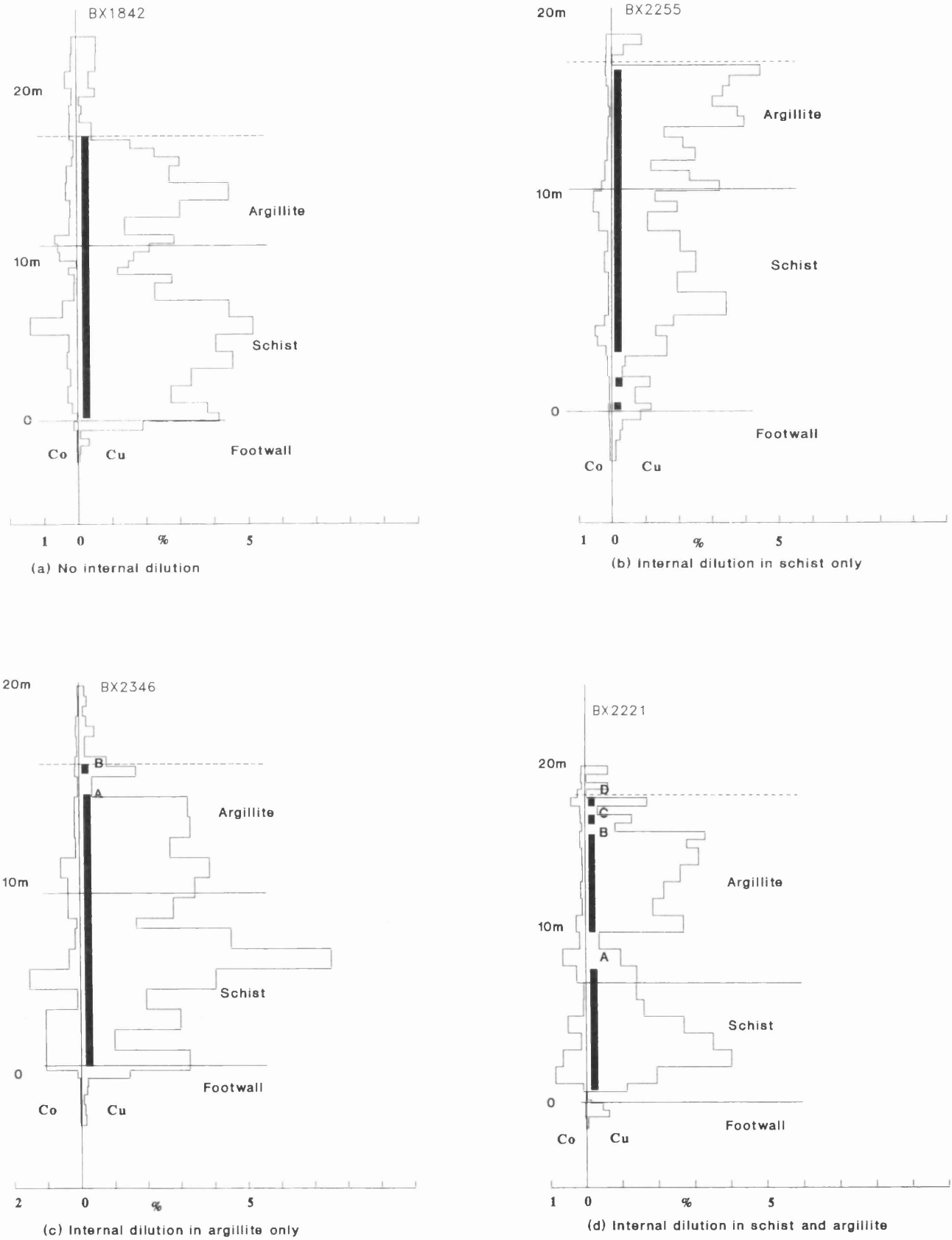

Figure 7.1: Modes of internal dilution displayed in the Baluba Centre Limb drill holes.

Based on the 1% copper cut off grade currently applied at Baluba to define the orebody in drill hole intersections four types of internal dilutions can be identified:

(i) no internal dilution at all, continuous orebody without any waste gaps,

(ii) internal dilution in schist only,

(iii) internal dilution in argillite only,

(iv) internal dilution in both schist and argillite.

The four scenarios are illustrated in Figure 7.1. Ideally the cutoff grade used to define the footwall and hangingwall should result in a continuous orebody as exemplified by drill hole BX1842 in Figure 7.1(a). The subjectivity associated with the positioning of the hangingwall is illustrated in drill holes BX2346 and BX2221 in Figure 7.1(c) and (d) respectively.

The optimum cutoff grade used to define the orebody should be one which, *inter alia*, gives rise to a minimum dilution. A measure of the internal dilutions obtained at different cutoff grades, therefore, has a connotation to the uncertainty associated with defining the orebody as the cutoff grade is varied. The cutoff grade should be high enough to maximise the metal concentration per tonne of rock mined.

7.3 SIGNIFICANCE OF COBALT

The cobalt assay grades of the samples are not used at Baluba mine for constraining the footwall and hangingwall bounds of the orebody. The importance of the cobalt associated with copper mineralisation in Baluba Centre Limb cannot, however, be ignored. Though the mean grade of cobalt (0.1 to 0.2%) is about one tenth of the mean copper grade, the market value of cobalt metal is 10 to 15 times that of copper.[1]

In the zonation model (Fig. 1.2) it is seen that cobalt mineralisation in the *pyrite zone* remains at similar levels (0.1-0.2%) as in the *chalcopyrite and pyrite zone* while copper grades decrease from about 1.5% in the *chalcopyrite and pyrite zone* to grades less than 1% in the *pyrite zone*. To assess the effect of the presence of cobalt mineralisation in the hangingwall region it is essential to take into account the concentrations of both copper and cobalt.

[1]The average cobalt sale price in the 1993/94 financial year was about £12,600/tonne compared to £900/tonne for copper (ZCCM, 1994).

7.4 OPTIMISATION OF THE DEFINITION OF THE FOOTWALL AND HANGINGWALL BOUNDS OF THE OREBODY

7.4.1 Moving window averages

To minimise the impact of erratic grades from discrete samples, moving average grades were applied to assess the hangingwall location. The grade assigned to each sample was the weighted mean grade of the sample and the neighbouring samples on either side of it. The 3-sample moving average grades were effectively grades of regularised samples. The impact of rich 'veins' within a poorly mineralised section of the orebody or of the poorly mineralised zones within an otherwise evenly mineralised section (say calcite or tremolite veins within an argillite with disseminated chalcopyrite mineralisation) was reduced. This procedure aimed at discounting the short range variations, essentially minimising erratic fluctuations in grades related to the nugget effect. Table 7.1 illustrates how the 3-sample moving averages were calculated in the Baluba Centre Limb.

Table 7.1: 3-sample moving window average calculation.

Sample length	Grade	3-sample moving average	Comments
l_1	g_1	-	
l_2	g_2	-	
l_3	g_3	-	[1]Footwall
l_a	g_a	g_a	[2]First sample (in schists)
l_b	g_b	$[(l_a x\ g_a) + (l_b x\ g_b) + (l_c x\ g_c)] / (l_a + l_b + l_c)$	
l_c	g_c	$[(l_b x\ g_b) + (l_c x\ g_c) + (l_d x\ g_d)] / (l_b + l_c + l_d)$	
l_d	g_d	-	Last sample (in argillites)

Notes:
1. A geological contact between the conglomerates and schists is used to position the footwall.
2. The grade of the first sample in the schists (at the contact with the footwall) is used without being averaged with the immediate neighbourhood. This avoids mixing schist samples with the footwall samples. The two are known to be derived from zones which are geologically and mineralogically distinct.

7.4.2 Minimisation of internal dilution

As was seen in Figure 7.1, as the frequency (and by implication the total length) of the internal dilutants increases so does the uncertainty of correctly positioning of the boundaries of the orebody.

The influence of internal dilutions is significant in the argillites, close to the pyrite zone, since the hangingwall is determined on the basis of grades only. The internal dilution was evaluated by measuring the widths of the waste portions included within the ore limits defined at varying cutoff grades. The mean width of the internal dilution was then calculated as a percentage of the mean ore width as a measure of the influence of internal dilution (Equation 7.1).

$$\%\ Internal\ dilution = \frac{included\ waste\ width}{ore\ width} \times 100 \qquad (7.1)$$

The internal dilution was evaluated using data from 40 drill holes from the Baluba Centre Limb. The data showing the widths of the ore intersections and the included waste on which the internal dilution was calculated is presented in Appendix H. Figure 7.2 shows the variation in internal dilution with applying different copper cutoff grades, ranging from 0.25% to 1.50%.

From Figure 7.2 it can be seen that the width of the internal dilution in the schists keeps on increasing as the cutoff grade is raised. This is because the schist is, by convention, wholly located within the ore section of the Baluba deposit. Therefore all 'below cutoff' grades that occur within the schists constitute internal dilution. The internal dilution in schist is accumulative. Contrast with the argillite where part of the waste may be located outside the limits of the orebody; effectively the hangingwall dilution as opposed to internal dilution. If too low a cutoff grade is used to define the orebody the position of the hangingwall is raised higher into the argillite and some of the waste initially located within the hangingwall becomes incorporated within the orebody and constitutes internal dilution. At too high a cutoff grade the internal dilution pockets within the argillite become wider. A balance occurs at some intermediate cutoff grade where the internal dilution obtained in the argillites is minimised.

From Figure 7.2 it is seen that the internal dilution in argillite is minimised at the cutoff grade of about 0.75% copper. Hence on the basis of the internal dilution phenomenon, a 0.75% total copper would be suggested to be the optimum grade to use in the definition of the hangingwall in the Baluba Centre Limb. Since the footwall boundary location is almost insensitive to changes in the grades, the geological footwall can be used as an assay footwall as well.

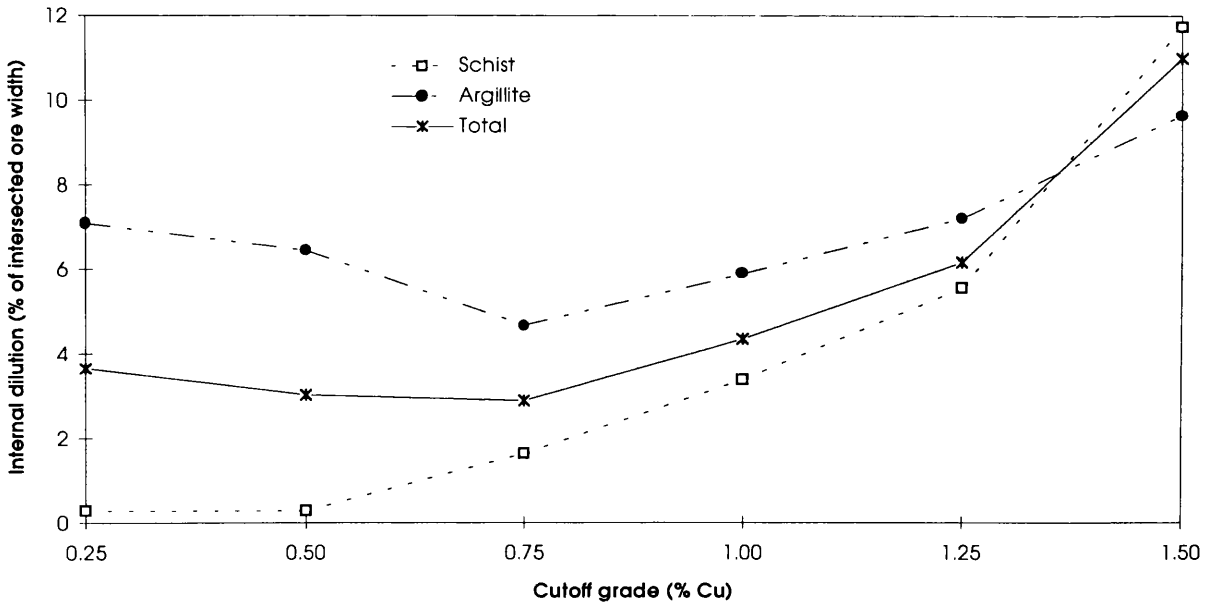

Figure 7.2: Internal dilutions achieved when different grades are used to position the footwall and hangingwall of the Baluba Centre Limb orebody. The internal dilution in argillite reaches a minimum at a cutoff grade of about 0.75%.

7.4.3 Effect of changing the cutoff grade on the definition of the orebody

As the cutoff grade is increased the thickness of the orebody so defined decreases but the mean grade increases.

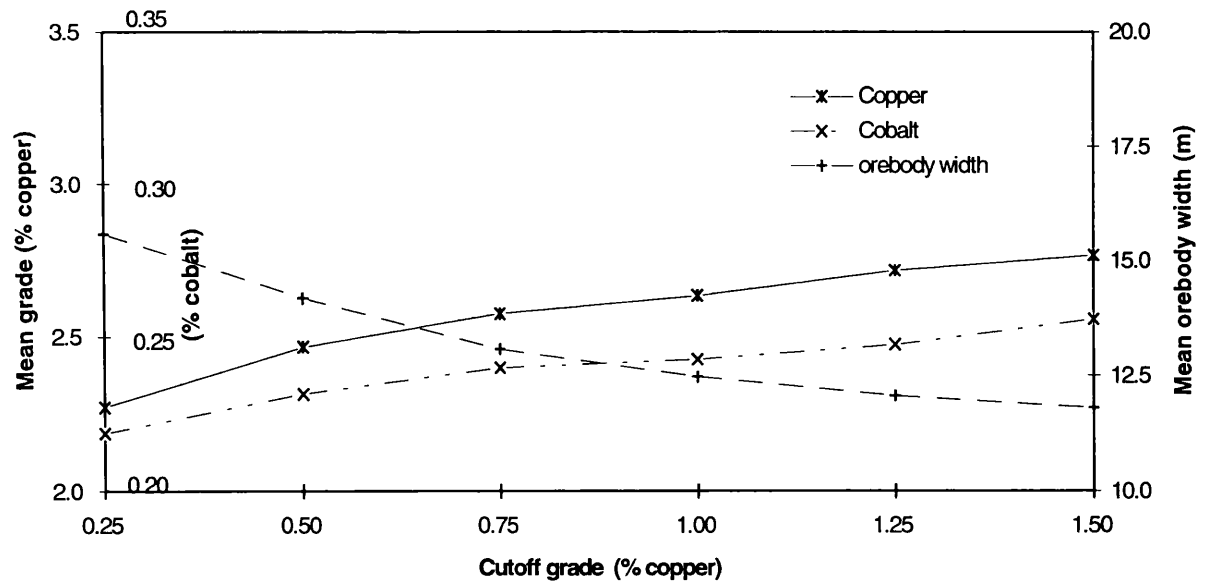

Figure 7.3: The plot illustrates how the orebody thickness and mean grade change in response to varying the cutoff grade in the Baluba Centre Limb.

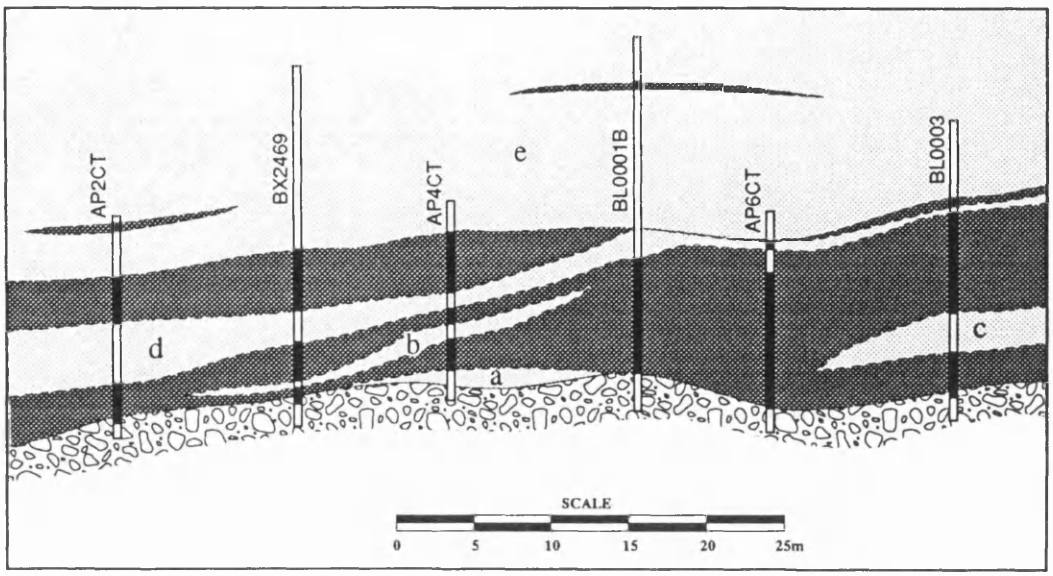

(a)

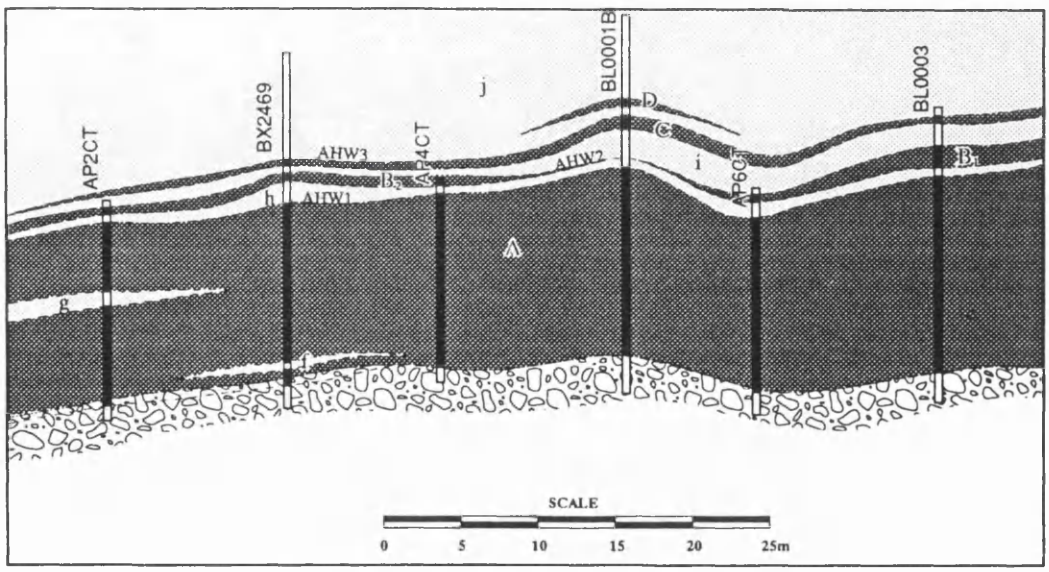

(b)

Darker shade = orebody

Figure 7.4: Effect of the definition of the orebody in response to the changes in the cut-off grade applied. In (a) a 1.5% copper cutoff grade is used to define the orebody. The resultant orebody is thin and has substantial internal waste dilution (a, b, c, d). In (b) a 0.25% copper cutoff grade is used to define the orebody. The main orebody (A) has little internal dilution (f, g). There is an occurrence of ore stringers (B_1, B_2, C, D) in the hangingwall waste. The hangingwall limit of the orebody could be placed along one of the lines AHW1, AHW2 or AHW3 depending on the effect of the dilution on the orebody. The geology of the section used in this figure is presented in Map 4 in Appendix J.

This is a manifestation of the typical grade-tonnage relationship (Annels, 1991; Taylor, 1972). The grade-orebody thickness relationship for the Baluba Centre Limb is illustrated in Figure 7.3. The data showing the mean copper and cobalt grades at different cutoff grades is presented in Appendix H.

Baluba Centre Limb drill hole data shows that if a high cutoff grade was applied (say 1.5% copper) to define the orebody, the resultant orebody is thin (as would be expected) and in addition is also discontinuous. Internal dilution is quite significant (Fig. 7.4(a)). If a low cutoff (say 0.25% copper) was applied the orebody becomes wider. However, the uncertainty in the positioning of the hangingwall increases since the grades in the vicinity of the hangingwall fluctuate about the cutoff grade (Fig. 7.4(b)). Therefore the gain in metal achieved due to widening the orebody by reducing the cutoff grade is offset by the uncertainty in positioning of the hangingwall and the associated increased dilution. An optimum cutoff grade should exist between the extremes of applying too low or too high a cutoff grade.

7.4.4 Unintentional dilution (Hangingwall dilution)

Thus far only the effects of dilution have been evaluated without considering the hangingwall dilution. In this section the effects of including hangingwall dilution will be considered.

In the numerical assessment of the effect of hangingwall dilution in this study, the dilution is defined according to David (1988) and David and Toh (1989) thus:

$$Grade\ Dilution\ \% = \left(\frac{undiluted\ \ grade\ -\ diluted\ \ grade}{undiluted\ \ grade}\right) \cdot 100 \qquad (7.2)$$

Note: Undiluted grade is the mean grade of the orebody (without hangingwall dilution). Diluted grade is the weighted average grade of the ore and hangingwall waste introducing dilution.

The hangingwall dilution for the Baluba Centre Limb has been evaluated for the effects of slices of 0.5m, 1.0m and 2.0m hangingwall waste (see Appendix H).

Figures 7.5(a) and 7.5(b) illustrate the predicted dilution on the copper and cobalt grades respectively due to the effect of hangingwall waste. For both graphs the dilutions are extended to the zero cutoff grade where theoretically the dilution should be zero - if it were possible to mine without using any

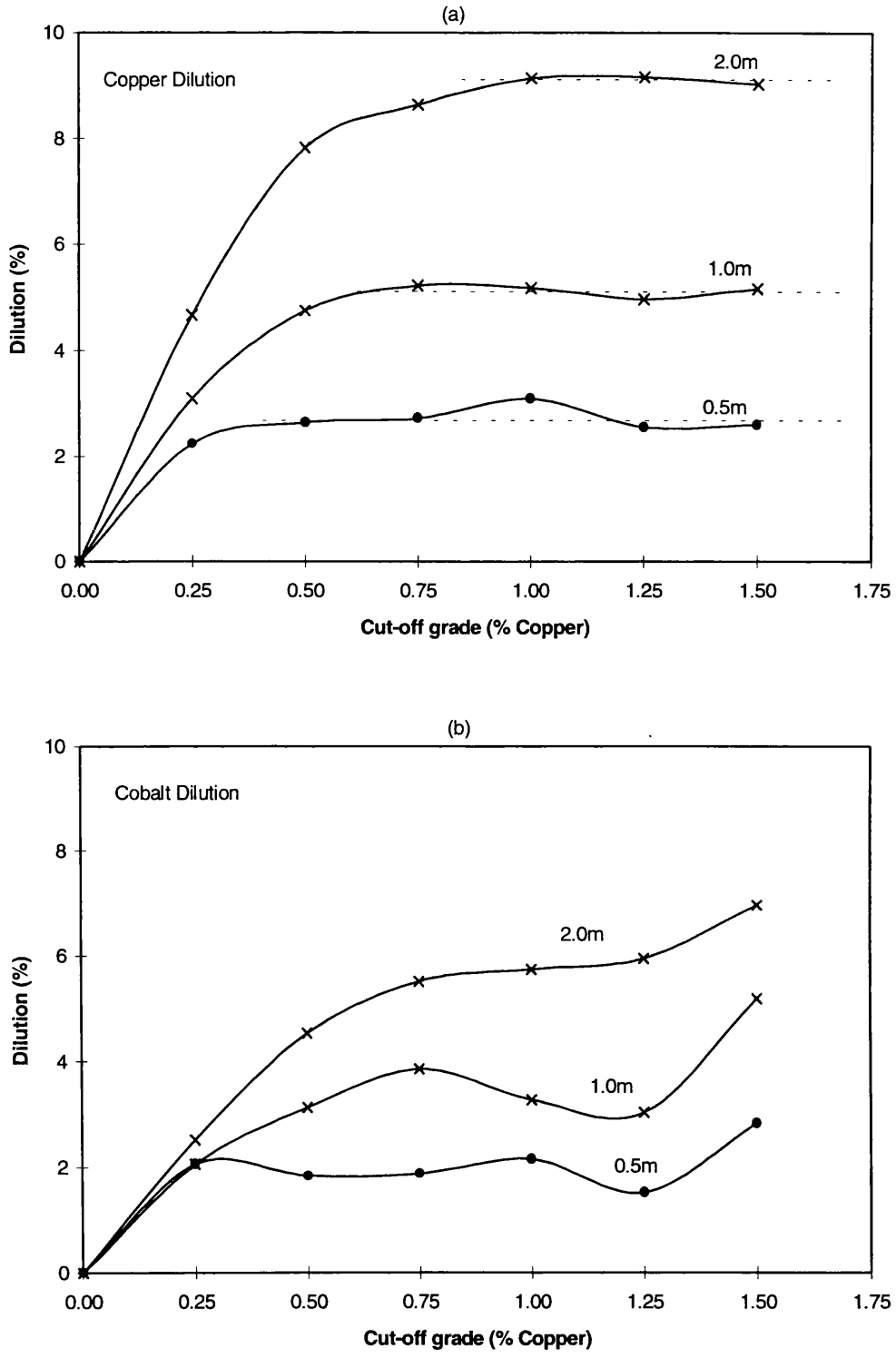

Figure 7.5: Estimation of dilution due to hangingwall waste being included with ore. Hangingwall waste dilution of slices of 0.5m, 1.0m and 2m above the hangingwall limit of the orebody is evaluated. In (a) the dilution is calculated on the copper grades and in (b) on the cobalt grades.

cutoff to segregate ore from waste, i.e. unselective mining. By definition, mining is a selective process and therefore some dilution will almost always be encountered.

For copper it is observed that the dilution rises from zero to a level of stationarity as the cutoff is increased. The levels where the dilution becomes stable are about 0.5%, 0.75% and 1.0% as hangingwall waste of 0.5m, 1.0m and 2.0m respectively is included to ore. These stationarity points signify the minimum cutoff grades that may be applied at given thicknesses of hangingwall overbreak. Taking the case of 1.0m hangingwall waste as an example, if 0.25% copper was used as a cutoff grade any high grading of the ore would require an increase in the cutoff grade and this would result in increased dilution. On the other hand if a cutoff grade of 0.75% or greater was applied, high grading of the ore could be achieved without incurring any further dilution.

In Figure 7.5(b) it is seen that the dilution defined on cobalt grades initially increases as the cutoff grade is increased from zero. Further increase in the cutoff grade results in a decrease in dilution to a local minimum level (or inflexion point) before the dilution increases again. The local dilution minima achieved can be attributed to the presence significant levels of cobalt mineralisation in the form of cobaltiferous pyrite in the immediate hangingwall. The dilution minima occur at a grade of around 1.25% copper up to a thickness of 2m hangingwall waste.

7.4.5 Effect of cobalt on cutoff grade and profit

Lane (1988) considers three types of situation in the determination of a cutoff grade: (i) where mining is the limiting factor, (ii) where treatment of the ore is limiting and (iii) where marketing of the product of mining is limiting. The Baluba case belongs to the first category. Lane proposes that in the case where mining is the limiting factor the cutoff grade can be as low as possible, so long as the difference between the price of the product and the cost of production was higher than the cost of treating the ore. Lane gives the following relationship as the breakeven point used to describe the cutoff grade:

$$g_m = \frac{h}{(p - k)\, y} \qquad (7.3)$$

where g_m is the mining cutoff grade
h is the treatment cost
p is the price of the product
k is the cost of production
y is the metallurgical recovery

From Equation 7.3 it is seen that a reduced cutoff grade could be applied if there was an increase in the metal price(p) or metallurgical recovery (y) or a decrease in the cost of production (k) or treatment cost (h).

The extra cobalt that could be produced in the Baluba Centre Limb by extracting part of the hangingwall argillite would be comparable to producing higher-priced copper - see footnote on p. 135). Therefore, assuming the capacity to mine the extra tonnage was available, a decrease in the copper cutoff grade could be applied so long as the cost of production or treatment of ore did not increase or the metallurgical recovery of either copper or cobalt decrease. No significant increase in production costs need be incurred since the development of underground excavations would have been undertaken for the production based on copper in any case.

7.4.6 Note on the optimisation of the hangingwall position

The position of the hangingwall in this study has been determined by the use of geology and the intrinsic grade distributions only, without applying classical economic analytical tools such as the discounted cash flow (DCF) methods. The aim of this study was to decide the geological constraints within which subsequent economic analysis could be applied. Unless the constraints of mineralisation can be defined geologically it would not be helpful to apply the economical analysis. Before using economics it is important that the geological and mineralogical behaviour of the metallic mineralisation be comprehended.

7.5 DENSITY ESTIMATION

The mineral reserves are estimated by the richness of the metal(s) in question (grade) as well as the mass of rock in which the metal bearing minerals occur (tonnage). In the estimation of mineral reserves it is essential that both the grade and tonnage of the mineralised rock are determined accurately. The mass is estimated by measuring the volume of mineralised rock which is converted to mass by multiplying the volume by the density of the rock mass in question.

Currently a density of 2.67 tonnes/m^3 is uniformly applied for the Baluba sulphide deposits. Variations in geology, however, affect the density and the value of 2.67 may not be the most suitable tonnage factor for the Baluba sulphide deposit.

Variations in densities for the different portions of the orebody are a function of the mineralogy of the host rocks and the metal bearing minerals present in the Baluba Centre Limb deposit. Table 7.2 lists the minerals found in the Baluba Centre Limb with their measured density values.

Based on the densities of the primary minerals of the Baluba Centre Limb rocks and the zonation model derived in Chapter 1, the following variations in densities can be predicted:

(i) The mineralised sections of the deposit comprising metal mineralisation (schists and argillites) will have a higher density than those sections devoid of metal mineralisation (footwall quartzites and conglomerates). The metal bearing minerals have higher densities (4.1-8.8) than those of the rock forming minerals (2.6-3.0).

(ii) The lower portion of the orebody is enriched in the high density minerals; chalcocite, cuprite and native copper. Therefore a high density can be expected in the base of the orebody.

(iii) The difference in the density between the cupriferous argillite (in the *chalcopyrite and pyrite zone*) and the hangingwall argillite (in the *pyrite zone*) is due the relative amounts of chalcopyrite and pyrite in the argillites. Pyrite has a higher density than chalcopyrite, and its concentration increases in the hangingwall argillite. It can therefore, be expected that the density will be lower in the cupriferous argillite than in the hangingwall argillite.

Density measurements were undertaken on 152 Baluba diamond drill core samples (see Appendix I). The mass was measured using an electronic weighing balance and the volume was estimated by the displacement of water.

Table 7.2: Densities of the main minerals found in the Baluba Centre Limb.

Mineral or rock type	Density (tonnes/m^3)
Rock-forming minerals	
Silica-rich rocks (footwall quartzites/conglomerate)	2.6
Tremolite	3.0-3.3
Biotite	3.0
Calcite/Dolomite	2.7-2.9
Metallic minerals	
Pyrite	5.0
Chalcopyrite	4.1 - 4.3
Bornite	5.1
Carrollite	4.8-5.0
Covellite	4.6
Chalcocite	5.5 - 5.8
Cuprite	6.0
Malachite	3.9 - 4.0
Native copper	8.9

Data compiled from Klein and Hurlbut (1993).

7.5.1 Determination of the optimum value of the density for the Baluba orebody rocks

Linear Regression

The density has been related to the copper grades using linear regression. Scattergrams have been plotted for each lithology (Fig. 7.6). The aim is to establish a relationship in each lithology that would estimate the density from the assay grades of copper, i.e. evaluate the relationship:

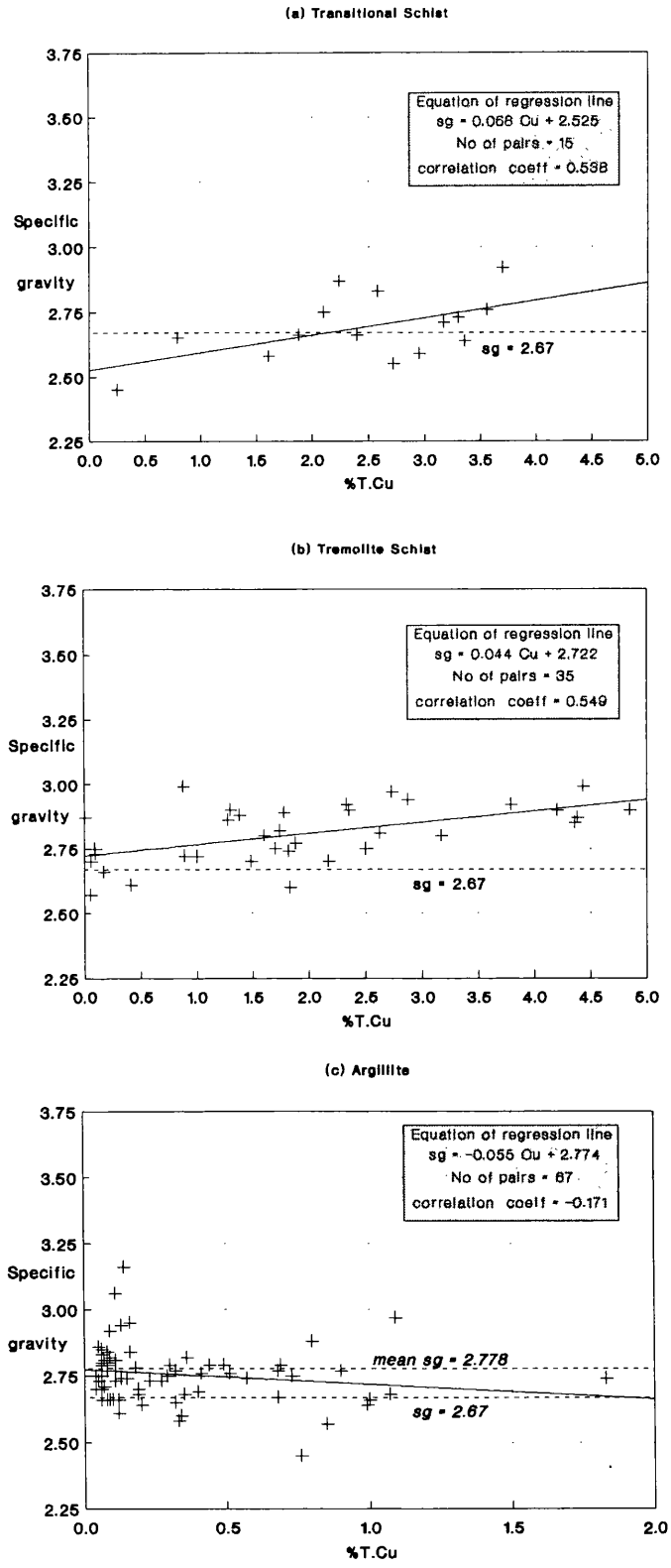

Figure 7.6: Variation of the density with copper concentration in the Baluba Centre Limb.

$$sg = (\beta \times \%Cu) + \alpha \qquad (7.4)$$

β is the slope of the regression line and α the intercept on the density axis. α gives the density when the copper grade is zero, i.e. the density of the unmineralised host rock. The best-fit line has been determined for each lithological category by linear regression. The gradient of the regression line, β, gives an indication of how the density varies as the grade of copper changes. In the special case where the gradient is zero, the regression line fitted would be horizontal and would represent a case where the density was constant for all values of the metal grade. This might arise if the density of the host rock was constant and the same as that of the metallic mineral/s present.

The values for β and α obtained from the regression lines fitted to the scatter plots for the Baluba Centre Limb area are presented in Table 7.3.

Table 7.3: Density estimation by regression analysis.

Lithology	slope,β	intercept,
Quartzite	0.284	2.571
Conglomerate	0.094	2.543
Transitional Schist	0.068	2.525
Tremolite Schist	0.044	2.722
Argillite	-0.055	2.774

Although the transitional schist hosts copper-bearing minerals of a higher density, the host rock is generally considerably leached. Owing to the leaching the transitional schists display a lower density than the tremolite schists, though the latter host metallic minerals of a lower density. The α values obtained were 2.525 tonnes/m^3 and 2.722 tonnes/m^3 for transitional schist and tremolite schist respectively.

From Figure 7.6 it is noted that in the transitional and tremolite schists the density increases with the increase in the concentration of copper, as expected. The spread of data in the argillite scatter does not seem to show any trend. Owing to the poor correlation of the two variables in argillite, linear regression has not been used to estimate density. The mean density has been used instead. The poor linear correlation of the data in argillite can be explained by the co-existence of chalcopyrite and pyrite mineralisation in argillite. Whereas the increase in the concentration of chalcopyrite results in the increase in both the copper grade and the density, the increase in the concentration of pyrite results in an increase in density only without the corresponding increase in the grade of copper. The combination of the effects of chalcopyrite and pyrite mineralisation is, therefore, antipathetic and causes the departure from a linear relationship between copper concentration and density that is observed in the schists. In the schists all the metallic minerals are copper bearing and have a complementary effect: the density increases as the concentration of the metallic minerals increases. Despite the co-existence of various metallic minerals in the schists, all the minerals behave similarly: the density increases with the copper concentration, hence the linear relationship between the density and copper grades.

Using the reserves data for the Baluba Centre Limb (ZCCM, 1990; ZCCM, 1994) and the average grades evaluated in Chapter 4, the mean in-situ copper grades for the orebody rocks are found to be 2.20% in the Transitional Schist, 2.50% in the dolomite schist and 2.15% in the cupriferous argillite. The average thicknesses are found to be about 3m, 9m and 3m in transitional schists, tremolite schists and argillites respectively. Applying the density regression equations derived above the mean densities obtained are 2.671 and 2.832 for transitional schist and tremolite schist respectively. The mean density, of 2.782, is used for argillite. A weighted combination for the schists orebody gives a mean density of 2.778 and a combined schist and argillite density of 2.779. Even allowing for possible voids and weathering in-situ, the density of 2.67 currently used for the Baluba orebody seems to be an underestimation of the tonnage factor.

7.6 DISCUSSION

The hangingwall optimisation in the Baluba Centre Limb has been assessed by evaluating the dilution associated with varying the cutoff grades. The effect of grade fluctuations introduced when discrete grades are used is a function of the variations in the metallic mineralisation within the Baluba Centre Limb rocks and was demonstrated by the presence of a nugget effect in Chapter 6. To reduce the

effect of discrete grades the 3-sample moving window averages were used to smoothen the short scale grade variations. It has been shown that a copper cutoff grade of 0.75% instead of the 1% currently used could be applied if there was only the influence of internal dilution. However, if an allowance was made for the dilution due to the collapse of the hangingwall in the roof of the stopes, then a higher cutoff grade of 1.25% could be applied.

The problem with hangingwall dilution is that when the hangingwall ground (roof of the stope) collapses it can lead to the hangingwall material blanketing off the ore, effectively making the broken ore in the stopes inaccessible. It is then necessary to remove the waste before the ore can be reached and extracted. If the volume of the material that collapses from the hangingwall is too great it will render the cost of reaching the ore buried beneath the collapse material prohibitive and the ore might be left unextracted leading to the loss of ore in-situ. The close collaboration and coordination between mining, rock mechanics and grade control sections in the management of hangingwall dilution cannot be overemphasised.

In the evaluation of the hangingwall position the significance of cobalt mineralisation in the pyritic argillite in the hangingwall section of the mineralised argillites has been recognised. It has been shown that there could be a gain in extracting the cobalt from the hangingwall provided that there were no substantial additional production costs as a result of extending the stoping into the hangingwall and that there was no decrease in the metallurgical recovery of copper or cobalt as a result of blending the immediate-hangingwall material (up to about 2m above the current hangingwall position) with the rest of the ore.

The density evaluation in the Baluba Centre Limb shows that the argillite has a mean value of 2.782 and the schist of 2.778. The variations in the densities in the different lithologies in Baluba Centre Limb are explained by assessing the variations in the host rock and metallic minerals. A uniform density of 2.67 is currently used at Baluba for all the sulphide orebodies. Even allowing for a decrease in the density due to the porosity there appears to be an underestimation of the tonnage factor by using the value of 2.67tonnes/m^3.

CHAPTER 8

DISCUSSION, CONCLUSIONS AND RECOMMENDATIONS

8.1 GEOLOGICAL SETTING AND MINERALISATION

The structure of the Copperbelt was formed mainly in response to the Lufilian Orogeny (circa 600 Ma). The present day structure of the Copperbelt is dominated by the Kafue Anticline which divides the deposits into the southwestern and northeastern flanks. On the southwestern flank the mineralisation is shale-hosted and on the northeastern side are arenite-hosted. The Baluba deposit belongs to the former group.

The copper and cobalt mineralisation in the Baluba deposit is hosted in Archean to Late Protorezoic tremolitic schists and argillites. The principal copper bearing minerals are chalcopyrite, bornite and chalcocite. Cobalt occurs in the form of carrollite in the schists and as cobaltiferous pyrite in the argillites. The metallic minerals occur as disseminated grains in the groundmass or in the massive form in the mineralised veins.

The primary metallic mineralisation in the Baluba deposit (and in other Copperbelt deposits) can be considered to have been introduced during sedimentary deposition. The Basement seems to be logical source of the copper mineralisation but not of cobalt. The Basement is enriched in copper and iron but not in cobalt. The source of cobalt is not clear. The mineralogy of the Basement seems to lack adequate levels of cobalt to account for the concentrations of cobalt seen in the Baluba Centre Limb.

Petrological studies indicate that the sediments have undergone low grade metamorphism of the greenschist facies. Local re-distribution of the metallic minerals is associated with the metamorphism. The minerals which have recrystallised in the massive form in the veins are noted to be of the same mineralogy as those in the immediately surrounding country rock. This suggests that the metamorphic reactions took place in a closed, isochemical system as there has been no addition or loss of metallic elements from outside the system subsequent to the original sedimentary deposition. The zonation into primary sulphide mineral groups associated with the sedimentary deposition has also been retained in the mineralised rocks. The recrystallisation has affected the distribution of copper and cobalt grades in the deposit and has implications on sampling and on the statistical and geostatistical characteristics of grades in the deposit.

The copper-bearing minerals of Baluba Centre Limb have compositions which are essentially the same as the expected theoretical stoichiometries. The cobalt bearing minerals have compositions which deviate considerably from the theoretical stoichiometries. The carrollites in Baluba are cobalt-rich and copper-poor compared to the theoretical composition of carrollite. The pyrites are found to be cobaltiferous. The cobaltiferous nature of the pyrites has an implication on the location of the hangingwall of the orebody- cobalt mineralisation extends beyond the hangingwall determined using copper grades only.

8.2 METAL SULPHIDE FORMATION AND VERTICAL GRADE VARIATION

The literature on the Copperbelt geology includes diagenetic and epigenetic ore genesis models. However, it is difficult to account for the large volumes of mineralised bodies using these models. Clearly, the deposits have been affected by post-sedimentary events, but it is unlikely that diagenesis and metamorphism were in themselves ore forming processes. There do not appear to be any discontinuities to suggest that the igneous bodies in the Basement are connected to the mineralised sediments of the Lower Roan. It is envisaged that the minerals were precipitated during sedimentary deposition and locally re-distributed and recrystallised during diagenesis and metamorphism.

In the absence of recrystallisation the grades would have been expected to vary steadily from the footwall to the hangingwall. Recrystallisation has introduced the small scale grade fluctuations. If the effects of metamorphic remobilisation and recrystallisation were removed from the vertical grade distribution pattern currently observed, a grade distribution pattern due to the primary sedimentary deposition could be determined.

8.2.1 Mathematical model of the synsedimetary ore deposition

In the description of the syngenetic model of ore genesis in Chapter 2 it was stated that the sulphide needed for the formation of metal sulphides was provided through the bacterial reduction of sulphates to sulphides in sea water. Rickard (1973) constructed a mathematical model to describe sulphide production in modern sediments due to sulphate-sulphide reduction by bacteria. Rickard's model is described by the equation:

$$C_c = C_{c(o)}\, e^{(-k/\sigma)x} \qquad \textbf{(8.1)}$$

where C_c is the concentration of bacterial carbon available for the reduction of sulphate
$C_{c(0)}$ is the metabolisable organic carbon initially available
k is the chemical reaction rate constant
σ is the sedimentation rate
x is the depth of water to the oxidation/reduction interface

Assuming a similar mode of formation of the sulphides in the Baluba deposit, it can be expected that the quantity of metal sulphides (hence the metal grades) will be related to the amount of bacterial carbon predicted in Rickard's model.

By analogy to Equation 8.1 the following relationship is proposed to describe the vertical grade variation in the Baluba deposit:

$$g = G\, e^{-(\frac{x-t}{a-t})^2} \qquad \textbf{(8.2)}$$

In this equation:

g is the grade of copper at a given position in the vertical profile of the orebody
G is the maximum copper grade (which is reached at the oxidation/reduction boundary)
x is the distance from the geological footwall contact
a is the distance from the geological footwall to the location of the 1% copper footwall (a_1) or hangingwall (a_2)
t is the width of the transitional schist

The convention adopted is that the geological footwall contact is the origin. Distances up into the orebody and hangingwall are positive and down into the footwall negative.

In the Baluba Centre Limb model the maximum grade, G, occurs at the contact between the transitional schist and tremolite schist The contact between the transitional and tremolite schists is considered to represent the oxidation/reduction boundary (*redoxcline*). The value of G is related to the available bacterial reducible sulphate, by analogy to Equation 8.1. Assuming the supply of sulphate from the sea water was not limiting, then the value of G would depend only on the availability of copper in solution. Hence the maximum grades would occur at the *redoxcline* where the metal availability would have been greatest - before any metals had precipitated from solution as metal sulphides.

a_1 is defined as the position of the footwall assay limit of the orebody. Since the geological and assay footwall contacts are coincident $a_1 = 0$. a_2 is the distance from the geological footwall to the position

of the 1% copper assay hangingwall. Note that by definition in Equation 8.2 the condition $a_2 \neq t$ must be met, or else the denominator in the exponential power term $(a - t)$ in Equation 8.2 becomes zero; division by zero cannot be evaluated. This implies that the hangingwall should be located beyond the transitional schist. This does not seem to create practical problems for the Baluba orebody since it is observed that the transitional schist is always mineralised and therefore the hangingwall is always located beyond the transitional schist, i.e. $a_2 > t$ at all times.

Two values of g are especially important in the model described by Equation 8.2, i.e. the values of g at the tremolite schist/transitional schist contact (*redoxcline*) and at the footwall contact. These two values depend on the value of the maximum grade G. At the transitional schist/tremolite schist contact (*redoxcline*) $x = t$, and the value of g at the redoxcline is evaluated to be G, the maximum grade. At the footwall contact x and a are both zero and g is calculated to be 0.37G, just over a third of the maximum grade.

8.2.2 Graphical representation of the mathematical model

The model proposed in Equation 8.2 was represented graphically by plotting the copper grades (g) on the y-axis against the distance from the footwall (x) on the x-axis. The data used were the averages of copper assay grades of drill holes from the same data base used to construct the zonation model in Figure 1.2. The width of the transitional schist (t) was determined as an average width of transitional schist from geological mapping data. Having fixed the value of t, G and a were then visually determined by iteratively fitting the mathematical model to the sampling data until the best curve to describe the drill hole data was achieved.

Figure 8.1 illustrates how the mathematical model represented Equation 8.2 has been used to fit a smooth curve to the sampling data. The values of t, G, and a used to fit the curve were 2m, 3.25% Cu and 17m respectively.

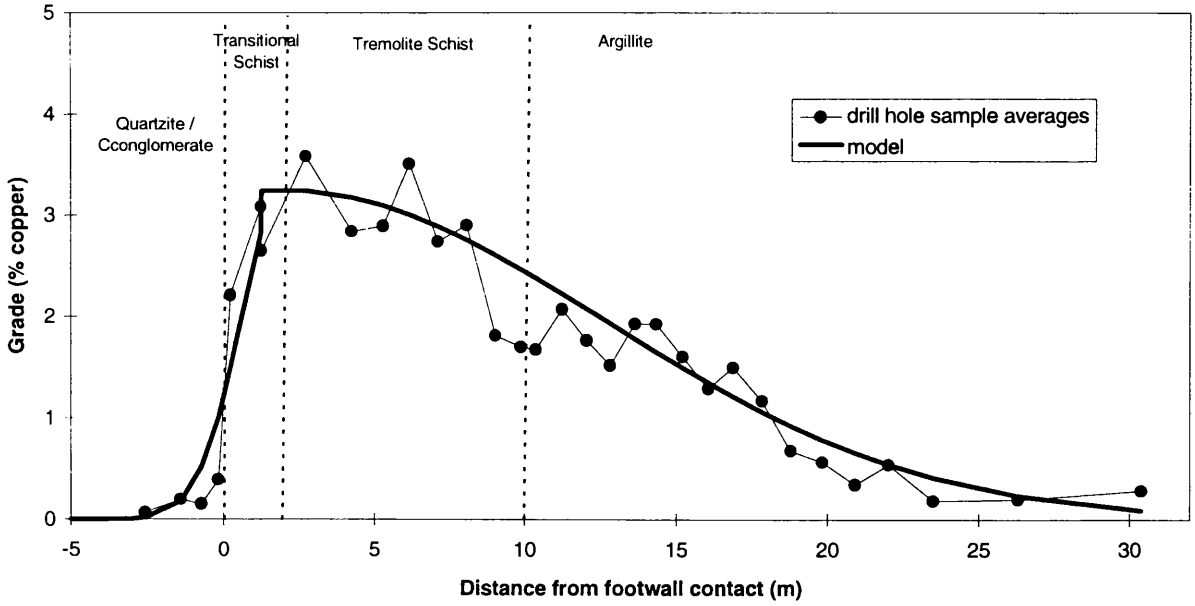

Figure 8.1: The mathematical model is used to fit a smooth curve to the Baluba Centre Limb sampling data. The curve described by the model possibly represents what the distribution of grades would have been in the absence of the post-sedimentary effects on the rocks.

The position of the assay footwall cutoff is fixed at $a = 0$ as described above. The position of the hangingwall (x_{hw}) can be read off the graph by finding the value of x where the value of the grade at $\log_e$ (G × cutoff grade) intersects the model curve. By default a 1% copper cutoff grade is used to describe the curve. Using this default value $\log_e (3.25 \times 1) = 1.18$ and the corresponding value of $a = 17$m, confirming the position of the hangingwall which was used to model the graph. As the cutoff grade is varied new positions of the hangingwall can be determined. For example if the cutoff grade was raised to 1.5%, then $x_{hw} = 15$m, and if it was lowered to 0.5%, $x_{hw} = 22$m.

8.2.3 Relationship of the mathematical model to the observed geological characteristics and grade distributions

In deriving the mathematical model for the sedimentary ore genesis the maximum grade, G, is located at the contact between transitional and tremolite schists, not at the geological footwall contact (see Equation. 8.2 and Fig. 8.1). The transitional schist has been grouped with the footwall

sediments rather than with the tremolite schists. This probably concurs with the stratigraphic correlation generally adopted for the Copperbelt rocks. The transitional schist is allocated to the Lower Roan 7 (RL7) formation together with the footwall quartzites and conglomerates, and not the RL6 formation to which the tremolite schists and argillites belong (see Baluba stratigraphy, Fig. 2.7). The transitional schists are therefore most likely an altered siliceous, clastic rock of the footwall type. The presence of copper mineralisation could be explained by the downward percolation and secondary oxidation enrichment of the primary sulphide mineralisation hosted in the tremolite schists. This is supported by the mineralisation in the transitional schists being dominated by secondary sulphides and oxides (see Fig. 2.1). Doubtless, the primary sulphide mineralisation proper commences in the tremolite schists.

The sharpness of the assay footwall contact can be explained by assuming a sudden influx of metals supplied from the basement landmass into the Katanga sediments as they were being deposited in the shallow shelf of the Katanga sea. Precipitation of the metallic minerals was determined by the stabilities of the metal sulphides in equilibrium with the metal ions (see Table 2.1). Assuming the sulphate availability was not limiting, a steady decrease in the metal availability as more metals were precipitated from the mineralising solution would be expected. This is represented by the steady decrease in the metal grades towards the hangingwall (as opposed to the steep gradient at the footwall). As x increases the curve becomes more asymptotic owing to the slowing in the rate of metal sulphide formation as the solution became further depleted in the metal. In theory if the cut off grade used were in the asymptotic part of the graph then the determination of the position of the hangingwall would be rendered difficult. Since the curve fitted to the vertical grade distribution indicates that the grade changes in the hangingwall region are expected to be smooth and gradual, the grade variations associated with the sedimentary deposition should be small.

The gradual grade change in the vicinity of the hangingwall coupled with the grade fluctuations due to recrystallisation render the optimisation of the location of the hangingwall difficult. The slow change in the grades towards the hangingwall is further supported by the variogram modelling results. The down-hole variograms showed that the range obtained in the argillites was longer than that in the schists (see Fig. 6.3).

The mathematical model described here seems to adequately describe the underlying sedimentary deposition of the metals, discounting the grade fluctuations introduced by post-sedimentary events.

8.3 USE OF GEOLOGY AS A CONTROL ON STATISTICS AND GEOSTATISTICS

For statistics and geostatistics to comply with the in-situ geological reality the assay data on which the statistics, geostatistics and other numerical evaluations are carried out should be an accurate reflection of the geological reality. The litho-strata displayed in the Baluba Centre Limb deposit and the zonation into metallic mineral categories serve as good natural geological boundaries to use in the assessment of the deposit. A complex behaviour of the variables is exhibited when the data are analysed together without regard to the associated geological and mineralogical classification. Simplified and more coherent statistical and geostatistical patterns are discernable when the data are grouped and analysed according to the lithological and mineralogical groups.

8.4 CUTOFF GRADES AND DEFINITION OF THE LIMITS OF THE OREBODY

The application of cut off grades to define the footwall and hangingwall of the orebody should be such that the ore and waste portions of the mineralised body are clearly segregated. This can best be achieved if the difference in the concentrations between the ore and waste are significant to allow an objective segregation between them. In the Baluba Centre Limb deposit it is seen that the assay grades vary rapidly from background copper and cobalt concentrations in the quartzites and conglomerates (less than 0.25% copper and 0.05% cobalt) to grades of well over 2% copper and 0.2% cobalt in the overlying schist. In addition, the change in mineralisation coincides with the geological contact between the conglomerates and schists. Hence, the footwall assay contact is essentially represented by a visual geological contact.

The geologically fixed footwall contrasts with the hangingwall which is determined on the basis of assay grades only without a corresponding geological marker. The demarcation of the orebody using cut off grades to define the hangingwall limit of mineralisation is affected by the subtle copper grade variations in the hangingwall region.

To optimise the location of the hangingwall the cutoff grades are evaluated by assessing the effects of internal and hangingwall dilution. The significance of cobalt mineralisation in the optimisation

of the hangingwall is acknowledged and a cutoff criterion combining the effects of copper and cobalt dilution is presented.

8.4.1 Grade control

Mining entails the depletion of mineral reserves, which like other natural resources must be optimally utilised. On one extreme it could be argued that all the available mineral resource should be extracted - maximising the utilisation of the resource. This would imply extracting the entire mineralised body (using only geological boundaries) without applying cutoff grades to discriminate between ore and waste. The other extreme of the argument would be to aim at the maximisation of the return on the investment. This would be achieved by extracting only the richest sections of the resource in order to maximise the profit per unit of rock mined.

Grade control is a process where the target grade is determined so as satisfy the objectives of mining operations (Dixon, 1979). It is the mechanism used to monitor and ensure that the material being mined is constrained within the defined ore limits and that the ore being sent to the mill is blended from different production blocks in such proportions that the ore produced has an actual grade within tolerable limits of the target grade (Lane, 1988; Annels, 1991). Grade control plays an important role in guiding mining and monitoring the production to ensure that the rock being mined and sent to the mill remains within the planned schedule.

Grade control is implemented on the basis of grade information obtained from sampling of production points. At Baluba grade control sampling is carried out by taking grab samples from draw points, ore passes and the cable belt. In order for grade control to be carried out effectively, reference must be made to expected grades during the production life of a stope. When grade control samples indicate grades lower than cutoff grade this should not necessarily suggest that a stope has advanced beyond the ore limits. As discussed in Chapter 7 some dilution may have to be included with ore in the definition of the orebody as intentional (planned) dilution. Hence the assays of grade control samples from production blocks should always be compared to the geological plans and sections showing the variations of expected in-situ grades.

The effectiveness of grade control is tested by comparing the calculated minerals reserves contained in the blocks and the ore actually received at the mill. This process of comparing the reserves and the milled reserves (reconciliation) can indicate when and where the grade control needs to be improved.

Table 8.1 presents a summary of how the geological features affect sampling and definition of the orebody in the Baluba Centre Limb.

8.5 SUGGESTED PARAMETERS TO USE

Based on the results drawn from this study the following parameters are recommended for use in the Baluba Centre Limb for the evaluation of mineral reserves:

(i) Currently samples of different lengths are taken along drill holes (see Fig. 4.11, Chapter 4). It is desirable that sampling should be constant through time and space (Journel and Huijbregts, 1978). It is suggested that samples of regular lengths of 1m should be taken along diamond drill holes to eliminate the bias due to the support effect. Based on the drill hole data from the Baluba Centre Limb the change to regular 1m sampling interval should reduce the number of samples by about 30% (911 samples unregularised to 649 regularised 1m samples). This should translate into a saving on the the cost of preparation and analysis of the samples.

(ii) A 1.25% copper cut off should be applied to define the hangingwall limit of the orebody. At this cutoff grade the dilution is minimised making an allowance for up to 2m of ground collapse from the hangingwall waste. If the hangingwall could be completely controlled then a lower cutoff grade of 0.75% could be used.

(iii) In the horizontal plane the copper variograms of the Baluba Centre Limb samples were isotropic with a range of 100m. Therefore, as a general guide, the drill holes should not be located longer than 100m apart or else part of the grade continuity information would be missed. The final layout of the drill holes should be determined using the information from variogram modelling so as to achieve a practical sampling pattern that would minimise the estimation variance.

Table 8.1: Summary of the main features of mineralisation and their effects on the definition of the orebody in the Baluba Centre Limb.

1. Ore Genesis

	Basement landmass	Katanga sea
Ingredients provided	Metals - Cu, Fe (± Co?) in solution from erosion of hinterland	Sulphur in sea water
Conditions	High Eh, low pH - oxidising and acidic	Low Eh, high pH - reducing and alkaline
Reactions/Products	Fe oxides	Bacterial reduction of sulphur to sulphide. Sulphide combines with metals to form metal sulphides

2. Observed features

	Footwall clastic sediments	Mineralised argillaceous sediments	
	Conglomerates and quartzites	Schists	Argillites
Primary Zonation of sulphides	Absence of metallic mineralisation	chalcocite → bornite → [carrollite] → chalcopyrite → pyrite **ZONATION MODEL : Chapters 1 & 2**	
Nature of copper assay contacts	Background Cu and Co mineralisation	Sharp assay footwall contact	Diffuse assay hangingwall contact **MATHEMATICAL MODEL FOR SEDIMENTARY MINERALISATION: Chapter 8**
Metamorphic effects on metallic mineralisation	----	Recrystallisation of minerals along schistose planes.	Recrystallisation of minerals along metamorphic veins.

Table 8.1 contd

	Conglomerates and quartzites	Schists	Argillites
Effects on sampling	----	Lower sampling variance	Higher sampling variance
		ANALYSIS OF VARIANCE: Chapter 5	
Effects on statistics/geostatistics	----	Higher variance, lower relative nugget effect	Lower variance, higher relative nugget effect
		VARIOGRAM MODELLING: Chapter 6	
Definition of orebody	----	Geological footwall contact coincides with assay footwall contact	Less well defined assay hangingwall contact. No corresponding geological marker
		ANALYSIS OF DILUTION : Chapter 7	
Effects on ore specific gravity	Specific gravity similar to average of common quartzitic rocks	Variable specific gravity owing to the mixed mineral assemblages. Specific gravity influenced by the presence of metallic minerals	
		DENSITY ANALYSIS: Chapter 7	

8.6 RECOMMENDATIONS FOR FURTHER WORK

8.6.1 Drill hole spacing

Although the drill hole sample data is used for the calculation of mineral reserves, the layout of drill holes in the Baluba Centre Limb is currently mainly planned for the purpose of elucidating the structure of the orebody for the design of mining blocks rather than for purposes of evaluating mineral reserves. For geostatistical applications, ideally the drill holes should be located on a regular grid pattern. It is recommended that for the future layout of drill holes in Baluba Centre Limb a compromise should be reached between the needs for design of mining blocks and for generating data for the reserve data base.

8.6.2 Chip sampling

It has been observed in this study that the chip samples in the Baluba Centre Limb give rise to sampling variances which are much higher compared to diamond drill sampling. It would be necessary to improve the chip sampling as it is currently practised at Baluba or to change to another non-drill sampling method which would give rise to smaller sampling variances. Channel (or groove) sampling is one method that could be used to reduce the sampling errors. Channel sampling provides continuous samples and can therefore be expected to give more reproducible samples and hence a smaller sampling variance. Caution must be taken, however, in the application of channel sampling. Practical experience indicates that although the channel samples are continuous, cutting of channel samples is difficult in hard rock (Annels, 1991).

Sample acquisition methods for reserve estimations and grade control should be clearly defined and easy to apply and monitor. They should be accurate and precise, without introducing obvious economic constraints. A balance between the reliability of sampling data and cost of sample acquisition needs to be considered (Springett, 1984; Storrar, 1987; Annels, 1991). Several alternative variants of chip and channel sampling could be tested for suitability in the Baluba Centre Limb and the results of sampling compared in terms of sample data quality and cost of sampling so as to select the best sampling method and procedure.

8.6.3 Grade continuity in schist

The down-hole variogram modelling has indicated that the grade continuity in the schists might be a pure nugget effect or one with a range just over 1m (Fig. 6.3). In selected drill holes, it might be appropriate to take samples of lengths shorter than the regular 1m lengths suggested in section 8.5. in order to verify the range (and nugget effect) associated with the mineralisation in schist. A sample length of 0.25m could be practical for this purpose.

8.6.4 Hangingwall dilution

It is clear that to fully comprehend the effects of hangingwall dilution it is important to analyse the geotechnical characteristics of the rock in the hangingwall. Sampling further into the hangingwall will be required to obtain grade and rock geotechnical information in order to assess the effects of cobalt mineralisation in the hangingwall and to evaluate the hangingwall dilution more thoroughly. It is proposed that a complete economic analysis be carried out to test the suitability of extending the orebody to extract the cobalt in the immediate hangingwall region of the orebody. Samples could be taken at least 10m into the hangingwall beyond the visual 1% copper hangingwall.

8.6.5 Application of cobalt in the definition of the hangingwall

As noted in this study possible economic cobalt mineralisation extends beyond the currently defined hangingwall. Instead of using only the copper grade in determining the footwall and hangingwall limits of the orebody, a combined relationship incorporating copper and cobalt could be applied. This approach would take into consideration the effect of cobalt mineralisation rather than regarding copper exclusive of the cobalt. In parts of the hangingwall the revenue from cobalt can be of more significance than copper.

The aim of using the combined copper-cobalt relationship would be to assist in determining which portions of the argillite in the hangingwall have high cobalt mineralisation and could therefore be included with the orebody on the account of cobalt mineralisation. A relationship between copper and cobalt would need to be established so that the grades of copper and cobalt could be combined. To achieve this will require evaluating the copper-equivalent grades of cobalt. As highlighted in Equation 7.3 in Chapter 7, the costs of production and treatment, the metal prices and metallurgical recoveries affect the assessment of the cutoff grades. By evaluating the relative costs, prices and

metallurgical recoveries for copper and cobalt the relationship of the form $(Cu + k.Co)$ would be determined so that cobalt grades were converted to copper equivalent. Previous work at the ZCCM Operations Centre in Kalulushi have suggested a value of k ranging from 3.5 to 15 (ZCCM, 1990). The determination of k has been inconclusive owing to the lack of reliability in the data of cobalt metallurgical recoveries in the hangingwall section of the orebody. As suggested in the previous section it is imperative in the assessment of cobalt recovery to include samples drawn from beyond the 1% copper hangingwall.

REFERENCES

AFIFI A. M and ESSENE E. J. 1988. MINFILE - a microcomputer program for storage and manipulation of chemical data of minerals, *Am. Mineral.*, **73**, p. 446-448.

ANNELS A. E. 1974. Some Aspects of the stratiform ore deposits of the Zambian Copperbelt and their genetic significance. In: Gisements stratiformes et Provinces cuprifères, Bartholomé P. (ed), Liège, *Soc. Géol. Belg.*, p. 235-254.

ANNELS A. E., VAUGHAN D. J. and CRAIG J. R. 1983. Conditions of ore mineral formation in certain Zambian Copperbelt deposits with special reference to the role of cobalt., *Minera. Deposita*, **18**, p. 71-88.

ANNELS A. E. and SIMMONDS J. R. 1984. Cobalt in the Zambian Copperbelt, *Precambrian Res.*, **25**, p. 75-98.

ANNELS A. E. 1984. The geotectonic environment of the Zambian copper/cobalt mineralization, *J. Geol. Soc. Lon.*, **141**, p. 279-289.

ANNELS A. E. 1989. Ore genesis in the Zambian Copperbelt, with particular reference to the northern sector of the Chambishi Basin. In: Sediment-hosted stratiform copper deposits, Boyle R. W. *et al.* (eds), *Geol. Assoc. Canada*, p. 427-452.

ANNELS A. E. 1991. Mineral deposit evaluation: A practical approach, Chapman & Hall, 436pp.

BANCROFT J. A. and PELLETIER R. A. 1929. Notes on the general geology of Northern Rhodesia, *Mining Mag.*, **41,** p. 369-372;, **42**, p. 47-50, 117-120, 180-182.

BAAS BECKING W. M. B. and MOORE D. 1961. Biogenic sulphides, *Econ. Geol.*, **56**, p. 259-272.

BATEMAN A. M. 1930. Ores of the Northern Rhodesian Copperbelt, *Econ. Geol.*, **25**, p 365-418.

BAXTER A. R. and HOOPER G. B. 1992. Use of "three-dimensional solids modelling" system for Baluba Centre/South Limb feasibility study at ZCCM, Ltd, *Trans. Instn Min. Metall. (Section B: Appl. earth sci.)*, **101**, p A41-A46.

BINDA P. L. 1969. The top of the RL7 at Muliashi South: Part II: Mineralisation and sedimentary Geology, Roan Selection Trust Technical Services, Unpublished Company report, 18pp.

BINDA P. L. and MULGREW J. R. 1974. Stratigraphy of copper occurreences in the Zambian Copperbelt. In: Gisements stratiformes et Provinces cuprifères, Liège, Bartholomé P. (ed), *Soc. Géol. Belg.*, p. 215-233.

BOWEN R. and GUNITALAKA A. 1977. Copper: its Geology and Economics, Applied Science Publ. 366pp.

BOYLE R. W., BROWN A. C., JEFFERSON C. W., JOWETT E. C. and KIRKHAM R. V. (eds) 1989. Sediment-hosted stratiform copper deposits, *Geol. Assoc. Can.*, Special Paper 36, 710pp.

BROCK B. B. 1963. On the structure and sedimentation of the Katanga basin. In: Stratiform Copper Deposits in Africa, Lombard J.and Nicolini P. (eds), *Assoc. Afr. Geol. Surveys*, Paris, p.166-142.

BROWN A. C. 1984. Alternative sources of metals for stratiform copper deposits, *Precambrian Res.*, **25**, p. 61-74.

BROWN A. C. 1992. Sediment-hosted stratiform Copper deposits, *Geosci. Can.*, **19,** p. 125-141.

BRUMMER J. J. 1955. The Geology of the Roan Antelope Orebody, *Trans Instn Min. Metall.*, **64**, p 257-318.

CAHEN L. 1970. Igneous activity and mineralisation episodes in the evolution of the Kibaride and Katangide orogenic belts of Central Africa. In: African magmatism and tectonics, Clifford T. N. and Gass I. G. (eds), Oliver and Boyd., p. 97-117.

CLARK I. 1979a. Practical Geostatistics, Elsevier Applied Science Publ., 129pp.

CLARK I. 1979b. The Semi variogram - Part I, *Engng. and Min. Journal*, **180** (7), p. 90-94.

CLARK I. 1979c. The Semi variogram - Part II, *Engng. and Min. Journal*, **180** (8), p. 92-97.

COWPER M. and RICKARD D. T. 1989. Mechanism of chalcopyrite formation from iron monosulphides in aqueous solutions (<100°C, pH 2-4.5), *Chem. Geol.*, **78**, p. 325-341.

CRAIG J. R., VAUGHAN D. J. and HIGGINS J. B. 1979. Phase relations in the Cu-Co-S System and Mineral Associations of the carrollite ($CuCo_2S_4$) - Linnaeite (Co_3S_4) Series, *Econ. Geol.*, **74**, p. 657-671.

DARNLEY A. G. and KILLINGWORTH P. J. 1962. Identification of carrollite from Chibuluma by X-ray scanning microanalyser, *Trans. Instn Min. Metall.*, **72**, p. 165-168.

DAVID M. 1988. Dilution and geostatistics, *CIM Bull.*, **81** (914), p. 29-35.

DAVID M. and TOH E. 1989. Grade control problems dilution and geostatistics: choosing the required quality and number of samples for grade control, *CIM Bull.*, **82** (931), p. 53-60.

DAVIS G. R. 1954. The Origin of the Roan Antelope copper deposit of Northern Rhodesia, *Econ. Geol.*, **49**, p. 575-615.

DE RUITER H. 1985. Problems of ore density determination at Nanisivik Mines, *Geol. en Mijnbouw*, **64**, p. 63-67.

DE WIJS H. J. 1972. Method of successive differences applied to mine sampling, *Trans. Instn Min. Metall.*, **81**, p. A78-81.

DIXON C. J. 1979. The role of the geologist in Grade Control, Unpublished course notes, Witwatersrand University.

DRYSDALL A. R., JOHN R. L., MOORE T. A. and THIEME J. G. 1972. Outline of the geology of Zambia, *Geol. en Mijn.*, **51**, p. 265-276.

FLEISCHER V. D., GARLICK W. G. and HALDANE R. 1976. Geology of the Zambian Copperbelt. In: Handbook of stratabound and stratiform ore deposits, vol. **6**: Cu, Zn, Pb and Ag deposits, Wolf K. H. (ed), Elsevier Scientific Publ., p 223-352.

GARLICK W. G. and BRUMMER J. J. 1951. The ages of the Granites of the Northern Rhodesian Copperbelt, *Econ. Geol.*, **46**, p. 478-497.

GARLICK W. G. 1953. Reflections on prospecting and ore genesis in Northern Rhodesia, *Trans. Instn Min. Metall.*, **63**, p. 9-20.

GARLICK W. G. 1964. Criteria for recognition of syngenetic sedimentary mineral deposits and veins formed by their remobilization, *Proc. 8th Congress Commonwealth Min. Metall.*, vol. **6** (General), p. 1393-1418.

GARLICK W. G. and FLEISCHER V. D. 1972. Sedimentary environment of the Zambian Copper deposition, *Geol. en Mijnbouw*, **51**, p. 277-298.

GARLICK W. G. 1976. Geology of the Zambian Copperbelt. In: Handbook of stratabound and stratiform ore deposits, vol. **6**: Cu, Zn, Pb and Ag deposits, Wolf K. H. (ed), Elsevier Scientific Publ., p 285-352.

GARLICK W. G 1989. Genetic interpretation from ore relations to algal reefs in Zambia and Zaire. In: Sediment-hosted stratiform copper deposits, Boyle R.W. *et al.*(eds), *Geol. Assoc. Can.*, p. 471-498.

GARRARD P. 1972. The Geology of the Chingola area, Zambia. PhD. thesis - Unpublished, University of London, 193pp + illustrations.

GRAY A. and PARKER R. J. 1929. The Copper deposits of Northern Rhodesia, *Engng. and Min. Journal*, **128**, p. 384-389, 429-434, 470-473.

GY P. M. 1974. The sampling of broken ores; a review of principle and practice. In: Geological, mining and metallurgical sampling , Jones M.J. (ed), *Instn Min. Metall.*, p. 194-205.

GY P. M. 1982. Sampling of particulate minerals: theory and practice, 2nd edition, Elsevier Scientific Publ. 431pp.

ISAAKS E. H. and SRIVASTAVA R. M. 1989. An introduction to Applied Geostatistics, Oxford Univ. Press, 561pp.

JOURNEL A. G. and HUIJBREGTS C. J. 1978. Mining Geostatistics, Academic Press, 600pp.

KERR P. F. 1945. Cattierite and Vaesite: New Co-Ni minerals from the Belgian Congo, *Am. Mineral.*, **30**, p. 483-497.

KLEIN C. and HURLBUT C. S. 1993. Manual of mineralogy, Wiley and Sons, 681pp.

KRIGE D. G. 1978. Lognormal de Wijsian Geostatistics for Ore Evaluation, *South Afr. Instn Min. Metall.*, 50pp.

LANE K. F. 1988. The Economic definition of ore: Cut-off Grades in Theory and Practice, Mining Journal Books Ltd., 211pp.

LINDGREN W. 1933. Mineral Deposits, McGraw Hill, , 930pp.

MABSON L. R. 1976. The development of Baluba Mine, *Min. Mag.*, **135,** p. 412-423.

MATHERON G. 1971. The Theory of Regionalized Variables and its applications, Ecole Nationale Superieur des Mines de Paris, 211pp.

MENDELSOHN F. 1959. The Structure of the Roan Antelope deposit, *Trans. Instn Min. Metall.*, **68**, p. 229-262.

MENDELSOHN F. (ed) 1961. The Geology of the Northern Rhodesian Copperbelt, MacDonald, 523pp.

MENDELSOHN F. 1962. The lithology of the Roan Antelope deposit. In: Stratiform Copper deposits in Africa Symposium, Lombard J and Nicolini P. (eds), *Assoc. Afr. Geol. Surveys*, Volume I, p. 173-179.

MENDELSOHN F. 1989. Central/Southern African Ore Shale deposits. In: Sedimentary hosted stratiform copper deposits, Boyle R. W. *et al* (eds), *Geol. Assoc. Can.*, p. 453-469.

MINING JOURNAL. 1992. ZCCM The way forward: Company Supplement, *Min. Journal*, **319**, 16pp.

MINING JOURNAL. 1994. Metals and Minerals Annual Review 1994. *Min. Journal*, p. 33-39, 61-62.

NOTEBAART C. W. and VINK B. W. 1972. Ore minerals of the Zambian Copperbelt, *Geol. en Mijnbouw*, **51**, p. 337-345.

PERRY J. H. E. and WIIK V. H. 1972. Unrolling of Copperbelt orebodies, *APCOM*, 10th Proceedings, p. 185-188.

PETERS W. C. 1987. Exploration and Mining Geology, John Wiley & Sons, 2nd edition, 696pp.

PRYOR R. N., RHODEN H. N. and VILLALON M. 1972. Sampling of Cerro Colorado, Rio Tinto, Spain, *Trans. Instn Min. Metall. (Section A: Min. industry)*, **81**, p. A142-A159.

RAMSAY C. R. and RIDGWAY J. 1977. Metamorphic patterns in Zambia and their bearing on problems of Zambian tectonic history, *Precambrian Res.*, **4**, p. 321-337.

RAMSEY M. H., THOMPSON M. and HALE M. 1992. Objective evaluation of precision requirements for geochemical analysis using robust analysis of variance, *J. Geochem. Expl.*, **44**, p. 23-36.

RAMSEY M. H. 1993. Sampling and Analytical Quality Control (SAX) for improved error estimation in the measurement of Pb in the environment using robust analysis of variance, *Applied Geochem.*, Supplementary Issue No. 2, p. 149-153.

RAMSEY M. H., POTSS P. J., WEBB P. C., WATKINS P., WATSON J. S. and COLES B. J. An objective assessment of analytical method precision: comparison of ICP-AES and XRF for the analysis of silicate rocks, *Chem. Geol.* In press.

RANTA D. E., WARD A. D. and GANSTER M. W. 1984. Ore Zoning Applied to Geologic Reserve estimation of molybdenum deposits. In: Applied Mining Geology, Erickson A. J. (ed), *AIME*, p. 83-114.

RAYBOULD J. G. 1978. Tectonic controls of Proterozoic stratiform mineralization, *Trans. Instn Min. Metall. (Section B: Appl. earth sci.)*, **87**, p. B79-B86.

R.C.M Ltd. 1978. Zambia's Mining Industry - The First 50 years. Roan Consolidated Copper Mines Ltd., unpublished company report.

RENDU J-M. 1979. Kriging, logarithmic kriging and conditional expectation: comparison of theory with actual Results, 16th APCOM symposium, *A.I.M.E.*, p. 199-212.

RENDU J-M. 1981. An Introduction to Geostatistical methods of Mineral Evaluation, 2nd edition, *South Afr. Instn Min. Metall.* , 84pp.

RENFRO A. R. 1974. Genesis of Evaporite Associated stratiform metalliferous deposits - a Sabkha process, *Econ. Geol.*, **69**, p 33-45.

RICHARDS G. W. 1965. Geology and Mineralization of the copper-cobalt deposits of the South Orebody, Nkana, Northern Rhodesia (Zambia). PhD. Thesis, Univ. London.

RICKARD D. T. 1973. Limiting conditions for the synsedimentary sulphide ore formation, *Econ. Geol.*, **68**, p. 605-617.

RILEY J. F. 1965. An intermediate member of the Binary System FeS_2 (pyrite) - CoS_2 (cattierite), *Am. Mineral.*, **50**, p. 1083-1086.

RILEY J. F. 1980. Ferroan carrollites, cobaltian vioarites, and other members of the linnaeite group: $(Co,Ni,Fe,Cu)_3S_4$, *Mineral. Mag.*, **43**, p. 733-739.

ROBERTS W. M. B. 1963. The low temperature synthesis in aqueous solution of chalcopyrite and bornite, *Econ. Geol.*, **58**, p. 52-61.

ROYLE A. G. 1979. Why Geostatistics?, *Engng. and Min. Journal*, **180** (7), p. 92-101.

SCHNEIDERHÖHN H. 1932. The Geology of the Copperbelt, Northern Rhodesia, *Min. Mag*, **46**, p. 241-245.

SIMMONDS J. R. 1979. Repetition of Luanshya cobalt assays using an X-ray Fluorescence Technique (XRF), Z.C.C.M Ltd, Luanshya Division Internal Report - Unpublished.

SIMMONDS J. R. 1980. Significance of the Baluba orebodies with respect to Zambian copper-cobalt mineralization. PhD. thesis - Unpublished, University of Wales.

SPRINGETT M. W. 1984. Sampling practices and problems, in: Applied Mining Geology, Erickson A. J. (ed), *AIME*, p. 189-195.

STORRAR C. D. (ed) 1987. South African Mine Valuation, 2nd edition, Chamber of Mines of South Africa, 470pp.

TARR W. A. 1935. The linnaeite group of cobalt-nickel-iron-copper sulfides, *Am. Mineral.*, **20**, p. 69-80.

TAYLOR H. K. 1972. General background theory of cutoff grades, *Trans. Instn Min. Metall. (Section A: Min. industry)*, **81**, p. A160-A179.

THOMPSON M. and HOWARTH R. J. 1976. A new approach to the estimation of analytical precision, *J. Geochem. Exploration*, **9**, p 23-30.

THOMPSON M. and WALSH J. N. 1983. A handbook of inductively coupled plasma spectrometry, Blackie, 273pp.

UNRUG R. 1989. Landsat-based Structural Map of the Lufilian Fold Belt and the Kundelungu Aulocogen, Shaba (Zaire), Zambia and Angola, and the Regional Position of Cu, Co, Au, Zn and Pb Mineralization. In: Sediment-hosted stratiform copper deposits, Boyle R. W. *et al.* (eds), *Geol. Assoc. Can.*, p. 519-524.

VINK B. W. 1972. Sulphide mineral zoning in the Baluba orebody, Zambia, *Geol. en Mijnbouw*, **51**, p. 309-313.

WOLF K. H. 1976. Handbook of stratabound and stratiform ore deposits, vol 6: Cu, Zn, Pb and Ag deposits, Elsevier Scientific Publ., 585pp.

Z.C.C.M Ltd. 1990. Baluba Centre/South Limb Study, Z.C.C.M Technical Services, Volume C, Zambia Consolidated Copper Mines Ltd., unpublished company report, 217pp.

Z.C.C.M Ltd. 1994. 1993/1994 Company Annual Report, Zambia Consolidated Copper Mines Ltd., 56pp.

ZEISS E. G. ALLEN E. T., MERWIN H. E. 1916. Some reactions involved in secondary copper sulphide enrichment, *Econ. Geol.*, **11**, p. 407-503.

APPENDIX A

SAMPLING DATA

Examples of geological diamond drill hole logs from the Baluba Centre Limb. The top page (sheet 1) contains the drill hole collar location, assay summary and plotting record. Subsequent pages (page 2 onwards) contain the geological and geotechnical descriptions of the rock.

ZCCM LUANSHYA DIVISION
DIAMOND DRILL HOLE LOG

Sheet No. 1 of: 02

DRILL HOLE No. BL0032

AREA: BALUBA CENTRE LIMB. LEVEL: 450 'D' FOOTWALL DRIVE SECTION: STRUCTURE SECTION 46 LOGGED BY: C.C. KAPUMPA

INCLINATION: -87.4° FINAL DEPTH: 7.0m BITSIZE: AXT DATE: 06.08.93

BEARING: 297.65° COLLAR CO-ORDINATES Y - 9220.4m X + 10376.7m COLLAR ELEVATION: 817.34m

1% SULPHIDE COPPER CUT-OFF

Limb	Orebody	Metrage	Width	Recovery	Av. Total	Av. Oxide	Av. Sul.	Av. Total
C/L	Incomplete orebody exposure							

PLOTTING RECORD

	SIGNATURE	DATE
Issue authorised by Geologist		
Plotted on section		
Plotted on plan		
Checked by Geologist		

METRAGE	Drilled	Recv'd	Horizon	ROCK TYPE	STRUCTURE			GROUND CONDITIONS		MINERALIZATION		ASSAYS						
					Sch	Metrage	Bdg	Cond'n	REMARKS	Zone	Accessory	Metrage	Drill	Recovery	Sample No.	Total	Oxide	Total
										cp^{10}	car^{4}	0.0-0.5	0.5	100	GA2273	3.39	0.30	0.25
										cp^{10}		0.5-1.0	0.5	100	2274	2.87	0.49	0.21
										cp^{11}	car^{4}	1.0-1.5	0.5	100	2275	2.80	0.33	0.24
										cp^{12}	bn^{2}	1.5-2.0	0.5	100	2276	1.53	0.13	0.17
										cp^{10}	bn^{1}	2.0-2.5	0.5	100	2277	1.57	0.15	0.10
										cp^{7}	cup^{2}	2.5-3.2	0.7	100	2278	2.33	0.23	0.11
										csc		3.2-3.7	0.5	100	2279	0.40	0.10	0.02
										NVM		3.7-4.2	0.5	100	2280	0.13	0.03	0.02
										NVM		4.2-4.7	0.5	100	2281	0.14	0.06	0.03
										NVM		4.7-5.7	1.0	100	2291	0.30	0.06	0.07
										NVM		5.7-7.0	1.3	100	2292	0.08	0.05	0.03

ZCCM LUANSHYA DIVISION
DIAMOND DRILL HOLE LOG

Page: 2 of: 02

DRILL HOLE No. BL0032

DISTANCE					ROCK TYPE	DESCRIPTION	ASSAY RESULTS						GROUND CONDITION					STRUCTURE				MINERALISATION		
From	To	Drilled	Recvry%	Form'n			Unit	Sample No	T.Cu%	Ox.Cu%	T.Co%	Cat	Metrage	RQD%	PLV(Mpa)	Cond'n	Remarks	Depth	Schs'ty	Bdg	Joints	Metrage	Zone	Accessory
0.0	2.5	2.5	100	RL6	BIOTITC	Greenish grey to black, med. grained, highly biotitic and tremolitic	OB					2				FAIR		1.0	85°				cpy	car
					TREM.	schsist.Schistosity highlighted by light coloured tremolitic portions and																		bn
					SCHIST	dark micaceous bands. Abundant acicular, radiating tremolite crystals																		
						common. Pink microcline feldspar band @ 2.0m (0.1m thick).																		
						Massive and disseminated cpy minz'n.																		
2.5	3.2	0.7	100	RL7	TRANS.	Black, highly biotitic and partly tremolitic rock. Moderately developed	OB					2				FAIR		2.6	85°				cpy	
					SCHIST	schistosity. Med. grained. Disseminated and massive cpy minz'n.										TO		2.8	80°					
																POOR								
3.2	5.7	2.5	100	RL7	FOOTWALL	A pebble conglomerate with vein qtz and qtzite clasts. Clasts are	FW					1				FAIR							-	csc
					CONGL.	rounded to sub rounded, sub-spherical, moderately sorted. Mtx is										TO								
						micaceous and tremolitic. Red Iron oxide coating along some clast										POOR								
						surfaces - near contact with transitional schist. Csc minz'n in the 0.1m																		
						portion next to the transitional schist.																		
5.7	7.0	1.3	100	RL7	ARG.	Med. grey, fine grained, massively bedded qtzite. Tremolitic in parts.	FW					1				GOOD		6.6		75°			NVM	
					QTZITE	Red Iron oxide staining common. Calcite infil along joints. No visible																		
						metallic minz'n (NVM).																		
						E.O.H @ 7.0m																		

Unit = FW (Footwall), OB (Orebody) or HW (Hangingwall)

Cat = Category = 1 for FW, 2 for OB or 3 for HW

RQD - Rock Quality Designation - $\frac{\Sigma \text{ unbroken drill core} > 10\,cm \text{ length}}{\text{Total length of drill run}} \times 100\ \%$

PLV = Point Load Test Value in Mpa
1MPa = 145psi

Condition:

Very Good	(100 - 81)
Good	(80 - 61)
Fair	(60 - 41)
Poor	(40 - 21)
Very poor	(20 - 0)

II. Example of a diamond drill hole report

DRILL HOLE REPORT HOLE: BX2221

COLLAR COORDINATES (Header Line)

HOLE #	NORTH	EAST	ELEVN	LENGTH	SECTION
BX2221	10489.9	-9306	791.5	100.4	48

GEOLOGY AND SAMPLING (Body)

DIST	HORIZON	LITH	CAT	TCu	OxCu	TCo	UNIT	MRMR	NORTHING	EASTING	ELEVN	LENGTH
1.5	RL7	ARQ	1				FW	30	10489.92	-9306.3	792.3	1.5
2	RL7	ARQ	1	0.06	0.00	0.01	FW	50	10489.94	-9306.3	793.3	0.5
2.7	RL7	ARQ	1	0.63	0.00	0.04	FW	50	10489.95	-9306.3	793.9	0.7
3.1	RL7	CON	1	0.46	0.00	0.04	FW	50	10489.96	-9306.3	794.4	0.4
3.5	RL7	CON	1	0.13	0.00	0.01	FW	50	10489.97	-9306.3	794.8	0.4
3.7	RL7	TSC	1	0.03	0.00	0.01	FW	50	10489.97	-9306.3	795.1	0.2
4.2	RL6	DSC	2	1.13	0.13	0.09	OB	30	10489.98	-9306.3	795.5	0.5
4.7	RL6	DSC	2	1.94	0.23	0.85	OB	30	10489.99	-9306.3	796	0.5
5.7	RL6	DSC	2	4.01	0.12	0.64	OB	30	10490	-9306.3	796.7	1.0
6.7	RL6	DSC	2	3.51	0.07	0.14	OB	30	10490.01	-9306.3	797.7	1.0
7.7	RL6	DSC	2	2.70	0.08	0.50	OB	30	10490.02	-9306.3	798.7	1.0
8.7	RL6	DSC	2	1.60	0.06	0.07	OB	30	10490.03	-9306.3	799.7	1.0
9.7	RL6	DSC	2	1.38	0.05	0.06	OB	30	10490.05	-9306.3	800.7	1.0
10.7	RL6	ARG	2	1.40	0.07	0.26	OB	10	10490.07	-9306.3	801.7	1.0
11.7	RL6	ARG	2	0.97	0.03	0.63	OB	30	10490.09	-9306.3	802.7	1.0
12.7	RL6	ARG	2	0.38	0.00	0.16	OB	30	10490.12	-9306.3	803.7	1.0
13.7	RL6	ARG	2	2.70	0.04	0.25	OB	30	10490.14	-9306.3	804.7	1.0
14.7	RL6	ARG	2	1.85	0.04	0.09	OB	30	10490.18	-9306.3	805.7	1.0
15.7	RL6	ARG	2	2.16	0.05	0.12	OB	30	10490.21	-9306.3	806.7	1.0
16.7	RL6	ARG	2	2.62	0.07	0.07	OB	30	10490.25	-9306.3	807.7	1.0
17.7	RL6	ARG	2	3.13	0.05	0.08	OB	50	10490.28	-9306.3	808.7	1.0
18.7	RL6	ARG	2	2.81	0.08	0.14	OB	50	10490.32	-9306.3	809.7	1.0
19.2	RL6	ARG	2	3.31	0.10	0.15	OB	50	10490.34	-9306.3	810.4	0.5
19.7	RL6	ARG	2	0.84	0.00	0.08	OB	50	10490.36	-9306.3	810.9	0.5
20.2	RL6	ARG	2	1.30	0.05	0.13	OB	50	10490.38	-9306.3	811.4	0.5
20.7	RL6	ARG	2	0.36	0.00	0.14	OB	50	10490.39	-9306.3	811.9	0.5
21.2	RL6	ARG	2	1.71	0.06	0.38	OB	50	10490.41	-9306.3	812.4	0.5
21.7	RL6	ARG	3	0.06	0.00	0.20	HW	50	10490.42	-9306.3	812.9	0.5
22.2	RL6	ARG	3	0.65	0.00	0.09	HW	50	10490.44	-9306.3	813.4	0.5
22.6	RL6	ARG	3	0.04	0.00	0.11	HW	50	10490.45	-9306.3	813.9	0.4
23.1	RL6	ARG	3	0.65	0.00	0.10	HW	50	10490.47	-9306.3	814.3	0.5
47.6	RL6	ARG	3				HW	30	10490.95	-9306.1	826.8	24.5
89.4	RL6	ARG	3				HW	50	10492.6	-9305.5	859.9	41.8
95.3	RL5	DOL	3				HW	50	10493.79	-9305.2	883.8	5.9
100.4	RL5	ARG	3				HW	50	10494.07	-9305.1	889.2	5.1

ABBREVIATIONS

ELEVN: Elevation
AZIM: Azimuth
DIST: Distance (from collar of drill hole)
LITH: Lithology
TCu: Total Copper
OxCu: Oxide Copper
TCo: Total Cobalt
MRMR: Modified Rock Mass Rating
CAT: Category
FW: Footwall (Category Code 1)
OB: Orebody (Category Code 2)
HW: Hangingwall (Category Code 3)

HORIZON CODES

RL(3 to 7): LOWER ROAN (3 to 7)
RU(1 to 2): UPPER ROAN (1 to 2)

LITHOLOGY CODES

ARG: Argillite
ARQ: Argillaceous Quartzite
CON: Conglomerate
DOL: Dolomite
DSC: Dolomite Schist
GRT: Grit
MQ: Medium Quartzite
QUA: Quartzite
QV: Quartz vein
SH: Shale
SL: Soil
SST: Sandstone
TSC: Transitional Schist

III. Description of samples

Sample No.	Location	Sample description	Type of sample
CK376	463m Block 'A' Haulage	Scapolitic argillite	Grab sample
CK480	480m Block 'A' Access Crosscut	Tremolite schist	Grab sample
CK1739	470m Block 'A' Haulage	Tremolite schist	Grab sample
CK1740	470m Block 'A' Crosscut 1	Argillite	Chip sample
CK1741	470m Block 'A' Crosscut 2	Conglomerate	Chip sample
CK1742	463m Block 'A' Access Crosscut	Argillite with calcite veining	Grab sample
CK2251	450m Block 'D' Haulage	Scapolitic argillite	Drill hole BL0033
CK2252	"	"	"
CK2253	"	"	"
CK2254	"	"	"
CK2255	"	"	"
CK2256	"	"	"
CK2257	"	Tremolitic argillite	"
CK2258	"	"	"
CK2259	"	"	"
CK2260	"	"	"
CK2261	"	"	"
CK2262	"	Scapolitic argillite	"
CK2263	"	"	"
CK2264	"	"	"
CK2265	"	"	"
CK2266	"	Tremolitic argillite	"
CK2267	"	"	"
CK2268	"	"	"
CK2269	"	Scapolitic argillite	"
CK2270	"	Tremolitic argillite	"
CK2271	"	"	"
CK2272	"	Scapolitic argillite	"
CK2273	"	Tremolite schist	Drill hole BL0032
CK2274	"	"	"
CK2275	"	"	"
CK2276	"	"	"
CK2277	"	"	"
CK2278	"	Biotite schist	"
CK2279	"	Conglomerate	"
CK2280	"	"	"
CK2281	"	"	"
CK2282	"	Tremolite schist	"
CK2283	"	"	"
CK2284	"	"	"

APPENDIX A.III (Contd)

Sample No.	Location	Sample description	Type of sample
CK2285	465m Block 'D' Haulage	Conglomerate	Drill hole BL0032
CK2286	"	Tremolite schist	"
CK2287	"	Conglomerate	"
CK2288	"	Tremolite schist	"
CK2289	"	"	"
CK2290	"	Conglomerate	"
CK2291	"	"	"
CK2292	"	Quartzite	"
CK2293	"	Conglomerate	"
CK2294	"	Quartzite	"
CK5879	463m Block 'A' Access Crosscut	Argillite with calcite veining	Chip sample
CK5880	"	"	"
CK5881	"	"	"
CK5882	"	"	"
CK5883	"	"	"
CK5885	470m Block 'A' Haulage	Tremolite schist	Grab sample
CK5886	"	"	Grab sample
CK5887	490m Block 'K' SS48 Crosscut	Tremolite Schist	Chip sample
CK5888	"	"	"
CK5889	"	Biotite Schist	"
CK5890	"	Tremolite schist	"
CK5891	"	"	"
CK5892	"	"	"
CK5894	470m Block 'A' Haulage	Argillite with tremolite veining	Grab sample
CK6483	463m Block 'A' Crosscut 2	Tremolitic argillite	Grab sample
CK6485	"	Argillite with tremolite veining	"
CK6487	"	Scapolitic argillite	"
CK6488	490m Block 'K' Crosscut 1	Tremolite schist	"
CK6489	"	"	"
CK6490	"	Biotite Schist	"
CK6491	"	Tremolite schist	"
CK6492	"	"	"
CK6493	"	"	"
CK6494	"	Biotite Schist	"
CK6495	"	Tremolite schist	"
CK6496	470m Block 'A' Crosscut No 10	Conglomerate	Chip sample
CK6497	"	Biotite Schist	"
CK6498	"	Tremolite schist	"
CK6499	"	"	"
CK6500	"	"	"

APPENDIX B

ZONATION MODEL

EVALUATION OF THE ZONATION MODEL

The zonation model presented in chapter 1 (Fig. 1.2) was constructed from the geological and grade information contained in geological and sampling reports (see Appendix A). The nature and tenor of the metallic minerals were extracted from the geologists' visual estimates in the geological logs of diamond drill core. The copper and cobalt grade variation was evaluated from assay reports of the drill hole logs.

The following parameters were used to calculate the distances and grades to represent the vertical grade variation in the zonation model.

d_i = actual depth of sample down the drill hole.
$a(0)$ = actual depth of the location of the geological footwall contact represented by the boundary between the conglomerates and the transitional schists.
$a(1)$ = actual depth of the location of the transitional schist/tremolite schist contact.
$a(2)$ = actual depth of the tremolite schist/argillite contact.
$d(0)_i$ = displacement of sample from the geological footwall contact.
$d(2)_i$ = displacement of sample from the tremolite schist/argillite contact.
$d(z)_i$ = adjusted, standardised depth of sample down the composite, model drill hole profile.
t_1 = intersected width of the transitional schist along a drill hole.
t_2 = intersected width of the tremolite schist along a drill hole.
w_1 = mean width of the transitional schist used for standardisation in the model (taken as 2m).
w_2 = mean width of the tremolite schist used for standardisation in the model (taken as 8m).
w_t = mean total width of the schists [transitional + tremolite schist] used for standardisation in the model, $w_t = w_1 + w_1 = 10$m
l_i = sample width.
$g(l)_i$ = grade of sample whose width is l.
s_i = mean sample width within a lithological unit.
x_i = mean depth within a prescribed distance interval.
g_i = mean grade within a prescribed distance interval.

(i) $d(0)_i = a(0) - d_i$ .....(B.1)
(ii) $d(2)_i = a(2) - d_i$ .....(B.2)
(iii) $t_1 = a(0) - a(1)$ .....(B.3)
$t_2 = a(1) - a(2)$
(iv) $d(z)_i$:
In conglomerates and quartzites: $d(z)_i = d(0)_i$ .....(B.4)
In Transitional schist: ..... $= d(0)_i \times w_1/t_1$
In Tremolite schist: ..... $= d(0)_i \times w_2/t_2$
In Argillite: ..... $= d(2)_i + w_t$

The parameters described above are schematically illustrated in Fig. B.1.

The procedure used to calculate the variables required for the construction of the grade variation in the model is described below.

(i) The geological footwall contact was used as a reference plane. Actual depths of samples down the drill holes were converted to displacements from the footwall contact (Eqn. B.1).
(ii) To allow for the variability of the widths of the lithologies intersected along several drill holes, the widths of the transitional and tremolite schists were fixed at 2m and 8m respectively. The depths

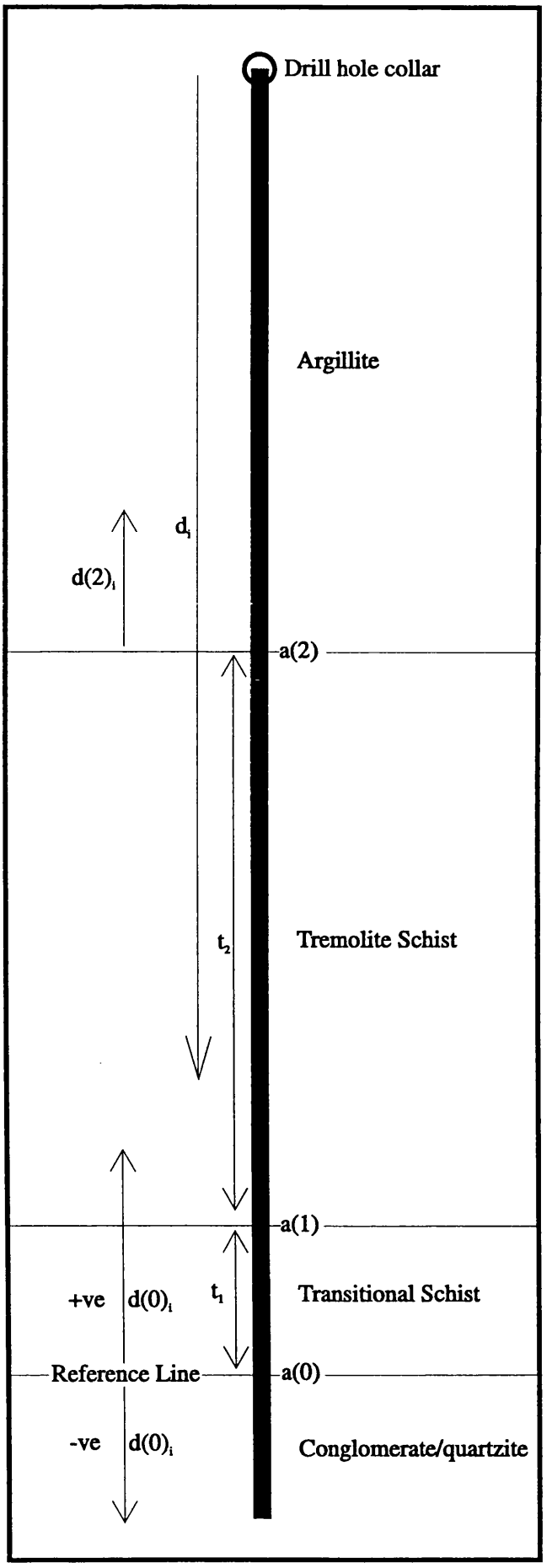

Figure B.1: Description of the terms used to evaluate the Baluba Centre Limb zonation model

down the drill holes were then converted to adjusted depths as shown is equation B.4.

(iii) The adjusted depths of the samples from all the drill holes were combined and sorted in an ascending order.

The mean sample length within each lithology was evaluated as:

$s_i = \sum l_i/N$, where N is the number of samples within the lithology ..... (B.5)

s_i was then used to classify the distance intervals within which the mean depth and mean grade were calculated. Within each lithological unit the first mean depth and grade were evaluated for the distance interval 0 to s_i from the lithological contact, the second sample for the interval s_i to $2s_i$ and so forth, until the last distance interval.

Within each distance interval the mean distance and grade were calculated thus:

Mean depth, $x_i = \sum d(z)_i/n$, where n is the number of samples within the distance interval (B.6)

Weighted mean grade, $g_i = \sum (g(l)_i \times l_i) / \sum l_i$, within each distance interval ..... (B.7)

Note that the grades were weighted by the lengths of the samples within each distance interval to account for the support effect.

(iv) x_i was then plotted against g_i for the total copper, acid soluble copper and cobalt assay grades.

APPENDIX C

SAMPLING AND CUTOFF GRADE CONVENTIONS

CUT OFF CRITERIA CURRENTLY IN USE AT BALUBA

At Baluba samples are assayed for total copper, acid soluble copper and total cobalt. A 1% sulphide copper (SCu) criterion is applied to define the footwall and hangingwall limits of the orebody. Sulphide copper is defined as total copper (TCu) less acid soluble copper (ASCu):

SCu = TCu - ASCu

Sulphide copper is an estimate of the proportion of total copper that is amenable to froth flotation and therefore available for recovery in the concentration process. Generally the amount of acid soluble copper is directly related to the amount of copper available in the form of oxides and carbonates. Hence the term oxide copper is sometimes used in the place of acid soluble copper. The two terms are, however, not synonymous since not all the oxide copper is acid soluble. A proportion of the oxide copper is acid insoluble and therefore responds to froth flotation in the concentrator mills.

In some areas the presence of high cobalt grades leads to portions in which the copper grades are marginally less than 1% being re-evaluated, provided the recovery of cobalt is possible. In such cases the cobalt grade is converted to an equivalent copper grade and the cut off analysis is conducted as though the mineralisation consisted only of copper. The copper equivalent of cobalt is currently taken as :3 * (%Co) and therefore the combined copper and cobalt represented in terms of the copper equivalent as: %SCu + 3 * (%Co)

The factor 3 is based on metal prices, metal recoveries and production costs (ZCCM, 1990).

Note that acid soluble copper assays are not always determined. Therefore it is usual to define the footwall and hangingwall cut offs based on total copper grades and not sulphide copper. In general the results can be accommodated notwithstanding the limitations of data available since the average acid soluble copper grades in the Baluba Centre Limb are normally low (0.04-0.05%) compared to total copper (~2.40%) and can therefore be considered negligible. It is however good practice to carefully examine all chip and drill core samples and determine visually the ore minerals present so that those parts of the deposit with obvious high copper oxide content are always assayed for acid soluble copper, to assist in carefully defining the orebody footwall and hangingwall assay cut offs.

APPENDIX D

DESCRIPTIONS OF ANALYTICAL PROCEDURES

I. MAJOR AND TRACE ELEMENT ANALYSIS BY INDUCTIVELY COUPLED PLASMA - ATOMIC EMISSION SPECTROMETRY (ICP-AES)

Chip samples collected from Baluba Centre Limb were used to carry out ICP-AES analyses in the Applied Geochemistry section at Imperial College, London. Analyses were carried out on the 3400C instrument following in-house procedures described below. The results obtained from the ICP-AES analyses were processed using the MINFILE computer program (After Afifi and Essene, 1988).

1. Sample comminution

The original nominal average size of the samples was about 100mm. The samples were first reduced to 50mm size using a hydraulic crusher and then to 25mm using a manual knife-edge cutter. They were then manually crushed to a 2mm size using a steel geological hammer and a steel pot. Subsequent pulverisation to 75μm was achieved by using a tema mill. All necessary care was taken to avoid contamination of the samples during the comminution stages.

2. Sample decomposition

(i) Three Acid Attack Method - Nitric, Perchloric and Hydrofluoric Acid Attack

0.1000g (±0.0001g) of the sample was weighed out into PFTE test tubes using a four point electronic scale. 2.0ml Nitric Acid was added followed by 1.0ml Perchloric Acid from calibrated Oxford dispensers. Then 5.0ml Hydrofluoric Acid was added using a hydrofluoric acid dispenser. The tubes were placed into the hot block and heated for 16 hours using a pre-set programmer, progressively increasing the temperature as follows: 90°C for the first 3 hours; 140°C for the next 3 hours and then 190°C for the last 10 hours.

The tubes were then removed from the hot block and cooled. After cooling, 2.0ml of 4 Molar Hydrochloric Acid was added from an Oxford dispenser. The solutions were leached at 70°C on a hot block for 1 hour, cooled and then 8.0ml of 0.3 Molar Hydrochloric Acid added. The resulting solutions were mixed thoroughly using a vertex tube mixer and decanted into disposable centrifuge tubes. The made up solutions needed to settle for at least 12 hours to equilibrate at room temperature before the analysis. Concentrations of 25 elements were determined from samples and reference materials prepared in this way.

(ii) Two Acid Attack Method - Nitric and Perchloric Acid Attack (Sulphur Analysis)

0.2500g was weighed out into glass test tubes using a four point electronic scale. 4.0ml Nitric Acid was added followed by 1.0ml Perchloric Acid from calibrated Oxford dispensers. The tubes were then placed into the hot block and heated for 34 hours using a preset programmer, progressively increasing the temperature as follows: 50°C for the first 3 hours; 150°C for the next 3 hours; 190°C for the subsequent 18 hours and then 195°C for the final 10 hours.

The tubes were then removed from the hot block and cooled in a fume cupboard. After cooling 2.0ml of 5 Molar Hydrochloric Acid was added from an Oxford dispenser. The solutions were leached at 60°C on a hot block for 1 hour, cooled and then 8.0ml of deionised water added. The resulting

solutions were mixed thoroughly using a vertex tube mixer and decanted into disposable centrifuge tubes. The made up solution in each tube was homogenised using a centrifuge mixer and then centrifuged at 2000 rpm for 2 minutes. The solutions were allowed to settle for at least 12 hours in order to equilibrate at room temperature before the analysis.

3. Quality control

In both two and three acid attack methods some samples were duplicated for analysis and reagent blanks were also processed with the batches to check the analytical accuracy. Two in-house reference materials (HRM1 and HRM2) and three international reference materials (GXR3, GXR4 and SU1) were analysed along with the batches as calibration solutions.

II. SCATTERED ELECTRON MICROPROBE ANALYSIS (SEM)

Analyses on some rock forming minerals (silicates and oxides) and metallic sulphide minerals were carried out on carbon coated polished thin sections using the ANALYTICAL JOEL 733 superprobe instrument fitted with a microanalyser in the Geology Department at Imperial College. Samples were carbon coated to render them electrically non-conducting. Carbon was coated onto the polished thin sections by thermal evaporation. A thin carbon film coated on the surface of the samples ensures that the sample current is drained to ground potential without development of an electric charge on the sample surface.

The analyses were done in the Energy Dispersive Spectrometry (EDS) mode. The instrument was operated at an accelerating voltage of 15kV and a beam current of 2nA, utilising a 100 second count time. Peak and noise calibration was achieved using a cobalt standard sample.

The data generated was corrected for atomic mass, absorption and fluorescence effects using an integrated ZAF correction computer program. The microanalyser data was normalised and stoichiometries were calculated with the aid of the MINFILE computer program (After Afifi and Essene, 1988).

APPENDIX E

CHEMICAL AND MINERALOGICAL ANALYSES

I. INDUCTIVELY COUPLED PLASMA (ICP) ANALYSES

	Units	CK376	CK480	CK1739	CK1740	CK1741	CK1742	CK2251	CK2252	CK2253	CK2254
Li_2O	%	0.03	0.01	0.04	0.05	0.01	0.02	0.07	0.06	0.06	0.04
Na_2O	"	0.53	0.15	0.72	2.9	0.35	0.04	0.97	0.55	0.14	0.74
K_2O	"	9.4	0.12	1.49	6.55	6.57	2.78	5.79	7.26	2.85	5.32
MgO	"	7.24	8.65	11.06	7.61	5.59	11.27	9.22	7.05	6.38	8.61
CaO	"	2.15	13.61	14.05	0.71	6.02	18.14	3.43	1.43	1.29	5.92
Al_2O_3	"	13.69	1.16	5.03	13.29	9.28	5.68	12.79	13.15	6.46	11.81
TiO_2	"	0.62	0.22	0.26	0.66	0.59	0.2	0.63	0.61	0.58	0.53
MnO	"	0.09	0.3	0.33	0.09	0.22	0.3	0.14	0.09	0.09	0.16
P_2O_5	"	0.18	0.11	0.13	0.14	0.13	0.05	0.14	0.16	0.15	0.15
Rb	ppm	180	10	66.67	250	130	56.67	200	200		110
Be	"	1.59	16.08	16.4	12.22	4.95	0.59	8.12	4.07	3.62	5.43
Sr	"	85.5	47.75	83.3	50.8	238.67	60.7	48.9	37.2	13.2	48.9
Ba	"	497	14.68	127.67	944.67	3816.7	148	380	590	58.9	325
La	"	41.5	11.63	24.17	37.17	42.83	18.5	51.5	43.5	46	46
V	"	122.7	167.5	108.17	147	103.1	49.1	142	160	139	155
Cr	"	99.5	53.13	38.5	63.33	81.5	42.17	75.5	73	21	62
Mo	"	7	89	28.17	0.5	0.5	0.5	71	9.5	24	39.5
Fe	%	4.54	9.67	5.93	2.63	1.76	4.24	4.27	3.38	2.42	3.46
Co	"	0.1	0.14	0.32	0.91	0.01	0.07	0.07	0.05	0.03	0.05
Ni	ppm	39.5	13.25	26.67	74.67	17.33	25.67	39	43	36.5	33.5
Cu	%	0.15	15.42	5.67	0.42	0.03	3.02	2.07	0.17	0.28	0.61
Ag	ppm	0.5	9	2.17	0.5	0.5	0.83	1	0.5	0.7	0.5
Zn	"	14.5	1046.3	401.17	51.5	5	201.33	169	23	45.3	51.5
Cd	"	0.42	4.88	1.75	1.67	0.33	0.42	0.75	0.5	0.25	0.25
Pb	"	5	66.88	21.67	25.83	2.5	3.33	12.5	2.5	10.5	2.5
S	%	3.13	11.41	5.41	1.71	0.04	3.91				

APPENDIX E.I (contd)

	Units	CK2255	CK2256	CK2257	CK2258	CK2259	CK2260	CK2261	CK2262	CK2263	CK2264
Li_2O	%	0.05	0.04	0.02	0.04	0.02	0.01	0.03	0.07	0.05	0.05
Na_2O	"	1.15	0.26	0.39	0.04	0.17	0.02	0.22	1.16	1.04	0.32
K_2O	"	6.94	2.11	3.96	1.6	2.55	0.43	4.28	6.25	6.55	2.6
MgO	"	7.78	6.27	10.08	4.01	10.66	2.21	10.33	9.1	7.71	6.6
CaO	"	2.95	4.32	9.72	4.49	11.94	10.83	10.84	3.25	2.91	1.72
Al_2O_3	"	13.17	5.8	9.16	6.61	9.26	3.72	10.09	13.94	13.02	6.44
TiO_2	"	0.58	0.36	0.35	0.41	0.37	0.2	0.41	0.65	0.6	0.49
MnO	"	0.12	0.12	0.23	0.09	0.27	0.13	0.26	0.14	0.12	0.09
P_2O_5	"	0.16	0.13	0.11	0.14	0.13	0.08	0.13	0.15	0.15	0.14
Rb	ppm	170		40		10		90	180	200	
Be	"	4.6	3.13	4.9	4.91	4.4	1.35	3.3	8.5	4.57	3.77
Sr	"	55.6	35.4	73.5	42	85.7	47	83.7	54	50	23.8
Ba	"	518	57.9	216	56.5	294	34	338	444	442	60
La	"	37.5	37	35.5	49.5	37	17.3	36.5	56.5	41.5	42.5
V	"	138	71.8	88.8	54.5	87.3	33.5	81.5	145	141	97.3
Cr	"	76	25	52.5	25	51.5	36.5	51	68.5	82.5	29.5
Mo	"	3.5	15	47	22.5	8	12.5	8.5	62.5	9	23.5
Fe	%	3.99	3.84	4.84	3.86	4.87	3.44	4.22	3.63	4.22	3.55
Co	"	0.07	0.06	0.1	0.07	0.08	0.05	0.06	0.05	0.07	0.06
Ni	ppm	44	38.5	37.5	31	37	24	30	35.5	46.5	43
Cu	%	0.46	0.16	0.41	0.19	0.61	0.13	0.29	1.37	0.56	0.1
Ag	ppm	0.5	0.4	0.5	0.9	0.5	1	0.5	0.5	0.5	0.9
Zn	"	44.5	13.9	35.5	31.6	51	61.1	31	114	52	18.6
Cd	"	0.25	0.25	0.25	0.25	0.25	0.25	0.25	0.25	0.5	0.25
Pb	"	2.5	7.5	2.5	15	2.5	18	2.5	2.5	2.5	10.5
S	%										

APPENDIX E.I (contd)

	Units	CK2265	CK2266	CK2267	CK2268	CK2269	CK2270	CK2271	CK2272	CK2273	CK2274
Li_2O	%	0.04	0.02	0.02	0.04	0.05	0.01	0.03	0.06	0.03	0.02
Na_2O	"	0.73	0.37	0.17	0.03	0.14	0.02	0.27	0.59	0.15	0.04
K_2O	"	5.52	3.75	2.7	1.53	2.81	0.48	4.31	7.26	1.52	1.22
MgO	"	8.67	9.85	10.45	3.8	6.27	2.09	10.51	7.46	11.84	6.62
CaO	"	5.95	10.66	12.01	4.6	1.31	9.89	11.52	1.75	16.09	13.67
Al_2O_3	"	12.15	9.13	9.62	6.63	6.41	3.57	10.28	13.47	4.27	3.19
TiO_2	"	0.54	0.34	0.37	0.49	0.58	0.2	0.43	0.64	0.17	0.14
MnO	"	0.16	0.24	0.27	0.1	0.1	0.1	0.27	0.1	0.38	0.28
P_2O_5	"	0.16	0.11	0.14	0.16	0.15	0.09	0.14	0.16	0.07	0.11
Rb	ppm	120	50	30				100	230	50	
Be	"	5.43	5.1	4.53	5.3	3.63	1.36	3.6	4.53	10.6	2.19
Sr	"	52.5	77.2	90	43.6	13.1	46.4	86.6	41.9	78.6	68.6
Ba	"	249	363	308	51	55.4	21.4	392	567	199	116
La	"	48	39	41.5	50	48.8	17.3	34.5	47	18.5	15.5
V	"	159	87.3	88	58.8	144	35.3	81.8	168	289	81.8
Cr	"	63.5	49	53	25.5	23	39.5	55	80	26.5	11.5
Mo	"	47	52.5	7.5	65.5	22.5	10.5	11	13	175	20.5
Fe	%	3.56	4.69	5.11	4.32	2.43	3.71	3.98	3.61	5.07	4.02
Co	"	0.05	0.09	0.09	0.08	0.03	0.06	0.06	0.06	0.16	0.21
Ni	ppm	39.5	33	35	35.5	36	23.5	27.5	44	21	25.5
Cu	%	0.63	0.34	0.55	0.18	0.34	0.15	0.28	0.19	3.2	3.06
Ag	ppm	0.5	0.5	0.5	0.8	1.1	0.4	0.5	0.5	0.5	1.5
Zn	"	54.5	32.5	49	19.5	46.5	39.5	29	24.5	233	111
Cd	"	0.25	0.25	0.5	1.25	1	0.75	0.5	0.5	1	1.75
Pb	"	2.5	2.5	2.5	15	18	19.5	2.5	12.5	10	34.5
S	%										

APPENDIX E.I (contd)

	Units	CK2275	CK2276	CK2277	CK2278	CK2279	CK2280	CK2281	CK2282	CK2283	CK2284
Li_2O	%	0.06	0.04	0.04	0.07	0.01	0.04	0.18	0.02	0.07	0.03
Na_2O	"	0.29	0.69	0.28	0.54	0.04	0.24	0.32	0.16	0.53	0.06
K_2O	"	7	5.78	5.72	6.04	0.3	4.53	1.64	1.22	5.67	1.63
MgO	"	9.54	9.04	7.81	9.24	1.56	2.87	3.3	11.57	9.34	6.8
CaO	"	5.53	8.76	12.93	8.23	11.18	12.98	5.44	16.23	8.51	12.35
Al_2O_3	"	10.98	9.86	9.37	10.86	0.92	7.33	4.59	3.93	10.52	4.02
TiO_2	"	0.52	0.49	0.4	0.5	0.06	0.26	0.12	0.16	0.5	0.2
MnO	"	0.22	0.25	0.28	0.24	0.13	0.2	0.17	0.38	0.24	0.28
P_2O_5	"	0.18	0.16	0.13	0.14	0.04	0.09	1.88	0.06	0.16	0.13
Rb	ppm	200	140	140	190		200		60	170	
Be	"	4.3	9.73	7.72	10.1	3.09	7.05	8.73	10.7	9.03	2.37
Sr	"	152	187	225	169	33.4	244	64.3	83.1	157	67.2
Ba	"	647	583	1480	431	156	2010	381	223	550	147
La	"	22.5	22.5	28.5	33	13.5	26.5	14.5	17	34.5	23.3
V	"	139	112	87.8	94.3	26	58.8	43	317	96	85
Cr	"	44	35	37.5	45.5	27.5	34.5	36.5	33.5	42.5	14
Mo	"	0.5	0.5	0.5	11	62	0.5	6	46.5	16	19
Fe	%	4.94	3.4	2.97	4.17	0.84	1.48	1.56	5.32	3.98	3.75
Co	"	0.26	0.17	0.09	0.09	0.01	0.01	0.01	0.31	0.09	0.14
Ni	ppm	30	24	23.5	27	21.5	16.5	19	37	30.5	21
Cu	%	2.86	1.58	1.72	2.45	0.39	0.11	0.14	3.65	2.26	2.51
Ag	ppm	1	0.5	0.5	1	0.1	0.5	0.4	14	0.5	1.3
Zn	"	229	128	141	198	2910	12	81.2	271	182	102
Cd	"	1	0.75	1	1	0.25	0.25	0.75	1.75	0.75	2
Pb	"	10	10	15	10	3	5	15	20	5	13.5
S	%										

APPENDIX E.I (contd)

	Units	CK2285	CK2286	CK2287	CK2288	CK2289	CK2290	CK2291	CK2292	CK2293	CK2294
Li_2O	%	0.01	0.03	0.04	0.04	0.04	0.15	0.04	0.04	0.07	0.05
Na_2O	"	0.05	0.12	0.22	0.71	0.3	0.62	0.05	1.07	0.38	0.08
K_2O	"	0.37	2	3.95	6.14	5.13	1.49	1.65	7.83	3.19	3.35
MgO	"	1.81	12.62	2.97	8.9	8.03	2.98	4.34	4.08	3.22	6.7
CaO	"	11.7	15.95	12.45	7.99	13.92	4.28	3.71	5.05	6.13	1.18
Al_2O_3	"	1.02	4.59	6.59	10.39	8.82	5.2	5.73	10.83	6.01	7.18
TiO_2	"	0.09	0.2	0.22	0.5	0.4	0.14	0.44	0.57	0.14	0.44
MnO	"	0.14	0.39	0.19	0.24	0.29	0.22	0.09	0.16	0.16	0.09
P_2O_5	"	0.06	0.13	0.07	0.15	0.13	0.58	0.14	0.15	0.05	0.14
Rb	ppm		80	180	140	140			190	250	
Be	"	3.44	3.95	6.47	10.1	7.75	9.13	4.29	6.5	7.05	3.5
Sr	"	37.5	82.1	208	182	195	53.3	32.2	134	114	13.4
Ba	"	140	240	1680	676	1050	410	45.7	2020	1480	98.7
La	"	18	24	25	22	27.5	14.3	49.3	40.5	19.5	45.8
V	"	28.3	196	59	108	85.8	44	63	97.3	42.5	131
Cr	"	21.5	31.5	83.5	36.5	36.5	37.5	23.5	56.5	53.5	23
Mo	"	58	11	3	0.5	0.5	6	32	0.5	2.5	16
Fe	%	0.91	4.32	1.52	3.35	2.76	1.44	3.52	3.19	1.08	2.81
Co	"	0.01	0.19	0.01	0.17	0.08	0.01	0.06	0.01	0.01	0.04
Ni	ppm	29	23	17	26	21.5	21	30.5	35.5	16	51
Cu	%	0.38	2.81	0.16	1.53	1.39	0.12	0.33	0.05	0.11	0.24
Ag	ppm	0.1	1.5	0.5	0.5	0.5	0.6	0.7	0.5	0.5	0.5
Zn	"	22.1	215	18.5	128	115	95.8	22.6	6.5	44	16.8
Cd	"	0.25	1	0.25	0.5	0.5	1	0.25	0.5	0.25	1.5
Pb	"	7.5	12.5	7.5	2.5	10	12	9	10	7.5	9
S	%										

APPENDIX E.I (contd)

	Units	CK5879	CK5880	CK5881	CK5882	CK5883	CK5885	CK5886	CK5887	CK5888	CK5889
Li_2O	%	0.03	0.03	0.02	0.02	0.01	0.02	0.03	0.04	0	0.01
Na_2O	"	0.22	0.56	0.03	0.14	0.05	0.09	2.4	0.95	0.07	0.09
K_2O	"	4.63	6.41	4.42	3.98	2.65	0.88	5.69	2.08	0.36	1.39
MgO	"	11.28	11.21	10.15	9.41	11.62	12.8	8.86	13.98	14.77	14.92
CaO	"	8.18	1.94	12.06	7.21	15.11	12.97	3.39	12.77	19.96	17.91
Al_2O_3	"	10.78	14.3	9.01	9.44	5.63	2.17	12.15	6.78	1.39	2.91
TiO_2	"	0.47	0.64	0.42	0.43	0.27	0.08	0.59	0.34	0.05	0.12
MnO	"	0.2	0.12	0.24	0.17	0.31	0.36	0.1	0.38	0.5	0.48
P_2O_5	"	0.16	0.24	0.12	0.12	0.07	0.05	0.14	0.1	0.03	0.05
Rb	ppm	113.33	140	90	80	50	33.33	130	70	10	30
Be	"	1.95	2.7	1.66	1.55	0.98	16.87	2.4	25.47	1.13	1.95
Sr	"	68.73	53.6	73.4	55.4	136	20.17	43.9	139.33	85.17	86.3
Ba	"	242.67	630	296.67	136.77	166	78.57	97.7	371.33	25.47	76.1
La	"	45	27.5	37	30.67	23.5	8.67	38.5	33.33	11.17	12
V	"	83.37	113	67.87	65.47	43	83.93	93.3	90.6	33.1	69.5
Cr	"	110.83	127	120	138.17	62	47.17	72	34	17.83	24
Mo	"	0.5	0.5	0.5	0.5	0.5	71.17	2	5.5	0.5	12.5
Fe	%	4.21	2.9	3.3	5.98	3.78	5.7	3.75	2.33	2.18	2.97
Co	"	0.11	0.04	0.07	0.2	0.08	0.88	0.47	1.19	0.06	0.06
Ni	ppm	23	23.5	22.17	63	27	57.5	58.5	59.67	6.67	10.5
Cu	%	3.16	1.19	1.82	4.82	3.27	6.16	1.74	0.64	1.99	2.57
Ag	ppm	1.33	0.5	0.67	2.17	1.5	2.33	0.5	0.5	1	1
Zn	"	229.67	99.5	136.5	349.67	232	417.67	127	44.17	127.67	176
Cd	"	0.75	0.25	0.25	1.08	0.5	2.17	0.75	1.33	0.25	0.75
Pb	"	8.33	2.5	2.5	14.17	2.5	29.17	7.5	13.33	2.5	5
S	%	3.24	1.18	2.39	5.79	3.44	5.97	3.04	1.29	1.62	2.08

APPENDIX E.I (contd)

	Units	CK5890	CK5891	CK5892	CK5894	CK6483	CK6485	CK6487	CK6488	CK6489	CK6490
Li_2O	%	0	0.05	0.03	0.04	0.02	0.06	0.09	0	0.05	0.02
Na_2O	"	0.1	1.59	0.11	3.13	0.49	0.54	0.41	0.03	2.03	0.81
K_2O	"	0.29	2.44	1.41	4.65	1.49	3.61	6.24	0.15	2.33	0.99
MgO	"	14.66	13.11	14.08	8.95	15.16	12.57	13.06	11.41	10.31	8.17
CaO	"	20.29	10.9	17.44	1.9	13.85	8.78	6.54	25.51	10.72	8.97
Al_2O_3	"	1.06	8.86	3.38	13.36	5.41	11.15	12.43	2.46	9.54	5.97
TiO_2	"	0.04	0.43	0.14	0.65	0.23	0.5	0.59	0.1	0.36	0.29
MnO	"	0.51	0.32	0.42	0.08	0.3	0.22	0.21	0.47	0.31	0.26
P_2O_5	"	0.02	0.11	0.07	0.14	0.07	0.15	0.16	0.1	0.15	0.11
Rb	ppm	10	83.33	63.33	160	40	126.67	226.67	10	83.33	36.67
Be	"	1.11	24.3	9.43	3.4	2.98	4.41	4.04	2.68	10.67	9.65
Sr	"	97.43	90.8	57.83	46.2	83.13	84.97	53.9	83.7	119.33	127.53
Ba	"	34.93	149	68.97	261	102.67	216.67	297.67	18.53	299	74.27
La	"	12.5	40.83	13.17	45.5	22.5	40.67	47.33	10.17	34.83	28.83
V	"	37.53	91.63	56.53	106	69.5	85.87	94.03	55.7	137.67	153.17
Cr	"	18	49.17	31.67	80	40.5	96.5	75.33	17.17	64.17	58.5
Mo	"	0.5	7.5	42	0.5	0.5	0.5	0.5	0.5	7.67	26.33
Fe	%	2.25	2.4	2.79	4.05	2.68	5.5	4.7	2.42	3.21	8.81
Co	"	0.06	0.91	0.39	0.18	0.04	0.11	0.09	0.08	0.52	2.02
Ni	ppm	6.67	50.67	22	37	15.33	40.17	34	6.33	39.67	120.17
Cu	%	2.09	0.77	2.71	2.6	0.22	2.29	0.85	2.45	3.76	11.81
Ag	ppm	0.5	0.67	2.33	1.5	0.5	0.5	0.5	0.67	3.5	6.83
Zn	"	137	55	184	199	15.67	160.67	68.17	158.33	258	863.67
Cd	"	0.25	1.25	1	0.75	0.25	0.5	0.25	0.58	1.17	5.17
Pb	"	2.5	10.83	15.83	12.5	2.5	2.5	2.5	8.33	21.67	83.33
S	%	1.64	1.39	1.85	2.46	1.14	3.28	2.98	2.39	2.21	7.68

APPENDIX E.I (contd)

	Units	CK6491	CK6492	CK6493	CK6494	CK6495	CK6496	CK6497	CK6498	CK6499	CK6500
Li_2O	%	0.07	0.03	0.06	0.02	0.07	0.01	0.1	0.01	0.07	0.01
Na_2O	"	1.1	0.09	1.16	2.21	0.91	0.45	0.23	3.96	0.6	0.05
K_2O	"	4.66	1.28	3.12	2	4.4	5.69	3.98	0.19	3.44	1.11
MgO	"	12.09	13.43	11.03	4.83	11.74	4.82	12.15	7.08	12.3	13.15
CaO	"	11.15	14.88	9.39	8.05	13.67	4.49	13.49	9.19	10.55	19.73
Al_2O_3	"	10.73	2.82	9.33	9.54	9.66	8.53	9.69	7.64	8.9	3.37
TiO_2	"	0.64	0.11	0.42	0.37	0.64	0.42	0.46	0.35	0.44	0.12
MnO	"	0.4	0.37	0.33	0.17	0.42	0.15	0.43	0.24	0.34	0.45
P_2O_5	"	0.15	0.05	0.28	0.2	0.23	0.09	0.06	0.1	0.14	0.14
Rb	ppm	240	66.67	156.67	60	203.33	116.67	220	10	166.67	37.5
Be	"	10.2	17.97	10.55	15.3	9.14	4.04	21.1	9.19	25	8.04
Sr	"	120	21.07	109.27	177	114.57	224.33	136	77.53	92.67	91.85
Ba	"	700	107.63	268.67	53.4	552.67	3240	847	141.3	220	41.3
La	"	16	8.33	32.83	31	20	35.67	22	14	25.67	15
V	"	141	91.1	168.67	88.5	136.67	99.93	92.1	31.63	127	70.95
Cr	"	41.5	44	41	57.5	38	86.83	32.5	73.67	40.33	20.38
Mo	"	7	43.17	1.67	4.5	6.67	0.5	10.17	3.33	0.5	3.25
Fe	%	3.35	5.72	5.24	7.54	2.92	1.4	3.66	2.46	5.05	3.52
Co	"	0.53	0.13	0.92	0.7	0.67	0.02	0.07	0.06	0.59	0.22
Ni	ppm	51	12.83	60.17	50	57	20.5	32.5	9.33	45.83	17.25
Cu	%	0.21	5.53	4.56	12.7	0.27	0.03	2.81	2.21	3.65	3.04
Ag	ppm	0.5	2.83	2.83	6.5	0.5	0.5	2.67	1.17	2.83	1.13
Zn	"	29.5	385.67	315.67	878	30.33	7	199.33	150.5	268.67	216.25
Cd	"	0.75	1.5	2	3.5	1.08	0.25	2.08	0.5	2.17	1.25
Pb	"	5	16.67	30	65	4.17	2.5	42.5	8.33	26.67	11.25
S	%	11.2	3.67	3.83	4.38	3.63	0.09	0.35	1.39	2.13	3.17

II. SCANNING ELECTRON MICROPROBE ANALYSES

(a) Rock Forming Minerals

(i) Feldspars

	CK376A	CK6487B	CK6487C	CK6496A	CK6496B	CK5115A
SiO_2	64.86	65.00	65.52	63.91	65.23	68.76
TiO_2	-	-	0.12	0.54	0.37	-
Al_2O_3	18.74	18.71	18.81	18.73	18.97	20.41
FeO	-	-	-	-	-	-
CaO	-	-	-	-	-	0.71
MnO	-	-	-	-	-	-
MgO	-	-	-	-	-	-
Na_2O	0.68	0.41	0.50	0.77	0.64	11.74
K_2O	16.42	16.93	16.74	15.64	16.51	-
Total	100.70	101.05	101.68	99.59	101.71	101.62
Ions						
#Si+4	2.98	2.98	2.98	2.96	2.97	2.96
#Ti+4	-	-	0.00	0.02	0.01	-
#Al+3	1.02	1.01	1.01	1.02	1.02	1.04
#Fe+2	-	-	-	-	-	-
#Ca+2	-	-	-	-	-	0.03
#Mn+2	-	-	-	-	-	-
#Mg+2	-	-	-	-	-	-
#Na+1	0.06	0.04	0.04	0.07	0.06	0.98
#K	0.96	0.99	0.97	0.93	0.96	-
Or	94.06	96.47	95.64	93.04	94.46	-
Ab	5.94	3.53	4.36	6.96	5.54	96.79
An	-	-	-	-	-	3.21
#TOTAL	5.02	5.02	5.02	5.00	5.02	5.01
#O-2	8	8	8	8	8	8

(ii) Tremolite

	CK376E	CK5890E	CK5892A	CK6487(2)	CK6496A	CK6496B	CK6500D
SiO_2	57.11	58.44	57.07	57.14	55.78	56.06	58.40
Al_2O_3	1.92	1.23	1.90	2.57	2.47	2.76	0.34
FeO	4.20	2.19	3.04	3.60	7.05	5.48	2.06
MnO	0.25		0.57	0.33	0.58	0.74	0.44
MgO	20.92	23.14	21.97	21.88	19.21	20.02	23.19
CaO	13.69	13.73	12.95	13.94	13.26	13.46	13.92
Na_2O		0.65	0.46	0.60	0.59	0.67	
K_2O				0.17	0.16	0.18	
H_2O	2.18	2.23	2.18	2.22	2.16	2.18	2.20
Total	100.26	101.61	100.14	102.46	101.26	101.56	100.55
Ions							
#Si IV	7.86	7.87	7.83	7.71	7.74	7.71	7.95
#Al IV	0.14	0.13	0.17	0.29	0.26	0.29	0.05
T site	8	8	8	8	8	8	8
#Al VI	0.17	0.07	0.14	0.12	0.14	0.16	0.00
#Mg	4.29	4.65	4.49	4.40	3.97	4.10	4.71
#Fe+2	0.48	0.25	0.35	0.41	0.82	0.63	0.23
#Mn	0.03		0.02	0.04	0.07	0.09	0.05
#Ca	0.03	0.04		0.03	0.00	0.02	0.01
M1,2,3 site	5	5	5	5	5	5	5
#Mn			0.05				
#Ca	2.00	1.98	1.90	2.00	1.97	1.98	2.00
#Na		0.02	0.05		0.03	0.02	
M4 site	2	2	2	2	2	2	2
#Ca	0	0		0	0	0	0.02
#Na		0.15	0.08	0.16	0.13	0.16	
#K				0.03	0.03	0.03	
A site	0.00	0.11	0.08	0.18	0.15	0.17	0.02
#O	22	22	22	22	22	22	22
#OH	2	2	2	2	2	2	2

(iii)Mica

	CK5879A	CK5882A	CK6487(3)	CK6490C	CK6500D	CK6500F
SiO_2	41.21	46.18	41.62	40.58	41.98	41.87
TiO_2			0.50	0.38	0.54	0.56
Al_2O_3	18.12	18.22	17.94	16.37	14.04	13.72
FeO	3.33	3.74	5.34	9.47	2.92	2.64
MnO			0.30	0.67		
MgO	21.57	17.79	20.94	18.35	25.71	25.92
CaO	0.09	0.30		0.14		0.30
Na_2O	0.40	0.33		0.21	0.44	
K_2O	10.53	8.51	10.98	10.19	10.34	10.69
H_2O	4.29	4.37	4.24	4.16	4.28	4.28
Cl		0.09				
O=Cl		0.02				
Total	99.54	99.51	101.86	100.53	100.25	99.98
Ions						
#Si IV	5.79	6.34	5.77	5.82	5.87	5.87
#Al IV	2.21	1.66	2.23	2.18	2.13	2.13
T site	8	8	8	8	8	8
#Al VI	0.79	1.29	0.70	0.59	0.18	0.14
#Ti VI			0.05	0.04	0.06	0.06
#Fe+2	0.39	0.43	0.62	1.14	0.34	0.31
#Mn	2.00			0.04	0.08	
#Mg	4.52	3.64	4.33	3.92	5.36	5.42
O site	5.70	5.35	5.74	5.77	5.94	5.93
#Ca	0.01	0.04		0.02		0.05
#Na	0.11	0.09		0.06	0.12	
#K	1.89	1.49	1.94	1.86	1.84	1.91
A site	2.01	1.62	1.94	1.94	1.96	1.96
#O	20	20	20	20	20	20
#OH	4.00	3.98	4.00	4.00	4.00	4.00
#Cl		0.02				

(iv) Chlorite

	CK5879F	CK5882B	CK6487C	CK6500E	CK6500F
SiO_2	30.36	31.10	38.02	36.54	36.66
TiO_2			0.61	0.40	0.10
Al_2O_3	20.86	22.07	16.50	12.88	12.96
FeO	5.05	5.44	5.45	7.05	7.63
MnO		0.26		0.39	0.33
MgO	29.80	30.53	18.50	27.38	27.19
CaO	0.09		0.20	0.63	0.46
Na_2O	0.54			1.44	0.79
K_2O			10.85	2.45	1.90
H2O	12.66	12.68	12.14	12.39	12.44
Cl	0.04				
O=Cl	0.01				
Total	99.38	102.08	102.28	101.53	100.47
Ions					
#Si IV	2.89	2.87	3.66	3.48	3.51
#Al IV	1.11	1.13	0.34	0.52	0.49
T site	4	4	4	4	4
#Al VI	1.24	1.28	1.53	0.92	0.98
#Ti			0.04	0.03	0.01
#Fe+2	0.40	0.42	0.44	0.56	0.61
#Mn+2		0.02		0.03	0.03
#Mg	4.24	4.21	2.66	3.88	3.89
#Ca	0.01		0.02	0.06	0.05
#Na	0.10			0.27	0.15
#K			1.33	0.30	0.23
O site	5.98	5.92	6.03	6.05	5.94
#O	10	10	10	10	10
#OH	7.99	8.00	8.00	8.00	8.00
#Cl	0.01				

(v) Epidote

	CK6484A	CK6484C	CK6484D	CK6490D
SiO_2	39.78	40.04	39.21	38.85
TiO_2			0.15	0.02
Al_2O_3	27.87	27.35	28.56	25.10
FeO	8.00	8.94	7.20	10.79
MnO			0.07	0.13
MgO				0.03
CaO	25.52	25.66	24.79	24.64
K_2O				0.01
Total	101.17	102.00	99.97	99.57
#Si+4	3.05	3.06	3.03	3.08
T site	3.05	3.06	3.03	3.08
Al IV	2.52	2.47	2.60	2.34
#Ti+4			0.01	0.00
#Fe+2	0.51	0.57	0.47	0.72
O site	3.04	3.04	3.07	3.06
#Mn+2			0.00	0.01
#Ca+2	2.10	2.10	2.05	2.09
A site	2.10	2.10	2.06	2.10
#Na	1.00			
#TOTAL	8.19	8.20	8.16	8.25
#O	12.50	12.50	12.50	12.50
#Al+3	2.52	2.47	2.60	2.34

(vi) Rutile

	CK6496E	CK6496F
SiO_2	1.39	0.95
TiO_2	98.16	99.40
Al_2O_3	0.08	
FeO	0.62	1.06
CaO	0.69	0.41
Na_2O		0.17
K_2O	0.15	
Total	101.09	102.00
#Si+4	0.02	0.01
#Ti+4	0.97	0.98
#Al	3.00	0.00
#Fe+2	0.01	0.01
#Mn	2.00	
#Mg	2.00	
#Ca+2	0.01	0.01
#Na+1		0.00
#K	0.00	
#TOTAL	1.01	1.01
#O-2	2	2

(vii) Sphene

	CK5115A	CK5115B	CK5115C	CK5115D	CK5883A
SiO_2	30.15	30.07	29.73	30.44	30.59
TiO_2	40.03	41.15	41.17	40.34	41.90
FeO	0.34		0.30	0.34	
CaO	28.27	28.36	28.45	29.02	29.12
K_2O	0.21	0.16		0.06	
Total	99.01	99.74	99.65	100.20	101.61
#Si+4	1.00	1.00	1.00	1.00	1.00
#Ti+4	1.00	1.03	1.04	1.00	1.03
#Al	3.00				
B site	1.00	1.03	1.04	1.00	1.03
#Fe+2	0.01		0.01	0.01	
#Ca+2	1.00	1.01	1.03	1.02	1.02
#K	0.01	0.01		0.00	
A site	1.01	1.02	1.03	1.02	1.02
#TOTAL	3.02	3.05	3.07	3.03	3.05

(b) Sulphide Minerals

(i) Carrollite

Sample grain No.	Cu	Co	Fe	S	Ni	Total
5879E	9.04	48.65	0.85	42.22	0.92	101.68
5881B	13.95	44.27	0.30	41.43	0.00	99.95
5882C	8.05	47.25	1.37	41.35	1.09	99.11
5887B	17.74	40.30	1.03	42.13	0.00	101.20
5891A	18.14	40.81	0.00	41.58	0.00	100.53
5891B	17.94	40.29	0.00	41.10	0.00	99.32
5891C	18.66	41.59	0.00	42.42	0.00	102.68
5892A	17.60	40.91	0.00	41.61	0.00	100.12
6498C	16.51	41.29	0.12	41.28	0.00	99.20
6500A	17.21	40.99	0.00	41.23	0.00	99.43
6500B	17.90	40.54	0.00	41.43	0.00	99.87

(ii) Pyrite

Sample grain No.	Cu	Co	Fe	S	Ni	Total
376A	0.00	1.44	45.84	53.79	0.00	101.07
5115/2A	0.00	0.00	47.34	54.25	0.00	101.60
5115/2B	0.00	0.00	47.18	54.12	0.00	101.29
5118B	0.00	0.00	46.13	53.32	0.00	99.45
5118C	0.00	0.00	46.31	53.19	0.00	99.49
5879C	0.00	0.76	45.54	53.92	0.00	100.22
5880C	0.00	19.21	27.73	52.69	0.00	99.63
5880D	0.00	10.84	36.91	53.43	0.00	101.18
5881A	0.00	1.80	45.51	54.33	0.00	101.64
5882B	0.00	10.22	36.95	52.99	0.00	100.15
6483A	0.00	3.01	44.11	53.93	0.00	101.06
5883A	0.00	0.00	47.00	54.34	0.00	101.35
6483B	0.00	3.18	43.59	53.80	0.00	100.56
6483C	0.00	4.50	42.31	53.46	0.00	100.27
6484A	0.00	8.63	38.91	53.31	0.00	100.84
6484B	0.00	3.66	43.58	54.07	0.00	101.32
6485/1A	0.00	2.62	44.33	53.08	0.00	100.04
6485/1B	0.00	1.06	45.73	53.86	0.00	100.65
6485/2A	0.00	13.06	34.99	53.08	0.00	101.13
6487A	0.00	5.74	40.70	53.06	0.00	99.50
5115/1A	0.00	2.34	44.09	53.24	0.00	99.67
5115/1B	0.00	1.05	45.72	53.50	0.00	100.27
5115/1C	0.00	0.00	46.74	53.79	0.00	100.53
5115/1D	0.00	1.74	44.89	53.40	0.00	100.03
5115/1E	0.00	1.55	45.23	54.19	0.00	100.96
5117A	0.00	3.02	43.18	52.98	0.00	99.18
5117B	0.00	1.60	44.89	53.34	0.00	99.83
5117C	0.00	2.48	44.41	53.26	0.00	100.15
5118A	0.00	0.28	46.36	53.68	0.00	100.32

(iii) Chalcopyrite

Sample grain No.	Cu	Co	Fe	S	Ni	Total
5115/2B	35.15	0.00	30.52	35.05	0.00	100.73
5879B	33.95	0.00	30.81	36.03	0.00	100.78
5879C	34.08	0.00	29.73	34.50	0.00	98.31
5879E	35.25	0.00	31.03	35.27	0.00	101.55
5880C	34.45	0.00	31.06	35.80	0.00	101.31
5881B	35.25	0.00	30.92	35.38	0.00	101.55
5882A	34.21	0.00	30.70	35.45	0.00	100.36
5882B	34.45	0.00	31.37	35.62	0.00	101.44
5882C	34.60	0.00	30.92	35.28	0.00	100.80
5883A	35.00	0.00	30.98	35.06	0.00	101.04
5887A	34.91	0.00	30.90	35.00	0.00	100.81
5889A	34.38	0.00	30.24	34.59	0.00	99.21
5890A	34.64	0.00	30.70	34.66	0.00	100.00
5892A	34.33	0.00	30.20	34.99	0.00	99.52
6483C	34.91	0.00	30.96	34.69	0.00	100.56
6484A	35.13	0.00	30.84	35.87	0.00	101.85
6485/1A	35.02	0.00	30.71	35.29	0.00	101.01
6485/1B	34.78	0.00	30.63	34.85	0.00	100.26
6485/2A	34.81	0.00	30.83	34.96	0.00	100.61
6487A	34.46	0.00	30.53	34.64	0.00	99.63
6490A	35.06	0.00	30.67	34.78	0.00	100.51
6498A	34.57	0.00	30.42	34.91	0.00	99.90
6498D	35.36	0.00	29.30	34.38	0.00	99.04
6498E	33.41	0.00	30.69	34.84	0.00	98.93
6500A	34.14	0.00	30.36	34.49	0.00	98.99
6500C	34.33	0.00	30.44	34.96	0.00	99.73

(iv)Bornite

Sample grain No.	Cu	Co	Fe	S	Ni	Total
5888A	62.51	0.00	11.19	25.45	0.00	99.15
5888B	62.88	0.00	11.37	25.55	0.00	99.81
5889A	60.16	0.00	12.25	27.33	0.00	99.74
5891A	59.92	0.00	12.03	28.34	0.00	100.29
5892B	62.44	0.00	11.75	26.53	0.00	100.71
5892C	62.63	0.00	11.83	26.80	0.00	101.26
6485/1A	62.37	0.00	11.91	26.84	0.00	101.12
6485/1B	61.44	0.00	11.72	27.06	0.00	100.22
6490A	62.39	0.00	12.10	26.40	0.00	100.89
6498E	60.99	0.00	11.84	26.37	0.00	99.19
6500A	61.76	0.00	11.59	26.06	0.00	99.42
6500C	62.63	0.00	11.51	26.42	0.00	100.55

(v) Covellite

Sample grain No.	Cu	Co	Fe	S	Ni	Total
6498A	67.73	0.00	0.17	33.54	0.00	101.43
6498B	66.05	0.00	1.59	33.21	0.00	100.85
6498C	65.11	0.00	2.69	33.13	0.00	100.93
6498D	64.67	0.00	2.77	33.13	0.00	100.58
6498E	64.68	0.00	2.06	33.11	0.00	99.85

(vi) Chalcocite

Sample grain No	Cu	Co	Fe	S	Ni	Total
5892B	75.49	0.00	0.14	24.87	0.00	100.50

APPENDIX F

DATA FOR ANALYSIS OF VARIANCE, PRECISION AND ACCURACY ESTIMATIONS

I. ANALYSIS OF VARIANCE DATA

(a) Drill hole samples

Drill Hole	Depth (m)		Sample Length	Lithology	Analysis 1			Analysis 2			Mean Grade
	From	To			1st core half	2nd core half	Mean Analysis 1	1st core half	2nd core half	Mean Analysis 2	
BL0016	0.0	1.00	1.0	Tremolite schist	6.17	5.95	6.06	6.16	5.77	5.97	6.01
	1.00	2.00	1.0	Tremolite schist	1.62	1.50	1.56	1.47	1.49	1.48	1.52
	2.00	3.00	1.0	Tremolite schist	2.50	2.30	2.40	2.31	2.27	2.29	2.35
	3.00	3.70	0.7	Tremolite schist	2.66	2.50	2.58	2.76	2.58	2.67	2.63
	3.70	4.30	0.6	Tremolite schist	2.31	2.18	2.25	1.86	1.79	1.83	2.04
	4.30	5.30	1.0	Argillite	2.28	2.21	2.25	1.71	1.69	1.70	1.97
	5.30	6.30	1.0	Argillite	2.65	2.57	2.61	2.13	2.09	2.11	2.36
	6.30	7.30	1.0	Argillite	2.85	1.11	1.98	2.84	2.78	2.81	2.40
	7.30	8.30	1.0	Argillite	3.72	1.41	2.57	3.67	3.35	3.51	3.04
	8.30	9.30	1.0	Argillite	3.45	3.25	3.35	3.67	3.47	3.57	3.46
	9.30	10.30	1.0	Argillite	3.26	1.24	2.25	3.15	3.03	3.09	2.67
	10.30	11.30	1.0	Argillite	1.84	1.76	1.80	1.83	1.77	1.80	1.80
	11.30	11.80	0.5	Argillite	3.51	3.49	3.50	3.77	3.49	3.63	3.57
	11.80	12.30	0.5	Argillite	0.82	0.71	0.77	0.66	0.65	0.66	0.71
	12.30	12.80	0.5	Argillite	0.68	0.62	0.65	0.48	0.48	0.48	0.57
	12.80	13.30	0.5	Argillite	0.35	0.35	0.35	0.31	0.31	0.31	0.33
	13.30	13.80	0.5	Argillite	0.18	0.18	0.18	0.13	0.13	0.13	0.16
	13.80	14.30	0.5	Argillite	0.40	0.39	0.40	0.45	0.45	0.45	0.42
	14.30	14.80	0.5	Argillite	0.13	0.12	0.13	0.11	0.09	0.10	0.11
	14.80	15.20	0.4	Argillite	0.15	0.16	0.16	0.16	0.16	0.16	0.16
BL0031	0.0	0.50	0.5	Transitional schist	2.50	1.79	2.15	2.38	1.93	2.16	2.15
	0.50	1.00	0.5	Tremolite schist	4.29	6.63	5.46	4.35	6.23	5.29	5.38
	1.00	1.50	0.5	Tremolite schist	4.93	4.79	4.86	4.95	4.63	4.79	4.83
	1.50	2.00	0.5	Tremolite schist	1.38	0.98	1.18	1.24	0.98	1.11	1.15
	2.00	2.50	0.5	Tremolite schist	1.43	1.80	1.62	1.46	1.77	1.62	1.62
	2.50	3.00	0.5	Tremolite schist	1.59	1.14	1.37	1.61	1.60	1.61	1.49
	3.00	3.50	0.5	Tremolite schist	1.37	1.35	1.36	1.41	1.33	1.37	1.37
	3.50	4.00	0.5	Tremolite schist	0.89	0.99	0.94	0.89	0.97	0.93	0.94
	4.00	4.50	0.5	Tremolite schist	0.57	0.48	0.53	0.48	0.52	0.50	0.51
	4.50	5.00	0.5	Tremolite schist	1.06	0.92	0.99	1.04	0.92	0.98	0.99
	5.00	5.50	0.5	Tremolite schist	1.37	1.71	1.54	1.40	1.70	1.55	1.55
	5.50	6.00	0.5	Argillite	1.30	1.42	1.36	1.20	1.53	1.37	1.36
	6.00	6.50	0.5	Argillite	0.45	0.37	0.41	0.45	0.41	0.43	0.42
	6.50	7.00	0.5	Argillite	0.68	0.55	0.62	0.68	0.59	0.64	0.63
	7.00	7.50	0.5	Argillite	1.62	1.85	1.74	1.59	1.88	1.74	1.74
	7.50	8.00	0.5	Argillite	1.45	1.55	1.50	1.40	1.57	1.49	1.49
	8.00	8.50	0.5	Argillite	1.72	1.42	1.57	1.70	1.49	1.60	1.58
	8.50	9.00	0.5	Argillite	3.10	2.81	2.96	3.07	2.66	2.87	2.91
	9.00	9.50	0.5	Argillite	1.12	1.10	1.11	1.11	1.25	1.18	1.15
	9.50	10.00	0.5	Argillite	2.01	2.59	2.30	2.01	2.55	2.28	2.29
	10.00	10.50	0.5	Argillite	1.46	1.37	1.42	1.41	1.36	1.39	1.40
	10.50	11.00	0.5	Argillite	1.10	0.64	0.87	1.02	0.66	0.84	0.86
	11.00	11.50	0.5	Argillite	2.88	2.52	2.70	2.91	2.51	2.71	2.71
	11.50	12.00	0.5	Argillite	0.67	1.06	0.87	0.67	1.09	0.88	0.87
	12.00	12.50	0.5	Argillite	2.07	3.66	2.87	2.06	2.57	2.32	2.59
	12.50	13.00	0.5	Argillite	2.93	3.17	3.05	2.81	3.17	2.99	3.02
	13.00	13.50	0.5	Argillite	1.56	1.55	1.56	1.56	1.55	1.56	1.56
	13.50	14.00	0.5	Argillite	0.48	0.59	0.54	0.56	0.46	0.51	0.52

Appendix F.I(a) Contd

Drill Hole	Depth (m)		Sample Length	Lithology	Analysis 1			Analysis 2			Mean Grade
	From	To			1st core half	2nd core half	Mean Analysis 1	1st core half	2nd core half	Mean Analysis 2	
BL0032	0.0	0.5	0.5	Argillite	0.28	0.29	0.29	0.39	0.60	0.50	0.39
	0.50	1.00	0.5	Tremolite schist	3.17	3.56	3.37	3.15	3.66	3.41	3.39
	1.00	1.50	0.5	Tremolite schist	3.06	2.69	2.88	3.18	2.56	2.87	2.87
	1.50	2.00	0.5	Tremolite schist	2.87	2.69	2.78	2.85	2.79	2.82	2.80
	2.00	2.50	0.5	Tremolite schist	1.56	1.50	1.53	1.54	1.53	1.54	1.53
	2.50	3.00	0.5	Tremolite schist	1.73	1.42	1.58	1.72	1.41	1.57	1.57
	3.00	3.70	0.7	Transitional schist	2.49	2.08	2.29	2.46	2.30	2.38	2.33
	3.70	4.20	0.5	Conglomerate	0.40	0.39	0.40	0.40	0.40	0.40	0.40
	4.20	4.70	0.5	Conglomerate	0.12	0.16	0.14	0.13	0.11	0.12	0.13
	4.70	5.20	0.5	Conglomerate	0.14	0.12	0.13	0.15	0.13	0.14	0.14
	5.20	6.20	1.0	Conglomerate	0.33	0.24	0.29	0.36	0.25	0.31	0.30
	6.20	7.50	1.3	Quartzite	0.05	0.10	0.08	0.07	0.10	0.09	0.08
BL0033	0.0	1.00	1.0	Argillite	2.10	1.31	1.71	2.15	1.33	1.74	1.72
	1.00	1.50	0.5	Argillite	0.19	0.60	0.40	0.19	0.21	0.20	0.30
	1.50	2.00	0.5	Argillite	0.28	0.11	0.20	0.30	0.35	0.33	0.26
	2.00	2.50	0.5	Argillite	0.64	0.67	0.66	0.64	0.66	0.65	0.65
	2.50	3.00	0.5	Argillite	0.47	0.37	0.42	0.45	0.60	0.53	0.47
	3.00	3.50	0.5	Argillite	0.15	0.57	0.36	0.17	0.12	0.15	0.25
	3.50	4.00	0.5	Argillite	0.42	0.18	0.30	0.42	0.37	0.40	0.35
	4.00	4.50	0.5	Argillite	0.19	0.36	0.28	0.19	0.18	0.19	0.23
	4.50	5.00	0.5	Argillite	0.64	0.15	0.40	0.64	0.58	0.61	0.50
	5.00	5.50	0.5	Argillite	0.14	0.30	0.22	0.14	0.16	0.15	0.19
	5.50	6.00	0.5	Argillite	0.32	0.21	0.27	0.32	0.29	0.31	0.29

Argillite (44 samples)

Source of Variation	Sum of squares	Degrees of freedom	Mean square	Variance estimated
Between samples	47.377	43	1.102	geochemical variance
Within samples, between sample splits	9.298	44	0.211	sampling variance
Within sample splits, between analyses	2.157	88	0.025	analytical variance
TOTAL	58.831	175	0.336	

Schist (22 samples)

Source of Variation	Sum of squares	Degrees of freedom	Mean square	Variance estimated
Between samples	43.994	21	2.095	geochemical variance
Within samples, between sample splits	6.298	22	0.286	sampling variance
Within sample splits, between analyses	0.129	44	0.003	analytical variance
TOTAL	50.421	87	0.580	

Conglomerate/Quartzite (5 samples)

Source of Variation	Sum of squares	Degrees of freedom	Mean square	Variance estimated
Between samples	0.071	4	0.018	geochemical variance
Within samples, between sample splits	0.013	5	0.003	sampling variance
Within sample splits, between analyses	0.001	10	0.000	analytical variance
TOTAL	0.085	19	0.004	

(b) Chip samples

Location	Lithology	1st sample split	2nd sample split	Mean
460m Block 'C' Crosscut No. 10	Argillite	0.35	0.08	0.22
"	Argillite	0.15	0.01	0.08
"	Argillite	0.47	0.36	0.42
"	Argillite	0.16	0.19	0.18
"	Argillite	0.15	0.17	0.16
465m Block 'C' Crosscut No. 7	Tremolite Schist	4.10	1.73	2.92
"	Tremolite Schist	3.45	4.02	3.74
"	Transitional Schist	2.12	1.98	2.05
"	Conglomerate	0.12	0.07	0.10
"	Conglomerate	0.08	0.10	0.09
"	Conglomerate	0.21	0.30	0.26
465m Block 'B' Crosscut No. 6	Tremolite Schist	8.30	9.50	8.90
"	Tremolite Schist	9.16	5.50	7.33
"	Tremolite Schist	2.61	2.87	2.74
"	Tremolite Schist	4.05	6.43	5.24
"	Transitional Schist	4.07	2.43	3.25
"	Transitional Schist	3.58	0.17	1.88
460m Block 'K' Haulage	Argillite	0.12	0.20	0.16
"	Argillite	0.15	0.07	0.11
"	Argillite	0.16	0.41	0.29
"	Argillite	0.50	0.14	0.32
"	Argillite	0.56	0.24	0.40
460m Block 'K' Crosscut No. 5	Argillite	0.30	0.30	0.30
"	Argillite	0.98	2.48	1.73
"	Argillite	0.63	0.63	0.63
"	Tremolite Schist	1.73	2.38	2.06
"	Tremolite Schist	3.28	2.98	3.13
"	Tremolite Schist	3.90	2.76	3.33
"	Tremolite Schist	3.47	0.23	1.85
460m Block 'J' Crosscut No. 9	Argillite	0.05	0.07	0.06
"	Argillite	0.06	0.11	0.09
"	Argillite	0.09	0.09	0.09
"	Argillite	0.12	0.09	0.11
"	Argillite	0.05	0.06	0.06
"	Argillite	0.03	0.05	0.04
"	Argillite	0.06	0.21	0.14
445m Block 'B' Crosscut No. 3	Argillite	0.15	0.12	0.14
"	Argillite	0.11	0.06	0.09
"	Argillite	0.08	0.05	0.07
"	Argillite	1.72	3.26	2.49
"	Tremolite Schist	2.20	2.61	2.41
"	Tremolite Schist	0.85	0.21	0.53
"	Tremolite Schist	3.46	2.10	2.78
460m Block 'K' Haulage	Argillite	0.06	0.06	0.06
"	Argillite	0.10	0.06	0.08
"	Argillite	0.21	0.05	0.13
"	Argillite	0.20	2.61	1.41
"	Argillite	0.28	0.07	0.18
"	Argillite	0.13	0.21	0.17
463m Block 'A' Crosscut No. 6	Argillite	0.82	0.48	0.65
"	Argillite	0.08	0.08	0.08
"	Tremolite Schist	0.28	0.15	0.22
"	Tremolite Schist	0.37	0.06	0.22
"	Tremolite Schist	0.19	0.42	0.31
"	Argillite	0.57	0.12	0.35

Argillite (33 samples)

Source of Variation	Sum of squares	Degrees of freedom	Mean square	Variance estimated
Between samples	9.081	32	0.284	geochemical variance
Within samples, between sample splits	5.635	33	0.171	technical variance
TOTAL	14.716	65	0.226	

Schist (19 samples)

Source of Variation	Sum of squares	Degrees of freedom	Mean square	Variance estimated
Between samples	92.799	18	5.156	geochemical variance
Within samples, between sample splits	27.875	19	1.467	technical variance
TOTAL	120.674	37	3.261	

Conglomerate (3 samples)

Source of Variation	Sum of squares	Degrees of freedom	Mean square	Variance estimated
Between samples	0.018	2	0.009	geochemical variance
Within samples, between sample splits	0.006	3	0.002	technical variance
TOTAL	0.024	5	0.005	

II. BALUBA REPLICATE AAS ANALYSES USED FOR PRECISION ESTIMATION

(a) Copper (%)

Drill Hole	Sample No.	Lithology	Analysis 1	Analysis 2	Mean Analysis	Difference between analyses
BL0016	301	Tremolite Schist	6.17	6.16	6.17	0.01
	302	Tremolite Schist	1.62	1.47	1.55	0.15
	303	Tremolite Schist	2.50	2.31	2.41	0.19
	304	Tremolite Schist	2.66	2.76	2.71	-0.10
	305	Tremolite Schist	2.31	1.86	2.09	0.45
	306	Argillite	2.28	1.71	2.00	0.57
	307	Argillite	2.65	2.13	2.39	0.52
	308	Argillite	2.85	2.84	2.85	0.01
	309	Argillite	3.72	3.67	3.70	0.05
	310	Argillite	3.45	3.67	3.56	-0.22
	311	Argillite	3.26	3.15	3.21	0.11
	312	Argillite	1.84	1.83	1.84	0.01
	313	Argillite	3.51	3.77	3.64	-0.26
	314	Argillite	0.82	0.66	0.74	0.16
	315	Argillite	0.68	0.48	0.58	0.20
	316	Argillite	0.35	0.31	0.33	0.04
	317	Argillite	0.18	0.13	0.16	0.05
	318	Argillite	0.40	0.45	0.43	-0.05
	319	Argillite	0.13	0.11	0.12	0.02
	320	Argillite	0.15	0.16	0.16	-0.01
	351	Tremolite Schist	5.95	5.77	5.86	0.18
	352	Tremolite Schist	1.50	1.49	1.50	0.01
	353	Tremolite Schist	2.30	2.27	2.29	0.03
	354	Tremolite Schist	2.50	2.58	2.54	-0.08
	355	Tremolite Schist	2.18	1.79	1.99	0.39
	356	Argillite	2.21	1.69	1.95	0.52
	357	Argillite	2.57	2.09	2.33	0.48
	358	Argillite	1.11	2.78	1.95	-1.67
	359	Argillite	1.41	3.35	2.38	-1.94
	360	Argillite	3.25	3.47	3.36	-0.22
	361	Argillite	1.24	3.03	2.14	-1.79
	362	Argillite	1.76	1.77	1.77	-0.01
	363	Argillite	3.49	3.49	3.49	0.00
	364	Argillite	0.71	0.65	0.68	0.06
	365	Argillite	0.62	0.48	0.55	0.14
	366	Argillite	0.35	0.31	0.33	0.04
	367	Argillite	0.18	0.13	0.16	0.05
	368	Argillite	0.39	0.45	0.42	-0.06
	369	Argillite	0.12	0.09	0.11	0.03
	370	Argillite	0.16	0.16	0.16	0.00
BL0031	95	Transitional Schist	2.50	2.38	2.44	0.12
	96	Tremolite Schist	4.29	4.35	4.32	-0.06
	97	Tremolite Schist	4.93	4.95	4.94	-0.02
	98	Tremolite Schist	1.38	1.24	1.31	0.14
	99	Tremolite Schist	1.43	1.46	1.45	-0.03
	100	Tremolite Schist	1.59	1.61	1.60	-0.02
	101	Tremolite Schist	1.37	1.41	1.39	-0.04
	102	Tremolite Schist	0.89	0.89	0.89	0.00
	103	Tremolite Schist	0.57	0.48	0.53	0.09
	104	Tremolite Schist	1.06	1.04	1.05	0.02

Appendix F.II(a) Contd

Drill Hole	Sample No.	Lithology	Analysis 1	Analysis 2	Mean Analysis	Difference between analyses
BL0031	105	Tremolite Schist	1.37	1.40	1.39	-0.03
	106	Argillite	1.30	1.20	1.25	0.10
	107	Argillite	0.45	0.45	0.45	0.00
	108	Argillite	0.68	0.68	0.68	0.00
	109	Argillite	1.62	1.59	1.61	0.03
	110	Argillite	1.45	1.40	1.43	0.05
	111	Argillite	1.72	1.70	1.71	0.02
	112	Argillite	3.10	3.07	3.09	0.03
	113	Argillite	1.12	1.11	1.12	0.01
	114	Argillite	2.01	2.01	2.01	0.00
	115	Argillite	1.46	1.41	1.44	0.05
	116	Argillite	1.10	1.02	1.06	0.08
	117	Argillite	2.88	2.91	2.90	-0.03
	118	Argillite	0.67	0.67	0.67	0.00
	119	Argillite	2.07	2.06	2.07	0.01
	120	Argillite	2.93	2.81	2.87	0.12
	121	Argillite	1.56	1.56	1.56	0.00
	149	Argillite	0.48	0.56	0.52	-0.08
BL0031	122	Transitional Schist	1.79	1.93	1.86	-0.14
	123	Tremolite Schist	6.63	6.23	6.43	0.40
	124	Tremolite Schist	4.79	4.63	4.71	0.16
	125	Tremolite Schist	0.98	0.98	0.98	0.00
	126	Tremolite Schist	1.80	1.77	1.79	0.03
	127	Tremolite Schist	1.14	1.60	1.37	-0.46
	128	Tremolite Schist	1.35	1.33	1.34	0.02
	129	Tremolite Schist	0.99	0.97	0.98	0.02
	130	Tremolite Schist	0.48	0.52	0.50	-0.04
	131	Tremolite Schist	0.92	0.92	0.92	0.00
	132	Tremolite Schist	1.71	1.70	1.71	0.01
	133	Argillite	1.42	1.53	1.48	-0.11
	134	Argillite	0.37	0.41	0.39	-0.04
	135	Argillite	0.55	0.59	0.57	-0.04
	136	Argillite	1.85	1.88	1.87	-0.03
	137	Argillite	1.55	1.57	1.56	-0.02
	138	Argillite	1.42	1.49	1.46	-0.07
	139	Argillite	2.81	2.66	2.74	0.15
	140	Argillite	1.10	1.25	1.18	-0.15
	141	Argillite	2.59	2.55	2.57	0.04
	142	Argillite	1.37	1.36	1.37	0.01
	143	Argillite	0.64	0.66	0.65	-0.02
	144	Argillite	2.52	2.51	2.52	0.01
	145	Argillite	1.06	1.09	1.08	-0.03
	146	Argillite	3.66	2.57	3.12	1.09
	147	Argillite	3.17	3.17	3.17	0.00
	148	Argillite	1.55	1.55	1.55	0.00
	150	Argillite	0.59	0.46	0.53	0.13
BL0032	CK2273	Tremolite Schist	3.17	3.15	3.16	0.02
	CK2274	Tremolite Schist	3.06	3.18	3.12	-0.12
	CK2275	Tremolite Schist	2.87	2.85	2.86	0.02
	CK2276	Tremolite Schist	1.56	1.54	1.55	0.02
	CK2277	Tremolite Schist	1.73	1.72	1.73	0.01
	CK2278	Transitional Schist	2.49	2.46	2.48	0.03

Appendix F.II(a) Contd

Drill Hole	Sample No.	Lithology	Analysis 1	Analysis 2	Mean Analysis	Difference between analyses
BL0032	CK2279	Conglomerate	0.40	0.40	0.40	0.00
	CK2280	Conglomerate	0.12	0.13	0.13	-0.01
	CK2281	Conglomerate	0.14	0.15	0.15	-0.01
	CK2291	Conglomerate	0.33	0.36	0.35	-0.03
	CK2292	Quartzite	0.05	0.07	0.06	-0.02
	CK2294	Quartzite	0.28	0.39	0.34	-0.11
	CK2282	Tremolite Schist	0.29	0.60	0.45	-0.31
	CK2284	Tremolite Schist	3.56	3.66	3.61	-0.10
	CK2286	Tremolite Schist	2.69	2.56	2.63	0.13
	CK2288	Tremolite Schist	2.69	2.79	2.74	-0.10
	CK2289	Tremolite Schist	1.50	1.53	1.52	-0.03
	CK2283	Transitional Schist	1.42	1.41	1.42	0.01
	CK2285	Conglomerate	2.08	2.30	2.19	-0.22
	CK2287	Conglomerate	0.39	0.40	0.40	-0.01
	CK2290	Conglomerate	0.16	0.11	0.14	0.05
	CK2294	Conglomerate	0.12	0.13	0.13	-0.01
	CK2293	Quartzite	0.24	0.25	0.25	-0.01
	CK2295	Quartzite	0.10	0.10	0.10	0.00
BL0033	CK2251	Argillite	2.10	2.15	2.13	-0.05
	CK2252	Argillite	0.19	0.19	0.19	0.00
	CK2253	Argillite	0.28	0.30	0.29	-0.02
	CK2254	Argillite	0.64	0.64	0.64	0.00
	CK2255	Argillite	0.47	0.45	0.46	0.02
	CK2256	Argillite	0.15	0.17	0.16	-0.02
	CK2257	Argillite	0.42	0.42	0.42	0.00
	CK2258	Argillite	0.19	0.19	0.19	0.00
	CK2259	Argillite	0.64	0.64	0.64	0.00
	CK2260	Argillite	0.14	0.14	0.14	0.00
	CK2261	Argillite	0.32	0.32	0.32	0.00
	CK2262	Argillite	1.31	1.33	1.32	-0.02
	CK2272	Argillite	0.60	0.21	0.41	0.39
	CK2269	Argillite	0.11	0.35	0.23	-0.24
	CK2265	Argillite	0.67	0.66	0.67	0.01
	CK2263	Argillite	0.37	0.60	0.49	-0.23
	CK2264	Argillite	0.57	0.12	0.35	0.45
	CK2266	Argillite	0.18	0.37	0.28	-0.19
	CK2268	Argillite	0.36	0.18	0.27	0.18
	CK2267	Argillite	0.15	0.58	0.37	-0.43
	CK2270	Argillite	0.30	0.16	0.23	0.14
	CK2271	Argillite	0.21	0.29	0.25	-0.08

(b) Cobalt (%)

Drill Hole	Sample No.	Lithology	Analysis 1	Analysis 2	Mean Analysis	Difference between analyses
BL0016	301	Tremolite Schist	0.65	0.20	0.43	0.45
	302	Tremolite Schist	0.05	0.05	0.05	0.00
	303	Tremolite Schist	0.15	0.10	0.13	0.05
	304	Tremolite Schist	0.05	0.15	0.10	0.10
	305	Tremolite Schist	1.59	1.41	1.50	0.18
	306	Argillite	1.31	1.17	1.24	0.14
	307	Argillite	0.76	0.55	0.66	0.21
	308	Argillite	0.25	0.70	0.48	0.45
	309	Argillite	0.43	0.40	0.42	0.03
	310	Argillite	0.40	0.45	0.43	0.05
	311	Argillite	0.40	0.45	0.43	0.05
	312	Argillite	0.40	0.40	0.40	0.00
	313	Argillite	0.10	0.10	0.10	0.00
	314	Argillite	0.20	0.15	0.18	0.05
	315	Argillite	0.20	0.20	0.20	0.00
	316	Argillite	0.10	0.10	0.10	0.00
	317	Argillite	0.15	0.05	0.10	0.10
	318	Argillite	0.15	0.10	0.13	0.05
	319	Argillite	0.15	0.10	0.13	0.05
	320	Argillite	0.15	0.20	0.18	0.05
	351	Tremolite Schist	0.25	0.20	0.23	0.05
	352	Tremolite Schist	0.08	0.06	0.07	0.02
	353	Tremolite Schist	0.13	0.14	0.14	0.01
	354	Tremolite Schist	0.10	0.14	0.12	0.04
	355	Tremolite Schist	1.40	1.43	1.42	0.03
	356	Argillite	1.27	1.20	1.24	0.07
	357	Argillite	0.73	0.53	0.63	0.20
	358	Argillite	0.62	0.69	0.66	0.07
	359	Argillite	0.43	0.42	0.43	0.01
	360	Argillite	0.42	0.35	0.39	0.07
	361	Argillite	0.35	0.33	0.34	0.02
	362	Argillite	0.37	0.37	0.37	0.00
	363	Argillite	0.16	0.16	0.16	0.00
	364	Argillite	0.18	0.19	0.19	0.01
	365	Argillite	0.18	0.21	0.20	0.03
	366	Argillite	0.10	0.10	0.10	0.00
	367	Argillite	0.15	0.12	0.14	0.03
	368	Argillite	0.14	0.13	0.14	0.01
	369	Argillite	0.11	0.12	0.12	0.01
	370	Argillite	0.15	0.14	0.15	0.01
BL0031	95	Transitional Schist	0.16	0.16	0.16	0.00
	96	Tremolite Schist	0.11	0.12	0.12	0.01
	97	Tremolite Schist	0.18	0.21	0.20	0.03
	98	Tremolite Schist	0.10	0.12	0.11	0.02
	99	Tremolite Schist	0.07	0.09	0.08	0.02
	100	Tremolite Schist	0.05	0.05	0.05	0.00
	101	Tremolite Schist	0.04	0.07	0.06	0.03
	102	Tremolite Schist	0.04	0.07	0.06	0.03
	103	Tremolite Schist	0.05	0.08	0.07	0.03
	104	Tremolite Schist	0.07	0.09	0.08	0.02
	105	Tremolite Schist	0.09	0.09	0.09	0.00
	106	Argillite	0.09	0.09	0.09	0.00

Appendix F.II(b) Contd

Drill Hole	Sample No.	Lithology	Analysis 1	Analysis 2	Mean Analysis	Difference between analyses
	107	Argillite	0.06	0.05	0.06	0.01
	108	Argillite	0.07	0.16	0.12	0.09
	109	Argillite	0.14	0.07	0.11	0.07
	110	Argillite	0.08	0.11	0.10	0.03
	111	Argillite	0.10	0.11	0.11	0.01
	112	Argillite	0.20	0.18	0.19	0.02
	113	Argillite	0.05	0.07	0.06	0.02
	114	Argillite	0.09	0.11	0.10	0.02
	115	Argillite	0.09	0.11	0.10	0.02
	116	Argillite	0.10	0.07	0.09	0.03
	117	Argillite	0.17	0.23	0.20	0.06
	118	Argillite	0.08	0.09	0.09	0.01
	119	Argillite	0.06	0.09	0.08	0.03
	120	Argillite	0.13	0.12	0.13	0.01
	121	Argillite	0.08	0.16	0.12	0.08
	149	Argillite	0.08	0.16	0.12	0.08
	122	Transitional Schist	0.12	0.16	0.14	0.04
	123	Tremolite Schist	0.11	0.12	0.12	0.01
	124	Tremolite Schist	0.14	0.14	0.14	0.00
	125	Tremolite Schist	0.07	0.09	0.08	0.02
	126	Tremolite Schist	0.06	0.07	0.07	0.01
	127	Tremolite Schist	0.04	0.05	0.05	0.01
	128	Tremolite Schist	0.04	0.05	0.05	0.01
	129	Tremolite Schist	0.06	0.07	0.07	0.01
	130	Tremolite Schist	0.05	0.05	0.05	0.00
	131	Tremolite Schist	0.07	0.10	0.09	0.03
	132	Tremolite Schist	0.11	0.10	0.11	0.01
	133	Argillite	0.08	0.09	0.09	0.01
	134	Argillite	0.06	0.09	0.08	0.03
	135	Argillite	0.08	0.07	0.08	0.01
	136	Argillite	0.16	0.17	0.17	0.01
	137	Argillite	0.14	0.17	0.16	0.03
	138	Argillite	0.10	0.10	0.10	0.00
	139	Argillite	0.15	0.16	0.16	0.01
	140	Argillite	0.07	0.07	0.07	0.00
	141	Argillite	0.09	0.12	0.11	0.03
	142	Argillite	0.09	0.10	0.10	0.01
	143	Argillite	0.08	0.16	0.12	0.08
	144	Argillite	0.13	0.17	0.15	0.04
	145	Argillite	0.08	0.07	0.08	0.01
	146	Argillite	0.08	0.07	0.08	0.01
	147	Argillite	0.06	0.09	0.08	0.03
	148	Argillite	0.08	0.09	0.09	0.01
	150	Argillite	0.08	0.16	0.12	0.08
BL0032	CK2273	Tremolite Schist	0.16	0.17	0.17	0.01
	CK2274	Tremolite Schist	0.23	0.25	0.24	0.02
	CK2275	Tremolite Schist	0.26	0.29	0.28	0.03
	CK2276	Tremolite Schist	0.16	0.17	0.17	0.01
	CK2277	Tremolite Schist	0.10	0.11	0.11	0.01
	CK2278	Transitional Schist	0.09	0.11	0.10	0.02
	CK2279	Conglomerate	0.02	0.02	0.02	0.00
	CK2280	Conglomerate	0.02	0.02	0.02	0.00

Appendix F.II(b) Contd

Drill Hole	Sample No.	Lithology	Analysis 1	Analysis 2	Mean Analysis	Difference between analyses
	CK2281	Conglomerate	0.02	0.04	0.03	0.02
	CK2291	Conglomerate	0.08	0.09	0.09	0.01
	CK2292	Quartzite	0.05	0.03	0.04	0.02
	CK2294	Quartzite	0.05	0.07	0.06	0.02
	CK2282	Tremolite Schist	0.33	0.35	0.34	0.02
	CK2284	Tremolite Schist	0.16	0.18	0.17	0.02
	CK2286	Tremolite Schist	0.20	0.22	0.21	0.02
	CK2288	Tremolite Schist	0.16	0.18	0.17	0.02
	CK2289	Tremolite Schist	0.09	0.10	0.10	0.01
	CK2283	Transitional Schist	0.11	0.12	0.12	0.01
	CK2285	Conglomerate	0.02	0.03	0.03	0.01
	CK2287	Conglomerate	0.02	0.03	0.03	0.01
	CK2290	Conglomerate	0.02	0.03	0.03	0.01
	CK2294	Conglomerate	0.05	0.07	0.06	0.02
	CK2293	Quartzite	0.01	0.03	0.02	0.02
	CK2295	Quartzite	0.10	0.10	0.10	0.00
BL0033	CK2251	Argillite	0.09	0.09	0.09	0.00
	CK2252	Argillite	0.07	0.08	0.08	0.01
	CK2253	Argillite	0.04	0.05	0.04	0.01
	CK2254	Argillite	0.07	0.07	0.07	0.00
	CK2255	Argillite	0.08	0.09	0.09	0.01
	CK2256	Argillite	0.08	0.08	0.08	0.00
	CK2257	Argillite	0.12	0.12	0.12	0.00
	CK2258	Argillite	0.09	0.10	0.09	0.01
	CK2259	Argillite	0.11	0.11	0.11	0.00
	CK2260	Argillite	0.07	0.07	0.07	0.00
	CK2261	Argillite	0.07	0.08	0.07	0.01
	CK2262	Argillite	0.07	0.07	0.07	0.00
	CK2272	Argillite	0.07	0.08	0.08	0.01
	CK2269	Argillite	0.04	0.04	0.04	0.00
	CK2265	Argillite	0.06	0.07	0.07	0.01
	CK2263	Argillite	0.09	0.10	0.09	0.01
	CK2264	Argillite	0.07	0.08	0.07	0.01
	CK2266	Argillite	0.11	0.11	0.11	0.00
	CK2268	Argillite	0.10	0.10	0.10	0.00
	CK2267	Argillite	0.11	0.11	0.11	0.00
	CK2270	Argillite	0.07	0.08	0.07	0.01
	CK2271	Argillite	0.07	0.07	0.07	0.00

III. BALUBA AAS ANALYSES AND IMPERIAL COLLEGE ICP ANALYSES USED FOR ACCURACY ESTIMATION

(a) Copper (%)

	AAS			ICP
Sample No	Baluba Analysis 1	Baluba Analysis 2	Baluba Mean	Imperial College Analysis
CK2251	2.10	2.15	2.13	2.07
CK2252	0.19	0.19	0.19	0.17
CK2254	0.64	0.64	0.64	0.61
CK2255	0.47	0.45	0.46	0.46
CK2257	0.42	0.42	0.42	0.41
CK2259	0.64	0.64	0.64	0.61
CK2261	0.32	0.32	0.32	0.29
CK2262	1.31	1.33	1.32	1.37
CK2263	0.60	0.60	0.60	0.56
CK2265	0.67	0.66	0.67	0.63
CK2266	0.37	0.37	0.37	0.34
CK2267	0.57	0.58	0.58	0.55
CK2271	0.30	0.29	0.30	0.28
CK2272	0.21	0.21	0.21	0.19
CK2273	3.17	3.15	3.16	3.2
CK2275	2.87	2.85	2.86	2.86
CK2276	1.56	1.54	1.55	1.58
CK2277	1.73	1.72	1.73	1.72
CK2278	2.49	2.46	2.48	2.45
CK2280	0.12	0.13	0.13	0.11
CK2282	3.56	3.66	3.61	3.65
CK2283	2.08	2.30	2.19	2.26
CK2286	2.69	2.79	2.74	2.81
CK2287	0.16	0.11	0.14	0.16
CK2288	1.50	1.53	1.52	1.53
CK2289	1.42	1.41	1.42	1.39
CK2292	0.05	0.07	0.06	0.05
CK2293	0.10	0.10	0.10	0.11

(b) Cobalt (%)

	AAS			ICP
Sample No	Baluba Analysis 1	Baluba Analysis 2	Baluba Mean	Imperial College Analysis
CK2251	0.09	0.09	0.09	0.07
CK2252	0.07	0.08	0.08	0.05
CK2254	0.07	0.07	0.07	0.05
CK2255	0.08	0.09	0.09	0.07
CK2257	0.12	0.12	0.12	0.10
CK2259	0.11	0.11	0.11	0.08
CK2261	0.07	0.08	0.08	0.06
CK2262	0.07	0.07	0.07	0.05
CK2263	0.09	0.10	0.10	0.07
CK2265	0.06	0.07	0.07	0.05
CK2266	0.11	0.11	0.11	0.09
CK2267	0.11	0.11	0.11	0.09
CK2271	0.07	0.07	0.07	0.06
CK2272	0.07	0.08	0.08	0.06
CK2273	0.16	0.17	0.17	0.16
CK2275	0.26	0.29	0.28	0.26
CK2276	0.16	0.17	0.17	0.17
CK2277	0.10	0.11	0.11	0.09
CK2278	0.09	0.11	0.10	0.09
CK2280	0.02	0.02	0.02	0.01
CK2282	0.33	0.35	0.34	0.31
CK2283	0.11	0.12	0.12	0.09
CK2286	0.20	0.22	0.21	0.19
CK2287	0.02	0.03	0.03	0.01
CK2288	0.16	0.18	0.17	0.18
CK2289	0.09	0.10	0.10	0.08
CK2292	0.01	0.03	0.02	0.001
CK2293	0.01	0.03	0.02	0.001

APPENDIX G

EXPERIMENTAL VARIOGRAM DATA

I. EXPERIMENTAL DOWN HOLE VARIOGRAM RESULTS FOR COPPER

(a) All lithologies

Lag No.	Sample Pairs	Mean Distance (m)	Variogram
1	78	0.78	1.80
2	55	1.65	1.17
3	54	2.67	1.97
4	65	3.66	2.17
5	53	4.62	2.14
6	46	5.64	2.00
7	49	6.56	1.90
8	28	7.62	3.29
9	32	8.60	1.47
10	37	9.54	2.85
11	31	10.64	2.36
12	28	11.52	1.76
13	26	12.68	3.43
14	22	13.62	3.76
15	15	14.56	1.40

(b) Schist

Lag No.	Sample Pairs	Mean Distance (m)	Variogram
1	137	0.79	2.29
2	127	1.68	3.58
3	96	2.68	3.02
4	98	3.68	3.21
5	80	4.60	3.57
6	67	5.66	2.58
7	42	6.59	3.67
8	32	7.53	3.22
9	18	8.56	1.94

(c) Argillite

Lag No.	Sample Pairs	Mean Distance (m)	Variogram
1	100	0.75	0.44
2	98	1.76	0.67
3	80	2.72	0.78
4	92	3.65	1.13
5	64	4.61	1.00
6	70	5.63	0.84
7	47	6.56	0.96
8	36	7.59	1.56
9	42	8.56	1.56
10	30	9.52	1.45
11	26	10.51	1.52

II. EXPERIMENTAL VARIOGRAM RESULTS FOR COPPER: 120°

(a) All lithologies

Lag No.	Sample Pairs	Mean Distance (m)	Variogram
1	14	18.49	0.21
2	25	38.77	0.20
3	38	64.56	0.36
4	55	85.76	0.30
5	52	113.11	0.38
6	61	138.17	0.32
7	71	160.45	0.56
8	54	187.50	0.43
9	46	212.78	0.70
10	58	236.94	0.37
11	60	260.74	0.26

(b) Schist

Lag No.	Sample Pairs	Mean Distance (m)	Variogram
1	14	18.49	0.36
2	25	38.77	0.38
3	38	64.56	0.53
4	55	85.76	0.36
5	52	113.11	0.53
6	61	138.17	0.37
7	71	160.45	0.64
8	54	187.50	0.56
9	46	212.78	0.81
10	58	236.94	0.57
11	60	260.74	0.38

(c) Argillite

Lag No.	Sample Pairs	Mean Distance (m)	Variogram
1	11	18.53	0.16
2	18	39.95	0.19
3	26	64.75	0.36
4	27	84.36	0.27
5	28	113.02	0.37
6	31	139.02	0.40
7	25	160.55	0.34
8	14	189.06	0.33

III. EXPERIMENTAL VARIOGRAM RESULTS FOR COPPER: 030°

(a) All lithologies

Lag No.	Sample Pairs	Mean Distance (m)	Variogram
1	10	14.55	0.10
2	38	36.29	0.18
3	44	63.13	0.25
4	37	88.36	0.31
5	27	111.87	0.49
6	20	133.78	0.44
7	23	161.01	0.52
8	5	186.59	0.11
9	7	212.33	0.19
10	2	241.58	0.16
11	2	261.22	0.28

(b) Schist

Lag No.	Sample Pairs	Mean Distance (m)	Variogram
1	10	14.55	0.15
2	38	36.29	0.29
3	44	63.13	0.39
4	37	88.36	0.40
5	27	111.87	0.53
6	20	133.78	0.63
7	23	161.01	0.62
8	5	186.59	0.18
9	7	212.33	0.31
10	2	241.58	0.04
11	2	261.22	0.78

(c) Argillite

Lag No.	Sample Pairs	Mean Distance (m)	Variogram
1	9	13.92	0.16
2	26	35.20	0.27
3	23	62.54	0.35
4	22	87.31	0.35
5	7	108.47	0.20
6	12	131.28	0.62
7	12	158.37	0.75
8	3	185.80	0.33
9	4	215.55	0.49
10	1	237.88	1.35
11	1	255.44	0.69

APPENDIX H

DILUTION

(a) INTERNAL DILUTION

Widths of ore and internal waste at different cutoff grades

Schist

Drill Hole	0.25% ore	0.25% int. dil	0.50% ore	0.50% int. dil	0.75% ore	0.75% int. dil	1.00% ore	1.00% int. dil	1.25% ore	1.25% int. dil	1.50% ore	1.50% int. dil
AP2CT	9.00	0.00	9.00	0.00	9.00	0.00	9.00	1.00	9.00	1.00	9.00	3.00
AP4CT	10.50	0.00	10.50	0.00	10.50	0.00	10.50	0.50	10.50	0.50	10.50	0.50
AP6CT	9.50	0.00	9.50	0.00	9.50	0.00	9.50	0.00	9.50	0.00	9.50	0.00
B287	6.70	0.00	6.70	0.00	6.70	0.00	6.70	0.00	6.70	0.00	6.70	0.00
B298	8.20	0.00	8.20	0.00	7.10	0.00	6.60	0.00	6.10	0.00	5.10	0.00
B300	7.30	0.00	7.30	0.00	7.30	1.40	7.30	1.90	7.30	1.90	7.30	1.90
B87	5.80	0.00	5.80	0.00	5.80	0.00	5.80	0.00	5.80	0.00	5.80	0.80
BL0001B	2.80	0.00	2.80	0.00	2.80	0.00	2.80	0.00	2.80	0.00	2.80	0.00
BL0003	6.00	0.00	6.00	0.00	6.00	0.00	6.00	0.00	6.00	0.00	6.00	0.00
BL0004	7.50	0.00	7.50	0.00	7.50	0.00	7.50	0.00	7.50	0.00	7.50	0.00
BL0008	7.30	0.00	5.90	0.00	5.90	0.00	5.90	0.00	5.40	0.00	5.40	0.00
BL0010	8.30	0.00	8.30	0.00	8.30	0.00	8.30	0.00	8.30	0.60	8.30	0.60
BL0011	6.80	0.00	6.80	0.00	6.80	0.50	6.80	0.50	6.80	0.50	6.80	1.90
BL0012	8.60	0.00	8.60	0.00	8.60	0.00	8.60	0.60	8.60	0.90	8.60	3.40
BL0013	5.80	0.00	5.80	0.00	5.80	0.50	5.80	0.50	5.80	0.50	5.80	0.50
BL0017	23.00	0.00	22.50	0.00	22.00	0.00	22.00	0.00	21.50	0.00	21.50	0.00
BL0021	5.10	0.00	5.10	0.00	5.10	0.00	5.10	0.00	5.10	0.00	5.10	0.00
BL0025	8.40	0.00	8.40	0.00	8.40	0.00	8.40	0.00	8.40	0.00	8.40	0.00
BX1455	6.90	0.00	6.90	0.00	6.90	0.00	6.90	0.00	6.90	1.00	6.90	1.00
BX1839	11.10	0.00	9.60	0.00	9.10	0.00	9.10	0.00	9.10	0.00	9.10	0.40
BX1840	7.00	0.00	7.00	0.00	7.00	1.00	5.50	0.00	5.50	0.00	4.50	0.00
BX1841	14.80	0.50	14.80	0.50	14.80	0.50	14.80	1.00	14.80	1.00	14.80	2.00
BX1842	10.40	0.00	10.40	0.00	10.40	0.00	10.40	0.00	10.40	0.00	10.40	0.40
BX1843	11.30	0.50	11.30	0.50	11.30	0.50	11.30	0.50	11.30	0.50	11.30	2.50
BX1844	9.50	0.00	9.50	0.00	9.50	0.00	9.50	0.00	5.50	0.00	4.50	0.00
BX1845	9.50	0.00	9.50	0.00	9.50	0.00	9.50	0.00	9.50	0.00	9.50	1.00
BX1846	15.70	0.00	15.70	0.00	15.70	0.00	15.70	0.00	15.70	0.50	15.70	4.00
BX2007	6.90	0.00	6.90	0.00	6.90	0.00	6.90	1.00	6.90	2.00	6.90	3.40
BX2008	17.90	0.00	17.90	0.00	17.90	0.00	17.90	0.00	17.90	0.00	17.90	0.00
BX2221	6.20	0.00	6.20	0.00	6.20	0.20	6.20	0.20	6.20	0.20	6.20	1.70
BX2255	8.20	0.00	8.20	0.00	8.20	1.00	8.20	2.30	8.20	3.10	8.20	3.10
BX2269	4.60	0.00	4.60	0.00	4.60	0.00	4.60	0.00	4.60	0.00	4.60	0.00
BX2346	8.90	0.00	8.90	0.00	8.90	0.00	8.90	0.00	8.90	0.00	8.90	0.40
BX2384	6.60	0.00	6.60	0.00	6.60	0.00	6.60	0.00	6.60	1.70	6.60	1.70
BX2385	6.20	0.00	6.20	0.00	6.20	0.00	6.20	1.00	6.20	1.00	6.20	2.00
BX2430	7.40	0.00	7.40	0.00	7.40	0.00	7.40	0.50	7.40	1.00	7.40	1.00
BX2434	8.50	0.00	8.50	0.00	8.50	0.00	8.50	0.00	7.50	0.00	7.50	0.00
BX2435	8.20	0.00	8.20	0.00	8.20	0.00	8.20	0.00	8.20	0.00	8.20	0.50
BX2436	5.10	0.00	5.10	0.00	5.10	0.00	5.10	0.00	5.10	0.60	5.10	1.10
BX2469	10.00	0.00	10.00	0.00	10.00	0.00	10.00	0.00	10.00	0.00	10.00	0.00
MEAN WIDTH	8.69	0.03	8.60	0.03	8.55	0.14	8.50	0.29	8.34	0.46	8.26	0.97
DILUTION	0.3		0.3		1.6		3.4		5.5		11.7	

Argillite

	0.25% ore	0.25% int. dil	0.50% ore	0.50% int. dil	0.75% ore	0.75% int. dil	1.00% ore	1.00% int. dil	1.25% ore	1.25% int. dil	1.50% ore	1.50% int. dil
AP2CT	3.50	0.00	3.50	0.00	3.50	0.00	3.00	0.00	2.50	0.00	2.00	0.00
AP4CT	1.00	0.00	1.00	0.00	0.50	0.00	0.00	0.00	0.00	0.00	0.00	0.00
AP6CT	3.00	0.00	2.00	0.00	2.00	0.00	2.00	0.00	2.00	0.50	2.00	0.50
B287	11.40	0.00	8.40	0.00	6.90	0.00	6.90	0.00	6.30	0.00	6.30	0.00
B298	3.80	0.00	2.80	0.00	0.00	0.00	0.00	0.00	0.00	0.00	0.00	0.00
B300	13.10	0.00	12.50	1.20	10.10	0.00	10.10	0.00	10.10	0.00	9.50	0.50
B87	6.10	0.00	5.20	0.00	4.30	0.00	3.70	1.80	1.20	0.00	0.60	0.00
BL0001B	12.90	0.00	12.40	2.50	12.40	4.00	6.50	0.00	5.20	0.00	4.50	0.00
BL0003	12.00	0.50	10.00	0.00	9.50	0.00	8.00	0.00	8.00	0.00	7.50	0.00
BL0004	7.10	3.60	2.00	0.50	2.00	0.50	2.00	0.50	2.00	0.50	0.50	0.00
BL0008	1.90	0.00	0.00	0.00	0.00	0.00	0.00	0.00	0.00	0.00	0.00	0.00
BL0010	8.80	0.00	8.80	0.00	8.30	0.00	7.80	0.00	7.80	0.00	7.80	0.00
BL0011	8.50	0.00	8.50	0.00	8.50	0.00	8.50	0.00	8.50	0.00	8.00	0.00
BL0012	6.50	0.00	6.00	0.00	6.00	0.00	6.00	0.00	6.00	0.00	6.00	3.00
BL0013	5.00	0.00	5.00	0.00	5.00	0.00	5.00	0.00	5.00	0.00	5.00	0.00
BL0017	0.00	0.00	0.00	0.00	0.00	0.00	0.00	0.00	0.00	0.00	0.00	0.00
BL0021	5.00	0.00	4.50	0.00	4.50	0.00	4.50	0.40	4.00	0.40	2.40	0.00
BL0025	6.00	0.00	6.00	0.00	6.00	0.00	6.00	0.00	6.00	0.50	6.00	1.50
BX1455	14.00	1.00	11.00	0.00	10.50	0.00	10.50	0.00	10.50	0.00	10.50	0.00
BX1839	2.50	0.50	0.00	0.00	0.00	0.00	0.00	0.00	0.00	0.00	0.00	0.00
BX1840	3.80	0.00	3.80	0.00	3.30	0.50	0.00	0.00	0.00	0.00	0.00	0.00
BX1841	13.50	0.00	12.00	0.50	12.00	2.50	11.00	3.50	11.00	6.00	7.50	2.50
BX1842	11.50	2.00	7.50	0.00	6.50	0.00	6.50	0.00	6.50	0.00	6.00	0.00
BX1843	11.90	0.50	11.40	0.50	11.40	1.00	8.20	1.00	8.20	1.00	7.20	1.50
BX1844	8.50	0.00	7.50	0.00	7.50	0.70	6.90	1.90	0.00	0.00	0.00	0.00
BX1845	9.60	1.00	6.60	0.00	5.60	0.00	5.60	0.00	5.60	0.00	5.10	0.00
BX1846	12.20	2.50	8.70	0.00	8.70	0.00	8.20	1.00	8.20	2.00	7.70	2.00
BX2007	20.70	7.00	10.70	0.00	9.70	0.00	9.70	0.00	9.10	0.00	9.10	0.60
BX2008	5.50	0.00	4.50	0.00	4.00	0.00	2.00	0.00	2.00	0.00	1.00	0.00
BX2221	12.90	0.00	12.00	0.00	12.00	0.50	11.00	1.50	10.00	2.00	10.00	3.00
BX2255	9.50	0.00	9.00	0.00	9.00	0.00	9.00	0.00	9.00	0.00	9.00	0.50
BX2269	9.00	0.00	9.00	0.00	9.00	0.00	9.00	0.00	9.00	0.70	9.00	1.50
BX2346	9.00	0.00	7.00	0.00	7.00	0.00	7.00	1.00	6.00	0.00	6.00	0.00
BX2384	16.00	1.50	15.00	4.00	8.50	0.00	8.50	0.00	7.00	0.00	7.00	0.00
BX2385	19.50	2.50	19.50	5.00	12.00	0.50	10.50	0.00	10.00	0.00	10.00	0.00
BX2430	2.00	0.00	2.00	0.00	2.00	0.00	2.00	0.00	2.00	0.00	2.00	0.00
BX2434	7.50	0.00	7.50	3.00	2.50	1.00	0.00	0.00	0.00	0.00	0.00	0.00
BX2435	13.70	0.00	4.50	0.00	4.50	0.00	4.50	0.00	4.00	0.50	4.00	0.50
BX2436	8.50	1.50	4.50	0.00	4.00	0.00	4.00	0.00	3.50	0.00	3.50	0.00
BX2469	3.50	0.00	2.50	0.50	0.50	0.00	0.00	0.00	0.00	0.00	0.00	0.00
MEAN WIDTH	8.51	0.60	6.87	0.44	5.99	0.28	5.35	0.32	4.91	0.35	4.57	0.44
DILUTION	7.1		6.4		4.7		5.9		7.2		9.6	

Total orebody

		0.25%		0.50%		0.75%		1.00%		1.25%		1.50%
	ore	int. dil	ore	int. dil	ore	int. dil	ore	int. dil	ore	int. dil	ore	int. dil
AP2CT	12.50	0.00	12.50	0.00	12.50	0.00	12.00	1.00	11.50	1.00	11.00	3.00
AP4CT	11.50	0.00	11.50	0.00	11.00	0.00	10.50	0.50	10.50	0.50	10.50	0.50
AP6CT	12.50	0.00	11.50	0.00	11.50	0.00	11.50	0.00	11.50	0.50	11.50	0.50
B287	18.10	0.00	15.10	0.00	13.60	0.00	13.60	0.00	13.00	0.00	13.00	0.00
B298	12.00	0.00	11.00	0.00	7.10	0.00	6.60	0.00	6.10	0.00	5.10	0.00
B300	20.40	0.00	19.80	1.20	17.40	1.40	17.40	1.90	17.40	1.90	16.80	2.40
B87	11.90	0.00	11.00	0.00	10.10	0.00	9.50	1.80	7.00	0.00	6.40	0.80
BL0001B	15.70	0.00	15.20	2.50	15.20	4.00	9.30	0.00	8.00	0.00	7.30	0.00
BL0003	18.00	0.50	16.00	0.00	15.50	0.00	14.00	0.00	14.00	0.00	13.50	0.00
BL0004	14.60	3.60	9.50	0.50	9.50	0.50	9.50	0.50	9.50	0.50	8.00	0.00
BL0008	9.20	0.00	5.90	0.00	5.90	0.00	5.90	0.00	5.40	0.00	5.40	0.00
BL0010	17.10	0.00	17.10	0.00	16.60	0.00	16.10	0.00	16.10	0.60	16.10	0.60
BL0011	15.30	0.00	15.30	0.00	15.30	0.50	15.30	0.50	15.30	0.50	14.80	1.90
BL0012	15.10	0.00	14.60	0.00	14.60	0.00	14.60	0.60	14.60	0.90	14.60	6.40
BL0013	10.80	0.00	10.80	0.00	10.80	0.50	10.80	0.50	10.80	0.50	10.80	0.50
BL0017	23.00	0.00	22.50	0.00	22.00	0.00	22.00	0.00	21.50	0.00	21.50	0.00
BL0021	10.10	0.00	9.60	0.00	9.60	0.00	9.60	0.40	9.10	0.40	7.50	0.00
BL0025	14.40	0.00	14.40	0.00	14.40	0.00	14.40	0.00	14.40	0.50	14.40	1.50
BX1455	20.90	1.00	17.90	0.00	17.40	0.00	17.40	0.00	17.40	1.00	17.40	1.00
BX1839	13.60	0.50	9.60	0.00	9.10	0.00	9.10	0.00	9.10	0.00	9.10	0.40
BX1840	10.80	0.00	10.80	0.00	10.30	1.50	5.50	0.00	5.50	0.00	4.50	0.00
BX1841	28.30	0.50	26.80	1.00	26.80	3.00	25.80	4.50	25.80	7.00	22.30	4.50
BX1842	21.90	2.00	17.90	0.00	16.90	0.00	16.90	0.00	16.90	0.00	16.40	0.40
BX1843	23.20	1.00	22.70	1.00	22.70	1.50	19.50	1.50	19.50	1.50	18.50	4.00
BX1844	18.00	0.00	17.00	0.00	17.00	0.70	16.40	1.90	5.50	0.00	4.50	0.00
BX1845	19.10	1.00	16.10	0.00	15.10	0.00	15.10	0.00	15.10	0.00	14.60	1.00
BX1846	27.90	2.50	24.40	0.00	24.40	0.00	23.90	1.00	23.90	2.50	23.40	6.00
BX2007	27.60	7.00	17.60	0.00	16.60	0.00	16.60	1.00	16.00	2.00	16.00	4.00
BX2008	23.40	0.00	22.40	0.00	21.90	0.00	19.90	0.00	19.90	0.00	18.90	0.00
BX2221	19.10	0.00	18.20	0.00	18.20	0.70	17.20	1.70	16.20	2.20	16.20	4.70
BX2255	17.70	0.00	17.20	0.00	17.20	1.00	17.20	2.30	17.20	3.10	17.20	3.60
BX2269	13.60	0.00	13.60	0.00	13.60	0.00	13.60	0.00	13.60	0.70	13.60	1.50
BX2346	17.90	0.00	15.90	0.00	15.90	0.00	15.90	1.00	14.90	0.00	14.90	0.40
BX2384	22.60	1.50	21.60	4.00	15.10	0.00	15.10	0.00	13.60	1.70	13.60	1.70
BX2385	25.70	2.50	25.70	5.00	18.20	0.50	16.70	1.00	16.20	1.00	16.20	2.00
BX2430	9.40	0.00	9.40	0.00	9.40	0.00	9.40	0.50	9.40	1.00	9.40	1.00
BX2434	16.00	0.00	16.00	3.00	11.00	1.00	8.50	0.00	7.50	0.00	7.50	0.00
BX2435	21.90	0.00	12.70	0.00	12.70	0.00	12.70	0.00	12.20	0.50	12.20	1.00
BX2436	13.60	1.50	9.60	0.00	9.10	0.00	9.10	0.00	8.60	0.60	8.60	1.10
BX2469	13.50	0.00	12.50	0.50	10.50	0.00	10.00	0.00	10.00	0.00	10.00	0.00
MEAN	17.20	0.63	15.47	0.47	14.54	0.42	13.85	0.60	13.24	0.82	12.83	1.41
DILUTION	3.6		3.0		2.9		4.3		6.2		11.0	

(b) HANGINGWALL DILUTION

0.5m hangingwall waste

Diluted copper and cobalt grades at different cutoff grades

Drill Hole	0.25% Cu	0.25% Co	0.50% Cu	0.50% Co	0.75% Cu	0.75% Co	1.00% Cu	1.00% Co	1.25% Cu	1.25% Co	1.50% Cu	1.50% Co
AP2CT	2.21	0.18	2.21	0.18	2.21	0.18	2.29	0.19	2.30	0.19	2.38	0.18
AP4CT	2.61	0.15	2.61	0.15	2.61	0.15	2.68	0.16	2.79	0.16	2.79	0.16
AP6CT	3.38	0.37	3.61	0.39	3.61	0.39	3.61	0.39	3.61	0.39	3.61	0.39
B287	2.32	0.23	2.58	0.25	2.90	0.27	2.74	0.26	3.09	0.29	3.09	0.29
B298	1.75	0.17	1.94	0.18	2.51	0.23	2.63	0.23	2.75	0.24	3.07	0.28
B300	1.99	0.09	2.06	0.09	2.40	0.08	2.34	0.08	2.34	0.08	2.40	0.08
B87	1.59	0.06	1.73	0.07	1.77	0.07	1.91	0.08	2.14	0.08	2.22	0.08
BL0001B	1.70	0.14	1.84	0.15	1.84	0.15	2.35	0.18	2.86	0.23	2.78	0.21
BL0003	1.95	0.19	2.13	0.21	2.20	0.21	2.32	0.22	2.32	0.22	2.42	0.28
BL0004	1.70	0.18	2.33	0.22	2.33	0.22	2.33	0.22	2.33	0.22	2.62	0.24
BL0008	2.20	0.13	2.91	0.15	2.91	0.15	2.91	0.15	3.13	0.16	3.13	0.16
BL0010	2.65	0.13	2.65	0.13	2.65	0.13	2.70	0.13	2.70	0.13	2.70	0.13
BL0011	2.21	0.24	2.21	0.24	2.21	0.24	2.21	0.24	2.21	0.24	2.21	0.24
BL0012	1.82	0.13	1.82	0.13	1.82	0.13	1.82	0.13	1.82	0.13	1.82	0.13
BL0013	2.51	0.18	2.51	0.18	2.51	0.18	2.51	0.18	2.51	0.18	2.51	0.18
BL0017	2.82	0.33	2.88	0.34	2.93	0.35	2.93	0.35	2.98	0.35	2.98	0.35
BL0021	2.50	0.21	2.61	0.22	2.61	0.22	2.61	0.22	2.73	0.23	3.08	0.25
BL0025	2.69	0.43	2.69	0.43	2.69	0.43	2.69	0.43	2.69	0.43	2.69	0.43
BX1455	2.94	0.23	3.30	0.24	3.38	0.25	3.38	0.25	3.38	0.25	3.38	0.25
BX1839	3.04	0.18	4.19	0.25	4.37	0.26	4.37	0.26	4.37	0.26	4.37	0.26
BX1842	2.55	0.29	2.90	0.30	3.07	0.31	3.07	0.31	3.07	0.31	3.14	0.31
BX1843	2.33	0.12	2.38	0.12	2.38	0.12	2.38	0.12	2.66	0.13	2.72	0.13
BX1844	1.46	0.13	1.53	0.13	1.53	0.13	1.57	0.13	2.48	0.15	2.75	0.15
BX1845	2.58	0.18	3.01	0.19	3.18	0.19	3.18	0.19	3.18	0.19	3.25	0.20
BX1846	2.32	0.21	2.62	0.23	2.62	0.23	2.67	0.23	2.67	0.23	2.72	0.23
BX1865	2.27	0.61	2.64	0.70	2.64	0.70	2.64	0.70	2.69	0.71	2.69	0.71
BX1866	2.04	0.45	2.28	0.50	2.37	0.52	2.37	0.52	2.44	0.54	2.44	0.54
BX2007	1.82	0.25	1.82	0.25	1.92	0.26	1.92	0.26	1.93	0.27	1.93	0.27
BX2008	2.37	0.28	2.46	0.29	2.51	0.30	2.65	0.30	2.65	0.30	2.73	0.31
BX2221	1.90	0.22	1.97	0.23	1.97	0.23	2.06	0.23	2.12	0.23	2.12	0.23
BX2255	2.01	0.20	2.01	0.20	2.01	0.20	2.01	0.20	2.01	0.20	2.01	0.20
BX2269	2.50	0.24	2.50	0.24	2.50	0.24	2.50	0.24	2.50	0.24	2.50	0.24
BX2346	2.55	0.36	2.83	0.39	2.83	0.39	2.83	0.39	2.99	0.41	2.99	0.41
BX2384	1.55	0.27	1.61	0.28	2.23	0.40	2.23	0.40	2.35	0.43	2.35	0.43
BX2385	1.73	0.16	1.73	0.16	2.31	0.21	2.43	0.22	2.50	0.23	2.50	0.23
BX2430	2.82	0.13	2.82	0.13	2.82	0.13	2.82	0.13	2.82	0.13	2.82	0.13
BX2434	1.72	0.15	1.72	0.15	2.19	0.16	2.57	0.17	2.81	0.18	2.81	0.18
BX2435	2.08	0.10	2.08	0.10	2.08	0.10	2.08	0.10	2.08	0.10	2.14	0.10
BX2436	1.58	0.12	2.10	0.14	2.21	0.14	2.21	0.14	2.32	0.14	2.32	0.14
BX2469	2.05	0.15	2.19	0.16	2.49	0.17	2.59	0.17	2.59	0.17	2.59	0.17
Mean diluted grades	2.22	0.21	2.40	0.23	2.51	0.24	2.55	0.24	2.65	0.24	2.69	0.25
Undiluted grades	2.27	0.22	2.47	0.23	2.58	0.24	2.63	0.24	2.72	0.25	2.77	0.25
% Dilution	2.2	2.1	2.7	1.8	2.7	1.9	3.1	2.1	2.6	1.5	2.6	2.8

1.0m hangingwall waste

Diluted copper and cobalt grades at different cutoff grades

Drill Hole	0.25% Cu	0.25% Co	0.50% Cu	0.50% Co	0.75% Cu	0.75% Co	1.00% Cu	1.00% Co	1.25% Cu	1.25% Co	1.50% Cu	1.50% Co
AP2CT	2.21	0.18	2.21	0.18	2.21	0.18	2.21	0.18	2.29	0.19	2.30	0.19
AP4CT	2.61	0.15	2.61	0.15	2.61	0.15	2.68	0.16	2.68	0.16	2.68	0.16
AP6CT	3.38	0.37	3.50	0.38	3.50	0.38	3.50	0.38	3.50	0.38	3.50	0.38
B287	2.32	0.23	2.58	0.25	2.90	0.27	2.90	0.27	2.90	0.27	2.90	0.27
B298	1.75	0.17	1.87	0.18	2.38	0.21	2.51	0.23	2.63	0.23	2.94	0.26
B300	1.91	0.09	2.06	0.09	2.26	0.08	2.26	0.08	2.31	0.08	2.34	0.08
B87	1.59	0.06	1.59	0.06	1.73	0.07	1.91	0.08	2.06	0.08	2.14	0.08
BL0001B	1.70	0.14	1.70	0.14	1.70	0.14	2.35	0.18	2.86	0.23	2.54	0.19
BL0003	1.95	0.19	2.08	0.20	2.13	0.21	2.29	0.22	2.29	0.22	2.32	0.22
BL0004	1.65	0.17	2.14	0.21	2.14	0.21	2.14	0.21	2.14	0.21	2.48	0.23
BL0008	2.20	0.13	2.72	0.14	2.72	0.14	2.72	0.14	2.91	0.15	2.91	0.15
BL0010	2.65	0.13	2.65	0.13	2.65	0.13	2.65	0.13	2.65	0.13	2.65	0.13
BL0011	2.21	0.24	2.21	0.24	2.21	0.24	2.21	0.24	2.21	0.24	2.21	0.24
BL0012	1.82	0.13	1.82	0.13	1.82	0.13	1.82	0.13	1.82	0.13	1.82	0.13
BL0013	2.51	0.18	2.51	0.18	2.51	0.18	2.51	0.18	2.51	0.18	2.51	0.18
BL0017	2.76	0.33	2.82	0.33	2.88	0.34	2.88	0.34	2.93	0.35	2.93	0.35
BL0021	2.40	0.21	2.50	0.21	2.50	0.21	2.50	0.21	2.61	0.22	2.98	0.24
BL0025	2.69	0.43	2.69	0.43	2.69	0.43	2.69	0.43	2.69	0.43	2.69	0.43
BX1455	2.94	0.23	3.22	0.24	3.30	0.24	3.30	0.24	3.30	0.24	3.30	0.24
BX1839	3.04	0.18	3.99	0.24	4.19	0.25	4.19	0.25	4.19	0.25	4.19	0.25
BX1842	2.55	0.29	2.90	0.30	2.90	0.30	2.90	0.30	2.90	0.30	3.07	0.31
BX1843	2.28	0.12	2.33	0.12	2.33	0.12	2.33	0.12	2.59	0.13	2.68	0.13
BX1844	1.43	0.13	1.49	0.13	1.49	0.13	1.57	0.13	2.48	0.15	2.75	0.15
BX1845	2.53	0.17	2.93	0.19	3.10	0.19	3.10	0.19	3.10	0.19	3.18	0.19
BX1846	2.32	0.21	2.57	0.23	2.57	0.23	2.62	0.23	2.62	0.23	2.67	0.23
BX1865	2.27	0.61	2.61	0.69	2.61	0.69	2.61	0.69	2.64	0.70	2.64	0.70
BX1866	2.04	0.45	2.28	0.50	2.35	0.52	2.35	0.52	2.42	0.54	2.41	0.53
BX2007	1.77	0.25	1.77	0.25	1.87	0.26	1.87	0.26	1.92	0.26	1.92	0.26
BX2008	2.32	0.28	2.42	0.29	2.46	0.29	2.65	0.30	2.65	0.30	2.73	0.31
BX2221	1.90	0.22	1.93	0.23	1.90	0.22	2.01	0.23	2.07	0.23	2.07	0.23
BX2255	2.01	0.20	2.01	0.20	2.01	0.20	2.01	0.20	2.01	0.20	2.01	0.20
BX2269	2.50	0.24	2.50	0.24	2.50	0.24	2.50	0.24	2.50	0.24	2.50	0.24
BX2346	2.49	0.35	2.76	0.38	2.76	0.38	2.76	0.38	2.99	0.41	2.99	0.41
BX2384	1.55	0.27	1.61	0.28	2.17	0.39	2.17	0.39	2.28	0.41	2.28	0.41
BX2385	1.73	0.16	1.73	0.16	2.25	0.20	2.38	0.22	2.43	0.22	2.43	0.22
BX2430	2.82	0.13	2.82	0.13	2.82	0.13	2.82	0.13	2.82	0.13	2.82	0.13
BX2434	1.72	0.15	1.72	0.15	2.11	0.15	2.44	0.17	2.67	0.18	2.67	0.18
BX2435	2.01	0.10	2.01	0.10	2.01	0.10	2.01	0.10	2.01	0.10	2.08	0.10
BX2436	1.52	0.12	2.00	0.14	2.10	0.14	2.10	0.14	2.21	0.14	2.21	0.14
BX2469	1.98	0.18	2.12	0.15	2.40	0.16	2.49	0.17	2.49	0.17	2.49	0.17
Mean diluted grades	2.20	0.21	2.35	0.22	2.44	0.23	2.50	0.23	2.58	0.24	2.62	0.24
Undiluted grades	2.27	0.22	2.47	0.23	2.58	0.24	2.63	0.24	2.72	0.25	2.77	0.25
% Dilution	3.1	2.1	4.8	3.1	5.2	3.9	5.2	3.3	5.0	3.0	5.2	5.2

2.0m hangingwall waste

Diluted copper and cobalt grades at different cutoff grades

Drill Hole	0.25% Cu	0.25% Co	0.50% Cu	0.50% Co	0.75% Cu	0.75% Co	1.00% Cu	1.00% Co	1.25% Cu	1.25% Co	1.50% Cu	1.50% Co
AP2CT	2.21	0.18	2.21	0.18	2.21	0.18	2.21	0.18	2.21	0.18	2.21	0.18
AP4CT	2.61	0.15	2.61	0.15	2.61	0.15	2.61	0.15	2.61	0.15	2.61	0.15
AP6CT	3.38	0.37	3.38	0.37	3.38	0.37	3.38	0.37	3.38	0.37	3.38	0.37
B287	2.32	0.23	2.45	0.24	2.58	0.25	2.74	0.26	2.74	0.26	2.74	0.26
B298	1.64	0.17	1.75	0.17	2.29	0.21	2.38	0.21	2.43	0.22	2.63	0.23
B300	1.91	0.09	1.99	0.09	2.18	0.08	2.18	0.08	2.55	0.08	2.22	0.08
B87	1.44	0.06	1.77	0.07	1.59	0.06	1.73	0.07	1.91	0.08	2.01	0.08
BL0001B	1.58	0.14	1.70	0.14	1.70	0.14	2.12	0.17	2.35	0.18	2.54	0.19
BL0003	1.95	0.19	1.99	0.20	2.02	0.20	2.20	0.21	2.20	0.21	2.25	0.21
BL0004	1.60	0.17	2.06	0.21	2.43	0.23	2.06	0.21	2.06	0.21	2.43	0.23
BL0008	2.20	0.13	2.38	0.13	2.38	0.13	2.38	0.13	2.49	0.14	2.49	0.14
BL0010	2.65	0.13	2.65	0.13	2.65	0.13	2.65	0.13	2.65	0.13	2.65	0.13
BL0011	2.21	0.24	2.21	0.24	2.21	0.24	2.21	0.24	2.21	0.24	2.21	0.25
BL0012	1.82	0.13	1.82	0.13	1.82	0.13	1.82	0.13	1.82	0.13	1.82	0.13
BL0013	2.51	0.18	2.51	0.18	2.51	0.18	2.51	0.18	2.51	0.18	2.51	0.18
BL0017	2.66	0.32	2.66	0.32	2.76	0.33	2.76	0.33	2.82	0.33	2.82	0.33
BL0021	2.30	0.20	2.30	0.20	2.30	0.20	2.30	0.20	2.40	0.21	2.73	0.23
BL0025	2.69	0.43	2.69	0.43	2.69	0.43	2.69	0.43	2.69	0.43	2.69	0.43
BX1455	2.94	0.23	3.08	0.23	3.14	0.24	3.14	0.24	3.14	0.24	3.14	0.24
BX1839	2.85	0.17	3.65	0.22	3.81	0.23	3.81	0.23	3.81	0.23	3.81	0.23
BX1842	2.55	0.29	2.76	0.30	2.83	0.30	2.83	0.30	2.83	0.30	2.90	0.30
BX1843	2.24	0.12	2.28	0.12	2.24	0.12	2.24	0.12	2.48	0.12	2.59	0.13
BX1844	1.39	0.13	1.43	0.13	1.43	0.13	1.49	0.13	2.27	0.15	2.48	0.15
BX1845	2.47	0.17	2.77	0.18	2.93	0.19	2.93	0.19	2.93	0.19	3.25	0.20
BX1846	2.24	0.21	2.48	0.22	2.48	0.22	2.52	0.22	2.52	0.22	2.57	0.23
BX1865	2.27	0.61	2.55	0.68	2.55	0.68	2.55	0.68	2.57	0.68	2.57	0.68
BX1866	2.01	0.45	2.25	0.50	2.31	0.51	2.31	0.51	2.40	0.53	2.40	0.53
BX2007	1.73	0.25	1.68	0.24	1.77	0.25	1.77	0.25	1.82	0.25	1.82	0.25
BX2008	2.28	0.28	2.32	0.28	2.37	0.28	2.55	0.30	2.55	0.30	2.65	0.30
BX2221	1.90	0.22	1.90	0.22	1.90	0.22	1.90	0.22	2.01	0.23	2.01	0.23
BX2255	2.01	0.20	2.01	0.20	2.01	0.20	2.01	0.20	2.01	0.20	2.01	0.20
BX2269	2.50	0.24	2.50	0.24	2.50	0.24	2.50	0.24	2.50	0.24	2.50	0.24
BX2346	2.43	0.34	2.62	0.37	2.62	0.37	2.62	0.37	2.83	0.39	2.83	0.39
BX2384	1.55	0.27	1.55	0.27	2.04	0.37	2.04	0.37	2.17	0.39	2.17	0.39
BX2385	1.73	0.16	1.73	0.16	2.17	0.20	2.31	0.21	2.36	0.22	2.47	0.27
BX2430	2.82	0.13	2.82	0.13	2.82	0.13	2.82	0.13	2.82	0.13	2.82	0.13
BX2434	1.72	0.15	1.72	0.15	1.92	0.15	2.32	0.16	2.44	0.17	2.44	0.17
BX2435	1.96	0.10	1.91	0.10	1.91	0.10	1.91	0.10	1.91	0.10	1.96	0.10
BX2436	1.48	0.13	1.84	0.14	1.91	0.14	1.91	0.14	2.00	0.14	2.00	0.14
BX2469	1.85	0.17	1.98	0.18	2.25	0.16	2.33	0.16	2.33	0.16	2.33	0.16
Mean diluted grades	2.16	0.21	2.27	0.22	2.36	0.23	2.39	0.23	2.47	0.23	2.52	0.24
Undiluted grades	2.27	0.22	2.47	0.23	2.58	0.24	2.63	0.24	2.72	0.25	2.77	0.25
% Dilution	4.7	2.5	7.8	4.5	8.6	5.5	9.1	5.7	9.2	6.0	9.0	7.0

APPENDIX I

DENSITY DATA

BALUBA CENTRE LIMB: DENSITY RESULTS

Drillhole No	Depth (metres)			Lithology	%T.Cu	Density
	From	To	Length			
BX1840	27.20	28.00	0.8	Conglomerate	0.03	2.53
	28.00	28.50	0.5	Conglomerate	0.04	2.51
	28.50	29.00	0.5	Conglomerate	0.02	2.50
	29.00	29.50	0.5	Conglomerate	0.46	2.57
	29.50	30.00	0.5	Tremolite Schist	4.20	2.90
	30.00	30.50	0.5	Tremolite Schist	4.43	2.99
	30.50	31.50	1.0	Tremolite Schist	3.59	3.04
	31.50	32.50	1.0	Tremolite Schist	2.35	2.90
	32.50	33.50	1.0	Tremolite Schist	2.33	2.92
	33.50	34.50	1.0	Tremolite Schist	0.88	2.99
	34.50	35.50	1.0	Tremolite Schist	0.77	3.03
	35.50	36.50	1.0	Tremolite Schist	0.41	2.61
	36.50	37.00	0.5	Argillite	0.73	2.75
	37.00	37.50	0.5	Argillite	1.83	2.74
	37.50	38.00	0.5	Argillite	0.40	2.69
	38.00	38.50	0.5	Argillite	1.00	2.66
	38.50	38.90	0.4	Argillite	1.07	2.68
	38.90	39.30	0.4	Argillite	0.99	2.64
	39.30	39.80	0.5	Argillite	0.57	2.74
	39.80	40.30	0.5	Argillite	0.06	2.70
	40.30	40.80	0.5	Argillite	0.08	2.66
	40.80	41.30	0.5	Argillite	0.06	2.66
	41.30	41.80	0.5	Argillite	0.06	2.79
	41.80	42.30	0.5	Argillite	0.06	2.83
BX1979	94.40	95.40	1.0	Conglomerate	0.03	2.60
	95.40	96.40	1.0	Conglomerate	0.02	2.60
	96.40	97.00	0.6	Conglomerate	0.03	2.58
	97.00	97.50	0.5	Transitional Schist	1.61	2.58
	97.50	97.90	0.4	Transitional Schist	2.24	2.87
	97.90	98.90	1.0	Tremolite Schist	4.38	2.87
	98.90	99.50	0.6	Tremolite Schist	2.17	2.70
	99.50	100.00	0.5	Tremolite Schist	0.70	3.10
	100.00	100.50	0.5	Argillite	0.76	2.45
	100.50	101.00	0.5	Argillite	0.68	2.67
	101.00	101.50	0.5	Argillite	0.12	2.66
	101.50	102.00	0.5	Argillite	0.16	2.95
	102.00	102.50	0.5	Argillite	0.09	2.30
	102.50	103.00	0.5	Argillite	0.34	2.60
	103.00	103.60	0.6	Argillite	0.14	3.16

APPENDIX I (contd)

Drillhole No	Depth (metres)			Lithology	%T.Cu	Density
	From	To	Length			
BX2077	9.50	10.50	1.0	Argillite	0.20	3.72
	10.50	11.50	1.0	Argillite	0.11	3.06
	11.50	12.50	1.0	Argillite	0.08	2.77
	12.50	13.50	1.0	Argillite	0.13	2.94
	13.50	14.50	1.0	Argillite	0.07	2.81
	14.50	15.50	1.0	Argillite	0.11	2.81
	15.50	16.50	1.0	Argillite	0.09	2.82
	16.50	17.50	1.0	Argillite	0.06	2.85
	17.50	18.50	1.0	Argillite	0.08	2.79
	18.50	19.50	1.0	Argillite	0.32	2.77
	19.50	20.50	1.0	Argillite	0.16	2.84
	20.50	21.50	1.0	Argillite	0.06	2.80
	21.50	22.50	1.0	Argillite	0.18	2.78
	22.50	23.00	0.5	Argillite	0.09	2.92
	23.00	23.50	0.5	Argillite	0.07	2.71
	23.50	24.00	0.5	Argillite	0.08	2.84
	24.00	24.50	0.5	Argillite	0.04	2.75
	24.50	25.00	0.5	Argillite	0.04	2.70
	25.00	25.50	0.5	Argillite	0.08	2.80
	25.50	26.00	0.5	Argillite	1.09	2.97
	26.00	26.50	0.5	Argillite	0.13	2.74
	26.50	27.00	0.5	Argillite	0.05	2.73
	27.00	27.50	0.5	Argillite	0.12	2.61
	27.50	28.00	0.5	Tremolite Schist	0.06	2.70
	28.00	28.50	0.5	Tremolite Schist	0.05	2.57
	28.50	29.50	1.0	Tremolite Schist	1.38	2.88
	29.50	30.50	1.0	Tremolite Schist	1.78	2.89
	30.50	31.50	1.0	Tremolite Schist	3.17	2.80
	31.50	32.50	1.0	Tremolite Schist	1.60	2.80
	32.50	33.00	0.5	Tremolite Schist	2.73	2.97
	33.00	33.50	0.5	Tremolite Schist	1.30	2.90
	33.50	33.90	0.4	Tremolite Schist	1.48	2.70
	33.90	34.20	0.3	Transitional Schist	2.10	2.75
	34.20	34.50	0.3	Transitional Schist	1.46	3.34
	34.50	35.00	0.5	Transitional Schist	3.35	3.15
	35.00	35.50	0.5	Transitional Schist	3.56	2.76
	35.50	36.00	0.5	Transitional Schist	1.88	2.66
	36.00	36.50	0.5	Transitional Schist	2.40	2.66
	36.50	37.00	0.5	Quartzite	0.06	2.70

APPENDIX I (contd)

Drillhole No	Depth (metres)			Lithology	%T.Cu	Density
	From	To	Length			
BX2078	71.60	72.60	1.0	Argillite	-	2.80
	72.60	73.10	0.5	Argillite	-	2.61
	73.10	73.60	0.5	Argillite	-	2.64
	73.60	74.60	1.0	Argillite	-	2.64
	74.60	75.60	0.0	Argillite	0.11	2.77
	75.60	76.10	0.0	Argillite	0.41	2.76
	76.10	76.60	0.0	Argillite	0.85	2.57
	76.60	77.10	0.5	Argillite	0.06	2.75
	77.10	77.60	0.5	Tremolite Schist	1.00	2.72
	77.60	77.90	0.3	Transitional Schist	3.70	2.92
	77.90	78.40	0.5	Quartzite	1.44	2.89
	78.40	78.90	0.5	Quartzite	1.75	2.88
	78.90	79.40	0.5	Quartzite	1.34	3.50
	79.40	80.40	1.0	Quartzite	1.02	2.60
	80.40	80.90	0.5	Quartzite	0.13	2.54
BX2083	9.10	9.60	0.5	Argillite	0.05	2.86
	9.60	10.10	0.5	Argillite	0.36	2.82
	10.10	10.60	0.5	Argillite	0.80	2.88
	10.60	11.10	0.5	Argillite	0.68	2.77
	11.10	11.60	0.5	Argillite	0.51	2.76
	11.60	12.00	0.4	Argillite	0.15	2.74
	12.00	12.40	0.4	Argillite	0.29	2.75
	12.40	12.90	0.5	Argillite	0.19	2.70
	12.90	13.40	0.5	Argillite	0.35	2.68
	13.40	14.40	1.0	Argillite	0.32	2.65
	14.40	15.40	1.0	Argillite	0.44	2.79
	15.40	16.40	1.0	Argillite	0.49	2.79
	16.40	17.40	1.0	Argillite	0.09	2.66
	17.40	18.40	1.0	Argillite	0.90	2.77
	18.40	19.40	1.0	Argillite	0.23	2.73
	19.40	20.40	1.0	Argillite	0.27	2.73
	20.40	21.40	1.0	Argillite	0.30	2.79
	21.40	22.40	1.0	Argillite	0.69	2.79
	22.40	22.90	0.5	Argillite	0.11	2.73
	22.90	23.90	1.0	Tremolite Schist	1.28	2.86
	23.90	24.60	0.7	Tremolite Schist	4.85	2.90
	24.60	25.20	0.6	Tremolite Schist	3.79	2.92
	25.20	26.20	1.0	Transitional Schist	2.58	2.83
	26.20	27.20	1.0	Transitional Schist	3.17	2.71
	27.20	27.70	0.5	Transitional Schist	0.25	2.45
	27.70	28.20	0.5	Transitional Schist	0.79	2.65
	28.20	28.80	0.6	Transitional Schist	3.36	2.64
	28.80	29.30	0.5	Conglomerate	0.18	2.54
	29.30	29.80	0.5	Conglomerate	0.03	2.57

APPENDIX I (contd)

Drillhole No	Depth (metres)			Lithology	%T.Cu	Density
	From	To	Length			
BX2105	34.20	35.20	1.0	Quartzite	0.04	2.59
	35.20	36.20	1.0	Conglomerate	0.07	2.50
	36.20	37.20	1.0	Conglomerate	0.03	2.54
	37.20	37.70	0.5	Conglomerate	0.02	2.58
	37.70	38.10	0.4	Conglomerate	0.94	2.68
	38.10	38.70	0.6	Transitional Schist	3.30	2.73
	38.70	39.20	0.5	Tremolite Schist	2.50	2.75
	39.20	40.20	1.0	Tremolite Schist	1.82	2.74
	40.20	41.20	1.0	Tremolite Schist	2.62	2.81
	41.20	42.20	1.0	Tremolite Schist	1.74	2.82
	42.20	43.10	0.9	Tremolite Schist	2.87	2.94
	43.10	43.60	0.5	Tremolite Schist	4.36	2.85
	43.60	44.10	0.5	Tremolite Schist	1.70	2.75
	44.10	44.60	0.5	Tremolite Schist	0.10	2.73
	44.60	45.10	0.5	Tremolite Schist	0.09	2.75
	45.10	45.60	0.5	Tremolite Schist	0.01	2.87
BX2106	37.30	38.30	1.0	Quartzite	0.02	2.52
	38.30	39.30	1.0	Conglomerate	0.02	2.51
	39.30	40.30	1.0	Conglomerate	0.03	2.55
	40.30	41.00	0.7	Conglomerate	1.13	2.62
	41.00	41.50	0.5	Transitional Schist	2.72	2.55
	41.50	42.00	0.5	Transitional Schist	2.95	2.59
	42.00	43.00	1.0	Tremolite Schist	1.83	2.60
	43.00	43.50	0.5	Tremolite Schist	1.88	2.77
	43.50	44.00	0.5	Tremolite Schist	0.89	2.72
	44.00	44.60	0.6	Tremolite Schist	0.17	2.66
	44.60	45.10	0.5	Argillite	0.33	2.58
	45.10	46.10	1.0	Argillite	0.20	2.64
	46.10	47.10	1.0	Argillite	0.19	2.68
	47.10	47.90	0.8	Argillite	0.10	2.66

APPENDIX J

MAPS

KEY TO MAPS 1 TO 7

Bedding (with angle of dip)

Jointing (with angle of dip)

Schist lineation (with angle of dip)

⊙ K5017 — Survey Peg

X + 10550m
Y - 9250m
} Local Mine Grid Coordinates

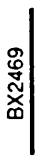

Drill hole

X/C — Crosscut

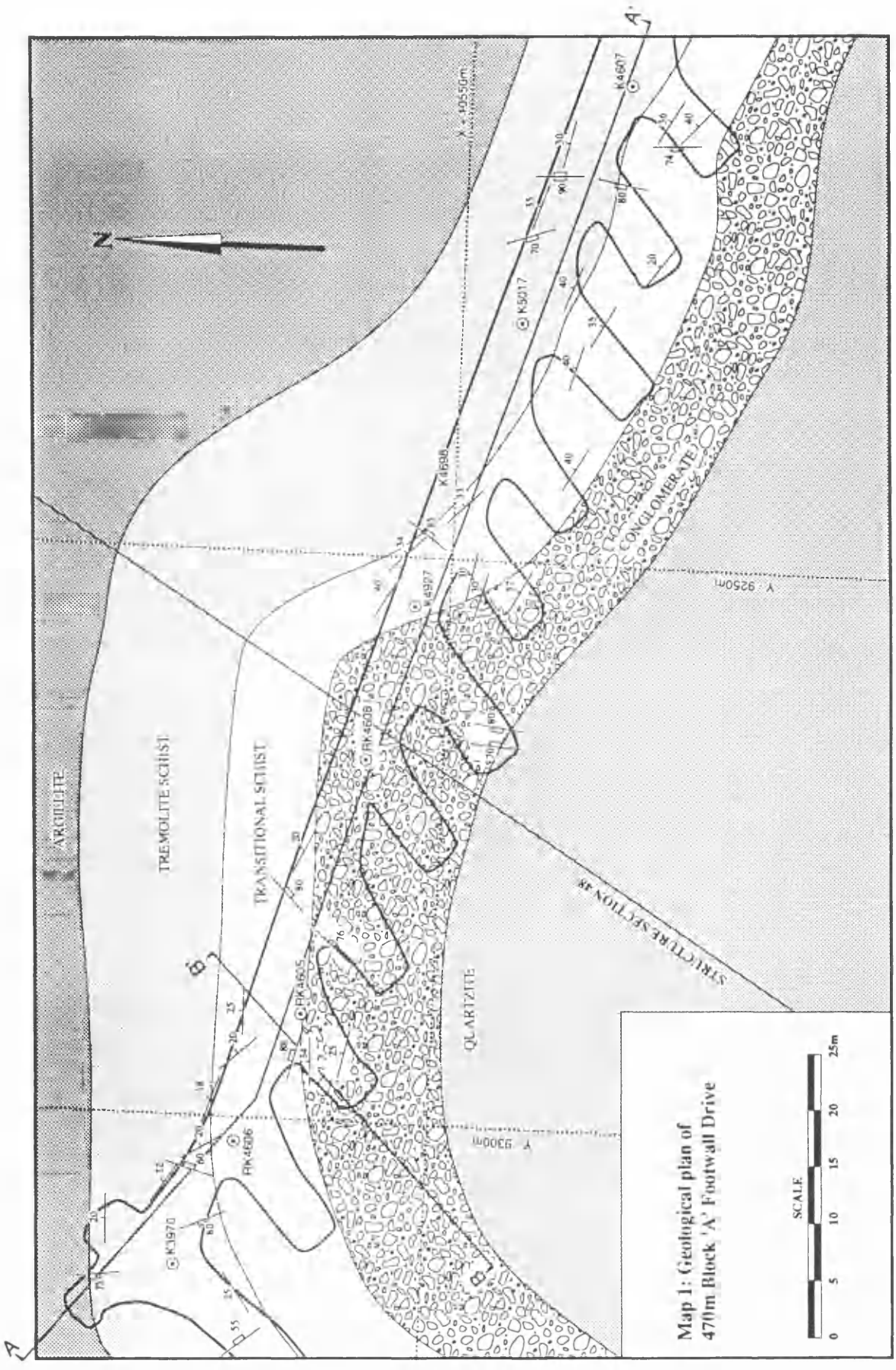
N
A
A'
B
B'
X = 4050m
Y 9250m
Y 9300m
K4607
K5017
K4698
K4927
K5070
RK4605
RK4606
RK4696
ARGILLITE
TREMOLITE SCHIST
TRANSITIONAL SCHIST
QUARTZITE
CONGLOMERATE
STRUCTURE SECTION 38
Map 1: Geological plan of
470m Block 'A' Footwall Drive
SCALE
0 5 10 15 20 25m

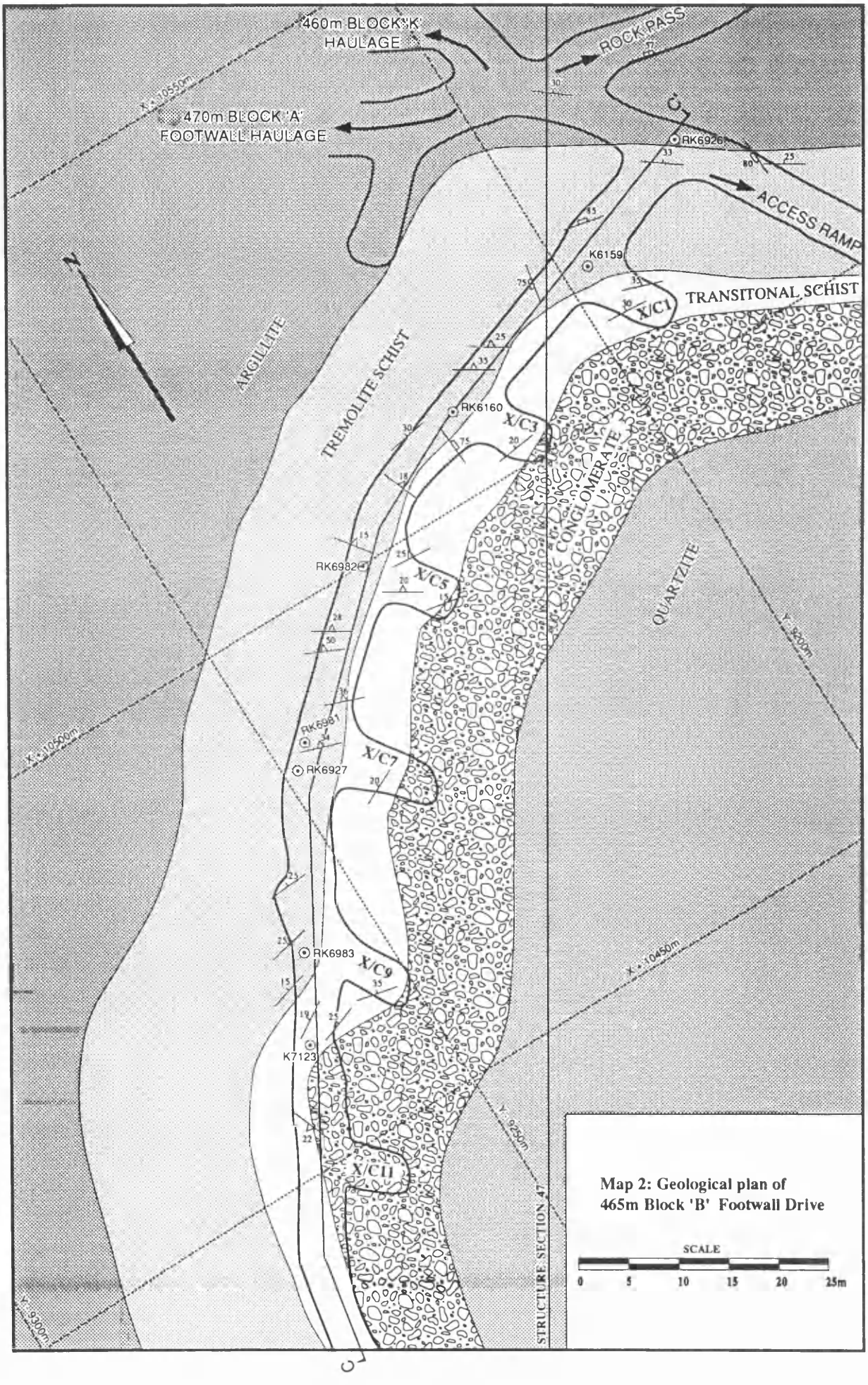

Map 2: Geological plan of 465m Block 'B' Footwall Drive

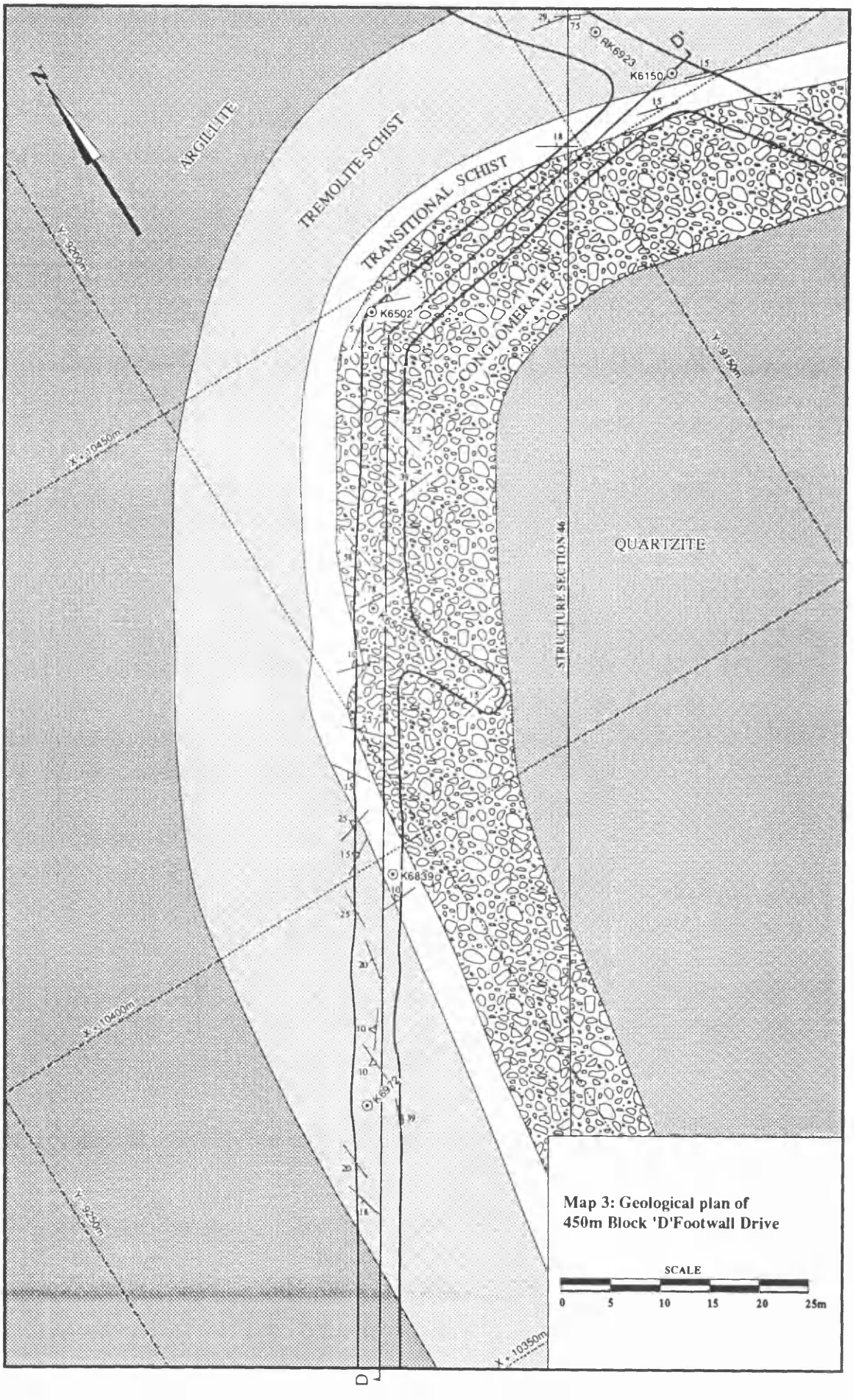

Map 3: Geological plan of 450m Block 'D'Footwall Drive

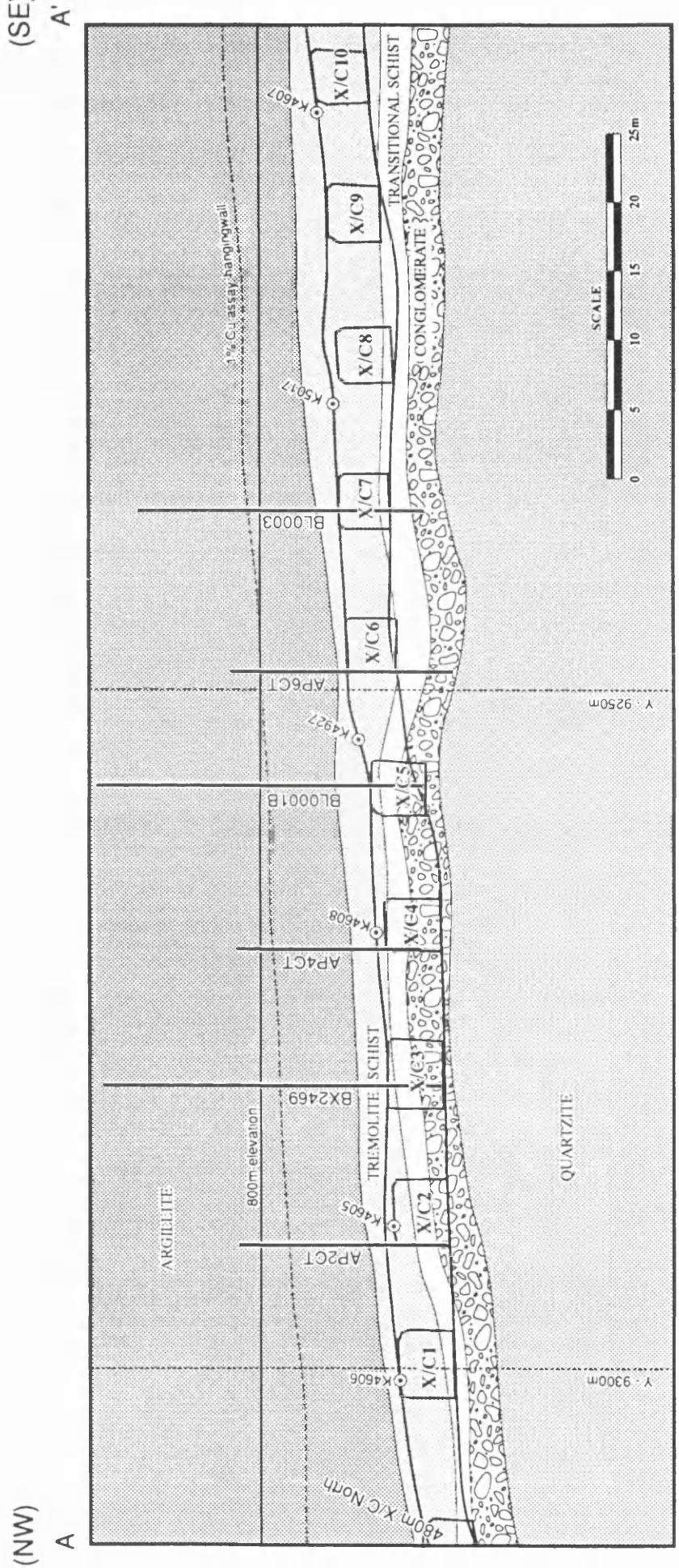

Map 4: Geological Section along 470m Block 'A' Footwall Drive

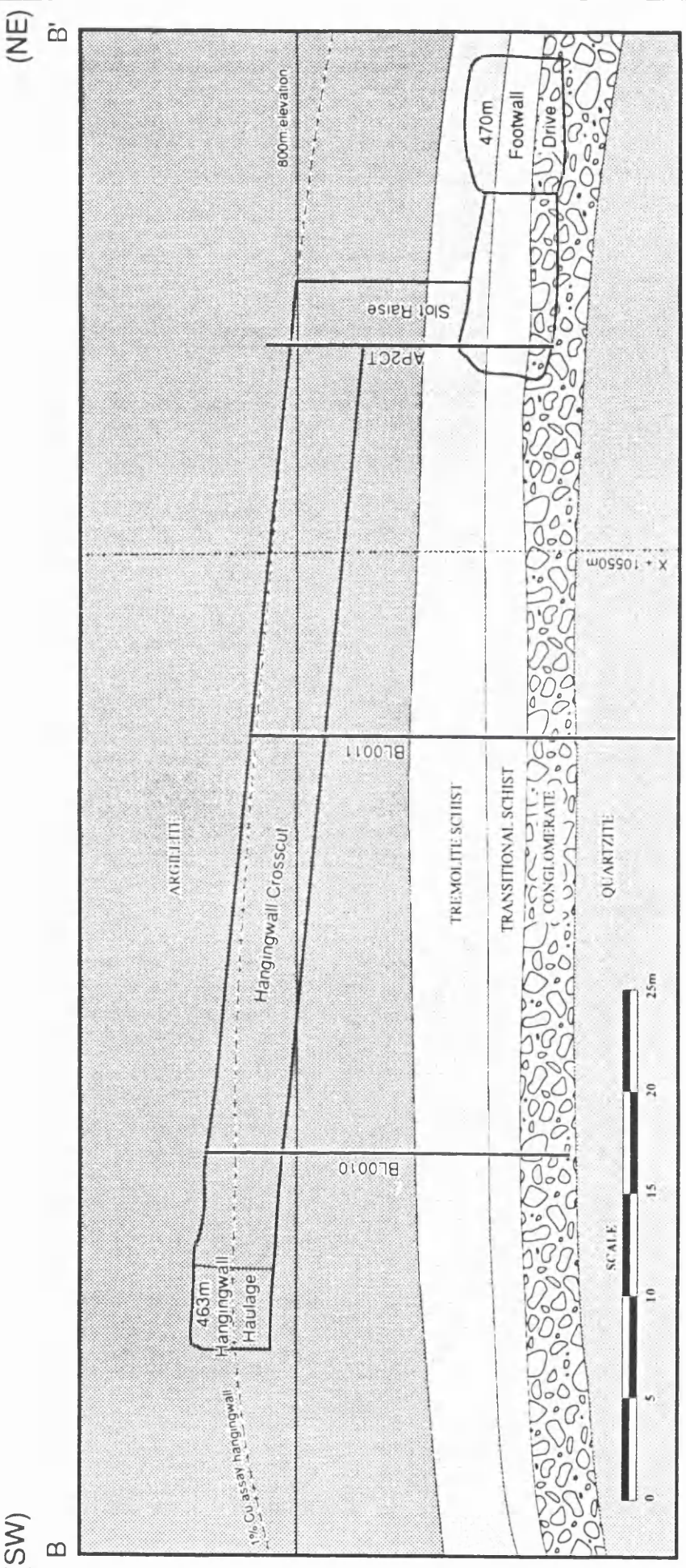

Map 5: Geological Section along crosscut 2; 470m Block 'A'

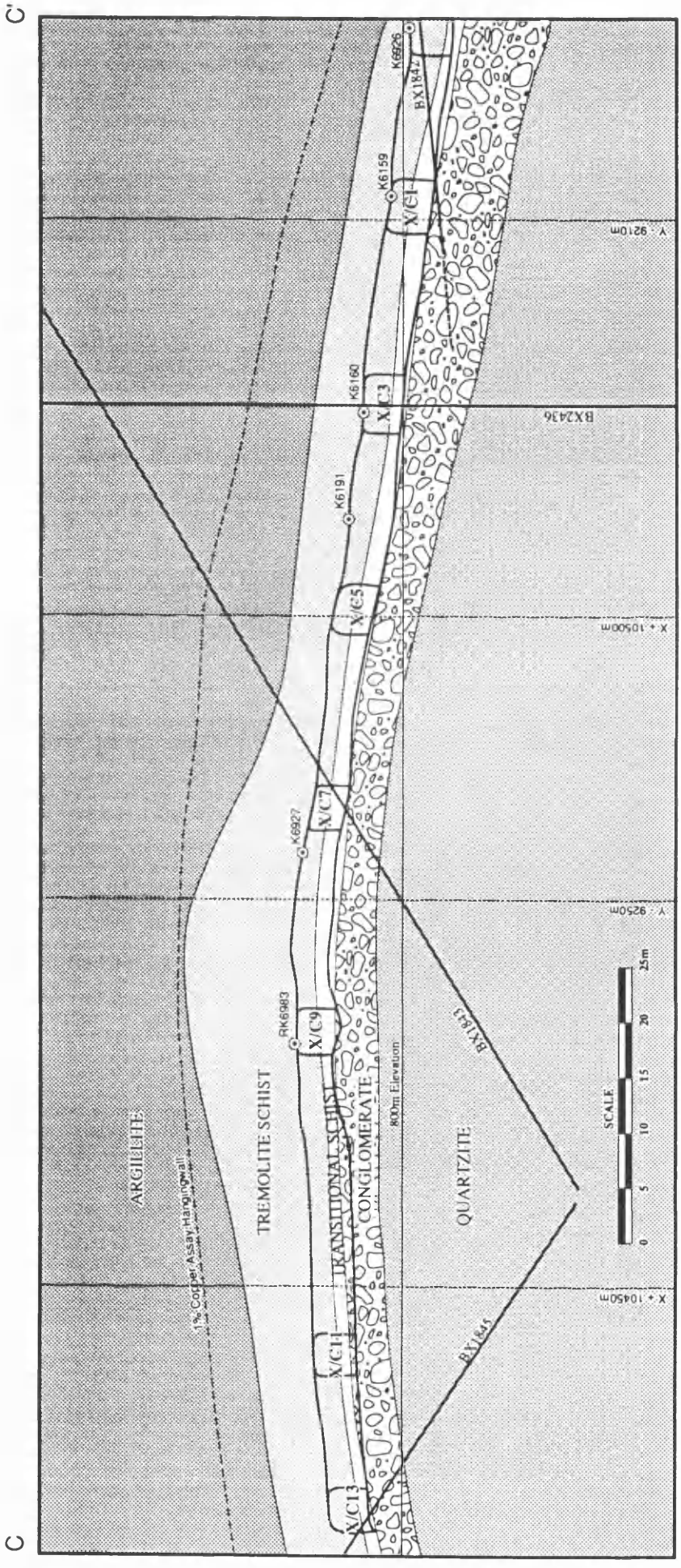

Map 6: Geological section along 465m Block 'B' Footwall Drive

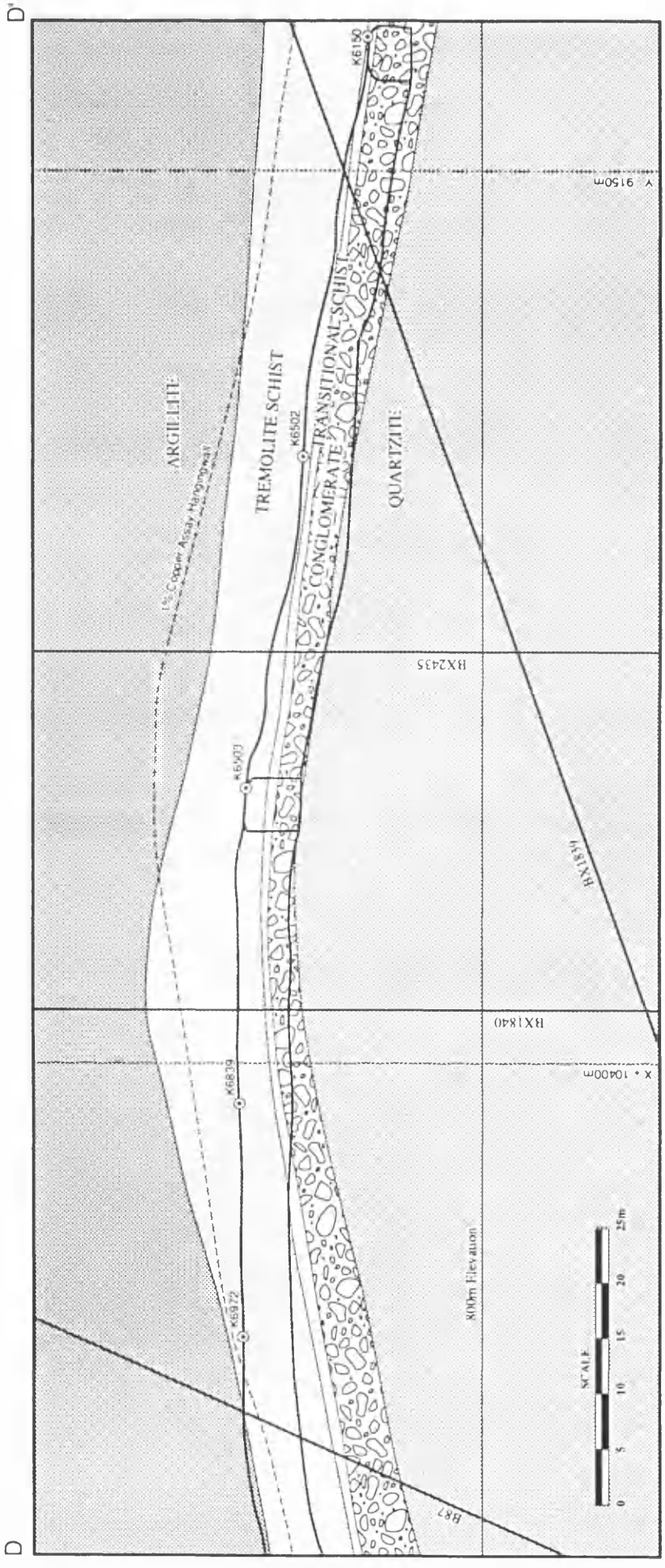

Map 7: Geological section along 450m Block 'D' Footwall Drive

KEY TO MAPS 8 TO 12


Sulphide mineral veins


Tremolite veins


Calcite/dolomite veins


Joints


Microfaults

□ CK5879 Hand specimen samples

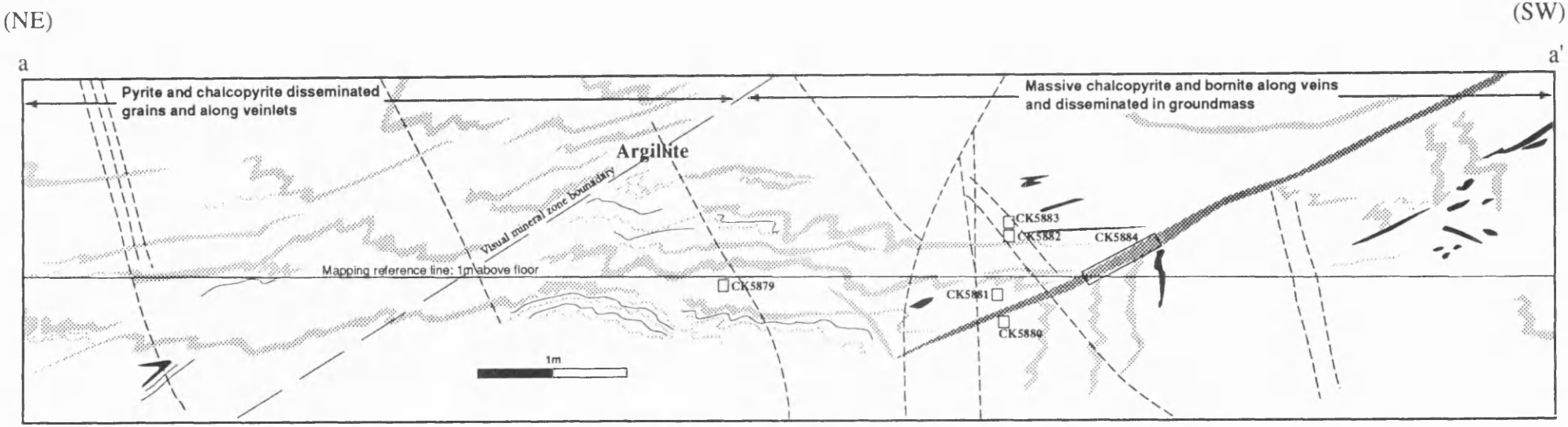

Map 8: Section along line a-a' in Figure 4.10 (enclosed in pocket of the back page). - 475m-463m Block 'A' Access crosscut; eastern wall
Samples CK5879-CK5884

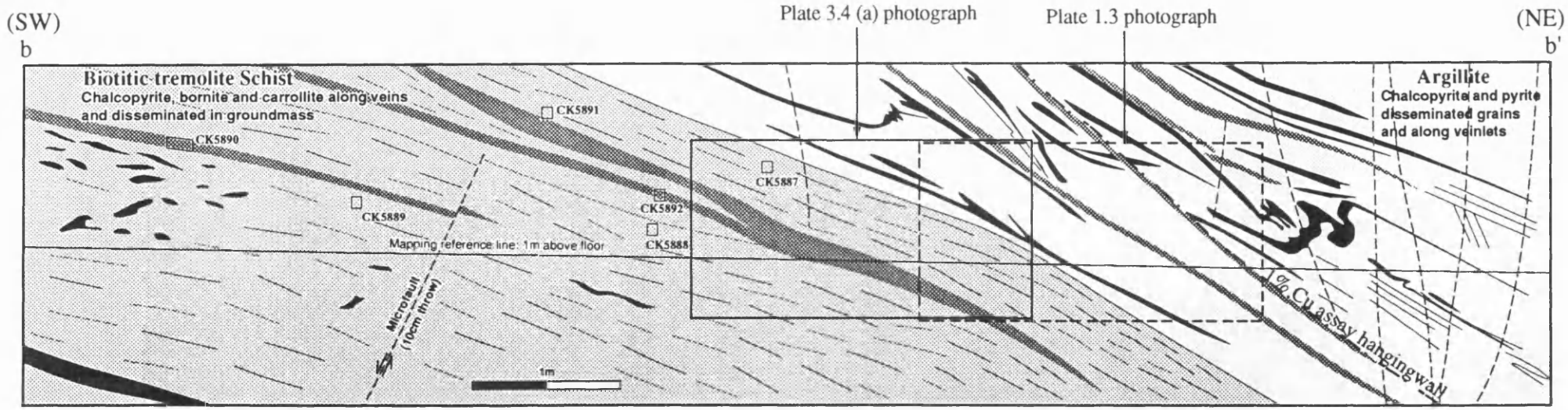

Map 9: Section along line b-b' in Figure 4.10 (enclosed in pocket of the back page) - 490m-Block 'K' Vent raise crosscut; western wall
Samples CK5887-CK5892

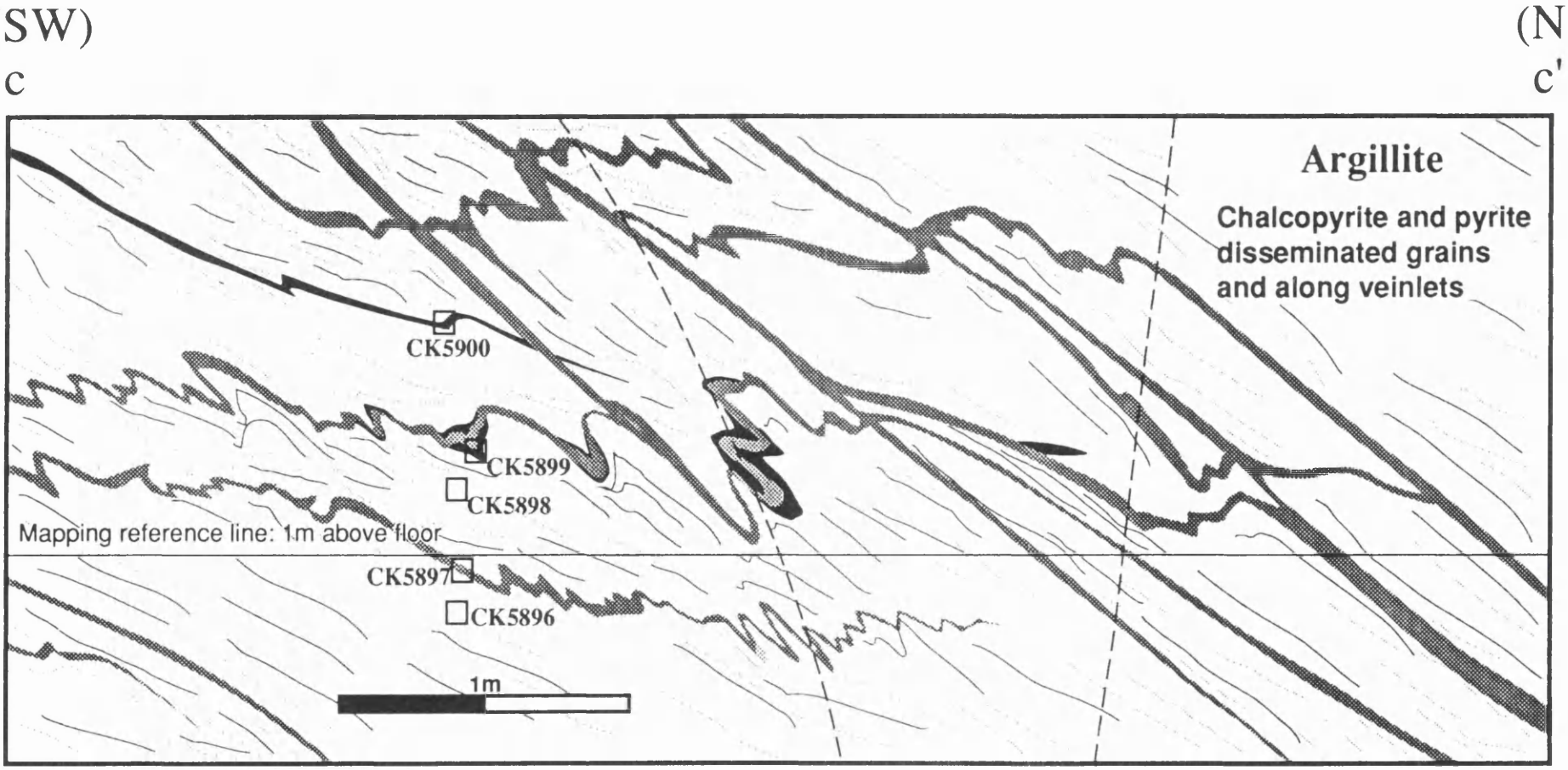

Map 10: Section along line c-c'in Figure 4.10 (enclosed in pocket of the back page).
463m-Block 'A' crosscut No 2; western wall
Samples CK5896-CK5900

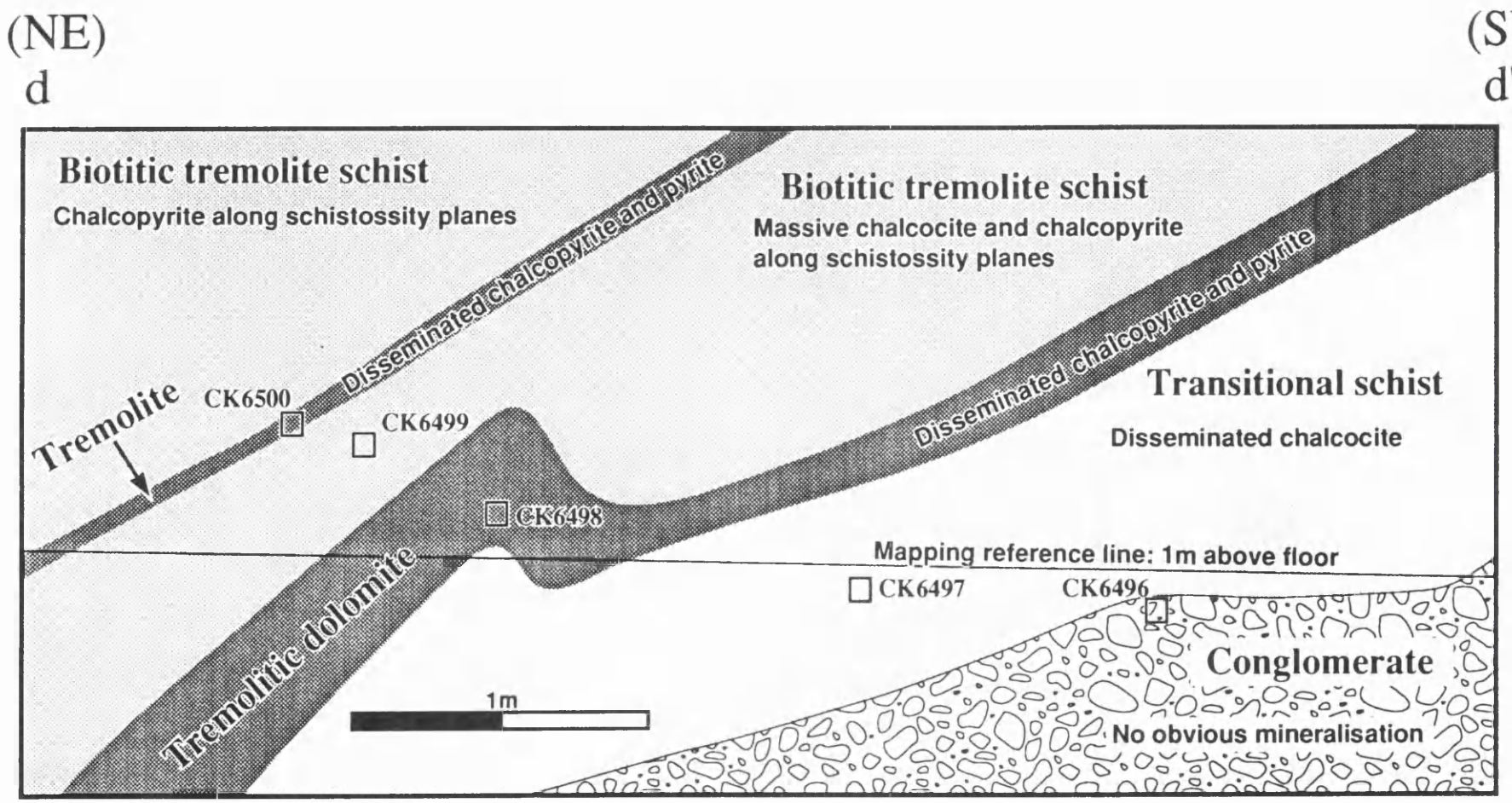

Map 11: Section along line d-d' in Figure 4.10 (enclosed in pocket of the back page).
470m-Block 'A' crosscut No 10; eastern wall
Samples CK6496-CK6500

(NE) e

(SW) e'

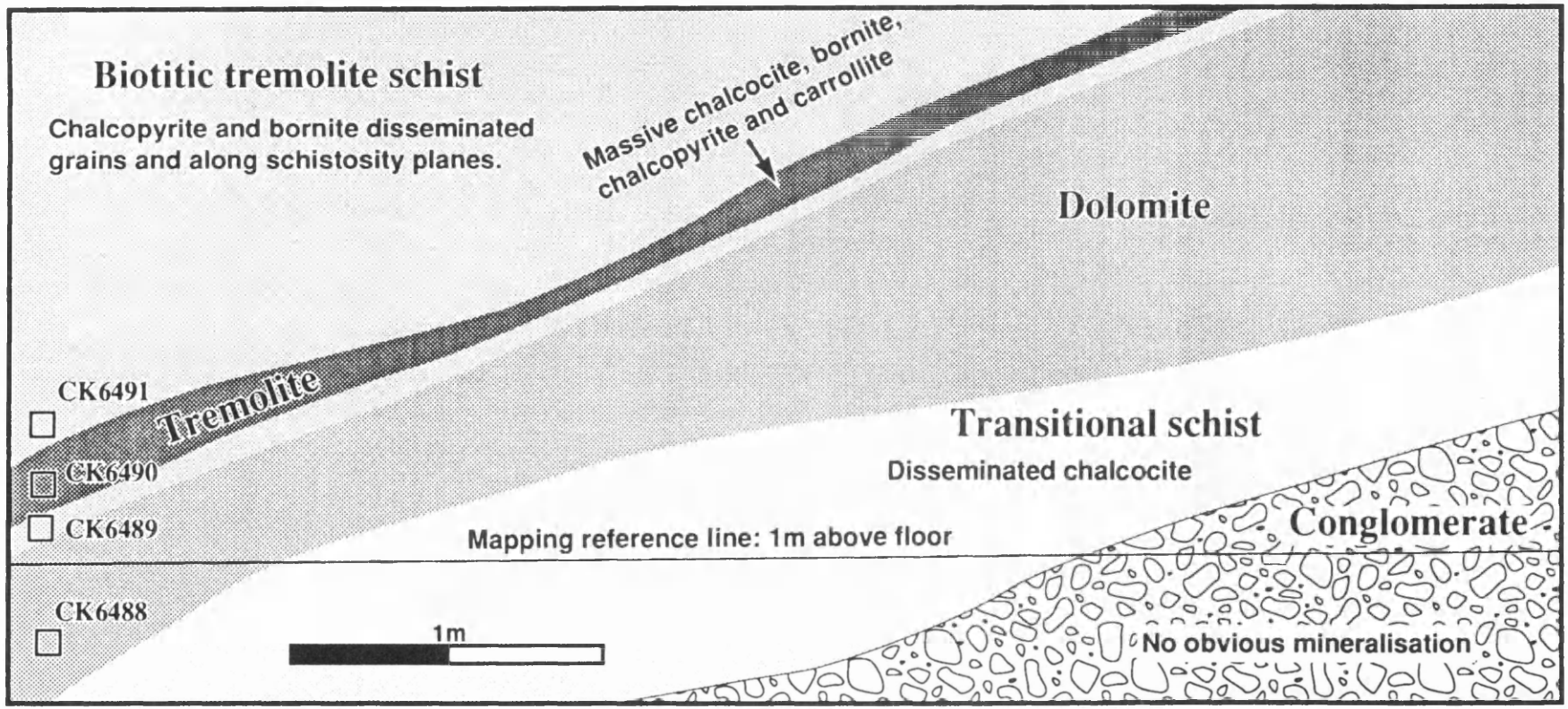

Map 12: Section along line e-e' in Figure 4.10 (enclosed in pocket of the back page).
490m-Block 'K' crosscut No 1; eastern wall
Samples CK6488-CK6491

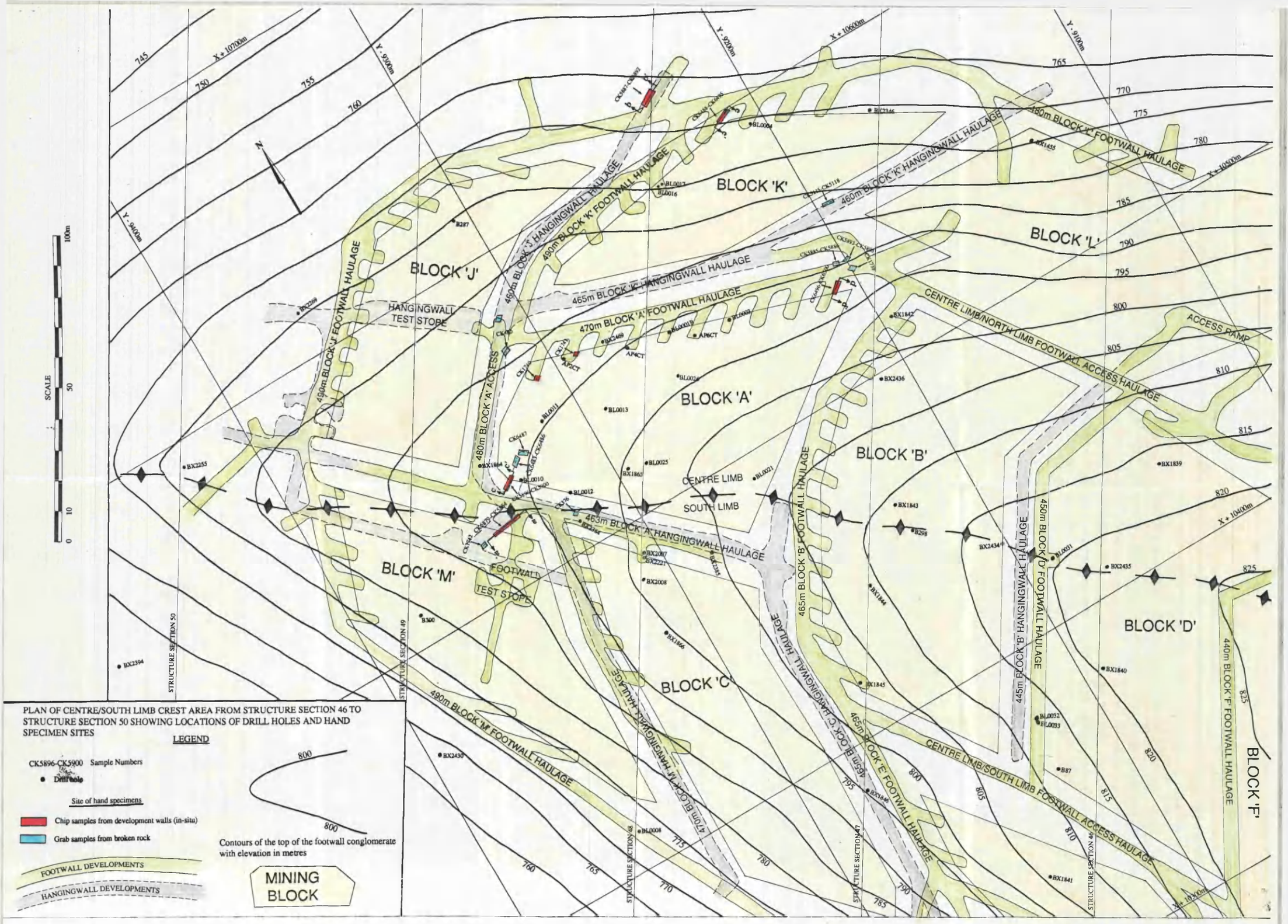

PLAN OF CENTRE/SOUTH LIMB CREST AREA FROM STRUCTURE SECTION 46 TO STRUCTURE SECTION 50 SHOWING LOCATIONS OF DRILL HOLES AND HAND SPECIMEN SITES

LEGEND

CK5896-CK5900 Sample Numbers

Drill hole

Site of hand specimens

Chip samples from development walls (in-situ)

Grab samples from broken rock

FOOTWALL DEVELOPMENTS

HANGINGWALL DEVELOPMENTS

800

800

Contours of the top of the footwall conglomerate with elevation in metres

MINING BLOCK